INVESTIGATION OF CARCINOGENIC PESTICIDE-ASSOCIATED *N*-NITROSO COMPOUNDS IN HUMAN SERUM AND URINE IN PRINCE EDWARD ISLAND

by

Crystal Lynn Sweeney

Submitted in partial fulfilment of the requirements
for the degree of Doctor of Philosophy

at

Dalhousie University
Halifax, Nova Scotia
August 2019

To a true mentor, Lyndon “Eric” Alcorn.

TABLE OF CONTENTS

List of Tables

List of Figures

Abstract

N-nitroso compounds form during acid-catalyzed reactions between certain nitrogen-containing compounds and nitrite. Approximately 90% of over 300 *N*–nitroso compounds have shown evidence of carcinogenicity. Pesticide-associated *N*-nitroso compounds (PA*N*Ns) may form endogenously from nitrosatable pesticide residues in food or water and may be detected in serum and urine. The objectives of this doctoral dissertation were to (i) develop analytical methods using ultra-high pressure liquid chromatography (UHPLC) high-resolution accurate mass (HRAM) orbital ion trap mass spectrometry (MS) for measuring 10 PA*N*N precursors in serum and urine; (ii) investigate PA*N*N formation in water by combining nitrosatable analytes with nitrite under environmentally-relevant conditions; and (iii) analyze serum and urine from a sample population in Prince Edward Island, the province with the highest pesticide-use intensity, and an urban control population (Halifax, Nova Scotia) for target analytes and PA*N*Ns. Three sample preparation methods were evaluated for extraction of target analytes from biomatrices. Deproteinization by methanol resulted in excessive ion enhancement of some analytes and complete loss of others. Solid-phase extraction showed less ion enhancement than did deproteinization; however, analyte loss remained an issue. The Quick, Easy, Cheap, Effective, Rugged, and Safe (QuEChERS) approach resulted in a novel method for extraction of target analytes with mean initial recoveries in serum ranging between 74 and 120% (% relative standard deviation, RSD <12) and 96% to 116% (%RSD ≤10) in urine. To assess PA*N*N formation, nine nitrosatable precursors were individually reacted at environmentally-relevant concentrations with sodium nitrite and hydrochloric acid in water. Ethylenethiourea (ETU) produced carcinogenic *N*-nitrosoethylenethiourea (*N*-ETU) in several experiments and at initial ETU concentrations as low as 7.5 µg L^{-1}. Finally, serum and urine from 64 healthy individuals in PEI and NS were analyzed for 10 PA*N*N precursors. ETU and 3,5,6-trichloro-2-pyridinol were detected in serum while atrazine and ETU were detected in urine with no significant differences in detection frequency in either biomatrix between provinces. Six and 10 PA*N*Ns were tentatively identified in serum and urine, respectively, in both provinces. Based on these findings, endogenous *N*-ETU formation may be a concern for individuals exposed to ETU and PA*N*Ns may be utilized as biomarkers of pesticide exposure.

List of Abbreviations Used

3,4-D – 3,4-dichloroaniline
5-HBC – methyl 5-hydroxy-2-benzimidazole carbamate
ACN – acetonitrile
AcOH – acetic acid
a.i. – active ingredient
AIF – all ion fragmentation
AM – atrazine mercapturate
As – arsenic
ATR – atrazine
Ba – barium
CAR – carbendazim
CAS – Chemical Abstracts Service
Cd – cadmium
CFM-ID – Competitive Fragmentation Modeling for Metabolite Identification
Cr – chromium
Cu – copper
CYP – cytochrome P450 enzyme
DACT – diaminochlorotriazine
DEA – desethylatrazine
DIA – deisopropylatrazine
DIM – dimethoate
di-*N*-ATR – di-*N*-nitroso atrazine
di-*N*-CAR – di-*N*-nitroso carbendazim
di-*N*-ETU – di-*N*-nitroso ethylenethiourea
di-*N*-TM – di-*N*-nitroso thiophanate methyl
DMM – double master mix
EBDCs – ethylene bis-dithiocarbamates
ETU – ethylenethiourea
EU – ethylene urea
Fe – iron
GC – gas chromatography
GIS – geographic information system
HCl – hydrochloric acid
HESI – heated electrospray ionization
HPLC – high performance liquid chromatography
HRAM – high-resolution accurate mass
HRW – Hills River watershed
IAG – indolyl-3-acryloylglycine
IARC – International Agency for Research on Cancer
IC – ion chromatography
ICP-MS – inductively coupled plasma-mass spectrometry
IMI – imidacloprid
IS – internal standard
IT – inject time

K – hydraulic conductivity
K_H – Henry's law constant
K_{OC} – normalized soil sorption coefficient
LCS – laboratory control sample
LIN – linuron
LOQ – limit of quantification
MAC – maximum acceptable concentration
MB – method blank
MCPA – 2-methyl-4-chlorophenoxyacetic acid
MDL – method detection limit
ME (%) – absolute matrix effect
MeOH – methanol
$MgSO_4$ – magnesium sulfate
Mn – manganese
MoNA – MassBank of North America
MPE – matrix post-extraction
MS – mass spectrometry
m/z – mass-to-charge ratio
NaCl – sodium chloride
$NaNO_2$ – sodium nitrite
NaOAc – sodium acetate
N-ATR – *N*-nitrosoatrazine
N-CAR – *N*-nitroso carbendazim
ND – not detected
N-DIM – *N*-nitroso dimethoate
NDMA – *N*-nitrosodimethylamine
N-ETU – *N*-nitrosoethylenethiourea
NF – not found
Ni – nickel
N-IMI – *N*-nitroso imidacloprid
N-LIN – *N*-nitroso linuron
N-OME – *N*-nitroso omethoate
NS – Nova Scotia
N-TCPy – *N*-nitroso 3,5,6-trichloro-2-pyridinol
N-TM – *N*-nitroso thiophanate methyl
OME – omethoate
PA*N*N – pesticide-associated *N*–nitroso
PATH – Partnership for Tomorrow's Health
Pb – lead
PE (%) – process efficiency
PEI – Prince Edward Island
ppm – parts per million
QA/QC – quality assurance/quality control
QuEChERS – quick, easy, cheap, effective, rugged, and safe
RE (%) – recovery efficiency
RSD – relative standard deviation

RWC – reagent water control
Se – selenium
SPE – solid-phase extraction
TCPy – 3,5,6-trichloro-2-pyridinol
TEA – thermal energy analyzer
tetra-*N*-TM – tetra-*N*-nitroso thiophanate methyl
TIC – total ion count
TM – thiophanate methyl
tri-*N*-TM – tri-*N*-nitroso thiophanate methyl
U – uranium
UHPLC – ultra-high pressure liquid chromatography
U.S. EPA – United States Environmental Protection Agency

Acknowledgements

It has been an absolute privilege to work in the Health and Environments Research Centre (HERC) Laboratory under the supervision of Dr. Jong Sung Kim. For all the twists, turns, obstacles, and celebrations of this PhD journey, Dr. Kim has always been involved every step of the way. Jong, I cannot thank you enough for your unwavering guidance and attentive support throughout my degree. I want to extend my gratitude to my committee members, Drs. Cathryn Ryan, Wenda Greer, and Ellen Sweeney, for their invaluable guidance and constructive advice throughout my program. Dr. Sweeney has also been instrumental in supporting and facilitating the collaboration of this research with Atlantic Partnership for Tomorrow's Health (PATH).

I am very appreciative of the many wonderful experiences I shared with past and present HERC Laboratory members. Nathan Smith, I am grateful for your assistance with the statistical analyses of this project, but I am even more grateful for your friendship. Nathan, you are like a brother to me and I cannot imagine where I would be without your unwavering and honest guidance. Eileen Burns, you will never know how much I appreciate your support throughout these years, both in and out of the lab. Though our shared experiences, we've become family and for that, I'm so grateful! Erin Keltie, thank you so much for your assistance with ICP-MS analysis and also for your awesome friendship. You are an excellent addition to the HERC Lab team! I'm also thankful to Andrew Rusnac for his problem-solving skills and forward-thinking during my program. Andrew, I look forward to monitoring your success throughout your career! Special thanks to my multi-talented friend, Matt Meuse-Dallian, who provided the geographic information system (GIS) elevation map data for the Hills River watershed in Prince Edward Island. I want to send a special thank you to Dr. Lynne Robinson, the Director of the Interdisciplinary PhD Program at Dalhousie University, for her encouragement and guidance. I also wish to express thanks to the Natural Sciences Engineering Research Council of Canada (NSERC), the Nova Scotia Health Research Foundation (NSHRF), and the Beatrice Hunter Cancer Research Institute (BHCRI) for financial support.

I am also extremely grateful to the many members of the Thermo Fisher Scientific team who have provided continuous analytical and technical support, especially Dr. Olivier Collin, Jason Lui, J.F. Carriere, Mark Belmont, Sebastien Morin, and Maroun El Khoury.

Dr. Alejandro Cohen, Scientific Director of the Proteomics and Metabolomics Core Facility at Dalhousie University, has also been an incredible support throughout my program and guided me through the generation of Q-Exactive orbital ion trap mass spectrometry data. To my mentors Dr. Yuri Park and Dr. Jordan Warford, thank you for your incessant guidance and support along the way. I would also like to thank Jonathan Langlois-Sadubin and Dr. Graham Gagnon for numerous helpful discussions. To my niece, Dreenan Shea, you have an incredible chemistry career ahead of you and I am forever grateful for your contributions to this work. I am extremely proud of your many accomplishments and unlimited potential!

To my husband, Mark Sweeney, I will be forever grateful for everything you've done for me, for us, over the course of this academic Everest. Your support and companionship gave me the strength I needed to push through my most difficult challenges. From bringing food to the lab all hours of the night to setting up my keyboard when I couldn't be there, you have been the reason I've been able to dedicate myself to this endeavour. Thank you from the bottom of my heart. To my amazing family, you have been cheering me on the entire time and although I missed so many family events, you've always made me see the light at the end of the tunnel. Your words of encouragement have always been my lighthouse. I look forward to endless nights of singing together! To my incredible friends, especially Darrin, Kirk, Tanya, Derek, Chrissy, and Lori…Oh, the Places *We'll* Go!

Chapter 1: Introduction

Pesticide use is often viewed as a double-edged sword, with its critical role in crop protection alongside growing concerns about environmental and human health effects. With a continuous increase in overall global pesticide use between 1990 and 2007 [1], pesticide dependence in agricultural regions has inevitably resulted in an increase in human exposure. Epidemiological studies have found positive associations between pesticide exposure and several types of cancers, including non-Hodgkin's lymphoma [2], leukemia [3], and cancers of the brain [4], breast [5], prostate [6], colon [7], liver [8], lungs [9], and bladder [10]. As such, it is important to monitor the presence of pesticides as they are inadvertently transported throughout the environment and into human populations.

Several pesticides used in Canada's maritime provinces, such as mancozeb, metiram, as well as their common metabolite, ethylenethiourea (ETU), are classified as "probable human carcinogens" by the United States Environmental Protection Agency (U.S. EPA) [11]. In addition to inherent toxicities of parent and degradation products, pesticides can also interact with other substances present in the environment to form products having greater toxicity than the parent compound itself. A prime example of this interaction is the formation of highly carcinogenic *N*-nitroso compounds from the reaction of some nitrosatable pesticides and metabolites and nitrite under acidic conditions [12]. The formation of such pesticide-associated *N*–nitroso (PA*N*N) compounds is an area of study that requires further investigation for cancer risk assessment in environments vulnerable to agricultural pesticide and nitrate pollution.

The characterization of carcinogenic potential of pesticides or other agents involves a *weight of evidence* approach, incorporating data from a range of studies, including laboratory animal tumour findings, physicochemical properties of the pesticides, structure-activity relationships in comparison with other known carcinogens, carcinogenesis mode of action (either *in vitro* or *in vivo*) and, when available, epidemiologic findings in humans [13]. Due to data gaps, notably those resulting from difficulties in obtaining accurate exposure assessments for time periods that may be relevant years before disease onset, the carcinogenicity of specific pesticides is often difficult to characterize [14]. However, the assertion that most *N*–nitroso compounds are carcinogenic is widely accepted, as they are

among the most broadly tested chemical group with 90% of approximately 300 *N*–nitroso compounds showing evidence of cancer development in all species of a wide range of laboratory animal models, including fish, snakes, and subhuman primates [15–17].

1.1 *N*-nitroso Compounds

N-nitrosamines and *N*-nitrosamides are two chemical classes of *N*–nitroso compounds formed from the nitrosation of amines and amides, respectively, from nitrite-derived nitrosating agents [18]. *N*-nitrosamines comprise the larger of the two *N*-nitroso compound groups and have the general structure of a nitroso functional group (–N=O) bonded to an amine with attached R_1 and R_2 groups, which may be in the form of a hydrogen atom or alkyl or aryl groups (Figure 1-1a) [19]. *N*-nitrosamides share a similar structure except that the carbon on one of the side chains is double bonded to oxygen and an alkyl or aryl group (Figure 1-1b). These structural blueprints allow for hundreds of *N*–nitroso compound configurations and the target organ of carcinogenicity appears to depend on molecular structure. These potent carcinogens exhibit high organ specificity, which means that different *N*-nitroso compounds have different target organs of carcinogenesis [20]. It has been observed in animal models, independent of the route of administration, that *N*–nitrosamines exhibiting symmetry with identical alkyl groups exert effects primarily in the liver, whereas a common target of asymmetrical *N*–nitrosamines is the esophagus, and cyclic *N*–nitrosamines promote tumour formation in various other tissues and organs, including the brain, stomach, gut, trachea, lung, kidney, bladder, pancreas, heart and skin [17,21].

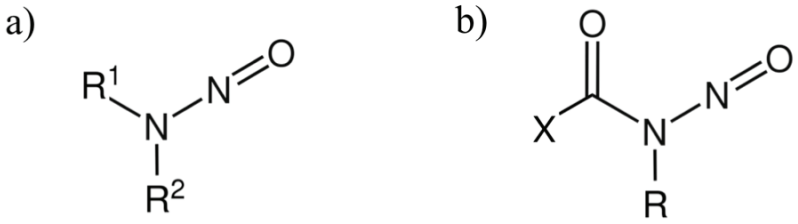

Figure 1-1. Generic structure of a) *N*-nitrosamines and b) *N*-nitrosamides [22].

In contrast to *N*-nitrosamides, *N*–nitrosamines require *in vivo* bioactivation into reactive intermediates to produce carcinogenic effects [23]. Cytochrome P450 (CYP) enzymes initiate α-hydroxylation to produce an unstable proximal carcinogen and then the oxidized side chain is cleaved, which leads to the formation of an ultimate carcinogen, an electrophilic alkylating agent (Figure 1-2) [21,24]. Due to inter-individual variation in CYP enzymes involved in *N*–nitrosamine metabolism, notably CYP2A6 and CYP2E1, bioactivation varies greatly among individuals [25]. Further variation in the metabolism of *N*-nitrosamines derives from differences in chemical structure and physicochemical properties [26–28].

Alkylating agents exert their carcinogenic effects by transferring an alkyl group onto the DNA strand to form altered bases, usually via G:C to A:T transitions [29]. While DNA alkylation may occur at various positions on the DNA strand (i.e. N-1, N-3, and N-7 positions of adenine; N-3, N-7, and O^6 of guanine; N-3 and O^2 of cytosine; N-3, O^4, and O^2 of thymine; and at the phosphate groups), observations from both *in vitro* and *in vivo* studies on *N*-nitroso carcinogenesis have shown that mutations resulting from alkylation at the oxygen atoms of DNA bases is more critical than those arising from alkylation at other positions [30]. Carcinogenesis resulting from *N*-nitrosamine exposure is more likely to occur following chronic exposure to small doses rather than acute exposure to a large single dose [20].

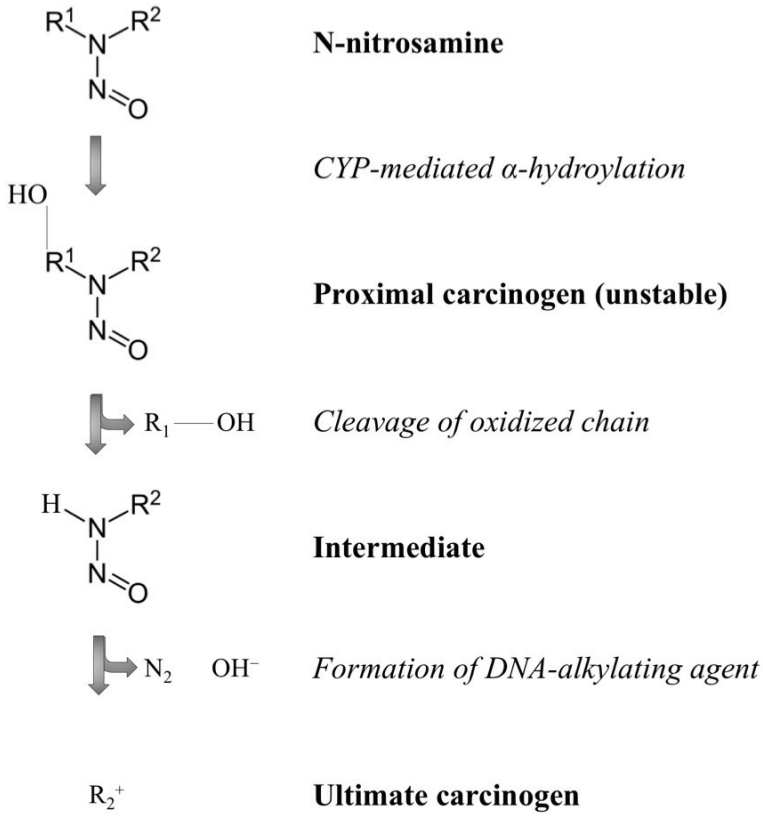

Figure 1-2. General bioactivation pathway for *N*-nitrosamines [21].

1.2 Endogenous/Exogenous *N*-nitroso Compound Formation

N-nitroso compounds are generally formed in acidic environments. *N*-nitrosamines are relatively stable in water, and are thermally stable under neutral conditions, but decompose with exposure to ultra violet light; in contrast, *N*-nitrosamides are unstable in aqueous solutions and in neutral and alkaline conditions, and decompose under normal and UV light and at temperatures above 100 ºC [31]. *N*-nitroso compounds are present in a variety of sources, including certain foods, pharmaceuticals, cosmetics, wastewater, air, soil, tobacco, detergents, rubber products, and pesticides [32]. In many of these products, *N*-nitroso compounds are formed during manufacturing processes [33]. In foods, *N*-nitrosamines are usually formed by the nitrosating agent, nitrous anhydride, which is generated from nitrite in acidic conditions [34]. This synthesis reaction can also be catalyzed by dissolved metals present [35]. It should be noted that nitrosation occurs when nitrite concentration exceeds that of the nitrosatable compound by at least fourfold [28].

The endogenous formation of *N*-nitrosamines from precursors nitrite, nitrate (present as food additives in a number food products, especially processed meats) and secondary amines accounts for 45 to 75% of total *N*-nitroso compound exposure [36]. Ingested nitrate can be reduced to nitrite *in vivo* (e.g. converted by oral bacteria to nitrite), which can subsequently participate in nitrosation reactions in the gastrointestinal tract and bladder with secondary amines to form *N*-nitrosamines [37,38]. In particular, the stomach provides a catalytic environment for the formation of *N*-nitroso compounds from dietary nitrite and nitrate because in gastric acid (pH ~ 2), nitrite is predominantly expressed in its protonated form (HNO_2), which is a direct source of the potent nitrosating nitrosonium ion (NO^+) [39]. As such, consumption of nitrate-contaminated drinking water may substantially increase the risk of endogenous *N*-nitroso compound formation [40]. Thiocyanates and heme-iron, such as that abundant in red meat, are associated with an increase in endogenous *N*-nitroso compound formation, whereas polyphenols, and vitamins C and E appear to show a protective effect against nitrosation [31,41–43].

1.3 Known Pesticide-Associated *N*-nitroso Compounds

The International Agency for Research on Cancer (IARC) lists over 30 PA*N*N compounds, noting that formation reaction rates vary widely due to dependence on type of precursor, pH, and temperature [44]. Many pesticides are often applied in conjunction with agricultural fertilizers, a rich source of nitrogen that may act as a precursor to *N*-nitroso compound formation. Environmental *N*-nitrosamine formation is most likely to form in soil, which is deprived of sunlight and can be acidic; these newly formed *N*-nitrosamines may leach through the soil into groundwater [45]. Two of the most commonly studied PA*N*N compounds that are relevant to this project are *N*-nitrosoatrazine (*N*-ATR) and *N*-nitrosoethylenethiourea (*N*-ETU).

1.3.1 *N*-nitrosoatrazine

The herbicide atrazine (ATR), a triazine herbicide used extensively in North America, is known to react with nitrite to easily form the stable *N*-ATR under acidic conditions (pH 3 to 3.5) (Figure 1-3) [46–48]. The two secondary amine moieties of the ATR molecule can be nitrosated to form either mono-*N*-ATR or di-*N*-nitrosoatrazine (di-

N-ATR), the latter of which is much less stable and rapidly decomposes to mono-*N*-ATR [49]. Moreover, two degradation products of ATR, desethylatrazine (DEA) and deisopropylatrazine (DIA), are known groundwater contaminants and can also undergo nitrosation. To illustrate the high toxicity of *N*-ATR compared to that of its parent compound, consider the following observations by Meisner *et al* (1993): *N*-ATR exposure to human lymphocyte cultures in concentrations as low as 0.0001 μg mL^{-1} resulted in significant elevations in chromosome damage whereas 1,000- to 10,000- fold greater concentrations of nitrates, nitrites, and/or ATR were required to produce comparable chromosome damage [48].

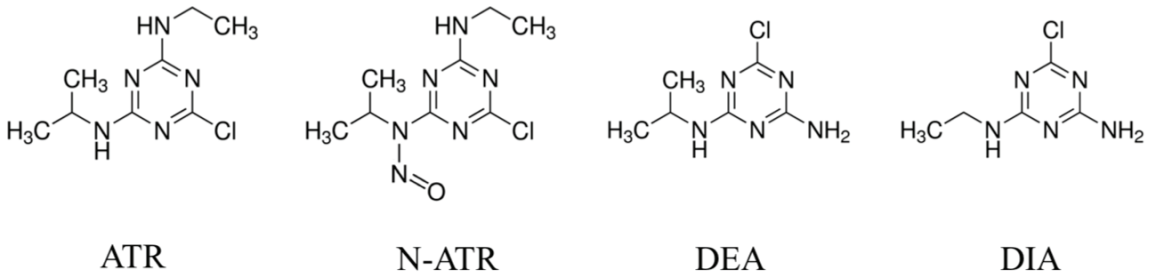

Figure 1-3. Structures of atrazine (ATR), *N*-nitrosoatrazine (*N*-ATR), desethylatrazine (DEA), and deisopropylatrazine (DIA).

Several studies have been performed to investigate the exogenous and endogenous formation of *N*-ATR. In 1977, Kearney *et al* failed to confirm the formation of *N*-ATR in soil at pH 5.0 to 7.0 after treatment with ATR at two parts per million (ppm) and high rates of nitrogenous fertilizer (100 ppm) [49]. However, in a 2011 study, *N*-ATR was detected in solutions containing 0.1 mM ATR and 0.4 mM sodium nitrite ($NaNO_2$) at pH 2 to 4, with product stability decreasing as acidity increased, and in soil at pH 4 to 5, reaching a maximum concentration at day seven and remaining constant until day 21 [50]. In addition, both acetate, a fermentation product, and fulvic acid, from soil organic matter, was found to promote nitrosation under near-neutral conditions. Further evidence supports that nitrosation of ATR and other pesticides in aqueous solutions is strongly inhibited at pH values above five [51].

In gastric juice samples (pH 1.5 to 2.0) collected from fasting individuals and treated with different concentrations of both $NaNO_2$ (0.5, 1.5, and 3 mM) and ATR, along with other triazine herbicides, (0.05 to 1 mM), maximum *N*-nitroso compound formation appeared at hour three and concentration slowly diminished after 4.5 hours [40]. Of importance, the concentrations of $NaNO_2$ used in the gastric juice experiment reflect the magnitude of the concentration of gastric nitrite present in the stomach after a meal that contains 38 mg of nitrate kg^{-1}. *N*-ATR excretion was investigated via oral administration of both ATR and *N*-ATR in rats, which resulted in urinary excretion of common metabolic biomarkers, ATR, diaminoatrazine, DEA, and DIA [52]. However, the total excretion of ATR and its metabolites after administration of ATR was 37% of the administered dose, compared to only 2% of the administered dose of *N*-ATR, which indicates a difference in metabolism of ATR and *N*-ATR. Interestingly, *N*-ATR was not detected in any of the rat urine samples.

1.3.2 *N*-nitrosoethylenethiourea

N-nitrosoethylenethiourea is formed via nitrosation of ETU [53], a common environmental degradation product and metabolite of ethylenebis-dithiocarbamates (EBDCs) (Figure 1-4) [54]. While information on this compound is limited, there exists evidence of its carcinogenic potential. In a tumorigenicity test of *N*-ETU in mice, 10 weekly oral doses between 0.66 and 2.64 mg resulted in dose-dependent increases in the number of mice having pulmonary and lymphocytic neoplasms [55]. Another experiment involving 10 weekly oral doses of ETU and $NaNO_2$ together in different combinations resulted in earlier development of tumours and/or dose-dependent increases in tumour formation in lymphatic tissue, lung, forestomach, Harderian gland, and uterus of mice; in contrast, evidence of carcinogenesis was absent after administration of either ETU or $NaNO_2$ alone [56]. These results support the assumption that *N*-ETU, believed to be formed *in vivo*, is a more potent carcinogen in mice than is ETU. In addition, concurrent oral administration of ETU and $NaNO_2$ to female Donryu rats resulted in endometrial adenocarcinomas, which is presumed to be a result of endogenously-formed *N*-ETU [57]. In a mutagenesis study, the formation of micronuclei (indicative of chromosome breakage) was observed in blood cells of female mice after the animals were fed a mixture of ETU

and $NaNO_2$, but not after administration of the single compounds [58]. As with previous studies, the authors postulated that endogenous formation of *N*-ETU and its delivery to target cells resulted in mutagenic effects observed.

ETU *N*-ETU

Figure 1-4. Chemical structures of ETU and *N*-ETU.

1.4 Pesticide and Nitrate Pollution in Prince Edward Island

Of considerable concern for exposure to PA*N*N compounds are environments that are vulnerable to pesticide and nitrate pollution. Perhaps the Canadian province of greatest vulnerability is Prince Edward Island (PEI), the producer of over 30% of Canada's total annual potato production [59]. PEI has been found to have the highest pesticide use intensity of all Canadian provinces [60]. While the island's cool, sandy and well-drained soils make the province ideal for potato production, the aquifer is highly vulnerable to pesticide contamination [61]. The PEI government operates a provincial pesticide monitoring program, which involves the analysis of groundwater (in January or February of each year) from over 100 drinking water wells of private homes, schools, municipalities, and seniors' housing facilities. Through this program, trace levels of several nitrosatable pesticides, including ATR, dimethoate (DIM), imidacloprid (IMI), and thiophanate methyl (TM), have been detected in drinking water samples [62].

Groundwater nitrate contamination is also an ongoing issue in PEI, as high fertilizer requirements for sufficient tuber yield and size make potato-growing regions particularly susceptible to leaching of nitrates into groundwater [63]. In PEI's farming-intensive watersheds, nitrate-N concentrations in 15 to 20% of tested drinking water wells exceeded

the Health Canada guideline of 10 mg L^{-1} [64]. Repeated fish kills and increasing estuarine anoxic events over the same period have alerted many Islanders about the potential for both pesticide and nitrate contamination of soils and groundwater and consequent health effects [65–67]. Considering that groundwater is the sole source of drinking water for PEI residents and it is vulnerable to pesticide and nitrate contamination, drinking water contaminated with these PA*N*N compound precursors presents a potential pathway of human exposure to *N*-nitroso compounds in PEI. There exists the potential for PA*N*N compound formation in PEI groundwater, soils, and endogenously, where nitrosatable pesticides and nitrites are present at a pH suitable for the reaction. However, these conditions must be explored further. These issues, combined with PEI's consistently higher than national cancer incidence rates [68], have created a need for more research on the relationship between pesticide exposure and cancer development in PEI.

1.5 Pesticide-Associated *N*-nitroso Compound Research Gaps

A majority of the information currently available on *N*-nitroso compounds was generated in the 1970s and 1980s. In addition to the surge in *N*-nitroso compound toxicity experiments of that era, several international symposia were held between 1971 and 1986 to address growing concerns related to these carcinogens [69–75]. In recent years, however, research on *N*-nitroso compounds has waned, leaving a number of research gaps, and thus opportunities, in the field. First, despite the advancement of technology used to identify a wide range of environmental pollutants and biomarkers, analytical methods have not yet been developed for semi-targeted analysis of *a priori* unknown *N*-nitroso compounds that are anticipated to form from nitrosatable pesticides, notably those used in PEI agriculture. Second, *N*-nitroso compound formation from these analytes has not yet been investigated using environmentally relevant concentrations of substrates. Furthermore, human biomonitoring data for PA*N*N compounds in PEI, an environment susceptible to nitrate and pesticide contamination, are lacking. To begin narrowing research gaps, and to develop feasible and specific aims for this work, these topics were further explored.

1.5.1 Laboratory Analysis of *N*-nitroso Compounds

The technology for detecting *N*-nitroso compounds has advanced significantly over the last four decades. In the mid 1970s, nanogram and picogram levels of *N*-nitroso compounds were analyzed in a range of matrixes, including complex biological materials and foods, by coupling gas chromatography (GC) and high performance liquid chromatography (HPLC) to a Thermal Energy Analyzer (TEA), a technique highly specific to the nitroso functional group [76–78]. As described by Ikeda *et al* (1990), TEA involves the thermal breakage of N-NO bonds of *N*-nitroso compounds within a flash catalytic pyrolyzer, which results in the formation of nitrosyl radicals [32]. All other organics, fragments, and solvent molecules are frozen in cold traps and removed, leaving only the nitrosyl radicals behind, which are subsequently oxidized via ozone to produce electronically excited nitrogen dioxide (NO_2*). The transformation of this unstable molecule back to its ground state emits characteristic electromagnetic radiation proportional to nitrosyl radical concentration. Despite the emphasis by Ikeda *et al* that highly specific TEA was the gold standard for *N*-nitroso compound analysis, it has been observed that some organic nitrites and nitrates, as well as some inorganic nitrites, produce undesired TEA responses, requiring unequivocal structure confirmation by an independent technique, usually mass spectrometry (MS) [79].

Mass spectrometry is a powerful tool used in identification and quantitation of a wide range of environmental and biological contaminants in trace concentrations. Commonly used types of MS in analytical toxicology are single quadrupole, triple quadrupole, and orbital ion trap MS, which are often coupled with GC or LC. In general, analytes separated in solution by chromatography are vaporized upon entry into the MS, are ionized, and sent to the detector for measurement of the mass-to-charge ratio (*m/z*) of each ion. For a given set of MS parameters, an ionized analyte will fragment into a set of discrete ions in consistently relative ratios, creating a characteristic mass spectrum used for compound identification. In addition to being used in targeted analysis of known analytes, the orbital ion trap MS can also be employed in semi- and non-targeted analyses, which is paramount for the study of unknown degradation and transformation products that may be more toxic than their parent compounds [80].

As previously mentioned, the group of *N*-nitroso compounds is comprised of hundreds of compounds that behave differently, not only toxicokinetically and toxicodynamically, but also analytically. This is to say that an analytical method developed to analyze a number of *N*-nitroso compounds may not be adequate for the analysis of other members of the group. In the case of PA*N*N compounds, the *N*-nitroso product formed from its parent pesticide is physicochemically similar (e.g. in molecular weight, retention characteristics, etc.) to its parent compound. Therefore, to analyze PA*N*N compounds, it may be more advantageous to develop a targeted/semi-targeted MS instrument method for the analysis of the parent pesticides (targeted analysis), with the capability of examining mass spectra of other closely related compounds in the sample (semi-targeted), than it would be to use a previously existing method for other *N*-nitroso compounds that share fewer structural similarities with the pesticides. For this reason, existing methods for other *N*-nitroso compounds (e.g. tobacco-specific nitrosamines) may not be suitable for the analysis of less structurally-similar PA*N*N compounds.

For precise identification of analytes in any type of targeted analysis, not only must the structure of the analyte be known, but retention characteristics and fragmentation data generated from analysis of a certified analytical standard should be used for verification. This poses a problem for studies, such as this, that aim to analyze compounds predicted to be present in a sample for which analytical standards are not readily available for purchase. In these cases, a semi-targeted approach is favoured. High-resolution accurate mass (HRAM) orbital ion trap MS allows the discovery of new pesticide biomarkers by screening for a virtually limitless number of analytes [81]. Despite the availability of this highly sensitive platform for semi-targeted analysis, it has not yet been employed in the investigation of PA*N*N compounds.

1.5.2 Pesticide-Associated *N*-nitroso Compound Formation

Several research groups have experimented with the formation of *N*-nitroso compounds from nitrosatable pesticides [45,50,82–85]. However, most studies experiment with high initial pesticide concentrations that are not typically found in the environment. For example, in a 2011 study of *N*-ATR formation in solution, concentrations used were much higher than are environmentally relevant (0.1 mM ATR = 21.56 mg L^{-1}; 0.4 mM

$NaNO_2$ = 18.40 mg L^{-1}) [50]. In some cases, the use of high initial pesticide concentrations may be due to a lack of a sensitive detection method while in others, study objectives may focus on the characterization of PA*N*N compound formation and identifying unknown physicochemical properties.

While it is important to investigate PA*N*N compound formation kinetics at high substrate concentrations under controlled laboratory conditions, it is also critical to explore whether synthesis occurs at concentrations to which people may be exposed in drinking water. Following a thorough review of the literature [45,50,82,84,85], the lowest initial pesticide concentration used in an *N*-nitroso compound formation experiment was found to be 20 μg L^{-1}; the study reported the synthesis of significant concentrations of *N*-nitrosodimethylamine (NDMA) (0.170 μg L^{-1}) during dichloramination of diuron [82]. However, this pesticide is not listed on the PEI Pesticide Sales Report [86] and is therefore not included in this study as an analyte of interest. Furthermore, when the literature was searched for *N*-nitroso compound formation from each individual analyte of interest, only two of 10 analytes (ATR and ETU) produced results [28,40,45,48–50,52,55–58,84,87–95]. As each PA*N*N compound bears its own physicochemical properties, formation kinetics may vary greatly among this group of carcinogens and, as such, should be examined individually.

1.5.3 Human Biomonitoring of Pesticide-Associated *N*-nitroso Compounds

Of the research gaps involving PA*N*N compounds discussed herein, human biomonitoring data are lacking the most. Studies identified that involved the analysis of PA*N*N compounds relevant to this work in biomatrices were not true biomonitoring studies. For example, *N*-ATR was studied in human gastric juice but under *in vitro* conditions [40]. Another study involved the analysis of *N*-ATR in urine, but samples were collected from rats [52]. Some biomonitoring studies involved non-specific analysis of *N*-nitroso compounds in human urine. For example, in 1982, an indiscriminate method was used for the screening of total *N*-nitroso content in human urine through detection of nitric oxide following denitrosation [96]. Other work examining specific nitrosamines in human biomatrices focused on tobacco-specific *N*-nitrosamines [97]. To the author's knowledge, there are no human biomonitoring data available to date from the analysis of PA*N*N

compounds related to any analyte of interest in this study with the exception of NDMA [98–101], a known pesticide contaminant.

1.6 Analytes of Interest

Analytes of interest in this study were chosen based on the following five inclusion criteria: (1) presence of secondary amines or amides (interaction potential with nitrates to form *N*-nitroso compounds); (2) sales group ranking in PEI Pesticide Sales Report; (3) detection in PEI environments based on data from the provincial pesticide monitoring program; (4) groundwater contamination potential, based on solubility, Henry's law constant (K_H), normalized soil sorption coefficient (K_{OC}), and persistence; and (5) toxicity potential (e.g., classified as carcinogenic by the U.S. EPA). Using the Retail Pesticide Sales Report issued by the PEI Department of Communities, Land and Environments, pesticides containing secondary amines or amides were ranked by amount of active ingredient (a.i.) sold in 2014, the most recent year for which sales data are available. Some of the highest ranked pesticides were eliminated due to analytical challenges. First, mancozeb, PEI's highest ranked pesticide in sales, is difficult to analyze using chromatographic techniques and has a high detection limit of 100 μg L^{-1} [102]. Glyphosate, ranking second, is also a major challenge to analyze on this platform without derivatization [103] and was excluded from the study. Metiram, also ranked in the top five, was excluded as its detection limit is 1,000 μg L^{-1} [102]. Of the remaining nitrosatable pesticides, the following five were selected for analysis: ATR, DIM, IMI, linuron (LIN), and TM (Figure 1-5).

Five additional analytes were also included in the study. ETU, a common metabolite of both mancozeb and metiram, two of PEI's highest ranked pesticides in sales, contains two secondary amines and is also classified as a "Group B Probable Human Carcinogen" by the U.S. EPA. MCPA (2-methyl-4-chlorophenoxyacetic acid), a phenoxy herbicide widely used in PEI, was also included in our study because, even though it does not contain a secondary amine or amide capable of interacting with nitrates to form *N*-nitroso compounds, it is often contaminated with the nitrosamine NDMA [104]. Other analytes of interest are primary metabolites of parent compounds, carbendazim (CAR), 3,5,6-trichloro-2-pyridinol (TCPy), and omethoate (OME), all of which are capable of forming *N*-nitroso compounds through interaction with nitrite (Tables 1 and 2).

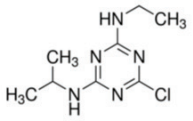

Atrazine (ATR)
CAS number: 1912-24-9
Molecular Formula: $C_8H_{14}ClN_5$
Molar mass: 215.68 g mol $^{-1}$

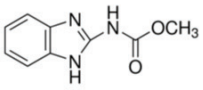

Carbendazim (CAR)
CAS number: 10605-21-7
Molecular Formula: $C_9H_9N_3O_2$
Molar mass: 191.19 g mol $^{-1}$

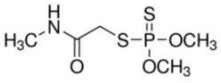

Dimethoate (DIM)
CAS number: 60-51-5
Molecular Formula: $C_5H_{12}NO_3PS_2$
Molar mass: 229.26 g mol $^{-1}$

Ethylenethiourea (ETU)
CAS number: 96-45-7
Molecular Formula: $C_3H_6N_2S$
Molar mass: 102.16 g mol $^{-1}$

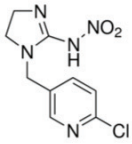

Imidacloprid (IMI)
CAS number: 138261-41-3
Molecular Formula: $C_9H_{10}ClN_5O_2$
Molar mass: 255.66 g mol $^{-1}$

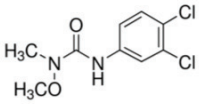

Linuron (LIN)
CAS number: 330-55-2
Molecular Formula: $C_9H_{10}Cl_2N_2O_2$
Molar mass: 249.09 g mol $^{-1}$

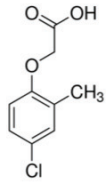

2-methyl-4-chlorophenoxyacetic acid (MCPA)
CAS number: 94-74-6
Molecular Formula: $C_9H_9ClO_3$
Molar mass: 200.62 g mol $^{-1}$

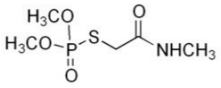

Omethoate (OME)
CAS number: 1113-02-6
Molecular Formula: $C_5H_{12}NO_4PS$
Molar mass: 213.19 g mol $^{-1}$

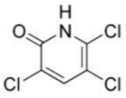

3,5,6-trichloro-2-pyridinol (TCPy)
CAS number: 6515-3
Molecular Formula: $C_5H_2Cl_3NO$
Molar mass: 198.43 g mol $^{-1}$

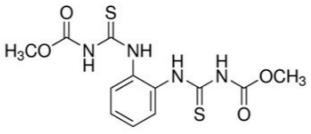

Thiophanate methyl (TM)
CAS number: 23564-05-8
Molecular Formula: $C_{12}H_{14}N_4O_4S_2$
Molar mass: 342.39 g mol $^{-1}$

Figure 1-5. Molecular structures, abbreviations, Chemical Abstracts Service (CAS) numbers, molecular formulas, and molar masses of target analytes.

Table 1-1. Groundwater contamination potential characteristics for analytes of interest based on (1) water solubility (mg L^{-1}); (2) K_H; (3) K_{OC}; and (4) persistence ($t_{1/2}$).

Analyte	Groundwater contamination potential				References
	Water solubility[a] (mg L^{-1})	K_H[b] (atm m^3 mol^{-1} @ 25 ºC)	K_{OC}[c] (L kg^{-1})	$t_{1/2}$[d] (days)	
ATR	Moderate	2.6 x 10^{-9}	54-1164	20-360	[105]
CAR	Low	1.5 x 10^{-12}	122.3-2805	320	[106,107]
DIM	High	2.4 x 10^{-10}	5.2-50	7-122	[108]
ETU	High	1.36 x 10^{-11}	13	<7	[109,110]
IMI	Moderate	1.65 x 10^{-15}	156 to 800	48-190	[111]
LIN	Moderate	1.97 x 10^{-9}	555 to 987	22-136	[112]
MCPA	Moderate	4.8 x 10^{-10}	50-62	<7 to 41	[113]
OME	High	4.6 x 10^{-14}	9.4	3.8-25	[114–116]
TCPy	Moderate	Unknown	27-389	42-117	[117]
TM	Moderate	1.21 x 10^{-9}	330	12-15	[118,119]

[a]Low water solubility is considered to be less than 10 mg L^{-1}, moderate solubility is between 10 and 1,000 mg L^{-1}, and high water solubility is more than 1,000 mg L^{-1} [120].
[b]Henry's law constant (K_H) is the ratio of a pesticide's concentration in air to that in water when in equilibrium and describes the tendency of a pesticide to volatilize out of an aqueous solution, with values less than 9.869 x 10^{-11} atm m^3 mol^{-1} denoting little tendency to volatilize [80].
[c]The normalized soil sorption coefficient (K_{OC}) is a measure of organic matter content of soil; pesticides are considered highly mobile if they have a K_{OC} value of less than 50 [80].
[d]Pesticide half-life ($t_{1/2}$) is the length of time in which it degrades to half of its initial concentration and may be considered low (less than 16 days), moderate (16 to 59 days), and high (over 60 days) [121]. These values pertain to soil except in the case with TM, which were calculated from plant leaves because TM soil $t_{1/2}$ is unknown.

Table 1-2. Analytes of interest based on (1) nitrosatability; (2) sales of pesticide (kg a.i.) in PEI; (3) detection in PEI groundwater; (4) groundwater contamination potential; and (5) toxicity potential.

Analyte	2014 PEI sales[a] (kg a.i.)	[Max] in PEI groundwater[b] ($\mu g\ L^{-1}$)	Groundwater contamination potential[c]	Toxicity potential[d]
ATR	2,870	0.65	Yes	High interaction potential with nitrate/nitrite
CAR	5,988[e]	N/A[f]	Yes	Possible human carcinogen; interaction potential with nitrate/nitrite
DIM	2,376	0.1	Yes	Possible human carcinogen; interaction potential with nitrate/nitrite
ETU	343,492[e]	N/A[f]	Yes	Probable Human Carcinogen; interaction potential with nitrate/nitrite
IMI	3,919	0.46	Yes	Interaction potential with nitrate/nitrite
LIN	27,528	≤ 0.06	Yes	Possible human carcinogen; interaction potential with nitrate/nitrite
MCPA	18,361	≤ 1	Yes	Often contaminated with NDMA
OME	2,376[e]	N/A[f]	Yes	Interaction potential with nitrate/nitrite
TCPy	741[e]	N/A[f]	Yes	High interaction potential with nitrate/nitrite
TM	5,988	0.55	Yes	Likely to be carcinogenic to humans; interaction potential with nitrate/nitrite

[a]Data acquired from 2014 PEI Pesticide Sales Report [86].
[b]Maximum concentration of analyte quantified in groundwater by Government of PEI pesticide monitoring program [102].
[c]Determined after considering contamination potential characteristics shown in Table 1.
[d]Carcinogen classification by U.S. EPA [11].
[e]Reflects sales of parent compound.
[f]Not included in the PEI government's pesticide monitoring program.

1.7 Objectives and Specific Aims

The primary objective of this study is to develop and employ a semi-targeted approach using HRAM orbital ion trap MS to identify specific nitrosatable pesticides and byproducts, as well as their associated *N*-nitroso compounds, in human serum and urine

from a healthy sample population in an area of intense agriculture in PEI and to determine whether these analytes are detected in serum and urine of a healthy sample population in Halifax, a non-agricultural urban area. The central hypothesis of this research is that *N*-nitroso compounds are formed endogenously after exposure to nitrosatable pesticides and nitrates/nitrites and that these carcinogens can be detected as biomarkers in biofluids of individuals living in areas of intensive pesticide use. It is also hypothesized that these PA*N*N compounds are undetectable in biofluids of individuals living in areas of non-intensive pesticide use. The assumption, based on the Government of PEI pesticide monitoring program data that confirm the presence of trace amounts of several nitrosatable pesticides in PEI groundwater, is that exposure to PA*N*N compound substrates is higher in the PEI population than in the Halifax population due primarily to contaminated drinking water. Three specific aims have been proposed to meet the objectives of this study.

Specific Aim 1: To develop sample preparation and semi-targeted analytical methods using HRAM orbital ion trap MS for identification and quantitation of nitrosatable pesticides and byproducts relevant to PEI agriculture and detection of PA*N*N compounds in human serum and urine.

Specific Aim 2: To investigate *N*-nitroso compound formation by combining nitrosatable target analytes with $NaNO_2$ under environmentally- and biologically-relevant conditions (maximum analyte concentration of 20 μg L^{-1}; nitrite concentration of 2.5 mg L^{-1}; pH values of 2 and 5; and metal catalyst concentrations of 50 μg L^{-1}) using HRAM MS.

Specific Aim 3: To use the semi-targeted methods developed in this project to analyze human serum and urine from a PEI population, as well as those biofluids from an urban control population, Halifax, for analysis of target analytes and screening of PA*N*N compounds.

This will be the first study to analyze human serum and urine in PEI for PA*N*N compounds, which may be important for large-scale cancer risk assessment projects. The detection of any of these analytes in human serum or urine signifies the discovery of novel pesticide-associated biomarkers that may be vital in carcinogenic risk assessment.

Chapter 2: Comparison of sample preparation approaches and validation of an extraction method for nitrosatable pesticides and metabolites in human serum and urine analyzed by liquid chromatography - orbital ion trap mass spectrometry

2.1 Abstract

In the acidic environment of the stomach, nitrosatable pesticide residues may react with nitrite to form potentially carcinogenic pesticide-associated *N*-nitroso (PA*N*N) compounds. The objective of this study was to develop a method for the analysis of 10 nitrosatable pesticides and breakdown products in human serum and urine. Three sample preparation methods were evaluated for extraction of target analytes from the biomatrices: deproteinization; solid-phase extraction (SPE); and the quick, easy, cheap, effective, rugged, and safe (QuEChERS) method. Deproteinization by methanol (MeOH) for 300-µL aliquots of serum with a final extract volume of 225 µL resulted in excessive ion enhancement of some analytes and suppression of others. Three types of SPE sorbents were tested for optimal analyte retention from 200-µL aliquots of serum with a final extract volume of 400 µL; this approach resulted in significant analyte loss for some compounds. The QuEChERS approach resulted in a suitable method for extraction of the analytes from each biomatrix and was further optimized. Biofluid samples (500 µL) were spiked to 100 µg L^{-1} with analytical standards and extracted using 500 µL of acetonitrile (ACN) with 4% acetic acid (AcOH) for serum and 0.1% AcOH in ACN for urine. Final extract volumes for both biomatrices using the QuEChERS method was 400 µL after dilution. For extraction, 200 mg magnesium sulfate ($MgSO_4$) and 50 mg sodium acetate were added for serum and 200 mg $MgSO_4$ and 50 mg sodium chloride were added for urine. Samples were analyzed via ultra-high pressure liquid chromatography (UHPLC)/high-resolution accurate mass (HRAM) orbital ion trap mass spectrometry (MS). Mean recoveries for target analytes in serum and urine ranged between 74 and 120% (% relative standard deviation (RSD) <12) and 96 to 116% (%RSD ≤10), respectively. These methods may be used in large-scale biomonitoring studies to analyze PA*N*N compounds and their precursors in human serum and urine.

Keywords: pesticides, QuEChERS, UHPLC/HRAM orbitrap MS, *N*-nitroso compounds, serum, urine

2.2 Introduction

Analysis of pesticide residues in food, air, and drinking water is an important step in characterizing pesticide exposure and assessing public health risks. However, these data provide only an estimate of pesticide exposure, rather than direct information on *internal* exposure. Biomonitoring is the analysis of a chemical and/or its metabolites in biological samples (e.g. blood, urine, hair, and saliva) to assess exposure [122]. Thus, pesticide biomonitoring is important in closing data gaps that remain by methods that estimate exposure through analysis of environmental samples. A key advantage of pesticide biomonitoring over analysis of environmental samples is that endogenously formed compounds resulting from pesticide exposure can also be examined. One highlighted example of endogenous formation of toxic pesticide byproducts is the formation of potentially carcinogenic *N*-nitroso compounds from nitrosatable pesticides and nitrites present in the body [123,124]. Although this reaction can occur in the environment under certain conditions, endogenous formation of *N*-nitrosamines accounts for up to 75% of total *N*-nitroso compound exposure [36]. This illustrates that biomonitoring of parent pesticides as well as their toxic byproducts and metabolites is necessary to better understand adverse health effects of pesticide exposure.

Worldwide, blood and urine analyses are considered the gold standards for pesticide biomonitoring [125]. Biomonitoring of pesticides in blood has several advantages. First, as many pesticides remain in their parent (unchanged) form for a given amount of time in the blood, detection of parent compounds offers confirmation of internal exposure to specific pesticides [126]. Another advantage of analyzing pesticides in blood is that blood volume is regulated, which means that fluctuations with water intake or other factors are prevented. Because of this regulation, calculations of body burden (the level of analyte relative to the total blood volume), do not require dilution corrections and are, thus, more accurate than measuring the pesticide or its metabolite in urine [127,128]. Furthermore, DNA adducts and other constituents that may represent early biomarkers of effect can also be measured in blood samples. Urine analysis also has several advantages.

Urine collection is completely non-invasive, sample volume is generally sufficient to acquire reliable analytical data, and concentrations of pesticides biomarkers are generally higher in urine than in blood due to higher rates of metabolism and excretion [128].

While blood and urine are the most commonly used biological matrices for pesticide analysis, there exist some challenges of analyzing these sample types. First, blood and urine are complex matrices, containing many hundreds or thousands of metabolites [129]. Blood is the more complex of the two, containing low-molecular-weight organic and inorganic chemicals as well as other higher-molecular-weight compounds such as proteins and RNA. These higher-molecular weight species are also present in urine, but in much lower concentrations. Matrix constituents can interfere with analysis and must be considered during sample preparation method development.

Another challenge in analyzing blood and urine for pesticides, metabolites, and byproducts is that these analytes are often present in very low concentrations (parts per billion or trillion). Detection and quantitation of analytes present in biological matrices in trace amounts places the onus on the sample preparation protocol to provide sufficient recoveries of the extracted analytes and on the instrument to be able to achieve increasingly lower limits of detection for target analytes. Fortunately, parameters of both the sample preparation and instrument methods can be optimized for maximum extraction efficiency and analyte signal intensity. However, this process becomes increasingly arduous as more target analytes from different chemical classes are added to the method.

To retain the maximum number of analytes, sample preparation may involve simple deproteinization, by addition of an organic solvent, followed by centrifugation to precipitate and remove high-molecular-weight interferents. This approach is illustrated in the Nature Protocols publication entitled, *Procedures for large-scale metabolic profiling of serum and plasma using gas chromatography and liquid chromatography coupled to mass spectrometry* [129]. This technique is appealing, as it is easy to perform and can accommodate the preparation of 30 samples per day. However, it may pose a problem for targeted analyses, as the indiscriminate extraction of thousands of non-target analytes may interfere with target compounds.

Solid-phase extraction is a popular sample preparation technique in pesticide analysis for its ability to concentrate target analytes and remove contaminants from a wide

range of complex sample matrices, including groundwater, surface water, wastewater, urine, and serum [130–133]. There are several ways to perform SPE, but generally, liquid sample is aspirated via gravity or low vacuum through sorbent material packed in a disposable cartridge. Analytes present in the matrix are retained by functional groups in the sorbent and are subsequently eluted with a small volume of organic solvent. The type of sorbent and elution solvent can be optimized, depending on the physicochemical properties of target compounds. Drawbacks of SPE include complex method development and costly one-use SPE cartridges.

A more recent sample preparation technique called QuEChERS (pronounced "catchers"), made its debut in 2003 and is now the gold standard for sample preparation of pesticides in a variety of food samples [80,134]. The premise of QuEChERS involves extraction of pesticides with ACN followed by the addition of $MgSO_4$ for salting out extraction/partitioning and an optional clean-up step using a primary-secondary amine sorbent and anhydrous $MgSO_4$ as a desiccant [135,136]. In mere minutes, QuEChERS can extract a large number of different classes of pesticides with acceptable recoveries from many samples [80]. However, no sample preparation method is without its disadvantages. First, ACN may not be an acceptable injection solvent for all methods and a solvent transfer may be required. Also, there are fewer data from studies involving the application of QuEChERS to biological samples. Finally, many acid- and base-sensitive pesticides show unacceptable recoveries with the original QuEChERS protocol, but the use of buffers have been shown to improve recoveries of such problematic pesticides [136].

Pesticides are most commonly analyzed via GC or LC coupled with MS [137]. This work will focus on LC-MS because it is the chosen platform for simultaneous analysis of pesticides and their metabolites, which tend to be more polar and less volatile than their parent compounds and less conducive to GC analysis [138]. In LC, the liquid mobile phase moves the sample through the analytical column and to the detector. To optimize analyte retention and separation in the column, characteristics of the mobile phase, including flow rate, percentage of organic solvent, gradient, and pH, can be modified. Generally, the rate of analyte elution from the column increases as the proportion of organic solvent in the mobile phase increases, resulting in a shorter retention time [139]. Buffered mobile phases

can be used to control the ionization state of acidic or basic analytes, altering retention characteristics such as retention time and peak shape [140].

Another parameter that requires optimization in pesticide method development is analytical column selection. HPLC columns are available with different types of stationary phase, including reversed phase, normal phase, ion exchange, and size exclusion [141]. Reverse phase, indicated by a hydrophobic stationary phase, is the most common type of chromatography [139]. The mobile phase is more polar than the stationary phase, which is often a C_{18} hydrocarbon. The physicochemical properties of pesticides influence how they interact with the stationary phase [142]. Column volume, dictated by length and internal diameter, influences system pressure and run time [143]. Some LC systems are equipped to operate under ultra-high pressure and are used with UHPLC columns that contain sub-2μm particles [144]. The result is improved throughput and resolving power, as separation efficacy increases as particle size decreases.

Mass spectrometry is a dynamic and reliable technique used for identification and quantitation of trace amounts of pesticides, their metabolites, and other degradation products. Single and triple quadrupole MS platforms are suited for targeted analysis of pesticides but are not conducive to semi- or non-targeted analysis. This is because non-targeted analysis requires MS operation in full scan mode, which significantly reduces sensitivity in these instruments [145]. In contrast, the orbital ion trap MS can be used to detect both known and unknown analytes. The orbital ion trap mass analyzer consists of a central spindle-like electrode and an outer barrel-like electrode [146]. The *m/z* of ion fragments is measured as ions become trapped in the orbital ion trap and oscillate both radially about the spindle electrode and in the z-direction, generating an axial frequency [147]. Key features of the orbital ion trap MS are its high resolution (up to 500,000), high mass accuracy (< 1 ppm), and wide mass range (50 to 4000 *m/z*) [148]. These HRAM performance characteristics make the orbital ion trap platform a key player in semi- and non-targeted pesticide analyses, as it can record a virtually unlimited number of analytes while operating in full scan mode [145].

The overall objective of this study is to develop a comprehensive sample preparation method for human serum and urine and a semi-targeted analytical method using HRAM MS technology for qualitative and quantitative analysis of a suite of

nitrosatable pesticides and identification of PA*N*N compounds. This study has been designed to meet this objective through a four-part plan involving the development of (1) the UHPLC-HRAM orbital ion trap MS instrument method; (2) the serum sample preparation method; (3) the urine sample preparation method development; and (4) the validation of each sample preparation method. The instrument method development will encompass optimization of several parameters, including ionization mode, analytical column, mobile phase, and heated electrospray ionization (HESI) source parameters. The sample preparation method development will involve experiments using three approaches: simple deproteinization; SPE; and QuEChERS. The method will be validated by determining the following method characteristics: specificity; accuracy; precision; recovery; matrix effects; linearity; method detection limit; and limit of quantitation.

It is hypothesized that these methods can be developed in a simplified manner to accommodate both types of biological matrices and that a single HRAM MS instrument method may be used to analyze both positive and negative mode analytes in a single injection via polarity switching. The primary objectives of this work were (i) to develop an instrument method for identification and quantitation of 10 nitrosatable pesticides and breakdown products using UHPLC/HRAM orbital ion trap MS; (ii) to compare deproteinization, SPE, and QuEChERS methods for extraction of target analytes from human serum and urine; and (iii) to optimize and validate the analytical methods. Various modifications of each sample preparation technique were investigated for maximum analyte recovery.

The suite of analytes chosen for this study is comprised of the following pesticides and metabolites: ATR, CAR, DIM, ETU, IMI, LIN, MCPA, OME, TCPy, and TM. With the exception of MCPA, all of these analytes are capable of forming *N*-nitroso compounds through interaction with nitrite. MCPA, a phenoxy herbicide, was also included in the study because, even though it is not capable of interacting with nitrates to form *N*-nitroso compounds, it is often contaminated with the carcinogenic nitrosamine NDMA [104]. In addition, each analyte is also expected to be a contaminant of concern in Atlantic Canada in terms of toxicity and exposure, based on provincial pesticide sales reports and detections in groundwater samples [60,62,86,149].

2.3 Materials and Methods

2.3.1 Analytical Standards, Solvents, and Reagents

Analytical standards for the following target analytes were purchased individually from Chromatographic Specialties (Brockville, ON, CA): ATR, CAR, DIM, ETU, IMI, LIN, MCPA, OME, TCPy, and TM. Chemical structure and molecular weight of each analyte are summarized in Figure 1-5. Carbendazim-d3 was chosen as the internal standard (IS) and was obtained in neat form from Sigma Aldrich Canada Co. (Oakville, ON, CA). All solvents and reagents used in this study were of HPLC-grade. MeOH, ACN, and ACROS Organics formic acid (>98% pure) were obtained from Thermo Fisher Scientific (Fair Lawn, NJ, US). Human sera (SKU: S7023-50ML), Surine™ Negative Urine Control (SKU: S-020), and AcOH were purchased from Sigma-Aldrich Canada Co. (Oakville, ON, CA). Certified ACS sodium acetate (NaOAc) anhydrous fused crystals, certified $MgSO_4$ anhydrous powder, and certified ACS crystalline sodium chloride (NaCl) were obtained from Fisher Chemical (Fair Lawn, NJ, US). Ultrapure laboratory grade water (Milli-Q water, a resistivity of 18.2 mΩ.cm and a total organic carbon (TOC) of less than 5 $\mu g\ L^{-1}$) was obtained from the Milli-Q plus system (Millipore, Bedford, MA, US). Ultra-high purity nitrogen for sample concentration was obtained from Praxair Canada (Dartmouth, NS, CA). SOLA™ HRP SPE cartridges (10 mg) were obtained from Thermo Scientific (Waltham, MA, US). Oasis HLB (30 mg) and Oasis PRiME HLB (10 mg) SPE cartridges were obtained from Waters (Milford, MA, US).

2.3.2 Sample Preparation Method Development

Sterile frozen liquid human sera (50 mL) and Surine™ Negative Urine Control (50 mL) were chosen as test sample matrices. Stock matrix was allowed to thaw at 4 ºC overnight and was aliquoted in volumes of 1 mL and refrozen. Each experiment batch consisted of three or five test sample replicates (depending on the type of experiment), one post-extraction spike control, and one matrix blank. Three different techniques were evaluated for the extraction of target analytes from biological matrices: deproteinization, SPE and QuEChERS. The optimized sample preparation method was deemed applicable

to the semi-targeted PA*N*N compounds of interest, as the chemical structures of the nitrosatable pesticides are similar to their *N*-nitroso counterparts. For each experiment, 1-mL aliquots of stock matrix were allowed to thaw refrigerated at 4 ºC overnight. Urine sample preparation for targeted analysis used methods optimized for serum as a starting point. A conceptual framework for sample preparation method development for this work is depicted in Figure 2-1.

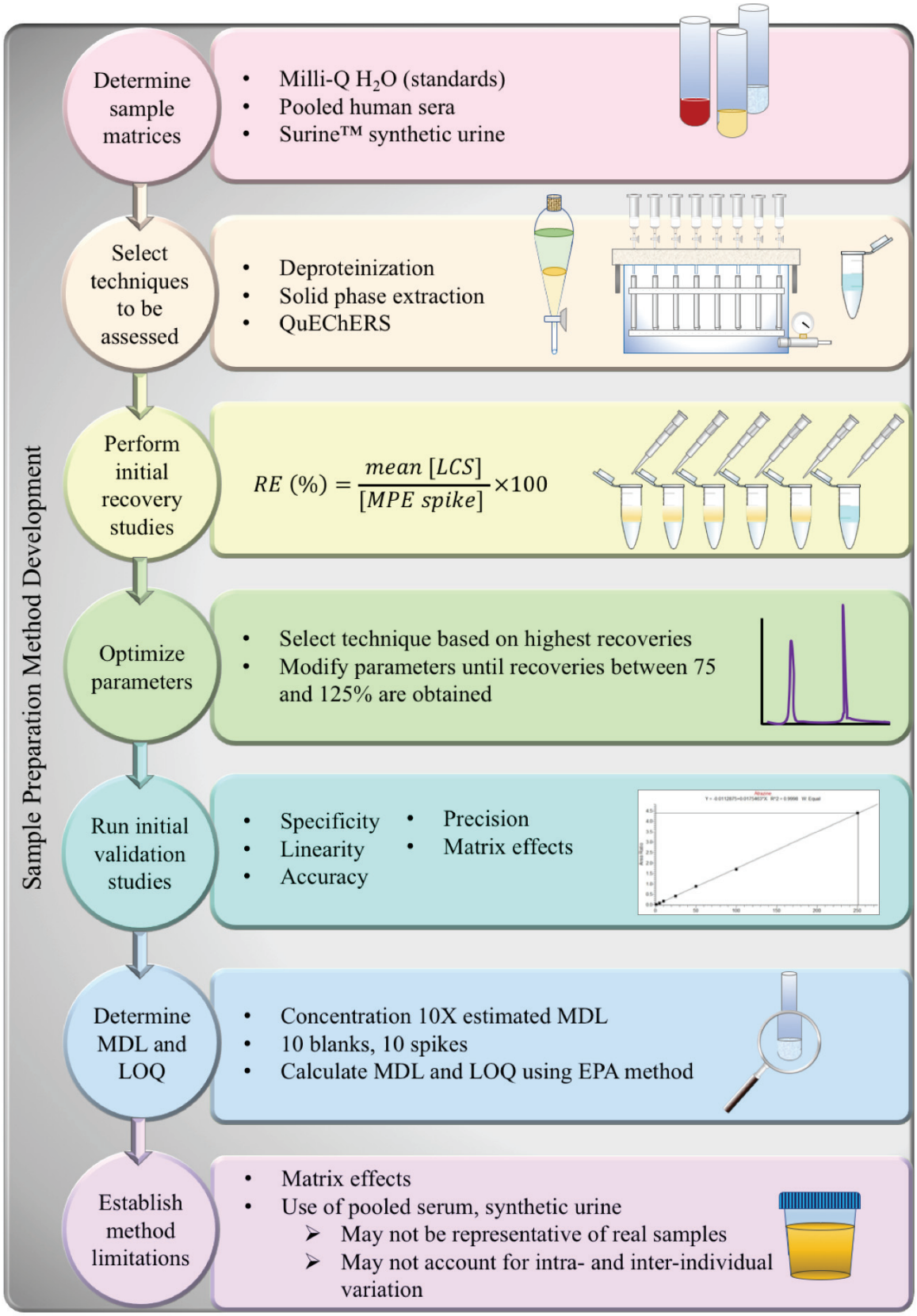

Figure 2-1. Conceptual framework for sample preparation method development.

Deproteinization procedure

Test samples (n=3) were made by adding 900 µL MeOH to 300 µL of stock serum in a 1.5-mL microcentrifuge tube and spiking with target analyte standards and IS to a final concentration of 100 µg L^{-1}. Samples were vortexed for 15 s and then centrifuged at room temperature for 15 min at 15,800 g. A volume of 1110 µL of the supernatant was transferred to a separate 1.5-mL centrifuge tube and evaporated under a gentle nitrogen stream at room temperature using the Reacti-Vap™/Reacti-Therm™. In this study, three different sample preparation methods were applied to compare. One batch of samples was evaporated to dryness and reconstituted in 250 µL of Milli-Q water. These samples were evaporated to dryness to obtain an injection solvent similar to the mobile phase starting conditions. To reduce risk of analyte loss during evaporation, a second batch was evaporated to 125 µL and diluted 1:1 with Milli-Q water and a third batch was evaporated down to 250 µL and left unmodified. Following reconstitution, each test sample was vortexed for 15 s and centrifuged at 4 ºC for 15 min at 15,800 g. A volume of 225 µL of the supernatant was transferred to a 2-mL amber glass autosampler vial fitted with a 400 µL glass insert, resulting in a final extract volume of 225 µL per 300 µL serum sample, and stored at 4 ºC until analysis.

SPE procedure

Samples were prepared by spiking 200 µL serum to 100 µg L^{-1} with target analyte standards and IS in a 1.5-mL microcentrifuge tube and vortexed for 15 s (n=3). Three types of SPE cartridges were tested for optimal analyte retention: SOLA™ HRP (10 mg), Oasis HLB (30 mg), and Oasis PRiME HLB (10 mg). Generic methods for sample pre-treatment, as described by the manufacturers, varied with SPE cartridge type. For the SOLA™ HRP cartridges, 0.1% (v/v) aqueous formic acid was added up to 400 µL after the addition of standards. For the Oasis HLB and PRiME HLB cartridges, serum was diluted 1:1 with 4% (v/v) aqueous phosphoric acid and spiked with standards following acidification for a total test sample volume of 650 µL. All samples were shaken vigorously by hand for 1 min, vortexed for 15 s, and then centrifuged at 4 ºC for 15 min at 15,800 g.

The SOLA™ HRP cartridges were conditioned with 500 µL MeOH and then equilibrated with 500 µL Milli-Q water. For each sample, the entire serum supernatant was loaded onto the cartridge followed by a wash volume of 500 µL 95 %:5 % Milli-Q water:MeOH solution. All cartridges were then eluted with 200 µL MeOH with 0.1% (v/v) aqueous formic acid followed by 200 µL Milli-Q water for a 1:1 dilution. The Oasis HLB cartridges were conditioned with 500 µL MeOH and then equilibrated with 500 µL Milli-Q water. The entire serum supernatant was loaded onto the cartridge followed by a wash volume of 500 µL Milli-Q water. The cartridge was then eluted with 500 µL MeOH followed by 200 µL Milli-Q water for a 1:1 dilution. The Oasis PRiME HLB cartridges need neither conditioning nor equilibration. The entire serum supernatant was loaded onto the cartridge followed by a wash volume of 500 µL Milli-Q water. The cartridge was then eluted with 500 µL MeOH followed by 200 µL Milli-Q water for a 1:1 dilution. For each SPE sorbent trial, final extract volume was 400 µL per 200 µL serum. All extracted samples were stored at 4 ºC until analysis.

QuEChERS procedure

Serum and Surine™ test samples were prepared for QuEChERS by vortexing 1-mL aliquots for 15 s and transferring 500 µL of sample matrix to 1.5-mL microcentrifuge tubes. Test samples (n=3) were spiked to a final concentration of 100 µg L^{-1} with target analyte standards and IS and vortexed for an additional 15 s. To each tube, 500 µL of extraction solvent (100% ACN, or 0.1%, 0.5%, 1%, or 4% AcOH in ACN) were added and samples were shaken vigorously by hand for 1 min. One of three premade QuEChERS salt mixtures (250 mg $MgSO_4$ only, 200 mg $MgSO_4$ + 50 mg NaOAc, or 200 mg $MgSO_4$ + 50 mg NaCl) was added to the sample to facilitate phase separation and extraction of target analytes. Samples were vortexed for 15 s to break up salt agglomerates and shaken vigorously by hand for 1 min. In some trials, the samples were sonicated for either 15 or 30 min. All samples were centrifuged at 4 ºC for 15 min at 15,800 g. A volume of 200 µL of the supernatant was transferred to a labelled autosampler vial, diluted 1:1 with Milli-Q water (for a final extract volume of 400 µL per 500 µL sample), vortexed for 15 s, and stored at 4 ºC until analysis.

Instrumentation

The Thermo Scientific Accela UHPLC system with the CTC Analytics PAL autosampler coupled to the Exactive Plus orbital ion trap mass spectrometer was used for all sample analyses. The Exactive Plus was programmed to employ "polarity switching", a feature that allows one full positive mode scan and one full negative mode scan in under a second, resulting in the acquisition of data from both ionization modes in a single data file. In general, positive ionization mode results in the protonated $[M+H]^+$ parent ion while negative mode ionization generates the deprotonated $[M-H]^-$ molecule [150]. Data analysis was performed using Thermo Scientific *Xcalibur* and *Tune* software. SPE was performed using the EluVac™ vacuum manifold (LCTech GmbH, Dorfen, Germany). Samples were concentrated using the Thermo Scientific Reacti-Vap™ III 27-port evaporator (TS-18826) and Reacti-Therm™ III triple block (TS-18824) heating module ensemble. Centrifugation was done using the Thermo Scientific Sorvall™ Legend™ X1R (75004261) centrifuge and salts were weighted on a Denver Instrument P-114 analytical balance (Bohemia, NY, US). A conceptual framework for each segment of instrument method development specific to this work is depicted in Figure 2-2.

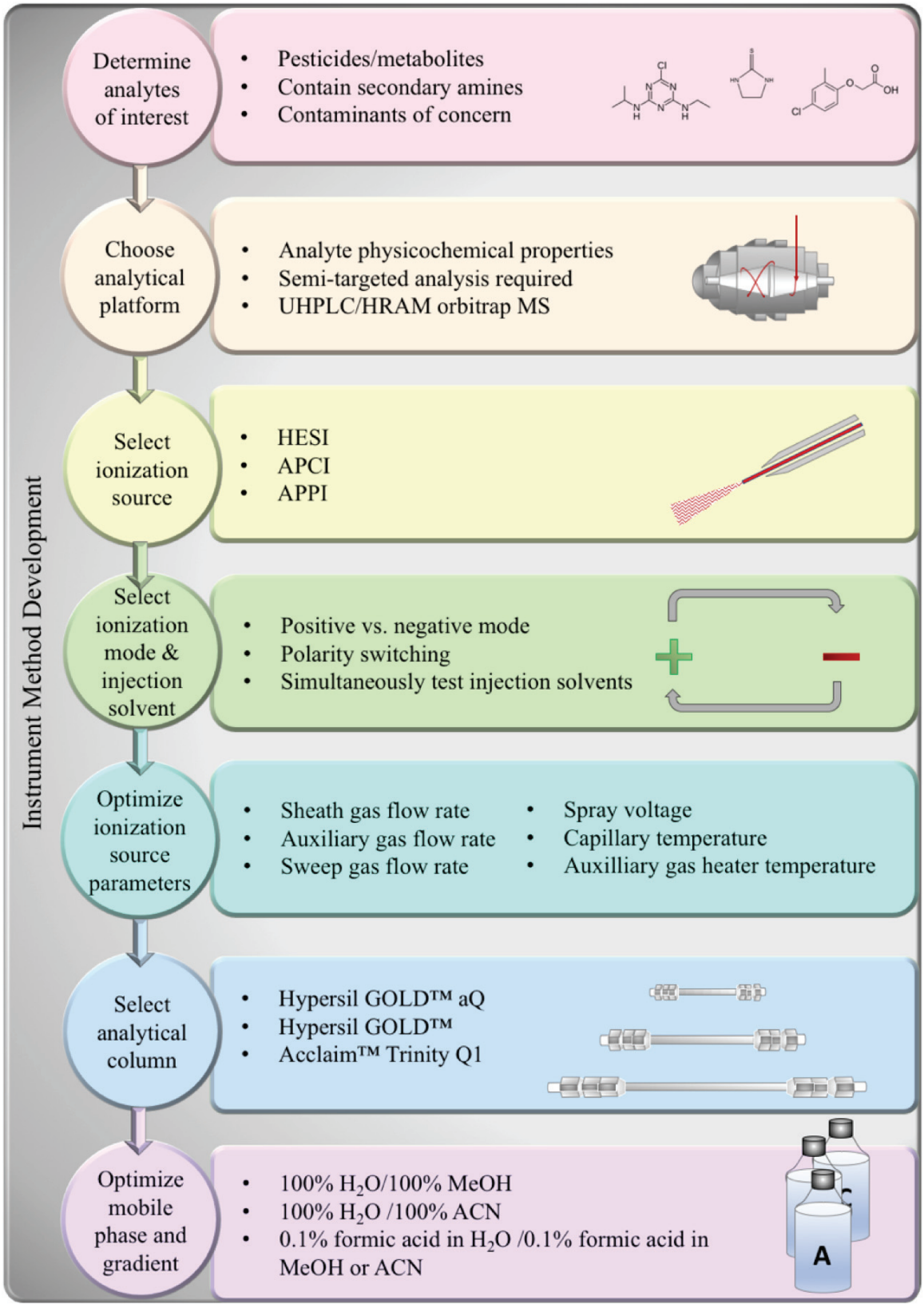

Figure 2-2. Conceptual framework for instrument method development.

UHPLC/orbital ion trap MS analysis

UHPLC separation was carried out using a Thermo Scientific Hypersil GOLD™ C18 analytical column (50 mm x 2.1 mm, 1.9 µm particle size) with a mobile phase flow rate of 400 µL min^{-1}. Mobile phase Solvent A consisted of 100 % Milli-Q water and Solvent B was 100 % MeOH. Solvent A began at 100 % and was held for 1 min. From min 1 to 7, Solvent B was increased to 100 % and held for 1 min. Minutes eight to 15 show a decrease of Solvent B back down to 0 % and 100 % Solvent A was pumped for the remaining two min of the run for a total run time of 17 min. The autosampler tray held samples at 4 ºC.

Standard solutions of each analyte were injected separately in both positive and negative HESI modes to determine which ionization mode results in a higher signal for each analyte. HESI source parameters, which were optimized based on UHPLC flow rate, were set to the following values: sheath gas flow rate, 50 au; auxiliary gas flow rate, 13 au; sweep gas flow rate, 0 au; spray voltage, 3.50 kV; capillary temperature, 263 ºC; S-lens RF level, 60.0 au; auxiliary gas heater temperature, 425 ºC. The MS scan parameters were set to the following values: scan type, full MS/all ion fragmentation (AIF); *m/z* range, 55-800 m/z; resolution, 70,000; automatic gain control target, 3e6; maximum inject time (IT), 200 ms; and collision energy, 20 eV.

Method validation

Initial recovery experiments conducted to assess the most efficient sample preparation technique were carried out using replicates of three. Mean recovery values with standard deviation (SD) were calculated. To assess the efficacy of each approach, recovery efficiency (RE (%)) was determined using Eq. (1).

$$RE\ (\%) = \frac{mean\ test\ sample\ concentration}{matrix\ post{-}extraction\ spiked\ control\ concentration} \times 100 \qquad (1)$$

Recovery efficiency of the most effective extraction method was evaluated by assessing analyte recoveries of test sample replicates (n=5) at two different concentrations (25 and 50 µg L^{-1}) and reported as %RSD of mean analyte peak area. Process efficiency (PE (%)) of the optimized extraction method for each sample matrix was determined using

five replicates at two different analyte concentrations, 25 and 50 µg L^{-1}, and calculated for each analyte using Eq. (2).

$$PE\ (\%) = \frac{mean\ test\ sample\ concentration}{concentration\ of\ spiked\ controls} \times 100 \qquad (2)$$

Intra-day precision was evaluated at 50 µg L^{-1} (n=3) by repeating the extraction procedure twice within a 24-hour period. Inter-day precision was evaluated at 50 µg L^{-1} and spiked samples (n=3) were analyzed daily for a period of three consecutive days.

Matrix effects are characterized by the occurrence of ion suppression or enhancement due to the presence of a matrix or interferences in the sample. The absolute matrix effect (ME (%)) was calculated for each analyte at three different analyte concentrations (10, 25, and 50 µg L^{-1}) by entering the values obtained for the post-extraction spike concentration and spiked control concentration into Eq. (3).

$$ME\ (\%) = \frac{matrix\ post{-}extraction\ spiked\ control\ concentration}{spiked\ control\ concentration} \times 100 \qquad (3)$$

The method detection limit (MDL) was determined in each sample matrix (rather than in pure solvent) using the US EPA procedures outlined in *Definition and Procedure for the Determination of the Method Detection Limit, Revision 2* [151]. First, MDLs were estimated to be around 1 µg L^{-1} from previously determined quantitation limits for several target analytes [81]. A concentration ten times this estimate (10 µg L^{-1}) was used to experimentally determine MDLs for each analyte. Ten spiked samples and 10 method blank samples were processed through all steps of the method (three test samples per day over two days and four on the third day) and analyzed. MDLs for each analyte in spiked samples and method blanks were then calculated; the greater of the two determined for each analyte represented the MDL. The limit of quantitation (LOQ) was calculated as ten times the SD of the 10 replicate spiked sample measurements.

For specificity and linearity, the molecular formula for each target analyte was entered into the *Tune* software's *Mass Calculator* to calculate theoretical *m/z* value of ions generated in both positive and negative ionization modes. Standards of target analytes were injected individually, and the theoretical *m/z* values were extracted from the resulting

chromatograms. Compound identification was confirmed by matching theoretical and experimental *m/z* values from the mass spectrum at each chromatographic peak corresponding to the target analyte (within 5 parts per million). Chromatographic peaks of each analytical standard for target compounds and IS (Figure 2-3) were further identified by retention time (t_r) (Table 2-1).

To assess linearity, Milli-Q water was spiked with a master mix containing all target analytes at seven different concentrations: 1, 5, 10, 25, 50, 100, and 250 μg L^{-1}. Each calibration level was also spiked with IS at a concentration of 100 μg L^{-1} for internal calibration. A calibration curve was generated for each analyte and linearity was evaluated using the correlation coefficient (R^2). A more detailed version of analytical method development can be found in Appendix A.

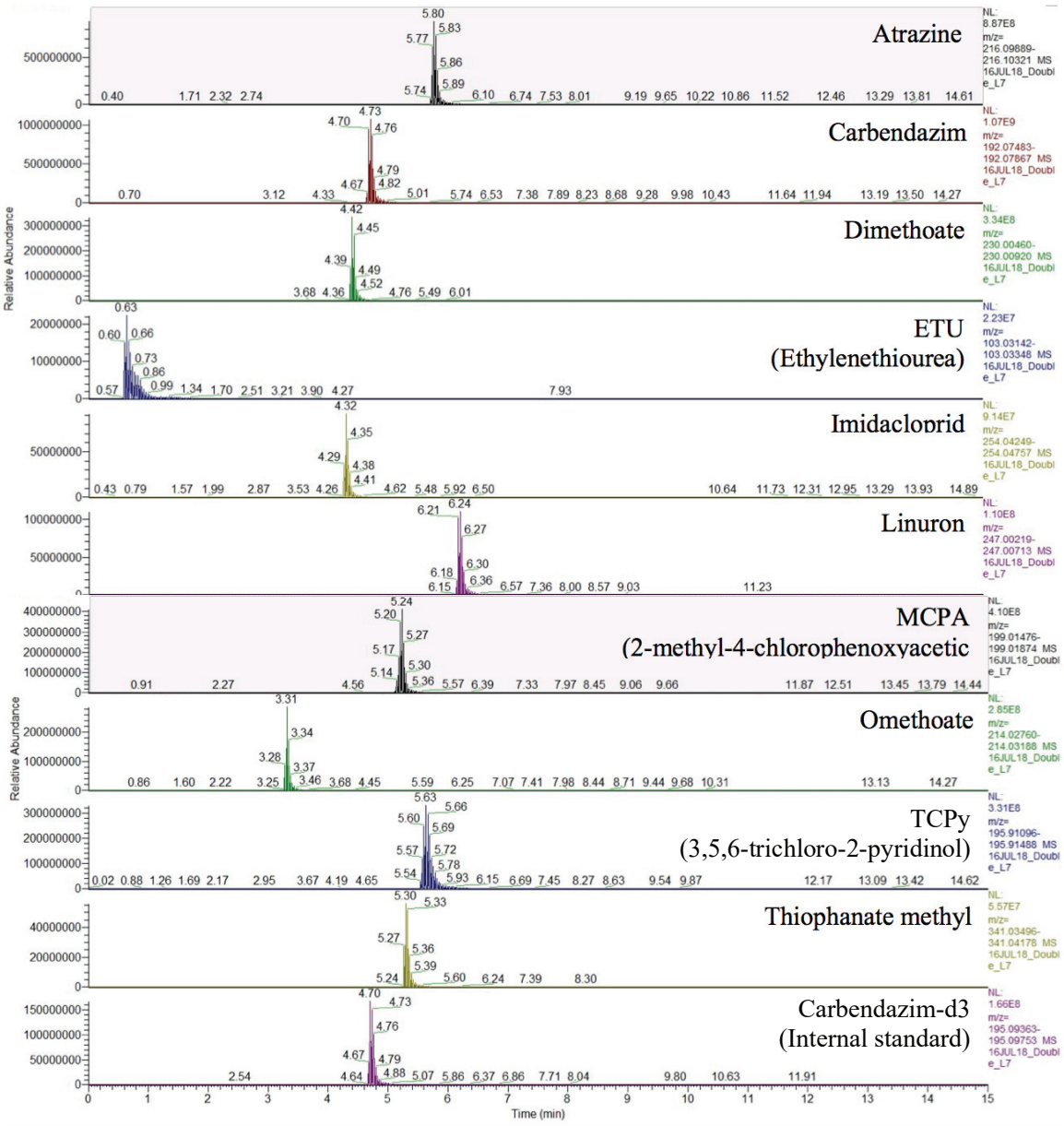

Figure 2-3. Representative chromatogram of a standard mixture of 10 target analytes and IS. Peaks were displayed by extracting the *m/z* values generated by the Exactive Plus Tune software.

Table 2-1. Theoretical *m/z* values extracted from chromatograms, ionization mode (positive, +, or negative, –), retention times (t_r), and R^2 values for seven-point calibration curves for each analyte. LOQ and MDL are given for each analyte in both biomatrices.

Analyte[a]	Theoretical mass (*m/z*)	Ionization mode	t_r (min)	R^2	Serum		Urine	
					LOQ[b] (µg L^{-1})	MDL[c] (µg L^{-1})	LOQ (µg L^{-1})	MDL (µg L^{-1})
ATR	216.10105	+	5.80	0.9998	4.1	1.4	5.8	1.9
CAR	192.07675	+	4.73	0.9999	1.8	0.6	2.3	0.8
DIM	230.00690	+	4.42	0.9999	7.4	2.5	9.2	3.1
ETU[d]	103.03245	+	0.63	0.9992	9.5	2.7	8.7	2.6
IMI	254.04503	–	4.32	0.9991	9.7	3.2	5.9	2.0
LIN	247.00466	–	6.24	0.9996	4.3	1.4	13.1	4.4
MCPA	199.01675	–	5.24	0.9994	6.7	2.2	3.7	1.2
OME	214.02974	+	3.31	0.9997	3.5	1.2	1.7	0.6
TCPy	195.91292	–	5.63	0.9999	8.1	2.7	6.7	2.2
TM[e]	341.03837	–	5.30	0.9992	9.9	3.3	20.4	6.8
CAR-D3*	195.09558	+	4.70	---	---	---	---	---

*Internal standard, carbendazim-d3

[a]ATR = atrazine; CAR = carbendazim; DIM = dimethoate; ETU = ethylenethiourea; IMI = imidacloprid; LIN = linuron; MCPA = 2-methyl-4-chlorophenoxyacetic acid; OME = omethoate; TCPy = 3,5,6-trichloro-2-pyridinol; TM = thiophanate methyl

[b]LOQ = limit of quantitation

[c]MDL = method detection limit

[d]A four-point calibration curve comprised of standards at the lowest ETU concentrations was used to determine LOQ and MDL for ETU in serum and urine because even slight changes in the calibration curve caused by incorporating points at high concentrations can affect quantitation at low concentrations.

[e]After calculating LOQ and MDL values for TM in both serum and urine using the EPA method, values for these parameters from blanks were higher than those from spiked levels and were therefore chosen as LOQs and MDLs.

2.4 Results and Discussion

2.4.1 Recovery Efficiency of Target Analytes Extracted from Serum and Urine

Three different sample preparation techniques were evaluated for the extraction of a suite of nitrosatable pesticides and byproducts from serum: deproteinization, SPE, and QuEChERS. Serum was chosen as the starting biomatrix for method development because it is more complex than urine [129]. The aim was to overcome extraction issues encountered from a higher concentration of interfering sample constituents in serum early in the method development process, making the adaptation to urine sample preparation method development more straightforward.

Recovery of target analytes from serum

Due to excessive ion enhancement of some target analytes and the absence of response for others, the deproteinization method was deemed unsuitable for targeted analysis of this suite of compounds in serum and was therefore not evaluated for urine analysis. Results of the serum deproteinization experiments are shown in Figure 2-4a. SPE recoveries of target analytes were better than those from the deproteinization method in serum (Figure 2-4b). Oasis PRiME HLB performed the best of all three cartridges with recoveries between 91 and 120% for eight target compounds: ATR, CAR, DIM, IMI, LIN, OME, TCPy, and TM. However, recoveries of ETU and MCPA from serum remained below 10%. ETU's relatively small molecular structure and polarity (log K_{OW} -0.66) [152] indicate that it is unlikely to be retained by nonpolar sorbents. For MCPA, analyte loss may be due to serum protein-binding. Chlorophenoxy herbicides, such as MCPA, bind extensively to albumin [153,154]. A study involving intentional self-poisoning with MCPA showed that the acidic pesticide bears protein-binding sites, one with an extremely high affinity [155]. Moreover, sample pre-treatment with 4% (v/v) aqueous phosphoric acid (Oasis HLB and PRiME HLB cartridges) rather than 0.1% (v/v) aqueous formic acid (SOLA™ HRP) may be more effective for deproteinization of some compounds, reducing the amount of serum protein-bound analyte and increasing analyte recovery. The QuEChERS technique resulted in the best recoveries for a majority of the target compounds

in serum. Results of the six QuEChERS method modifications are summarized in Figure 2-4c. Overall, 4% AcOH in ACN using the buffered QuEChERS protocol with a 15-min sonication step resulted in recoveries for all target analytes between 74 (ETU) and 120% (DIM).

Recovery of target analytes from urine

The buffered QuEChERS method using 4% AcOH in ACN and 4:1 $MgSO_4$:NaOAc salt mix) and a 15-min sonication step was used as a starting point for urine sample preparation method development. All analyte recoveries were between 91 and 104% except ETU, which showed a recovery of 55%. As shown in Figure 2-4d, several modifications of this protocol did not result in significant changes in analyte recoveries. Finally, by reducing the strength of AcOH in ACN from 0.5 to 0.1% while keeping the 4:1 $MgSO_4$:NaCl salt mix, all analyte recoveries were between 96% (OME) and 116% (IMI).

The deproteinization method, applied in studies involving large-scale metabolic profiling of serum and plasma [129], is better suited for analysis of non-targeted compounds when identification (rather than quantitation) is a priority. It has been demonstrated here that this technique does not perform well on a semi-targeted analysis platform, as ion enhancement and complete loss of analytes impede recovery and quantitation of target compounds. Furthermore, the SPE method was not chosen for optimization and validation because recoveries from the first SPE trials did not surpass those of the QuEChERS approach. However, the SPE protocol used in this study was the generic method suggested by the manufacturer as a starting point and could have been modified to attain better recoveries for this suite of analytes by optimizing method parameters.

During the optimization of the QuEChERS methods for biomatrices, trends in method performance were observed. In serum, it became clear that buffering was necessary and that the concentration of AcOH in ACN needed to be greater than in the original buffered QuEChERS method to adequately extract this suite of analytes. In urine, it was observed that neither the buffered nor original method was ideal for extraction of all analytes. However, a compromise of a low concentration of AcOH in ACN (0.1%) and the original salt mix proved to be best suited for extraction of these target analytes in urine.

Interestingly, the addition of a 15-minute sonication step to the QuEChERS method in this case appeared to increase the recovery of analytes that were difficult to extract. Due to the best performance and several advantages of the QuEChERS method, it was selected for further optimization and validation.

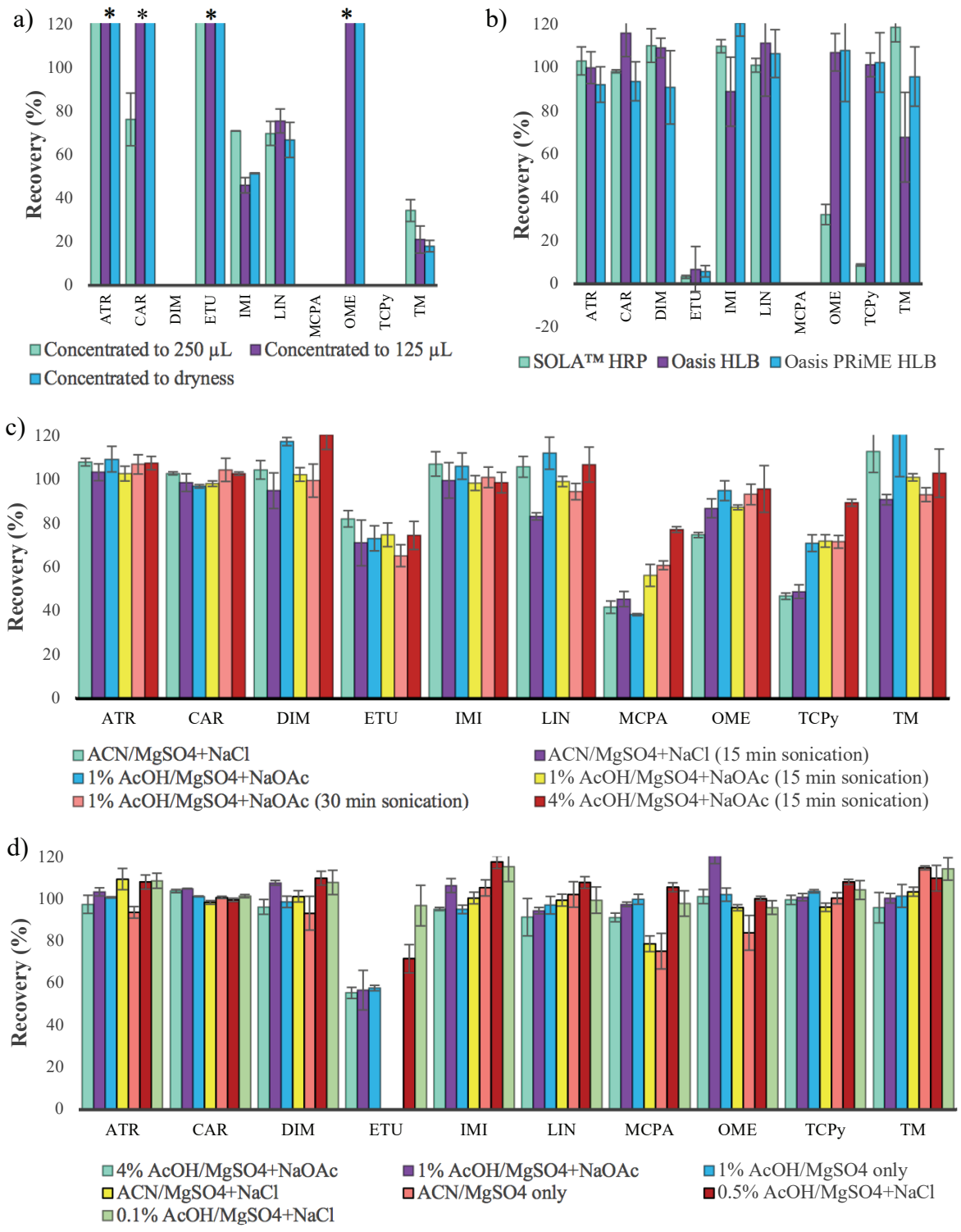

*Compounds with recoveries greater than 125%; error bars not shown if SD > 100%.

Figure 2-4. Recovery (%) of each target analyte extracted from a) serum, via the deproteinization approach; b) serum, by SPE; c) serum, using QuEChERS; and d) urine, via QuEChERS procedure (n = 3).

2.4.2 Analytical Method Validation Procedures

Analytical performance characteristics evaluated for the QuEChERS methods optimized for extraction of target analytes in serum and urine include specificity, linearity, accuracy (recovery and process efficiencies), precision (intra-day precision, and inter-day precision), matrix effects, MDL, and LOQ. Determination of the recovery and process efficiencies, and matrix effects in quantitative bioanalytical methods using HPLC-MS has been detailed by Matuszewski *et al*. (2003) [156] and adapted for this study.

Analytical method performance

Accuracy was generally consistent across sample preparation methods for both serum and urine and at both spike levels (n=5) for ATR, CAR, DIM, IMI, LIN, and TM, with PE ranging from 74 and 135% and RE between 94 and 114% (Table 2-2). For serum ETU, PE was 33 and 36% for 25 and 50 µg L^{-1} spike levels, respectively, while RE decreased from 78 to 55 % at the lower spike concentration. Urine ETU PE values were much lower at 11 and 24% for 25 and 50 µg L^{-1} spike levels, respectively. In contrast to RE for the serum method, better recovery was observed at the higher spike concentration (85%) than at the lower level (52%). However, %RSD for RE at the higher concentration was 26%. Both PE and RE remained between 48 and 54% for MCPA extraction from serum while better method performance was observed for the analyte in urine test samples with PE and RE values between 84 and 97%. PE for OME was higher for serum samples (70 and 86%) compared to that in urine samples (59 and 63%) while RE remained within 90 and 103% for this analyte in both methods. TCPy PE and RE in serum test samples were between 58 and 65%, while accuracy was much better for extraction of the analyte for the urine method with parameters for both spike concentration levels between 95 and 100%. The %RSD was below 20% for all experiments except for recovery of ETU in urine test samples at 50 µg L^{-1}.

Table 2-2. Serum and urine method process efficiency, recovery efficiency, and %RSD (n=5).

Analyte	Spike level (µg L^{-1})	Serum			Urine		
		PE[a] (%)	RE[b] (%)	RSD[c] (%)	PE[a] (%)	RE[b] (%)	RSD[c] (%)
ATR	25	104	104	4	104	107	5
	50	94	99	2	115	102	6
CAR	25	100	98	4	101	101	3
	50	97	99	2	100	99	1
DIM	25	97	107	4	112	99	4
	50	95	100	2	133	106	8
ETU	25	33	78	11	11	52	15
	50	36	55	8	24	85	26
IMI	25	101	100	4	80	101	2
	50	91	92	2	76	104	19
LIN	25	78	101	5	92	94	4
	50	74	95	3	89	101	15
MCPA	25	54	51	7	84	90	2
	50	48	48	5	88	97	8
OME	25	86	100	5	59	90	2
	50	70	90	3	63	103	3
TCPy	25	58	65	6	97	95	4
	50	63	64	4	95	100	14
TM	25	135	104	3	107	98	3
	50	108	94	2	93	114	14

[a]PE = Precision efficiency; [b]RE = Recovery efficiency; [c]RSD = relative standard deviation

Overall, good precision was obtained for all target analytes across both sample matrix types for intra-day and inter-day precision assessments at 50 µg L^{-1} spike (n=3). Values for RSD were <10% for 36 of 40 precision experiments (90%) with only one trial resulting in a RSD value over 20% (ETU intra-day precision RSD for serum method, 20.6%) (Table 2-3).

Table 2-3. Serum and urine matrix effects at 10 and 50 µg L^{-1} spike levels and intra- and inter-day precision at 50 µg L^{-1} spike level (n=3).

Analyte	Serum				Urine			
	ME (%)[a]		Intra-day precision (%RSD)	Inter-day precision (%RSD)	ME (%)		Intra-day precision (%RSD)	Inter-day precision (%RSD)
	10 µg L^{-1}	50 µg L^{-1}			10 µg L^{-1}	50 µg L^{-1}		
ATR	101	102	2	3	110	103	4	3
CAR	102	102	<1	1	105	101	<1	<1
DIM	92	100	2	1	115	113	3	5
ETU	36	79	9	21	9	28	<1	15
IMI	95	98	8	2	89	84	4	6
LIN	80	78	6	4	93	97	6	9
MCPA	103	104	7	2	95	93	1	3
OME	79	90	4	4	68	62	1	1
TCPy	86	95	5	2	102	95	<1	<1
TM	115	106	1	11	139	104	2	19

[a]ME (%) = absolute matrix effect

Matrix effects were assessed using Eq. (3) with values less than 100% indicating ion suppression, ME (%) >100 indicating ion enhancement, and ME (%) of 100 denoting no observable matrix effects. For post-extraction spike levels 10 and 50 µg L^{-1}, three replicates were used for each spike level. Most ME (%) values fell between the range of 80 and 120%. The strongest matrix effects were observed for ETU, increasing from 36 to 79% with spike concentration in the serum test samples and from only 9 to 28% in urine test samples. Minimal but consistent matrix effects were detected with LIN in the serum test samples with ME (%) values ranging from 78 to 80%; LIN did not appear to be affected by urine matrix. In contrast, greater matrix effects were observed in urine than serum for OME, with ME (%) values ranging between 62 and 68% in urine and increasing from 79 to 90% in serum. Only TM showed notable ion enhancement with a ME (%) value of 139% at a concentration of 10 µg L^{-1} spike in urine (n=3).

LOQ values are <10 µg L^{-1} for all analytes in both matrices except for LIN and TM, which have LOQ values of 13.1 and 20.4 µg L^{-1}, respectively, in urine. The lowest LOQ in serum and urine was achieved for CAR (1.8 µg L^{-1}) and OME (1.7 µg L^{-1}), respectively. MDLs were <1 µg L^{-1} for CAR (serum and urine) and OME (urine) and between 1 and 4.4

μg L^{-1} for all remaining analytes in both matrices except for TM, which had an MDL value of 6.8 μg L^{-1} for urine.

2.5 Conclusions

This work demonstrates that a simple and cost-effective QuEChERS method resulted in highest recovery efficiencies of three sample preparation techniques assessed for the extraction of a diverse group of nitrosatable pesticides and byproducts from serum. After further optimization for serum and urine analysis, the method resulted in satisfactory analyte recoveries for a majority of the target analytes. Furthermore, most analytes showed minimal matrix effects (between 80 and 120%) in both biomatrices. Analytes that appeared to be most affected by the biomatrices were ETU in both serum and urine and OME in urine. While it may not be feasible to reduce or eliminate matrix effects, it is imperative that they are identified and quantified [157].

One of the potential limitations of this study is that this method was developed and validated using a pooled human serum sample (from an unknown number of male donors) and synthetic urine. These matrices may not accurately represent serum and urine from each individual in a future study. Due to intra- and inter-individual variations in serum and urine composition, the parameters of this method (i.e. recovery efficiency, matrix effects, etc.) may vary during analysis of real samples. Another limitation of this study, which is evident in the degree of matrix effects for ETU, is that only one isotopically-labeled IS was used to represent all ten target analytes, even though they present a wide range of physicochemical properties. While a deuterated ETU IS would greatly diminish matrix effects for ETU, future studies should also consider further optimization of the method for an overall greater process efficiency for this analyte. Ultimately, these validated sample preparation methods add to the growing range of applications for the QuEChERS method, advantageous due to its simplicity, efficiency, cost-effectiveness, and safety.

Chapter 3: *N*-nitrosoethylenethiourea formation at environmentally-relevant concentrations of ethylenethiourea in a pooled groundwater sample

3.1 Abstract

N-nitroso compounds form from the interaction between nitrosatable precursors and nitrite under acidic conditions. A majority of the more than 300 *N*-nitroso compounds are carcinogenic in animal models. Most research on the formation of pesticide-associated *N*-nitroso (PA*N*N) compounds involve high pesticide concentrations that are not typically found in groundwater. In this work, nine nitrosatable pesticides and degradation products were individually reacted at environmentally-relevant concentrations with sodium nitrite ($NaNO_2$) and hydrochloric acid (HCl) in water at to assess PA*N*N compound formation. Analysis of target compounds and predicted PA*N*N compounds was performed using UHPLC/HRAM MS. At initial analyte and $NaNO_2$ concentrations of 20 µg L^{-1} and 2.5 mg L^{-1}, respectively, four experimental conditions were tested: (i) pH 2.62 ± 0.10; (ii) pH 5.02 ± 0.21; (iii) pH 2.22 ± 0.09 with dissolved copper (Cu) at 50 µg L^{-1}; and (iv) pH 2.00 ± 0.08 with dissolved iron (Fe) at 50 µg L^{-1}. Only ethylenethiourea (ETU) showed evidence of PA*N*N compound formation and only under conditions i, iii, and iv. *N*-ETU formation was assessed in a pooled groundwater sample collected from an agricultural region of Prince Edward Island, where nitrate contamination is a known concern. Evidence of *N*-ETU formation in the groundwater sample was observed within 30 minutes at concentrations 20, 10, and 7.5 µg L^{-1}, but not at 5 µg L^{-1}. HRAM technology confirmed in-house synthesis of *N*-ETU with a molecular ion ($[M+H]^+$) *m/z* value of 132.02252 (0.7 ppm mass error) and a retention time of 1.22 ± 0.04 minutes. ETU is recognized by the U.S. EPA as a Group B Probable Human Carcinogen. The results of this study suggest that ETU is capable of forming the potentially carcinogenic *N*-ETU at environmentally relevant concentrations at pH values comparable to that of gastric pH. Based on these findings, it is believed that endogenous *N*-ETU formation may be a concern for individuals exposed to low concentrations of ETU.

Keywords: pesticide-associated *N*-nitroso (PA*N*N) compounds, UHPLC/HRAM orbitrap MS, *N*-nitrosoethylenethiourea, *N*-nitrosoatrazine, groundwater.

3.2 Introduction

PEI is one of the most intensely farmed provinces in Canada, having over 40% of its total land mass cleared for agriculture [158]. Pesticides used in PEI crop production can leach into the highly permeable sandstone aquifer, contaminating the sole source of drinking water for the island's residents [61]. Generally, the extent of groundwater contamination and movement of pesticides in any groundwater flow system depends on many factors including the framework of the location (e.g. soil type, the presence of confining layers in an aquifer, weather patterns, and hydraulic conductivity (K), the measure of a soil's ability to transmit water), physicochemical properties of pesticides, presence of buffer zones created by forests, and farming intensity [46,159–163].

The famous red soil of PEI is predominantly Charlottetown soil, characterized as well-drained, sandy, rich in iron-oxide, and ideal for farming [164]. It covers an unconfined/semi-confined fractured-porous sandstone aquifer [63]. Field soil experiments conducted at the Agriculture and Agri-Food Canada's Harrington Experimental Farm near Charlottetown, PEI on the metre-thick surface soil have shown that ground surface K is over one order of magnitude greater than at the lower soil level and that K measurements from laboratory matrix core samples are lower (mean K value of 10^{-7} m s^{-1}) than those observed in field pumping tests (K values between 10^{-6} and 10^{-4} m s^{-1}) [165]. These finding implicate fractures rather than the matrix in dominating control of groundwater flow in the aquifer, which means that water and its dissolved pollutants can be transported very rapidly both in the saturated zone and at times in the unsaturated zone (i.e. following a significant precipitation event when unsaturated zone fractures may become temporarily saturated).

Pesticides are more likely to be present in shallow groundwater and in areas where soil permeability and K are the greatest [166,167]. Pesticide transport to groundwater occurs when rainfall or irrigation, or both, results in groundwater recharge [168]. Pesticides applied to the land surface can infiltrate the soil and traverse the underlying vadose zone (also known as the unsaturated zone) to the water table; as such, groundwater pesticide concentrations fluctuate as the groundwater levels rise and fall throughout the year [166].

In contrast to pesticide transport in streams, dissolved forms of pesticides and environmental breakdown products travel substantial distances in groundwater, as particle-bound pesticides are more likely to be retained by the soil [169].

Groundwater and surface water are interactive components of the hydrologic system and, consequently, contamination of one commonly affects the other [170]. For example, a 2007 study of groundwater contribution to surface water contamination of problematic nutrients and heavy metals in a region with intensive agricultural land use in The Netherlands found that groundwater was a dominant source of surface water contamination [171]. This example demonstrates the role of groundwater as a transporter of chemicals into discharge areas. In contrast, contaminants from surface water can be incorporated into nearby groundwater regions through induced recharge, a process in which groundwater pumping stress induces infiltration of surface water into the formation and supplements the groundwater resource [172]. Induced recharge occurs when pumping stress lowers the water table below the water level in the nearby surface water. Due to the dynamic relationship between surface water and groundwater, movement of pesticides in groundwater is difficult to characterize because groundwater flow is often unpredictable and elaborate.

For decades, western PEI surface waters have been notorious for agricultural pollution. Mill River, a West Prince County estuary, has been plagued by several eutrophication events. In 2002, Martec Limited constructed a report for the Mill River Watershed Roundtable on a modelling study that was launched to identify sources of eutrophication episodes, determine relative contributions of each and, ultimately, present recommendations to restore the river's ecosystem [67]. Agricultural land use was found to be the largest contributor of nitrogen to the Mill River estuary. Over the last few decades, nitrate levels have more than doubled in Mill River and this trend of increasing nitrate concentrations correspond to an increase in row crop production in the watershed [173].

Further evidence of PEI's vulnerable surface water is the number of fish kills that have occurred in recent years. Between 1995 and 1999, PEI endured 12 fish kills purportedly caused by pesticide contamination [174]. In December 2018, the Government of PEI published an online information resource entitled, "*Fish Kill Information and Statistics*" that allows the public to review details of 51 fish kills reported in the last 56

years on PEI linked to pesticides [65]. In her informative briefing on fish kills to the Prince Edward Island Legislative Assembly in September 2017, Kate MacQuarrie (Provincial Director of Forests, Fish and Wildlife) described a number of interventions aimed at preventing the occurrence of fish kills, including the following: (i) buffer zones larger than the 15 m minimum required by legislation; (ii) soil conservation practices and erosion control structures, some of which are supported by the Alternative Land Use Services program; (iii) retirement of high risk fields; (iv) use of lower risk pesticides and restriction of high risk pesticides; and (v) partnerships between government, industry, producers and watershed groups to assist in implementing these changes [66].

Groundwater vulnerability to pesticide and nitrate pollution is also a concern in PEI. Groundwater beneath two PEI potato fields was periodically tested for nitrate and aldicarb, a highly toxic pesticide, between the years of 1985 to 1988; the oral median lethal dose (LD_{50}, the amount of a substance that kills 50% of a test animal model population within a short duration) for aldicarb is 0.9 mg kg^{-1} in rats [61]. Aldicarb concentrations exceeded the drinking water guideline of 9 µg L^{-1} in 12% of all samples and nitrate levels in 32% of the samples exceeded the drinking water guideline of 10 mg L^{-1}. Although aldicarb was voluntarily withdrawn from potato production in 1990 [175], the pesticide was detected in PEI's sandstone aquifer more than two years after its last application [176]. The PEI government has also detected trace levels of several pesticides, including ATR (0.03 to 0.65 µg L^{-1}), DIM (0.1 µg L^{-1}), IMI (0.02 to 0.31 µg L^{-1}), and TM (0.01 to 0.55 µg L^{-1}, with all detections reported for the 2017 sampling year), through their provincial pesticide monitoring program, which involves the analysis of groundwater (in January or February of each year) from over 100 drinking water wells of private homes, schools, municipalities, and seniors' housing facilities [62]. While the island's cool, sandy and well-drained soils make the province ideal for potato production, the aquifer is highly vulnerable to pesticide contamination [61].

A largely overlooked concern involving the contamination of PEI groundwater is that nitrosatable pesticides and byproducts (including several of those detected in PEI groundwater) may interact with nitrite present in groundwater to form *N*-nitroso products in the presence of gastric acid [12,50]. There exist hundreds of *N*–nitroso compounds, a majority of which are potent carcinogens [15–17]. However, most research involving the

formation of PA*N*N compounds experiment with high initial pesticide concentrations that are not typically found in groundwater [45,50,82–85].

N-nitroso compounds are known to form favourably in acidic media where conversion of nitrite to nitrous acid facilitates nitrosation [12]. The formation of *N*-nitroso compounds may be catalyzed by metal ions such as Cu (II), Fe (II), manganese (Mn) (II), and nickel (Ni) (II) [177]. It has also been observed that nitrosation of secondary amines becomes more favourable as amine basicity (i.e. pK_a) decreases [12]. Even at low formation yields, *N*-nitroso compound synthesis remains a health concern because of their potent carcinogenicity at very low concentrations [178]. For example, Health Canada's maximum acceptable concentration (MAC) for NDMA is 0.04 µg L^{-1} while that for benzene, classified as a "known human carcinogen" by the U.S. EPA, is 5 µg L^{-1} [179].

For the purpose of characterizing exposure to toxic pesticides, metabolites and environmental breakdown products to assess potential human health effects, additional analyses of catalytic metals and nitrates/nitrates in groundwater samples are important. The analytes selected for investigating PA*N*N compound formation were ATR, CAR, DIM, ETU, IMI, LIN, OME, TCPy, and TM. All compounds of interest are capable of forming *N*-nitroso compounds through interaction with nitrite and have PEI groundwater contamination potential. Very little is known about the potential PA*N*N compounds formed by these analytes. For example, most have no CAS numbers and are not even commercially available as an analytical standard. As such, the substrate concentrations at which they are formed are also unknown.

The main hypothesis of this research project is that nitrosatable pesticides and byproducts that are contaminants of concern in PEI groundwater are susceptible to nitrosation in water when mixed with $NaNO_2$ and acidified to a pH value comparable to that of human gastric acid. It is also possible that certain metal ions common in PEI groundwater (e.g., Cu and Fe) catalyze PA*N*N compound formation. The primary objectives of this work were to (i) screen nine nitrosatable pesticides for *N*-nitroso compound formation when mixed with $NaNO_2$ in Milli-Q water under various conditions using UHPLC/HRAM MS; (ii) synthesize two representative PA*N*N compounds (*N*-ATR and *N*-ETU) and confirm that the analytical method is capable of detecting them via semi-

targeted analysis; and (iii) determine the lowest analyte concentration that produces PA*N*N compounds in a pooled PEI groundwater sample.

3.3 Materials and Methods

3.3.1 Analytical Standards, Solvents, Reagents, Working Solutions, and Intermediates

Analytical standards were purchased individually from Chromatographic Specialties (Brockville, ON, CA): ATR, CAR, DIM, ETU, IMI, LIN, MCPA, OME, TCPy, and TM. Carbendazim-d3 was chosen as the IS and was obtained in neat form from Sigma Aldrich Canada Co. (Oakville, ON, CA). Structures of anticipated PA*N*N compound structures resulting from interaction of nitrosatable compound with nitrite are shown in Figure 3-1. All solvents and reagents used in this study were of HPLC-grade. MeOH and TraceMetal grade HCl were obtained from Thermo Fisher Scientific (Fair Lawn, NJ, US). Neat $NaNO_2$ and Fe and Cu, purchased as Inductively Coupled Plasma-Mass Spectrometry (ICP-MS) standards at 100 µg mL^{-1} in 2 to 5% nitric acid, were obtained from Chromatographic Specialties (Brockville, ON, CA). Milli-Q water was obtained from the Milli-Q plus system (Millipore, Bedford, MA, US).

For each analyte, a 250 µg L^{-1} working solution was made by adding 25 µL of a 100-µg mL^{-1} analytical standard in 10 mL of Milli-Q water in a volumetric flask. Using a disposable glass pipet, the solution was topped up with Milli-Q water to the 10-mL mark, vortexed for 15 seconds, and transferred to a labeled 11-mL amber glass vial. Two intermediates of neat $NaNO_2$ were required. The first intermediate was made by adding 250 mg solid $NaNO_2$ to 10 mL of Milli-Q water for a total concentration of 25 mg mL^{-1}. The second intermediate was made by adding 200 µL of the 25 mg mL^{-1} intermediate in 10 mL of Milli-Q water for a total $NaNO_2$ concentration of 0.5 mg mL^{-1}. In addition, each metal standard was obtained in a concentration of 100 µg mL^{-1}. An intermediate for each was made by adding 1 mL of metal standard in a 10-mL volumetric flask using a 1,000 µL syringe and topping up to the 10-mL mark with Milli-Q water for a final concentration of 10 µg mL^{-1}.

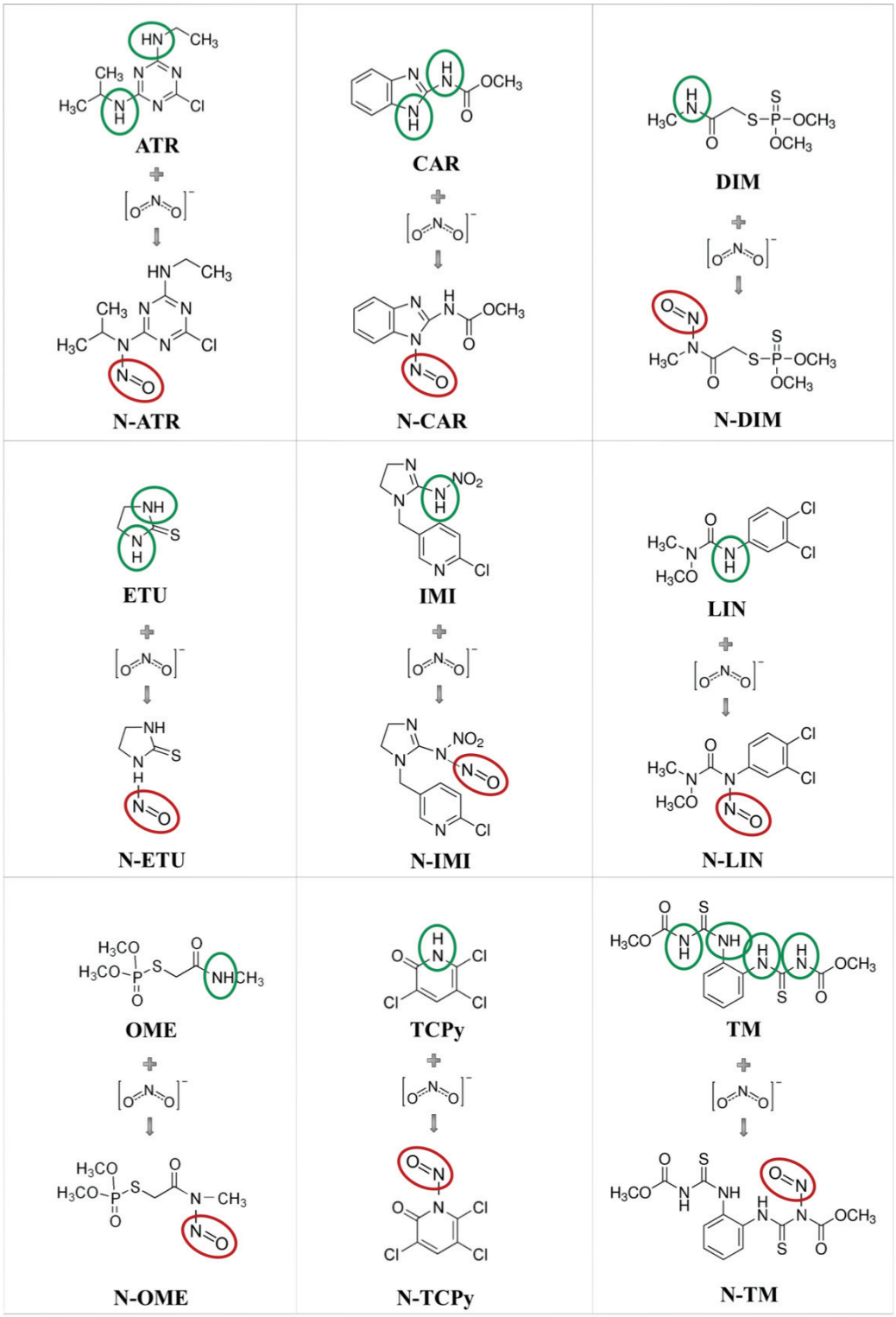

Figure 3-1. Structures of anticipated PA*N*N compound structures resulting from interaction of nitrosatable compound with nitrite. Green ellipses depict potential nitrosation sites and red ellipses highlight the nitroso group on a potential *N*-nitroso product.

3.3.2 Theoretical Mass-to-Charge Values for PA*N*N Compound Identification

The instrument's *Tune* software was used to generate theoretical *m/z* values in both positive and negative ionization modes from the chemical formulas of each predicted PA*N*N compound (Table 3-1). These theoretical *m/z* values were extracted from chromatograms resulting from analysis of samples in PA*N*N compound formation experiments. The mass spectra of peaks identified by extracting theoretical PA*N*N compound *m/z* values were examined for prominent ions that match theoretical values. These ions were entered into the *Xcalibur* software program, which generates the most probable chemical formula of the unknown analyte from its experimental *m/z* and matches it to the corresponding chemical formula of the PA*N*N compound within 5 ppm. A workflow for compound identification is illustrated in Figure 3-2.

Table 3-1. Theoretical *m/z* values for PA*N*N compounds calculated by *Tune* software in both positive and negative ionization modes.

PA*N*N compound	Molecular formula	Molar mass	[H+] theoretical mass (*m/z*)	[H-] theoretical mass (*m/z*)
N-ATR[a]	$C_8H_{13}ClN_6O$	244.08	245.09121	243.07666
di-*N*-ATR[b]	$C_8H_{12}ClN7O_2$	273.68	274.08138	272.06682
N-CAR[a]	$C_9H_8N_4O_3$	220.06	221.06692	219.05236
di-*N*-CAR[b]	$C_9H_7N_5O_4$	249.18	250.05708	248.04253
N-DIM[a]	$C_5H_{11}N_2O_4PS_2$	257.99	258.99706	256.98251
N-ETU[a]	$C_3H_5N_3OS$	131.02	132.02261	130.00806
di-*N*-ETU[b]	$C_3H_4N_4O_2S$	160.15	161.01277	158.99822
N-IMI[a]	$C_9H_9ClN_6O_3$	284.04	285.04974	283.03519
N-LIN[a]	$C_9H_9Cl_2N_3O_3$	277.00	278.00937	275.99482
N-OME[a]	$C_5H_{11}N_2O_5PS$	242.01	243.01991	241.00535
N-TCPy[a]	$C_5HCl_3N_2O_2$	225.91	226.91764	224.90308
N-TM[a]	$C_{12}H_{13}N_5O_5S_2$	371.04	372.04309	370.02853
di-*N*-TM[b]	$C_{12}H_{12}N_6O_6S_2$	400.39	401.03325	399.01870
tri-*N*-TM[c]	$C_{12}H_{11}N_7O_7S_2$	429.39	430.02341	428.00886
tetra-*N*-TM[d]	$C_{12}H_{10}N_8O_8S_2$	458.39	459.01358	456.99902

[a]PA*N*N compounds formed by nitrosation at a single site on parent analyte; *N*-ATR = *N*-nitrosoatrazine; *N*-CAR = *N*-nitroso carbendazim; *N*-DIM = *N*-nitroso dimethoate; *N*-ETU = *N*-nitrosoethylenethiourea; *N*-IMI = *N*-nitroso imidacloprid; *N*-LIN = *N*-nitroso linuron; *N*-OME = *N*-nitroso omethoate; *N*-TCPy = *N*-nitroso 3,5,6-trichloro-2-pyridinol; *N*-TM = *N*-nitroso thiophanate methyl;

[b]PA*N*N compounds formed by nitrosation at two sites on parent analyte; di-*N*-CAR = di-*N*-nitroso carbendazim; di-*N*-ETU = di-*N*-nitroso ethylenethiourea; di-*N*-TM = di-*N*-nitroso thiophanate methyl

[c]PA*N*N compounds formed by nitrosation at three sites on parent analyte; tri-*N*-TM = tri-*N*-nitroso thiophanate methyl

[d]PA*N*N compounds formed by nitrosation at four sites on parent analyte; tetra-*N*-TM = tetra-*N*-nitroso thiophanate methyl

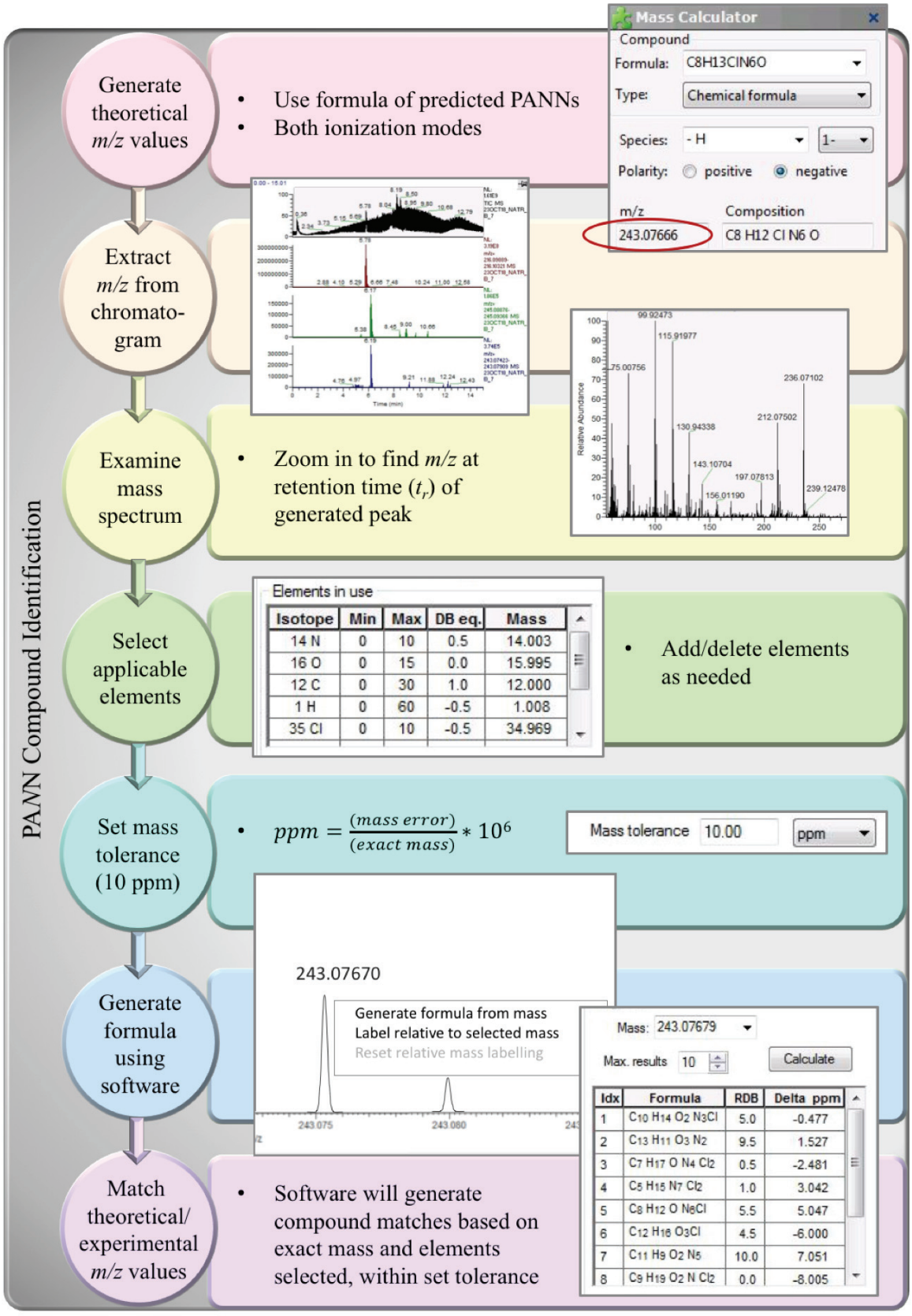

Figure 3-2. Workflow for compound identification using *Tune* and *Xcalibur* software.

3.3.3 Instrumentation

The Thermo Scientific Accela UHPLC system with the CTC Analytics PAL autosampler coupled to the Exactive Plus orbital ion trap mass spectrometer, equipped with a HESI source, was used for analysis of nitrosatable analytes and PA*N*N compounds (Thermo Fisher Scientific, MA, USA). Nitrate and nitrite were measured using the Thermo Scientific Dionex ICS-5000 ion chromatograph and elemental analysis was performed using the Thermo Fisher Scientific ICAP-Q ICP-MS paired with an ESI SC-4DXS autosampler (Elemental Scientific, NE, USA). Data analysis was performed using Thermo Scientific *Xcalibur* and *Tune* software. Solid standards were weighed on a Denver Instrument P-114 analytical balance (Bohemia, NY, US). Solution pH was measured on the Fisher Scientific Accumet AB200 pH/conductivity benchtop meter. Samples were vortexed using the Thermo Scientific MaxiMix I vortex mixer.

3.3.4 UHPLC/Orbital Ion Trap MS Analysis

The development of chromatographic and detection methods involving the targeted analysis of nitrosatable pesticides and the semi-targeted analysis of PA*N*N compounds of interest in this study is described in Chapter 2. UHPLC separation was carried out using a Thermo Scientific Hypersil GOLD™ aQ C18 (20 mm x 2.1 mm x12 µm) analytical column with a mobile phase flow rate of 400 µL min^{-1}. Mobile phase Solvent A consisted of 100% Milli-Q water and Solvent B was 100% MeOH. Solvent A began at 100% and was held for one minute. From minute one to seven, Solvent B was increased to 100% and held for one minute. Minutes eight to 15 show a decrease of Solvent B back down to 0% and 100% Solvent A is pumped for the remaining two minutes of the run for a total run time of 17 minutes. The refrigerated autosampler tray held samples at 4 ºC.

HESI source parameters were optimized based on UHPLC flow rate and set to the following values: sheath gas flow rate, 50 au; auxiliary gas flow rate, 13 au; sweep gas flow rate, 0 au; spray voltage, 3.50 kV; capillary temperature, 263 ºC; S-lens RF level, 60.0 au; auxiliary gas heater temperature, 425 ºC. The orbital ion trap MS was operated using the following scan parameter settings: scan type, full MS/AIF; *m/z* range, 55-800 m/z; resolution, 70,000; AGC target, 3e6; maximum IT, 200 ms; and collision energy, 20 eV. The orbital ion trap was also programmed to operate in polarity switching mode, a feature

that allows the acquisition of data from both positive and negative mode scans in a single data file, to maximize the probability of detecting PA*N*N compounds.

3.3.5 "In-House" Synthesis of *N*-ATR and *N*-ETU at High Initial Analyte Concentrations

As analytical standards are not readily available for PA*N*N compounds, nor are the mass spectra provided in *m/z* databases, established methods were used to synthesize *N*-ATR [50] and *N*-ETU [53] "in house" to confirm identification of the two semi-targeted analytes. *N*-ATR was synthesized based on methods outlined by Wei et al [50]. A 0.1mM ATR solution was made by adding 21.6 mg ATR in 1L of Milli-Q water. Since ATR is only moderately soluble in water [105], the ATR was dissolved in a small volume (~ 5 mL) of MeOH before being added to the water. A 0.4mM $NaNO_2$ solution was made by adding 27.6 mg of $NaNO_2$ to 1L of Milli-Q water. A volume of 5 mL of each solution was combined and adjusted to a pH value of approximately 2.5 by addition of 200 µL stock HCl. The solution was allowed to sit at room temperature; at two time points (one, six, and 12 hours), a 100-µL aliquot was removed from the stock, diluted 100 times with Milli-Q water, and analyzed by UHPLC/MS. These time points were selected because peak *N*-ATR formation at pH 2 and 3 was observed after one hour and 12 hours, respectively. Since the pH of our solution was between 2 and 3, both time points, plus a time point in the middle, were selected for analysis of the diluted stock solution. This experiment was carried out in duplicate along with a control stock solution without the addition of HCl that contained only 5 mL of each ATR and $NaNO_2$ solution.

To synthesize *N*-ETU, Yamamoto *et al* (1983) detailed a method in which a 300-mL solution containing 3.5 g $NaNO_2$ and 1.5 g ETU was adjusted to various pH values with HCl [53]. In a scaled-down version of this method, 117 mg $NaNO_2$ and 50 mg ETU was added in 10 mL Milli-Q water in a volumetric flask, keeping the $NaNO_2$:ETU ratio of the original method at 2.3:1. Before adjusting the pH with the addition of HCL, a 100-µL aliquot of the 10-mL solution was diluted to 250 µg L^{-1} ETU and analyzed as the control sample, as there should not be any *N*-ETU formed in the absence of HCl. A volume of 200 µL of stock HCl was added to the remaining solution, which resulted in a pH value of 2.30. The solution was left to sit at room temperature for 10 minutes wrapped in aluminum foil.

Two 100-µL aliquots of the acidified solution were diluted down to an ETU concentration of 250 µg L^{-1} and analyzed immediately.

3.3.6 Analyte Screening for PA*N*N Compound Formation in Milli-Q Water

Analytes of interest were screened for PA*N*N compound formation by analyzing them in Milli-Q water with $NaNO_2$ under four different conditions: pH ~ 2.5; pH ~ 5; with dissolved Cu at a concentration of 50 µg L^{-1} at a target pH of 2.5; and with dissolved Fe at a concentration of 50 µg L^{-1} at a target pH of 2.5. Initial analyte and $NaNO_2$ concentrations for experimental stock solutions were 20 µg L^{-1} and 2.5 mg L^{-1}, respectively. The starting analyte concentration was chosen based on MAC values in Health Canada's *Guidelines for Canadian Drinking Water Quality*, for which only two of the nine target analytes have been assigned: ATR (5 µg L^{-1}) and DIM (20 µg L^{-1}) [179]. The greater of the two MAC values was chosen as the highest experimental concentration in this study because even though concentrations exceeding this value are unlikely in PEI groundwater (based on results from the PEI Pesticide Monitoring Program), the potential exists for pesticide concentrations to reach 20 µg L^{-1}, as aldicarb has been detected at 15 µg L^{-1} in groundwater beneath a PEI potato field [61]. The starting nitrite concentration of 2.5 mg L^{-1} was chosen because the average nitrate level for PEI groundwater samples tested in 2013 was 15.5 mg L^{-1} ± 12.4 (3.5 mg L^{-1} ± 2.8 nitrate-N) [180] and as about five to 10 percent of total nitrate intake is converted to nitrite endogenously [181], a value of 2.5 mg L^{-1} was chosen. Moreover, these concentrations exceeded the $NaNO_2$:analyte ratio of 4:1 favourable for *N*-ATR formation [50].

Copper and Fe were selected for catalysis experiments. Of the four metals associated nitrosation catalysis (Cu, Fe, Mn, and Ni), Cu had the highest mean concentrations in PEI groundwater samples in 2013 (42.4 ± 50 µg L^{-1}), ranging from 5 to 410 µg L^{-1} [180]; although Mn had a higher mean concentration (16.6 ± 113 µg L^{-1}, ranging from 0.5 to 18,168 µg L^{-1})[1] than Fe (12.8 ± 60 µg L^{-1} with concentrations ranging from 2

[1] The Health Canada Guidelines for Canadian Drinking Water Quality lists the MAC for Mn as 120 µg L^{-1} [179]. Between 2013 and 2017, 165 PEI groundwater samples analyzed by the PEI government as a part of an ongoing monitoring program contained Mn at concentrations between the MAC and 18,168 µg L^{-1}. Considering that about 20% of mancozeb is elemental Mn [182], the extensive use of this fungicide in the province may be a significant source of groundwater Mn contamination.

to 38,335 µg L^{-1}), the maximum value for Fe was more than double that for Mn. Therefore, Fe was chosen as the second metal for assessing nitrosation catalysis. Metal concentrations of 50 µg L^{-1} were chosen because these values have been reported in PEI groundwater samples in 2013 for Cu and Fe [180]. *N*-nitroso compound formation occurs largely in acidic media. As such, target pH values of 2.5 and 5 were selected to represent that of gastric acid (pH 1.5 to 3.5) and the recorded pH of some acidic PEI soils [183], respectively.

For each of the nine analytes (ETU, ATR, LIN, TM, CAR, DIM, OME, IMI, and TCPy), two replicates of three 10-mL test solutions for each analyte were made in Milli-Q water by adding (i) 800 µL of the 250 µg L^{-1} analyte solution for a total analyte concentration of 20 µg L^{-1}; (ii) 50 µL of the 0.5 mg mL^{-1} $NaNO_2$ intermediate for a total $NaNO_2$ concentration of 2.5 mg L^{-1}; and (iii) 100 µL of the 10 mg mL^{-1} IS intermediate for a final concentration of 100 µg L^{-1} (Figure 3-3). For samples involving metals, a volume of 50 µL of metal intermediate in 10 mL gave a final metal concentration of 50 µg L^{-1}.

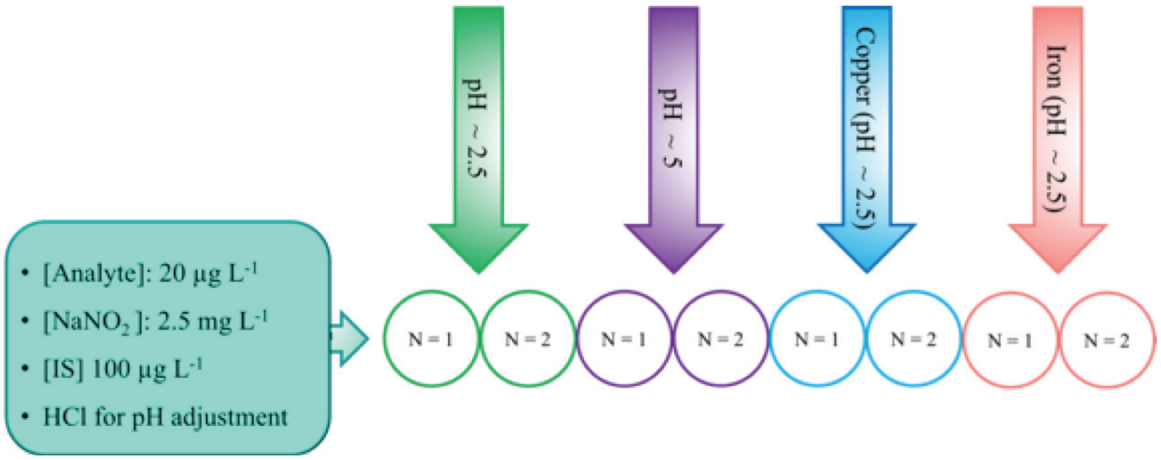

Figure 3-3. Overview of PA*N*N compound synthesis screening experiment.

The pH of each test solution was adjusted with stock HCl; pH was measured and recorded immediately after components were added and thoroughly mixed. Test solutions were stored at room temperature in amber glass vials wrapped in aluminum foil to avoid photodegradation. At the following time points, a 150 µL fraction was taken from each test

solution for UHPLC-MS analysis to assess PA*N*N compound formation: 0 hours (immediately after the addition of HCl); 4 hours; and 12 hours.

3.3.7 *N*-nitroso Compound Formation in PEI Groundwater

Other constituents present in PEI groundwater may enhance or interfere with PA*N*N compound formation. To assess whether PA*N*N compound formation is a favourable reaction in actual groundwater, a site for groundwater collection in PEI was chosen. The U.S. EPA states that small watershed size and high pesticide use intensity are factors that indicate vulnerability of water systems to pesticide contamination [184]. Watershed vulnerability to pesticide pollution in western PEI was assessed by overlaying the Land in Potato Rotation map (indicating pesticide use intensity) on watershed boundary files for the region (Figure 3-4). A highly vulnerable watershed, Hills River Watershed (HRW) was chosen as the study unit based on the following criteria: relatively small watershed area (13.96 km^2); greater than 75% land in potato rotation; Hills River is a sub-basin of Mill River, where several anoxic events have occurred; substantial hydrogeological data exist for this watershed; the 2003 Mill River Estuary Modelling Study indicated that this watershed is a known location of groundwater nitrate contamination and that agriculture was a major contributor [67].

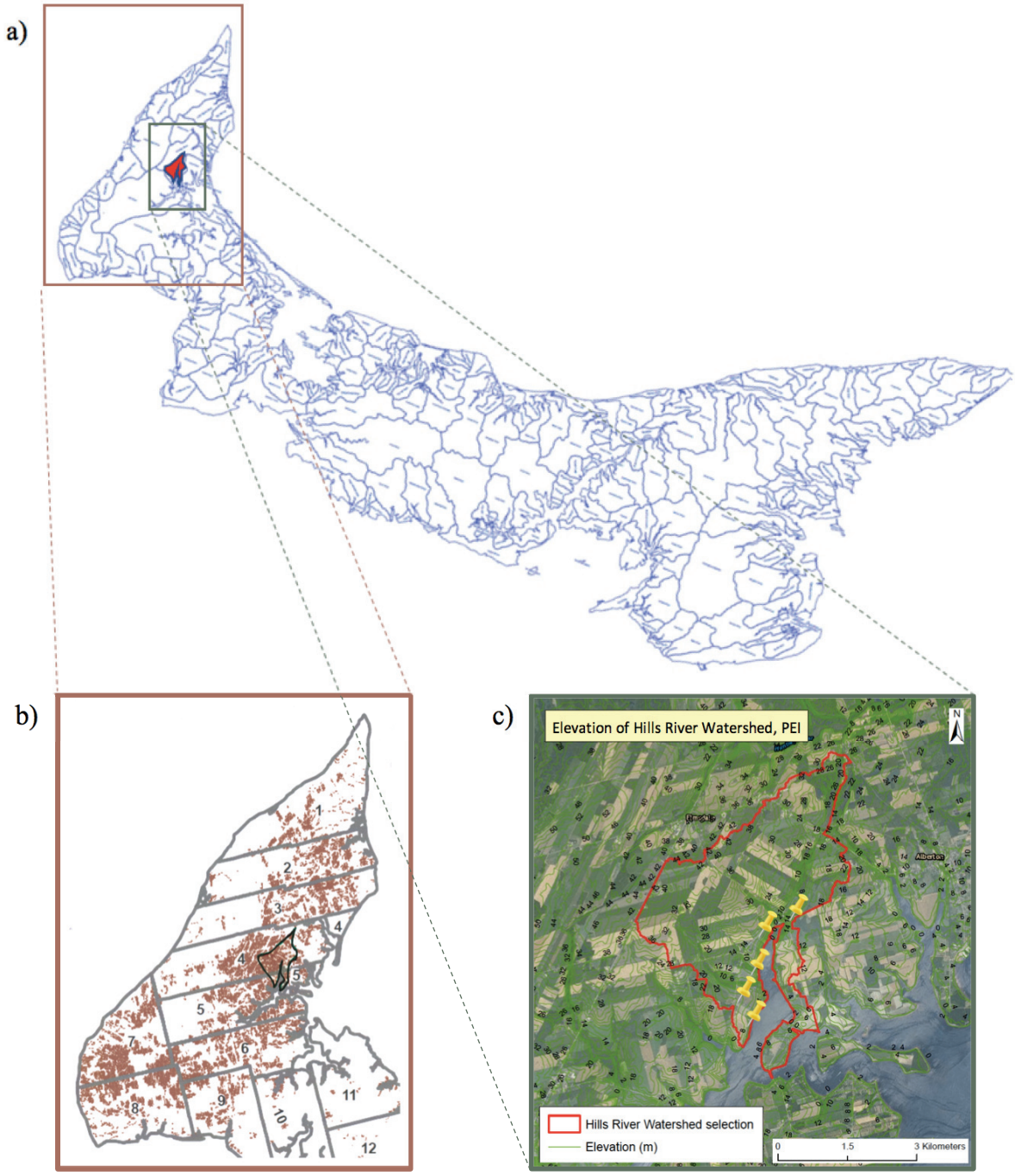

Figure 3-4. (a) Delineation of the watersheds in PEI with the HRW highlighted in red; (b) Western Prince County, PEI land in potato rotation (2006 to 2009) with HRW delineation; and (c) groundwater sampling sites within the HRW shown on an elevation map.

All groundwater samples were voluntarily submitted by participants at each location. Sampling protocols were followed as per established methods [185]. Two 30-mL amber glass jars were used to collect groundwater for UHPLC analysis of pesticides, byproducts, and *N*-nitroso compounds (without rinsing with groundwater sample before collection) and stored in darkness on ice during transport to the laboratory. Glass reduces plasticizer contamination, which can interfere with analysis, and the amber glass reduces photodegradation of analytes. Laboratory analysis occurred within seven days and so pH adjustment was not required. For ion chromatography (IC) and ICP-MS analyses of nitrate/nitrate and select elements, respectively, groundwater was collected in two 15-mL polypropylene centrifuge tubes. Individual groundwater samples were analyzed for target analytes, nitrate/nitrite, and elements of interest while a pooled sample created from all five samples was used for PA*N*N compound formation experiments.

Ion chromatography analysis

Ion chromatography is a form of liquid chromatography that involves the separation of ions in solution based on their interaction with a resin inside a pressurized analytical column [186]. The sample is carried by an ion extraction liquid (eluent) through the column as ions in the sample are separated depending on ion species type and size. Nitrate and nitrite were measured in the PEI groundwater samples by IC using a previously developed method.

A Dionex ICS-5000 IC, equipped with a Dionex Ion Pac AS20 analytical column and conductivity detector, was used to determine nitrite and nitrate concentrations in PEI groundwater samples. A six-point calibration curve was constructed to quantify the anions in water samples. The following concentrations were used for the calibration curve: 50, 100, 200, 1000, 2000, and 4000 µg L^{-1}. Calibration levels were prepared using IC standards containing 1 g L^{-1} of each analyte from Fluka Analytical. Samples were introduced unfiltered and carried through the analytical column under isocratic conditions by 30 mM potassium hydroxide eluent at a flow rate of 1 mL min^{-1}. Eluent conductivity suppression was achieved by a Dionex Anion Self-Regenerating Suppressor (ASRS, 4mm), a component that enhances sample ion conductivity and increases detection sensitivity.

Inductively coupled plasma-mass spectrometry analysis

ICP-MS is an analytical platform used in elemental analysis, favoured for metal analysis [187]. An argon plasma ionizes the sample and the MS determines the *m/z* of the ions. An existing ICP-MS method for 37 elements was used to determine the concentration of dissolved metals and other elements in PEI groundwater. Of the 37 elements, the following 11 were quantified: arsenic (As); barium (Ba); cadmium (Cd); chromium (Cr); Cu; Fe; Mn; Ni; lead (Pb); selenium (Se); and uranium (U). Cu, Fe, Mn, and Ni were selected because they have been known to catalyze homogeneous nitrosation involving nitric oxides [177] and may be involved in catalyzing nitrosation of pesticides. As, Ba, Cd, Cr, Pb, Se, and U were selected because they are among the chemical parameters included in routine testing of PEI groundwater that have health-based drinking water guidelines and assigned MACs [188].

Groundwater samples were acidified to 2% (v/v) nitric acid by adding 60 µL of concentrated nitric acid (70%, TraceMetal grade, Fisher Scientific) to 2.940 mL of each water sample, to a final volume of 3 mL. Samples were introduced into the ICAP-Q ICP-MS by the ESI SC-4DXS autosampler. The instrument was operated in kinetic energy discrimination (KED) mode, using high purity helium as the collision gas. To quantify elements of interest in water samples, an eight-point calibration curve was generated for each using the following concentrations: 0.1, 0.5, 1, 5, 10, 20, 50, and 100 µg L^{-1}. Online IS addition was performed using 50 µg L^{-1} scandium and an SC FAST Valve (Elemental Scientific, NE, USA). A dwell time of 0.01 seconds was programmed for all analytes, with 25 sweeps and three main runs per sample.

PANN compound formation in pooled PEI groundwater sample

As with PA*N*N compound formation experiments in Milli-Q water, two replicates of three 10-mL test solutions for each analyte capable of forming *N*-nitroso compounds in Milli-Q water in previous experiments were made in amber glass vials wrapped in aluminum foil using the pooled PEI groundwater sample. Volumes of 800 µL of the 250 µg L^{-1} analyte solution, 50 µL of the 0.5 mg mL^{-1} $NaNO_2$ intermediate, and 100 µL of the 10 mg mL^{-1} IS intermediate were added. The pH was adjusted to ~ 2.5 with stock HCl.

Test solutions were stored at room temperature and analyzed by UHPLC/MS in fractions of 150 µL at 0 hours, 4 hours, and 12 hours.

3.3.8 Kinetics of PA*N*N Compound Formation in PEI Groundwater

To better determine the time of optimal PA*N*N compound formation, experiments were carried out in both Milli-Q water and a pooled PEI groundwater sample with analytes showing evidence of nitrosation before the four-hour time point. Test solutions for both media had initial analyte, $NaNO_2$, and IS concentrations of 20 µg L^{-1}, 2.5 mg L^{-1}, and 100 µg L^{-1}, respectively, and were adjusted to pH ~ 2.5 using stock HCl. Test sample fractions of 150 µL were analyzed at 30-minute intervals up to 4 hours. Each experiment was replicated for three consecutive days to obtain triplicate measurements. The extent of PA*N*N compound formation was assessed using the following calculation: (analyte peak area/IS peak area) x 100. The time point that corresponded to the highest value for analyte peak area:IS peak area ratio was considered the time of maximum PA*N*N compound formation for that particular analyte.

3.3.9 Minimum Concentration of Analytes for PA*N*N Compound Formation in PEI Groundwater

To assess PA*N*N compound formation in a pooled PEI groundwater sample at lower analyte concentrations, individual stock solutions of analytes were made by adding 100, 200, 300, and 400 µL of the 250 µg L^{-1} working solution to 10-mL of groundwater, resulting in starting concentrations of 2.5, 5, 7.5, and 10 µg L^{-1}, respectively. These experiments were carried out in triplicate measurements. Test sample solutions were adjusted to pH ~ 2.5 using stock HCl. The single time point chosen for analysis was the time of maximum *N*-nitroso compound formation determined in the experiment involving PA*N*N compound formation in PEI groundwater at 30-minute intervals.

3.3.10 Quantitation of Target Analytes and Calculation of Peak Area Ratios for PA*N*N Compounds

Quantitation of target analytes was carried out using calibration standards prepared at seven different concentrations in Milli-Q water to construct a seven-point calibration curve for each target analyte. Since accurate quantitation for PA*N*N compounds is not possible without certified analytical standard, a peak area ratio technique was formulated

to measure relative response of PA*N*N compounds. Once identified using the *Tune* and *Xcalibur* software, PA*N*N compound peak area was divided by the IS peak area and multiplied by 100 (e.g. 100**N*-ETU peak area/IS peak area). This ratio represented the PA*N*N compound's relative response and was used to determine whether the compound concentration was increasing or decreasing over time.

3.3.11 Method Detection Limit and Limit of Quantitation

The MDL was determined using U.S. EPA procedures [151]. Ten spiked samples at 5 μg L^{-1} and 10 method blank samples were analyzed. MDLs for each analyte in spiked samples and method blanks were then calculated; the greater of the two determined for each analyte represented the MDL. The LOQ was calculated as ten times the standard deviation of the 10 replicate spiked sample measurements.

3.3.12 Statistical Analysis

Initial PA*N*N compound formation screening experiments (pH ~ 2.5: pH ~ 5; with dissolved Cu; and with dissolved Fe), PA*N*N compound formation in PEI groundwater (initial analyte concentration of 20 μg L^{-1}), and in-house synthesis of *N*-ATR and *N*-ETU at high initial analyte concentrations were carried out using replicates of two at each time point. Experiments involving PA*N*N compound formation at lower initial analyte concentrations and at 30-minute increments were carried out in triplicate measurements. For all experiments, mean analyte concentration values were calculated and standard deviation was used to determine error bars. To assess significance of changes in mean analyte concentration over time during PA*N*N compound formation screening experiments, a paired t-test ($\alpha = 0.05$, two-tailed) was performed for each analyte to compare mean concentration between 0 and 4 hours, 4 and 12 hours, and 0 and 12 hours.

3.4 Results and Discussion

3.4.1 Confirmation of *N*-ATR and *N*-ETU Synthesis

Synthesis of *N*-ATR resulted in a compound that matched the theoretical *m/z* values of *N*-ATR generated by the *Tune* software in both positive and negative ionization modes. Extraction of these theoretical *m/z* values from the chromatogram showed that the

compound eluted at a retention time of 6.17 ± 0.01 minutes (Figure 3-5a). No *N*-ATR was identified in control samples containing only ATR and $NaNO_2$ without HCl acidification (Figure 3-5b). The compound's negative ion showed a greater response with a mean peak area of 406,823 compared to its positive ion, which had a mean peak area of 225,389. Hence, the negative ion was used for compound identification. Examination of the mass spectrum at that retention time showed that the most prominent experimental ion matching the theoretical value of 243.07666 was 243.07668 (Figure 3-5c). Mass accuracy, generally reported as mass error in ppm, was calculated using the following equation [189]:

$$Mass\ error = \left(\frac{Theoretical\ mass - Experimental\ mass}{Theoretical\ mass}\right) \times 10^6$$

The mass error between experimental and theoretical *m/z* values for *N*-ATR was 0.08 ppm. With elements carbon, hydrogen, chlorine, nitrogen, and oxygen selected and a mass tolerance set to 5 ppm, the *Xcalibur* software matched the formula for *N*-ATR to potential matches for the compound. All criteria were met for identification of *N*-ATR.

The formation of *N*-ATR was assessed at three different time points: after 1, 6, and 12 hours (n=2). Since *N*-ATR appears to ionize more favourably in negative mode, its negative ion was used to monitor its relative abundance (via peak area) across the three time points. Of the three time points, *N*-ATR formation appeared to have peaked after 6 hours (Figure 3-6). Moreover, ATR concentration decreased over time, which may indicate that ATR is being used up in the *N*-ATR synthesis reaction. These findings are consistent with observations from a previous study that found that at pH 2, *N*-ATR was transformed back to ATR and hydroxyatrazine after 6 hours and ATR concentrations decreased in the initial hours of the 48-hour experiment [50].

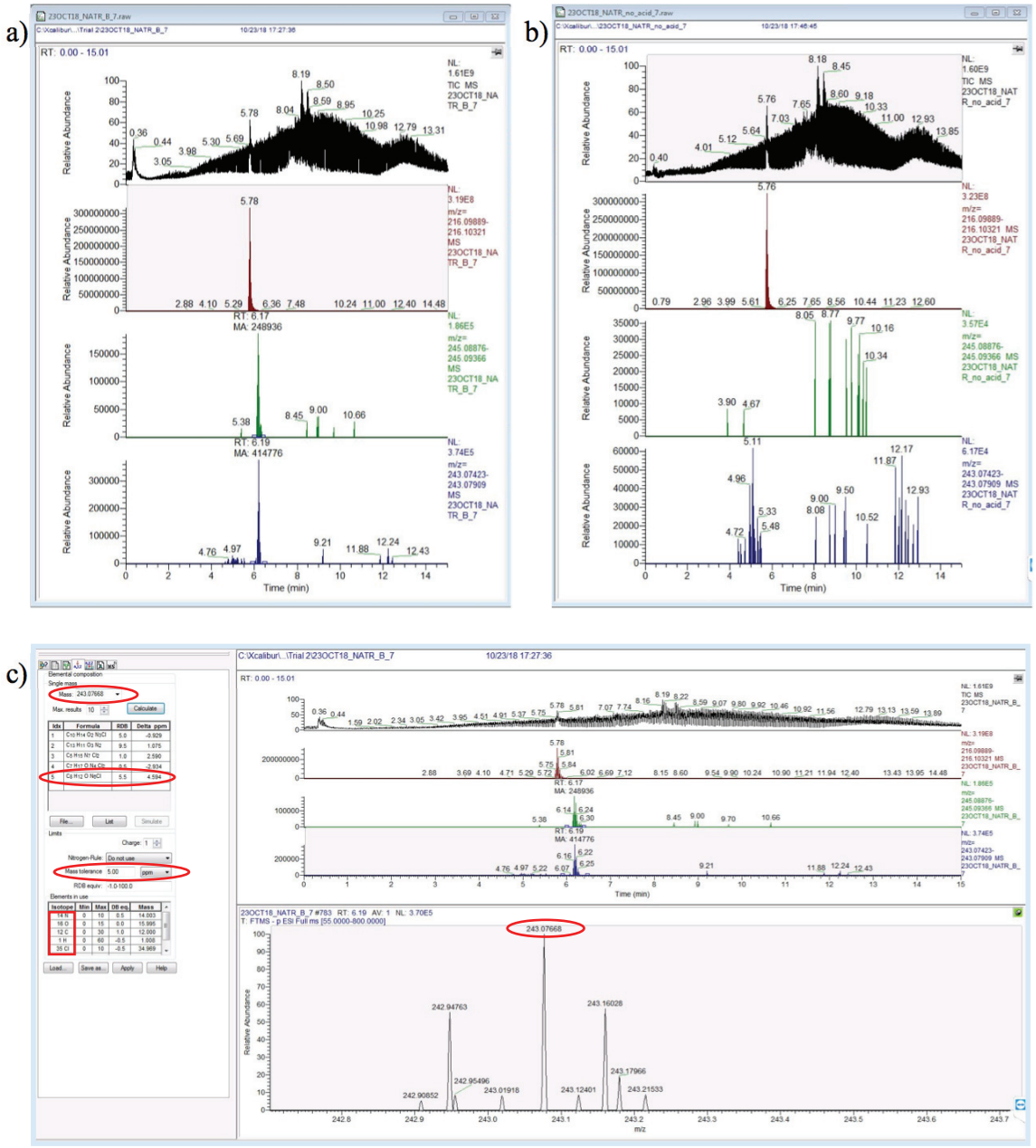

Figure 3-5. Chromatograms showing a) *N*-ATR synthesis after six hours and b) the absence of *N*-ATR in a control solution containing ATR and $NaNO_2$ without HCl acidification. The top row of each chromatogram depicts the total ion count (TIC), the second row represents the extracted ion for ATR, and the third and last rows show peaks generated by extraction of theoretical *N*-ATR ions in positive and negative ionization modes, respectively; c) confirmation of *N*-ATR identification required matching the theoretical *m/z* value of *N*-ATR to the experimental *m/z* value shown in the red ellipse in the mass spectra at $t_r = 6.19$. The bottom left of the figure shows the theoretical formula of the compound generated from the experimental *m/z* value within 5 ppm.

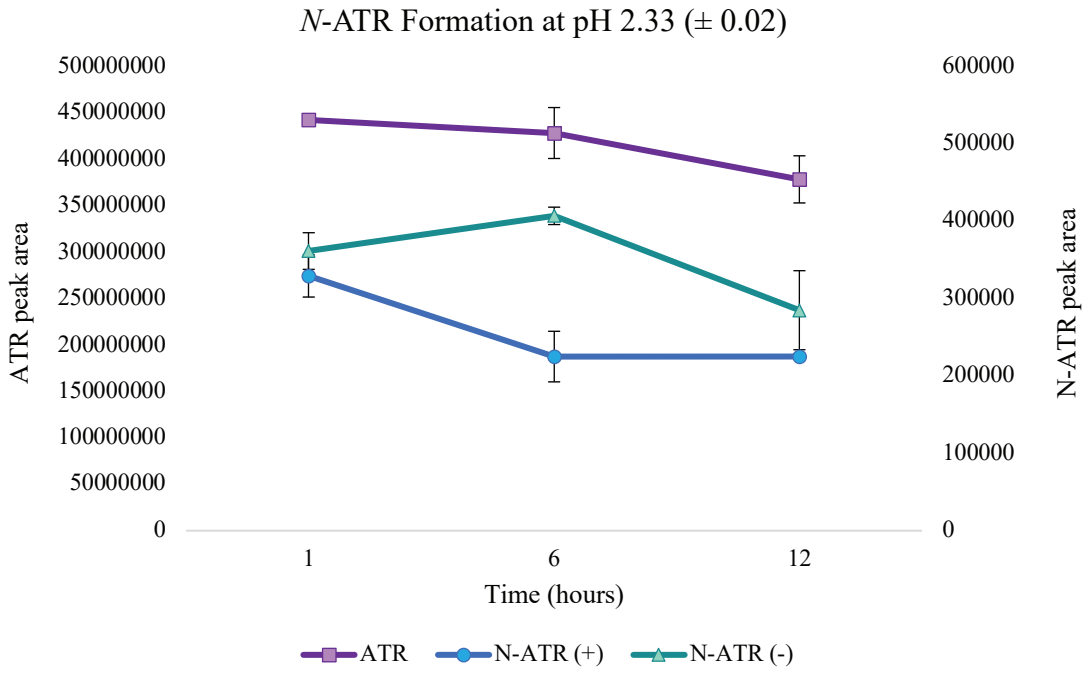

Figure 3-6. Change in ATR and *N*-ATR peak area after 1, 6, and 12 hours (n=2). *N*-ATR peak area was determined after extracting both positive (blue) and negative (teal) mode ions from the chromatogram.

The synthesis of *N*-ETU resulted in a yellow solution (Figure 3-7). This is consistent with the observation that *N*-nitrosamines usually produces a yellowish oil that is subsequently purified [190]. A proposed set of chemical reactions for the formation of *N*-ETU is shown in Figure 3.8. As with *N*-ATR, synthesis of *N*-ETU resulted in a compound that matched the *Tune* software's theoretical *m/z* values for *N*-ETU in both positive and negative ionization modes. Extraction of theoretical *m/z* values from the chromatogram showed that the compound eluted at a retention time of 1.22 ± 0.04 minutes (Figure 3-9a). No *N*-ETU was identified in control samples containing only ETU and $NaNO_2$ without HCl acidification (Figure 3-9b). Contrary to *N*-ATR ionization, the compound's positive ion showed a greater response than its negative ion, with mean peak areas of 14,344,029 and 219,816, respectively. Therefore, the compound's positive ion was used for identification. Examination of the mass spectrum at that retention time showed that the most prominent experimental ion matching the theoretical value of 132.02261 was 132.02252 (Figure 3-9c). The mass error between experimental and theoretical *m/z* values

for *N*-ETU was 0.7 ppm. The *Xcalibur* software generated a single positive match for the *N*-ETU formula with a potential formula for the compound within these criteria with elements carbon, hydrogen, nitrogen, oxygen, and sulfur selected and a mass tolerance set to 5 ppm. The ETU (parent) peak split into two separate peaks, indicating that the ion is detected at both t_r = 0.69 minutes and t_r = 1.24 minutes. This suggests that in addition to the elution of the intact parent compound at 0.69 minutes, the ionization of *N*-ETU at 1.24 minutes, (the same time that *N*-ETU elutes), results in a fragment identical to ETU.

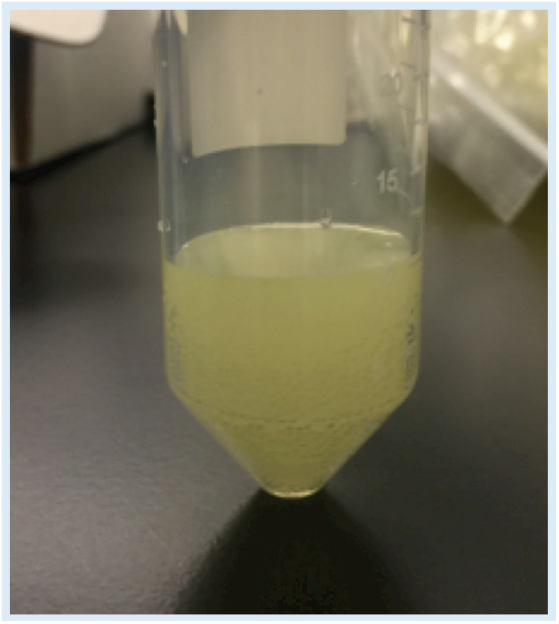

Figure 3-7. Synthesis of *N*-ETU from 50 mg ETU and 117 mg $NaNO_2$ in 10 mL Milli-Q water, adjusted to pH 2.30 with HCl, resulted in a yellow solution (undiluted sample).

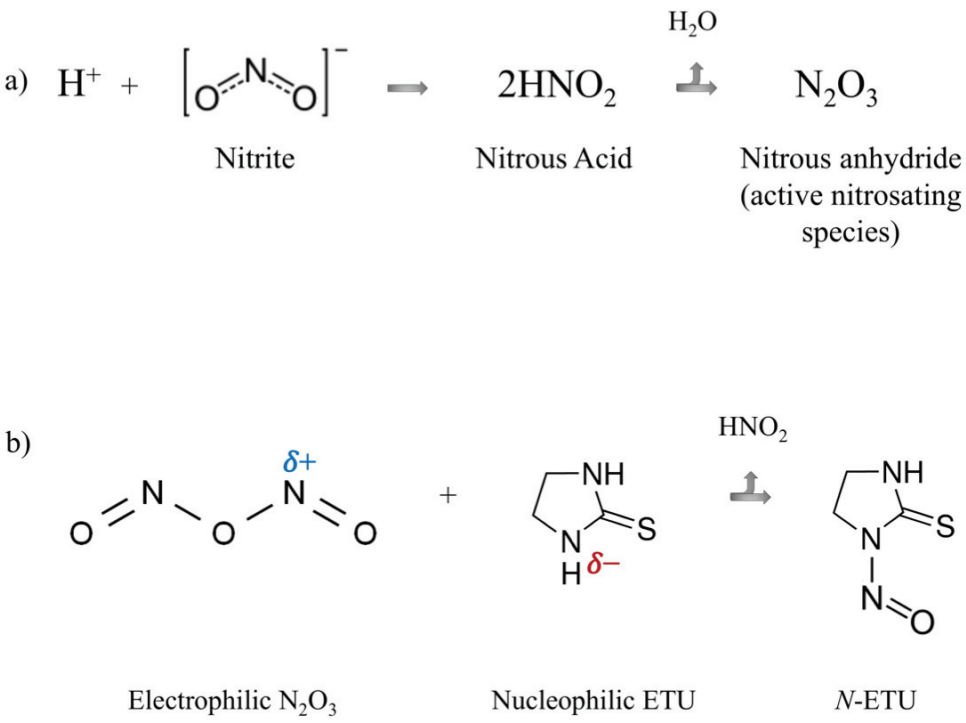

Figure 3-8. Proposed chemical reactions for the formation of *N*-ETU: a) formation of the active nitrosating species, and b) electrophilic attack resulting in *N*-ETU.

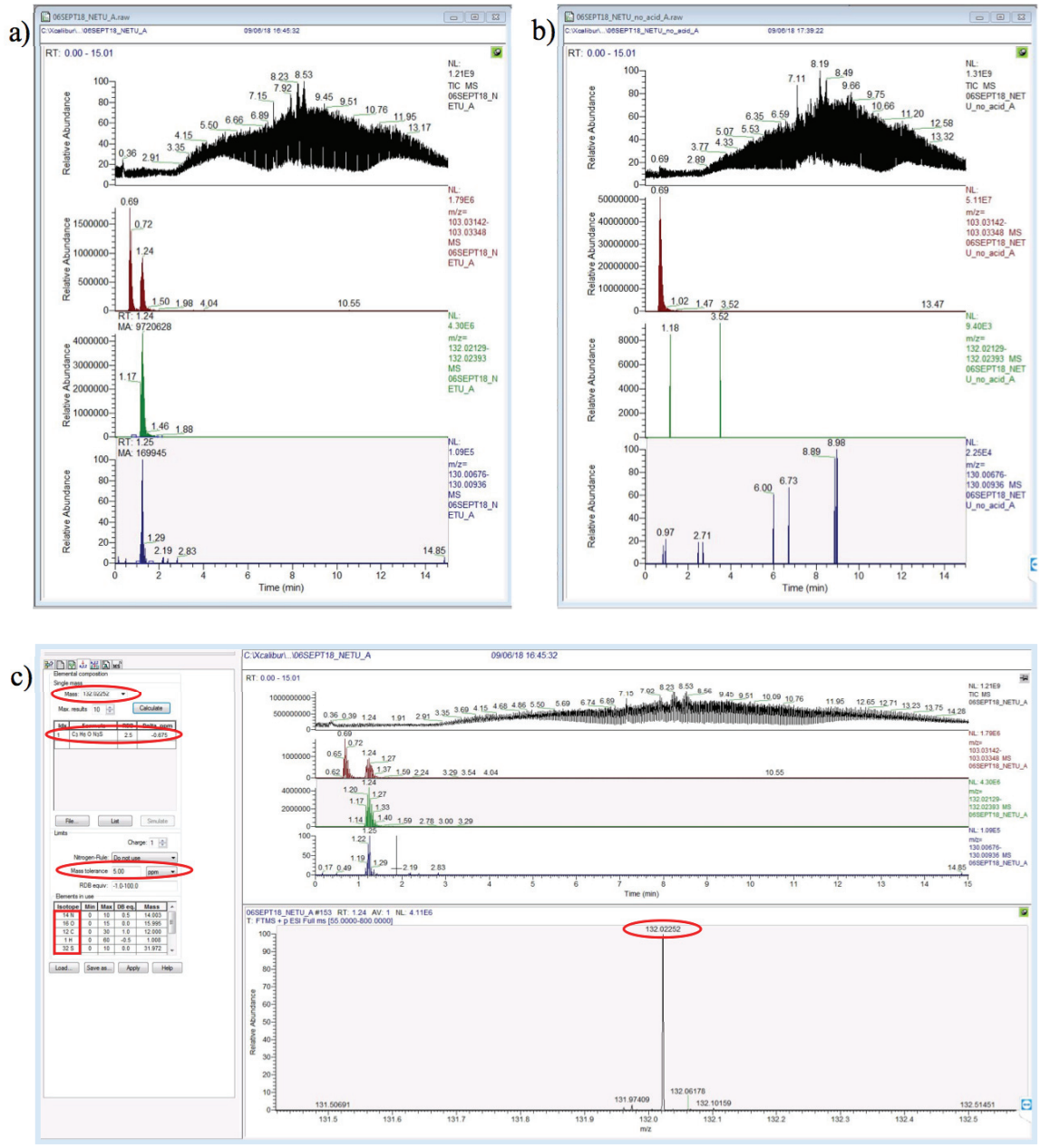

Figure 3-9. Chromatograms showing a) *N*-ETU synthesis after 10 minutes and b) the absence of *N*-ETU in a control solution containing ETU and $NaNO_2$ without HCl acidification. The top row of each chromatogram depicts the total ion count (TIC), the second row represents the extracted ion for ETU, and the third and last rows show peaks generated by extraction of theoretical *N*-ETU ions in positive and negative ionization modes, respectively; c) as with *N*-ATR, confirmation of *N*-ETU identification required matching the theoretical *m/z* value of *N*-ETU to the experimental *m/z* value shown in the red ellipse in the mass spectra at t_r = 1.24. The bottom left of the figure shows the theoretical formula of the compound generated from the experimental *m/z* value within 5 ppm.

3.4.2 Screening of Target Analytes for PA*N*N Compound Formation

PA*N*N compound formation was determined by two factors: (i) decrease in concentration of target analyte over time, which may indicate that the parent compound was being used up in the PA*N*N compound synthesis reaction, and (ii) the presence of a peak in the resulting chromatogram that matched the theoretical *m/z* values of predicted PA*N*N compounds. First, change in analyte concentration over time was assessed for each analyte screening experiment (Figure 3-10). For each experiment, analyte concentration began at 20 µg L^{-1}. Analyte concentrations reported *above* 20 µg L^{-1} demonstrate that ion enhancement has occurred as a result of matrix constituents (i.e. addition of HCl or metals may enhance analyte response). However, concentrations reported *below* 20 µg L^{-1} indicate that one of three events had occurred: (i) overall ion suppression (without a marked change in analyte concentration over time); (ii) depletion of the parent compound over time due to interaction with matrix constituents (without the formation of PA*N*N compounds); or (iii) depletion of the parent compound as a result of *N*-nitroso compound formation. It should be noted that all vertical axes in Figure 3-10 represent analyte concentrations from 0 to 35 µg L^{-1} except those for ETU and OME, which display concentrations from 0 to 80 µg L^{-1} to show the occurrence of ion enhancement.

Acidification is generally performed by adding concentrated acid to a solution until the desired pH is achieved. However, in this case, different volumes of acid may be required for different analyte solutions to reach the same pH level. Since changes in volume affect concentration (and therefore, quantitation), it was necessary to keep the volume of acid added to all analyte solutions constant. For example, the target pH value for the first round of screening experiments was 2.5 and the addition of 200 µL stock HCl to each test solution resulted in a mean pH value of 2.62 (± 0.10). For the second round, the addition of 155 µL 2.5mM HCl resulted in an average pH value of 5.02 (± 0.21), very close to the targeted pH of 5. Target pH values for experiments involving metals was also 2.5. A volume of 200 µL stock HCl to analyte solutions containing Cu and Fe resulted in mean pH values of 2.22 (± 0.09) and 2.00 (± 0.08), respectively.

Change in analyte concentration over time

For ATR, the most notable decrease in concentration occurred with the addition of Cu from 28.2 to 20.6 µg L^{-1} ATR over 12 hours, while pH ~ 2.5 showed a slight decrease in ATR concentration over time from 26.4 to 24.3 µg L^{-1} (Figure 3-10a). Solutions at pH ~ 5 and with Fe show very little fluctuation in ATR concentration over the duration of the experiment. Concentration did not appear to change significantly with time under any experimental conditions for CAR (Figure 3-10b), DIM (Figure 3-10c), IMI (Figure 3-10e), LIN (Figure 3-10f), and TCPy (Figure 3-10h). Paired t-tests ($\alpha = 0.05$) showed statistically significant differences in mean analyte concentration for IMI (with Fe) and LIN (at pH ~ 2.5) from 4 to 12 hours and for TCPy (with Fe) from 0 to 4 hours, but this was likely due to small variances. Interestingly, it is apparent that low pH conditions, as with experiments at pH ~ 2.5, and Cu and Fe addition, supress analyte response for IMI, LIN, TCPy, and TM (Figure 3-10i). This suppression may be a result of a number of potential interactions with constituents present in the acidic solution, as these analytes present suitable leaving groups that could facilitate the formation of resonance-stabilized reactive intermediates via thermodynamically-supported reactions. These side reactions may occupy reactants, thereby interfering with *N*-nitroso compound formation.

Although a gradual decline in OME concentration over time was observed at pH ~ 2.5 and between 0 and 4 hours with the addition of Cu, neither experiment resulted in a statistically significant change in OME concentration over time (Figure 3-10g). Statistically significant decreases in TM concentration were seen at pH ~ 2.5 and with addition of Cu and Fe over the duration of the experiment (0 to 12 hours). All three concentration curves took on a characteristic “hockey stick” shape. This concentration curve shape was also seen with statistically significant decreases in ETU concentration over time at pH ~ 2.5 and with the addition of Fe, and also with the addition of Cu (although not statistically significant for the latter (Figure 3-10d). Of the four PA*N*N compound formation screening experiments for ETU, pH ~ 5 was the only one that did not result in a marked decrease in ETU concentration over time.

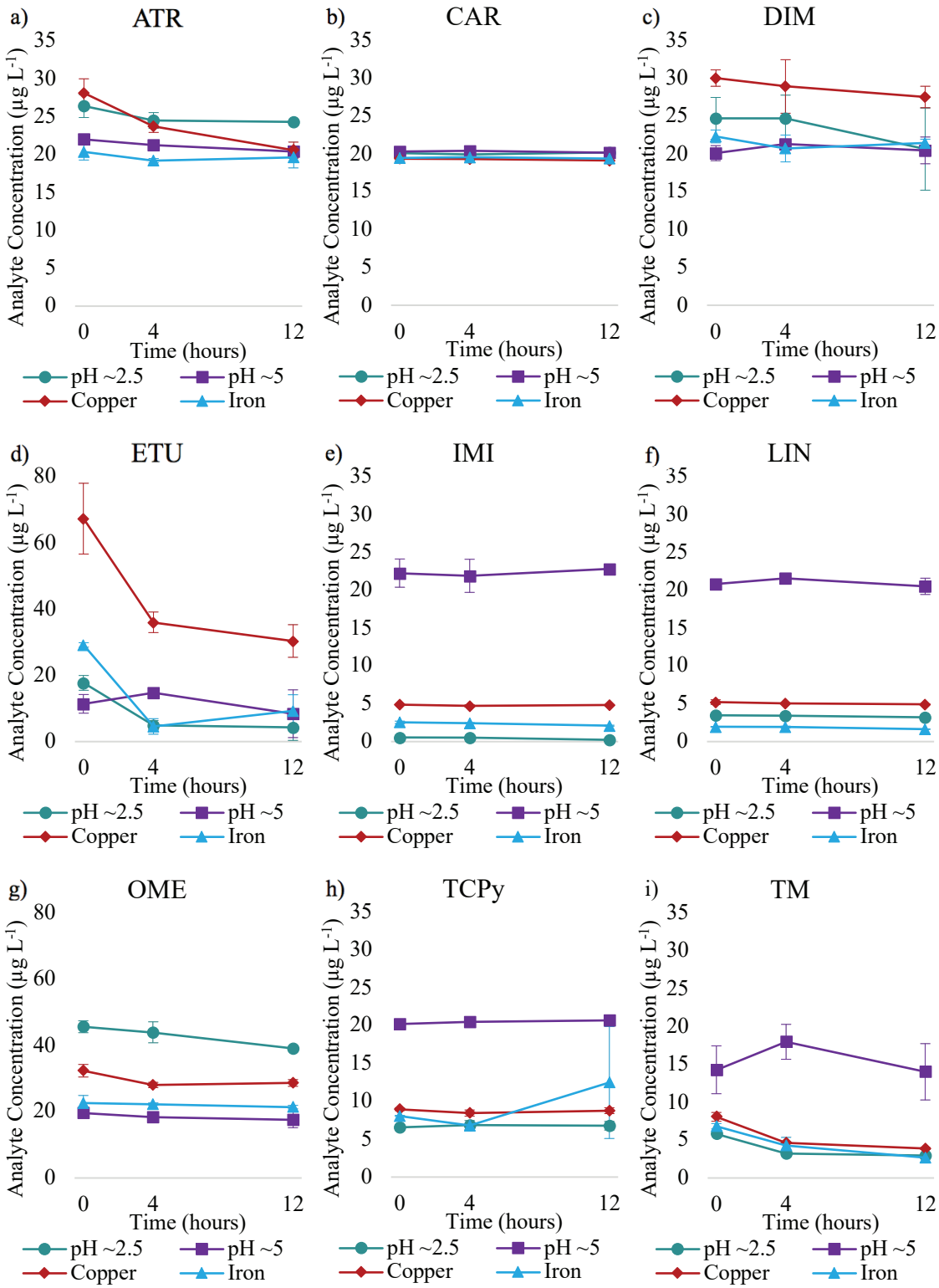

Figure 3-10. Change in analyte concentration at three time points (t = 0, 4, and 12 hours) at pH ~2.5, pH ~5, and with dissolved Cu or Fe for a) ATR; b) CAR; c) DIM; d) ETU; e) IMI; f) LIN; g) OME; h) TCPy; and i) TM.

Extraction of theoretical m/z values of PANN compounds from chromatograms

Following analysis of each test solution, theoretical PA*N*N compound molecular ions listed in Table 3-1, for both positive and negative ionization modes, were extracted from the chromatogram. Of the nine nitrosatable analytes, only ETU appeared to be involved in PA*N*N compound formation. Peaks for theoretical *m/z* values for *N*-ETU were observed in experiments at pH ~ 2.5, and with the addition of Cu and Fe, but not at pH ~ 5 (Figure 3-11). Moreover, the addition of Cu and Fe are associated with higher *N*-ETU responses (*N*-ETU response = 140,000 counts, Figure 3-11c and 3-11d) than with only HCl and $NaNO_2$ (*N*-ETU ion response = 80,000 counts, Figure 3-11a). This is consistent with previous findings that Cu and Fe may catalyze *N*-nitroso compound formation [177]. Only the positive *m/z* value for *N*-ETU was identified in the chromatograms. This is consistent with the observation that in the *N*-ETU synthesis experiment at high concentrations, the peak area ratio of positive to negative mode *N*-ETU *m/z* values was 65:1.

Despite the notable decrease in analyte concentration over time for ATR, OME, and TM, the extracted chromatograms provided no indication of PA*N*N compound formation at any of the time points. Decrease in concentration for these three analytes may be due to competing reactions, such as simple protonation (e.g. OME), the loss of a leaving group with resonance stabilization (e.g. ATR), or both (e.g. TM). These potential outcomes account for analyte depletion without the apparent formation of respective PA*N*N compounds. Chromatograms for ATR at pH ~2.5, pH ~5, and with the addition of Cu and Fe showing ion extractions for *N*-ATR (and the absence of *N*-ATR peaks) are shown in Figure 3-12 (chromatograms for other analytes that do not appear to be participating in PA*N*N compound formation are not shown).

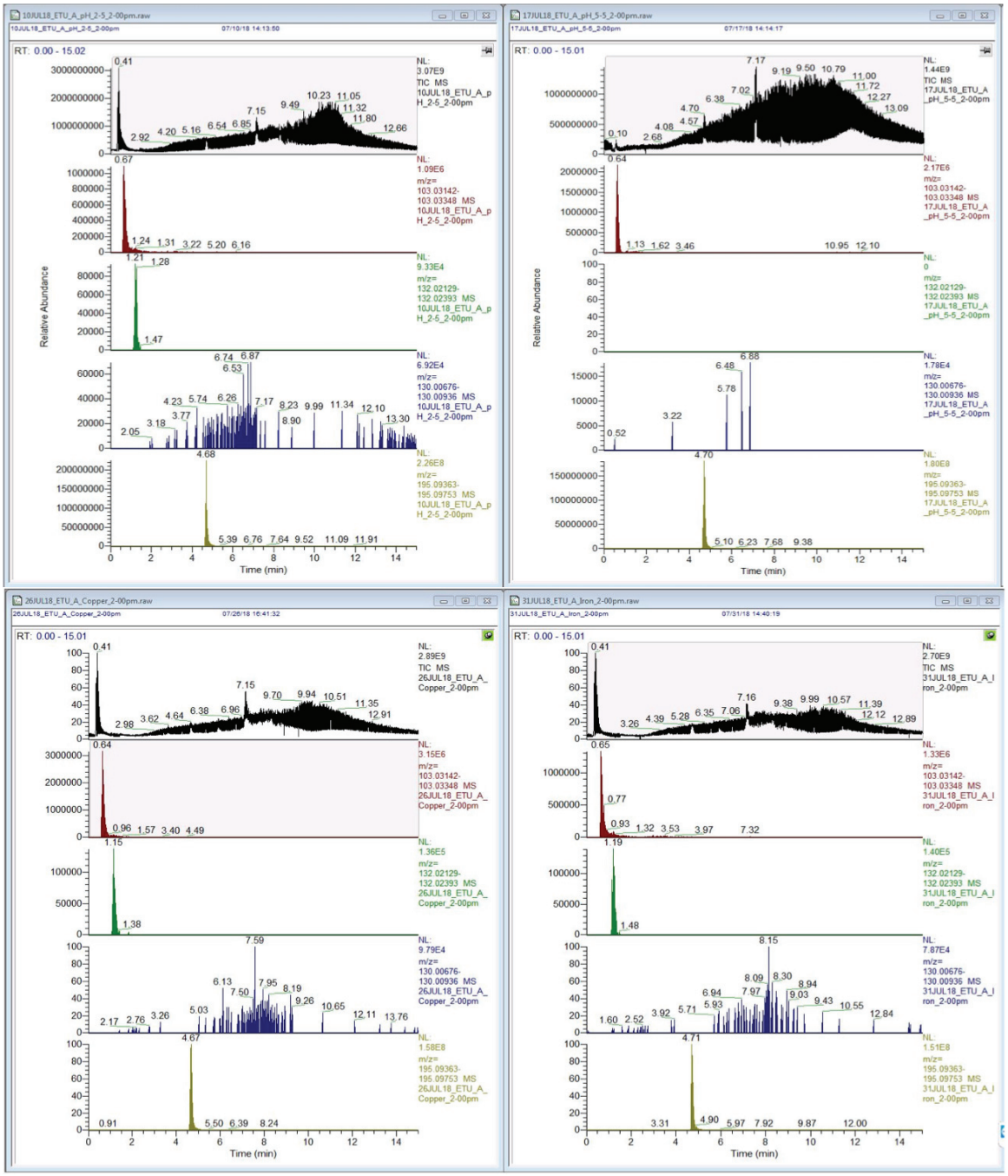

Figure 3-11. Extracted ion chromatograms of *N*-ETU at pH ~ 2.5 (top left); pH ~ 5 (top right); with Cu (bottom left); and with Fe (bottom right). The top row of each chromatogram depicts the total ion count (TIC), the second row represents the extracted ion for ETU, the third and fourth rows show peaks generated by extraction of theoretical *N*-ETU ions in positive and negative ionization modes, respectively, and the bottom row shows the IS peak. Confirmation of the positive mode *N*-ETU peak is shown in green (third row of each chromatogram) in all experiments but at pH ~5.

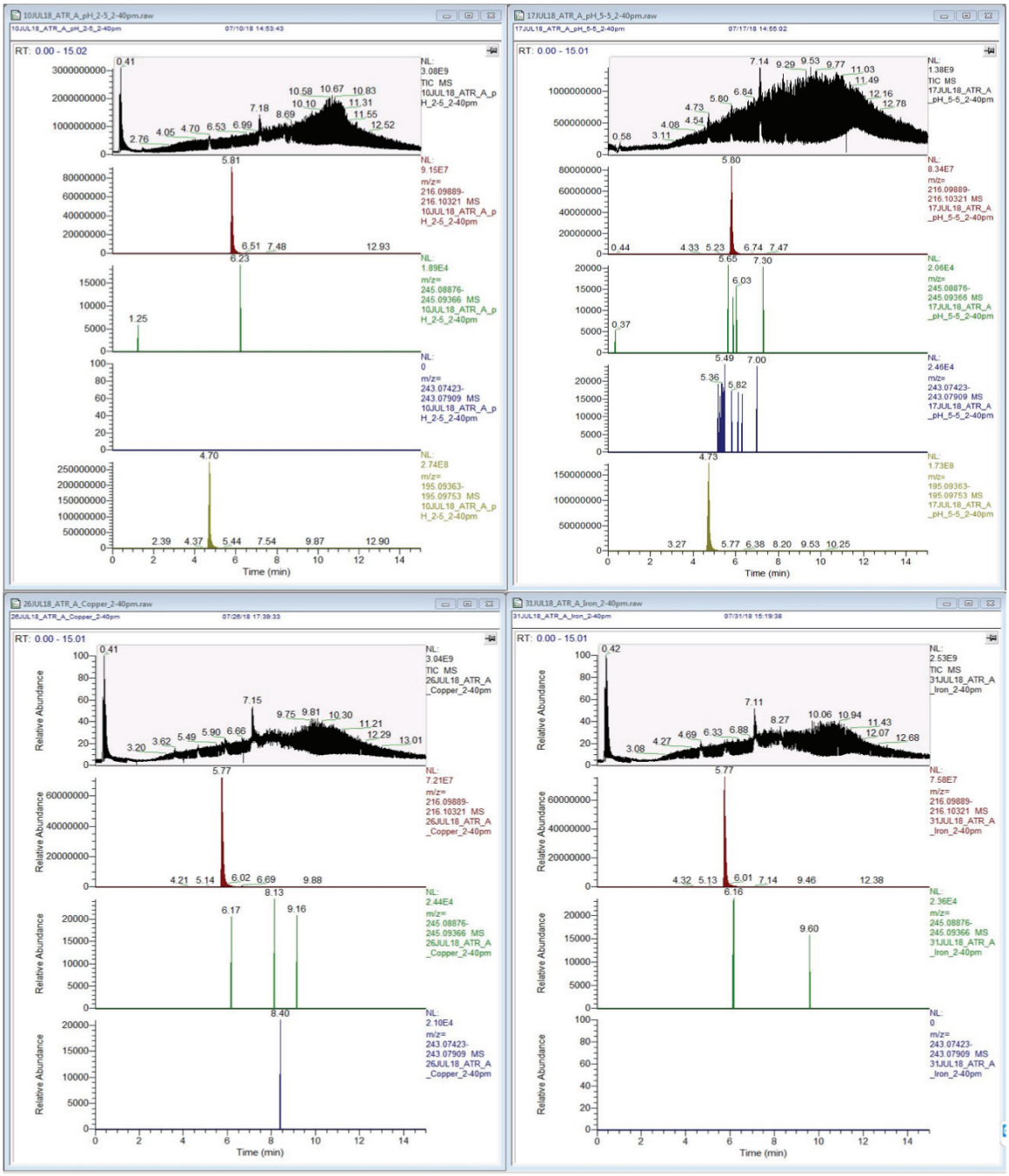

Figure 3-12. Extracted ion chromatograms of *N*-ATR at pH ~ 2.5 (top left); pH ~ 5 (top right); with Cu (bottom left); and with Fe (bottom right). The top row of each chromatogram depicts the total ion count (TIC), the second row represents the extracted ion for ATR, the third and fourth rows show peaks generated by extraction of theoretical *N*-ATR ions in positive and negative ionization modes, respectively, and the bottom row shows the IS peak. The absence of peaks in third and fourth rows of each chromatogram indicates that PA*N*N compound formation has not occurred under these experimental conditions.

3.4.3 UHPLC/HRAM MS, IC, and ICP-MS Analyses of PEI Groundwater Samples

Target analytes in groundwater samples

Five PEI groundwater samples were analyzed by UHPLC/HRAM MS to determine whether target analytes were present in appreciable amounts in any of the samples (Table 3-2). The MDLs and LOQs for each analyte in both matrices are provided in Table 3-3. Two samples from each location were analyzed. None of the groundwater samples contained any of the analytes above the LOQ. In all five samples, ATR was detected in trace amounts, but concentrations were below the MDL of 0.5 μg L^{-1}. CAR and TM were also found in trace amounts in all five samples above the MDLs of 0.1 and 0.7 μg L^{-1}, respectively. However, they could not be accurately quantified because concentrations were below the LOQs of 0.5 and 2.1 μg L^{-1}, respectively. Interestingly, each sample contained very similar quantities of both TM (1.3 to 1.5 μg L^{-1}) and its primary metabolite, CAR (0.4 μg L^{-1} in all five samples). Since CAR is not sold in PEI, it is assumed that its presence in groundwater is a direct result of TM conversion. The U.S. EPA applies a maximum conversion factor of 0.827, derived from results of an aerobic soil metabolism study, to account for TM conversion to CAR [191]. However, the rate of TM conversion to CAR depends on soil pH (conversion is faster in neutral versus acidic soils), microorganism activity, and temperature [192].

Table 3-2. UHPLC/HRAM MS analysis of target compounds in PEI groundwater samples.

Analyte[a]	Mean analyte concentration (μg L^{-1})				
	Sample 1	Sample 2	Sample 3	Sample 4	Sample 5
ATR	< MDL	< MDL	< MDL	< MDL	< MDL
CAR	0.4 ± 0.02[b]	0.4 ± 0.003[b]	0.4 ± 0.005[b]	0.4 ± 0.002[b]	0.4 ± 0.003[b]
DIM	NF[c]	NF	NF	NF	NF
ETU	NF	NF	NF	2.5 ± 0.4[b]	1.1 ± 0.4[b]
IMI	NF	0.9[b]	NF	NF	1.0 ± 0.004[b]
LIN	NF	NF	NF	NF	NF
OME	NF	< MDL	NF	NF	NF
TCPy	< MDL	< MDL	< MDL	NF	NF
TM	1.5 ± 0.02[b]	1.4 ± 0.02[b]	1.3 ± 0.01[b]	1.4 ± 0.04[b]	1.3 ± 0.03[b]

[a]ATR = atrazine; CAR = carbendazim; DIM = dimethoate; ETU = ethylenethiourea; IMI = imidacloprid; LIN = linuron; MCPA = 2-methyl-4-chlorophenoxyacetic acid; OME = omethoate; TCPy = 3,5,6-trichloro-2-pyridinol; TM = thiophanate methyl.
[b]Higher than MDL but below LOQ
[c]NF = not found

Table 3-3. MDLs and LOQs for target analytes in Milli-Q water and a pooled PEI groundwater sample.

Analyte	Milli-Q water		Pooled PEI groundwater sample	
	MDL ($\mu g\ L^{-1}$)	LOQ ($\mu g\ L^{-1}$)	MDL ($\mu g\ L^{-1}$)	LOQ ($\mu g\ L^{-1}$)
ATR	0.6	2.0	0.5	1.5
CAR	0.4	1.3	0.1	0.5
DIM	1.5	4.9	0.6	1.8
ETU	0.5	1.7	1.0	3.2
IMI	1.2	3.8	0.9	2.7
LIN	0.7	2.3	0.6	1.9
OME	1.5	4.9	1.1	3.4
TCPy	0.8	2.5	0.8	2.4
TM	1.0	3.1	0.7	2.1

ETU was detected in two of the five groundwater samples. As with CAR, ETU is not sold or used as a standalone product on PEI but is a common metabolite of two of the most commonly used fungicides in PEI, mancozeb and metiram. Both detections (mean concentrations of 1.1 and 2.5 $\mu g\ L^{-1}$) were above the MDL of 1.0 $\mu g\ L^{-1}$ but below the LOQ of 3.2 $\mu g\ L^{-1}$ in groundwater. Similarly, TCPy is present in PEI environments only as a degradation product of the organophosphorus insecticide chlorpyrifos. The metabolite was detected in three of the five samples at trace levels, but concentrations were below the groundwater MDL of 0.8 $\mu g\ L^{-1}$. IMI was detected in two of the five groundwater samples, one at and one slightly above the MDL of 0.9 $\mu g\ L^{-1}$ but both concentrations were below the LOQ of 2.7 $\mu g\ L^{-1}$. DIM, LIN, and OME were not found (NF) in any of the samples.

As all analyte concentrations in the PEI groundwater samples were below respective LOQs and substantially lower than those used in PA*N*N compound formation experiments, it was presumed that analyte concentrations in a pooled groundwater sample would be unlikely to interfere with PA*N*N compound formation. Analyte concentrations in a pooled groundwater sample were considered negligible, not necessarily from a public health perspective, but for the purpose of conducting subsequent PA*N*N compound formation experiments. Therefore, it was deemed appropriate for a pooled groundwater sample to be made from all five samples to assess PA*N*N compound formation in groundwater.

Nitrate and nitrite in groundwater samples

IC analysis was performed to determine existing concentrations of nitrate and nitrite in groundwater samples (Table 3-4). Duplicates of each sample were tested. Nitrite was not detected in any of the samples. Nitrate concentration ranged from 7.3 to 26.5 mg L^{-1}, below the MAC of 45 mg L^{-1}.

Table 3-4. IC analysis of nitrate and nitrite in PEI groundwater samples.

Analyte[1]	Mean anion concentration (mg L^{-1})				
	Sample 1	Sample 2	Sample 3	Sample 4	Sample 5
Nitrate	7.3 ± 0.2	23.0 ± 0.3	19.9 ± 0.3	13.9 ± 0.1	26.5 ± 0.4
Nitrite	NF	NF	NF	NF	NF

Nitrate MAC = 45 mg L^{-1}; nitrite MAC = 3 mg L^{-1} [179].

Elements of interest in groundwater samples

PEI groundwater samples were analyzed by ICP-MS for the 12 elements of interest (Table 3-5). Concentrations were reported with at least two significant figures and a standard deviation having at least one significant figure and one decimal place. None of the samples contained any element above its health-based drinking water guideline. Copper concentration, a potential nitrosation catalyst, varied greatly among samples (2.2 to 103.7 µg L^{-1}). Iron, another presumed catalyst in the nitrosation reaction, was detected in four of the five samples at a concentration between 1.0 and 10.8 µg L^{-1}. Instrument limits of detection (LODs) for each parameter are given beneath Table 3-5.

Table 3-5. ICP-MS analysis of groundwater samples for target metals and other elements associated with *N*-nitroso compound formation or included in routine testing of PEI groundwater that have health-based drinking water guidelines and assigned MACs [179,188].

Element[a]	Mean elemental concentration (μg L^{-1})[b]				
	Sample 1	Sample 2	Sample 3	Sample 4	Sample 5
^{75}As	2.89 ± 0.05	2.04 ± 0.03	0.350 ± 0.004	0.23 ± 0.01	1.07 ± 0.07
^{137}Ba	54.5 ± 0.7	3.0 ± 0.7	1.1 ± 0.2	270.1 ± 6.4	756.6 ± 23.3
^{111}Cd	BDL	BDL	0.000682 ± 0.000005	0.0016 ± 0.0007	BDL
^{52}Cr	0.33 ± 0.01	0.28 ± 0.06	0.1821 ± 0.0005	0.17 ± 0.01	0.174 ± 0.003
^{63}Cu	27.8 ± 3.4	2.6 ± 0.4	103.7 ± 46.8	12.3 ± 1.7	2.2 ± 1.2
^{57}Fe	1.2 ± 0.7	1.0 ± 0.6	BDL	5.2 ± 1.6	10.8 ± 1.8[c]
^{55}Mn	0.017 ± 0.002	BDL	0.023 ± 0.017	0.11 ± 0.02	Excluded[d]
^{60}Ni	0.050 ± 0.002	0.079 ± 0.036	0.62 ± 0.09[c]	0.086 ± 0.019	0.12 ± 0.05
^{208}Pb	0.034 ± 0.008	0.034 ± 0.003	0.39 ± 0.22	0.061 ± 0.043	Excluded[d]
^{77}Se	0.014 ± 0.009	0.015 ± 0.005	BDL	BDL	0.0095 ± 0.0001
^{238}U	0.93 ± 0.03	0.43 ± 0.01	0.0235 ± 0.0005	0.087 ± 0.003	0.39 ± 0.02

[a]As = arsenic (MAC = 10 μg L^{-1}, LOD = 0.0024 μg L^{-1})
Ba = barium (MAC = 1,000 μg L^{-1}, LOD = 0.052 μg L^{-1})
Cd = cadmium (MAC = 5 μg L^{-1}, LOD = 0.00018 μg L^{-1})
Cr = chromium (MAC = 50 μg L^{-1}, LOD = 0.0081 μg L^{-1})
Cu = copper (aesthetic objective = 1,000 μg L^{-1}, LOD = 0.0032 μg L^{-1})
Fe = iron (aesthetic objective = 300 μg L^{-1}, LOD = 0.14 μg L^{-1})
Mn = manganese (MAC = 120 μg L^{-1}, LOD = 0.015 μg L^{-1})
Ni = nickel (MAC = N/A, LOD = 0.00062 μg L^{-1})
Pb = lead (MAC = 10 μg L^{-1}, LOD = 0.0078 μg L^{-1})
Se = selenium (MAC = 50 μg L^{-1}, LOD = 0.13 μg L^{-1})
U = uranium (MAC = 20 μg L^{-1}, LOD = 0.00057 μg L^{-1})
[b]BDL = below detection limit
[c]Due to suspected contamination of one of the sample pair, one sample was analyzed twice
[d]Measurement excluded due to inconsistent element responses

3.4.4 *N*-ETU Formation in Pooled PEI Groundwater Sample

To determine if there are differences in rate and magnitude of *N*-ETU formation in pure water versus a real groundwater sample, *N*-ETU formation was assessed at 30-minute intervals over four hours in Milli-Q water and in a pooled PEI groundwater sample (n=3). Both sets of experiments involved initial analyte concentrations of 20 μg L^{-1} and 2.5 mg L^{-1} of $NaNO_2$ with a target pH value of 2.5. At the beginning of the experiment, the Milli-Q

water and groundwater sample pH values were 2.09 (± 0.08) and 2.08 (± 0.16), respectively. After four hours, the pH measured 2.27 (± 0.13) for the Milli-Q water and 2.30 (± 0.05) for the groundwater. This insignificant difference in pH between the two media shows that the buffering capacity of this particular groundwater sample is not sufficient in preventing the pH from dropping to a value similar to that of Milli-Q water.

In both media, an increase in *N*-ETU/IS peak area ratios was most prominent in the first 30 minutes while a marked decrease in ETU/IS peak area ratios occurred in the same time frame (Figure 3-13). In addition, neither ETU nor *N*-ETU response appeared to change significantly after 60 minutes. At this starting ETU concentration of 20 μg L^{-1}, the peak area ratio of ETU:*N*-ETU from 60 minutes to four hours was slightly lower in groundwater (25 ± 3:1) than in Milli-Q water (30 ± 3:1). While the rate of *N*-ETU formation in groundwater appeared to coincide with that in Milli-Q water, the larger peak areas for *N*-ETU in Milli-Q water indicate that groundwater constituents (e.g. dissolved ions) may inflict an overall suppressive effect on *N*-ETU response or directly interfere with *N*-ETU formation. This is understandable, as Milli-Q water contains far fewer reactants that may potentially suppress ETU response or participate in competing reactions.

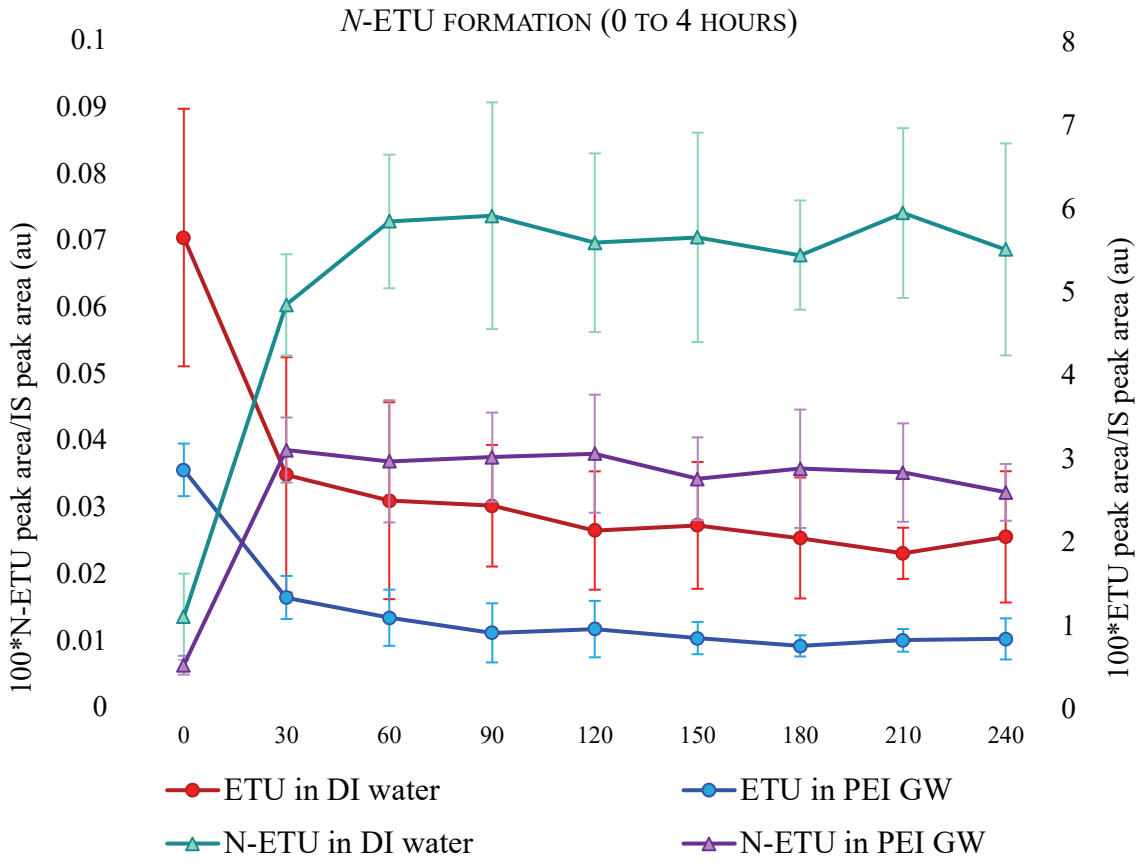

Figure 3-13. Change in *N*-ETU and ETU response (expressed as 100*analyte peak area/IS peak area) in 30-minute increments over 4 hours in Milli-Q water and a pooled PEI groundwater sample (target pH = 2.5; n=3). In both media, the first 30 minutes showed a significant increase in *N*-ETU/IS peak area ratio and a marked decrease in ETU/IS peak area ratio. Overall *N*-ETU peak area ratios were larger in Milli-Q water than in groundwater.

3.4.5 *N*-ETU Formation with Lower Initial Concentrations of ETU

Further *N*-ETU formation experiments were conducted with a series of lower initial ETU concentrations (10, 7.5, and 5 µg L^{-1}), 2.5 mg L^{-1} of $NaNO_2$, and a target pH value of 2.5 to determine the lowest starting ETU concentration that produced a detectable level of *N*-ETU in PEI groundwater. The mean pH value of analyte solutions for this set of experiments was 2.36 (± 0.09). Since *N*-ETU peak area reached a maximum at 30 minutes during *N*-ETU formation in PEI groundwater over four hours and did not change significantly for the remainder of the experiment, samples were analyzed after 60 minutes.

N-ETU formation was observed after one hour with initial ETU concentrations of 10 and 7.5 µg L^{-1}, but not at 5 µg L^{-1} (Figure 3-14a). For this reason, experiments with starting concentrations of 2.5 µg L^{-1} were not carried out. As expected, *N*-ETU peak area decreased with lower ETU starting concentrations, as there is less of the reactant species to participate in the *N*-ETU formation reaction. Interestingly, compared to the ETU/*N*-ETU peak area ratio of 25 ± 3:1 in groundwater (between 60 minutes and four hours) with a starting ETU concentration of 20 µg L^{-1}, ETU/*N*-ETU peak area ratios for initial ETU concentration of 10 and 7.5 µg L^{-1} at the 60-minute mark were 16:1 and 12:1, respectively (Figure 3-14b). Stated another way, the peak area ratio of ETU:*N*-ETU decreases as initial ETU concentration decreases, which may indicate that the *N*-ETU formation reaction becomes more favourable as starting ETU concentration decreases. It is unclear what is causing this observed effect, as the opposite (a larger peak area ratio) was expected based on simple kinetic laws. However, this may be due to the increase in the molar ratio between $NaNO_2$ and ETU, as $NaNO_2$ concentration remained at 2.5 mg L^{-1} while ETU concentration decreased.

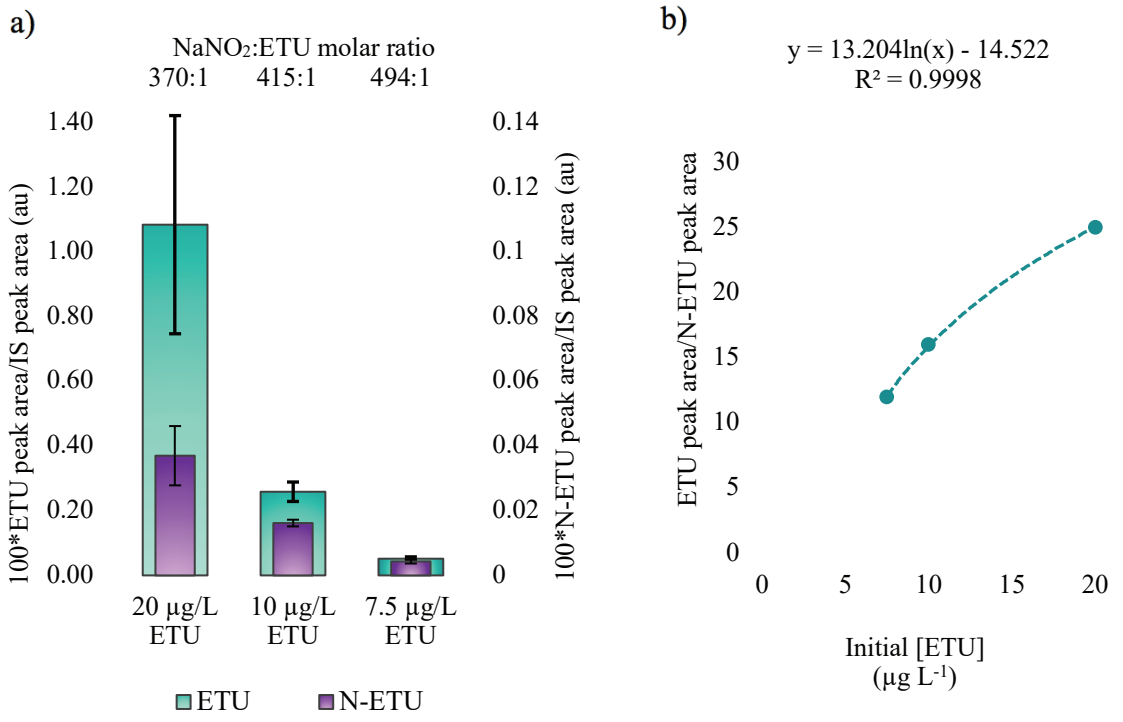

Figure 3-14. a) Peak area ratios of ETU/ID and *N*-ETU/IS at initial ETU concentrations of 10 and 7.5 µg L^{-1} at pH 2.36 (± 0.09); b) ETU peak area/*N*-ETU peak area decreases on a logarithmic scale as initial ETU concentration is lowered.

3.5 Conclusions

ETU is a contaminant of concern in PEI environments for several reasons. First, it is a common metabolite of two parent compounds (mancozeb and metiram) that are currently two of the most widely used pest control products on the island, with a combined amount of 343,492 kg a.i. sold in 2014 [86]. In fact, the Pest Management Regulatory Agency (PMRA) is currently in the process of reissuing a Proposed Re-evaluation Decision document for mancozeb and its associated end-use products (e.g. ETU) [193]. Second, ETU is classified by the U.S. EPA as a Group B Probable Human Carcinogen [11]. In addition, based on its high water solubility (20,000 mg L^{-1}) and low K_{OC} (13 L kg^{-1}), ETU is a potential groundwater contaminant [109,110].

The results of this study suggest that ETU present at environmentally relevant concentrations (20, 10, and 7.5 µg L^{-1}) is capable of forming the highly carcinogenic *N*-ETU in a pooled PEI groundwater sample at pH values comparable to that of gastric pH. *N*-ETU formation was rapid, with greatest analyte peak area observed after 30 minutes, but it is possible that formation peaks earlier. Despite the presence of numerous ions and dissolved minerals in the pooled groundwater sample that may participate in competing side reactions with ETU, *N*-ETU formation was still observed.

One potential limitation of this study is that the pooled groundwater sample used in the PA*N*N compound formation experiment may not be representative of all PEI watersheds. Groundwater composition varies between watersheds, depending upon a number of both natural (e.g. mineral content) and anthropogenic (e.g. agricultural activity) factors. It is possible that groundwater in other areas of the island contain different levels of elements that may interfere with *N*-ETU formation. Another limitation of this work is that it is not known with certainty if the analytical method is capable of detecting other semi-targeted PA*N*N compounds that were not confirmed via in-house synthesis. Although there was no evidence presented here that any analyte other than ETU participated in PA*N*N compound formation, the reaction may still have occurred without being detected by this method (i.e. PA*N*N compounds may have remained undetected due to method incompatibility, as the assumption is that the method suitable for the parent compound is also suitable for its respective PA*N*N compounds).

Future studies may aim to refine this method with a specific focus on *N*-ETU formation and quantitation. In doing so, the method run time could be reduced, thereby allowing evaluation of *N*-ETU formation in less than 30-minute intervals. Additionally, further development could be done to lower the MDL and LOQ for ETU so that *N*-ETU formation from lower concentrations of ETU may be assessed. It would also be advantageous to synthesize the remaining analytes at high concentrations and analyze them using HRAM MS to determine their retention times and experimental *m/z* values using this analytical method. Further testing of PA*N*N compound formation could involve a greater pH variation (to account for individual differences in gastric pH), PA*N*N compound formation at physiological temperature or in human gastric fluid, or different concentrations of $NaNO_2$.

It remains uncertain whether the following factors provide the perfect storm for endogenous PA*N*N compound formation: low gastric pH; nitrate-to-nitrite conversion within the body; and ingestion of groundwater containing trace amounts of nitrosatable pesticides. However, based on the results of this work, it is believed that endogenous *N*-ETU formation is a legitimate concern. Perhaps a first step would be to include ETU as a measured analyte in the PEI pesticide monitoring program. Ultimately, it would be beneficial to further this research through a biomonitoring study of nitrosatable pesticides in PEI, notably ETU and *N*-ETU.

Chapter 4: Analysis of Human Serum and Urine for Tentative Identification of Potentially Carcinogenic Pesticide-Associated *N*-nitroso Compounds using a Semi-Targeted Approach

4.1 Abstract

Human serum and urine samples were analyzed for a suite of nitrosatable pesticides and potentially carcinogenic pesticide-associated *N*–nitroso (PA*N*N) compounds. Formation of PA*N*N compounds may occur *in vivo* after consumption of food or water containing trace amounts of nitrosatable pesticide residues and nitrite. Using a modified version of the Quick, Easy, Cheap, Effective, Rugged, and Safe (QuEChERS) method, 10 nitrosatable pesticides and byproducts were extracted from serum and urine from 64 individuals from two different sample populations: (i) Prince Edward Island, a region where nitrate and trace amounts of nitrosatable pesticides have been detected in groundwater; and (ii) Halifax, Nova Scotia, a non-agricultural urban area. Samples were then analyzed using UHPLC coupled with HRAM orbital ion trap MS, which allows for semi-targeted analysis and tentative identification of a virtually limitless number of biomarkers retrospectively. Two nitrosatable target analytes, ethylenethiourea (ETU), a common metabolite of EBDCs, and 3,5,6-trichloro-2-pyridinol (TCPy), a metabolite of organophosphate insecticides chlorpyrifos and chlorpyrifos-methyl, were found in serum, while ATR, a triazine herbicide, and ETU were detected in urine. Six and 10 PA*N*N compounds were tentatively identified in serum and urine, respectively. The two PA*N*N compounds that were most frequently tentatively identified in serum were *N*-nitroso dimethoate (*N*-DIM) and *N*-nitroso omethoate (*N*-OME) with a detection frequency of 78% and 95%, respectively. In urine, significantly more tentative identifications were found in PEI samples for di-*N*-nitroso carbendazim (di-*N*-CAR, $p = 0.045$). This is the first biomonitoring study of its kind to investigate PA*N*N compounds in human serum and urine.

Keywords: pesticide-associated *N*-nitroso (PA*N*N) compounds, UHPLC/HRAM orbitrap MS, serum, urine, biomonitoring, QuEChERS.

4.2 Introduction

Exposure to pesticides is a global health concern. The general population can be exposed to pesticides through drift during and following application, contamination of drinking water and food, and bioconcentration through the food chain [14]. While direct analysis of pesticides in an individual's environment provides an estimate of exposure, it is not always feasible nor does it offer information about the absorption (internal dose) of the pesticide, which is most relevant for assessing health risk [194]. Pesticide biomonitoring allows investigation of *endogenously* formed compounds resulting from pesticide exposure. The potential formation of *N*-nitroso compounds *in vivo* through the interaction between nitrosatable pesticides and nitrite in the acidic but favourable environment of the stomach warrants investigation [44]. The IARC lists over 30 PA*N*N compounds, many of which have been investigated for carcinogenicity potential [44]. In short-term mutagenicity tests, several PA*N*N compounds have been shown to induce DNA damage, mitotic gene conversion, gene mutation, mitotic recombination, chromosomal aberrations, sister chromatid exchange, and dominant lethal mutation. In some cases, PA*N*N compounds exhibit higher carcinogenic potential than their parent pesticides [48,56].

One region particularly vulnerable to exposure to PA*N*N compound precursors is Prince Edward Island (PEI). PEI has been reported to have the highest pesticide use intensity of all Canadian provinces [8]. Several of the pesticides sold in PEI are nitrosatable, including ATR, DIM, IMI, LIN, and TM [86]. The island also has a history of pesticide and nitrate contamination of its surface waters and aquifer [61,62,65–67,174,176,180,195]. It is also the only Canadian province that uses groundwater as the sole source of drinking water for its residents [196]. Considering its vulnerability to agricultural pollution, PEI groundwater contaminated with nitrate and nitrosatable pesticides presents a potential pathway of human exposure to potentially carcinogenic *N*-nitroso compounds in PEI. Furthermore, PEI has also seen consistently higher than national cancer incidence rates [68]. Many concerned residents and health professionals have attributed extensive pesticide use to the increased cancer rates in PEI [197].

The main objective of this cross-sectional biomonitoring study was to employ HRAM MS to identify specific pesticide-related biomarkers in human serum and urine from a healthy sample population in an area of intense agriculture in PEI and from a healthy

sample population in Halifax, a non-agricultural urban area. The hypothesis of this research was that potentially carcinogenic *N*-nitroso compounds formed endogenously after exposure to drinking water contaminated with nitrosatable pesticides and nitrates (e.g., PEI residents drinking well water) and other pesticide-related metabolites may be detected as biomarkers in biofluids of individuals living in areas of intensive pesticide use. It was also expected that significantly lower concentrations and fewer detections of these biomarkers would be observed in biofluids of individuals living in areas of non-intensive pesticide use (e.g., Halifax residents drinking tap water).

4.3 Materials and Methods

Biomarkers of interest were allocated into three groups. Group I was comprised of 10 nitrosatable pesticides and degradation products used in PEI agriculture. These compounds were considered target analytes because the availability of certified analytical standards allowed their identification and quantitation. Group II analytes included PA*N*N compounds that could potentially have formed endogenously after exposure to nitrate (converted in the body to nitrite) and analytes in Group I. Since reference standards were not obtained for Group II analytes (a majority were not commercially available), Group II compounds were analyzed using a semi-targeted approach with tentative identification based on their theoretical accurate mass calculations. Group III was comprised of other common biomarkers associated with target compounds in Group I. As with Group II, quantitation of these analytes was not feasible without obtaining analytical standards. Therefore, Group III compounds were analyzed using a semi-targeted approach with tentative identification. Three focused objectives for this work were established: (i) to analyze serum and urine samples from the two sample populations for biomarkers from analyte Groups I, II, and III; (ii) to determine if there were significant differences in mean concentrations of target analytes (Group I) or number of biomarker detections (Groups II and III) in serum or urine of the two sample populations; and (iii) to determine specific biomarkers of concern for the two sample populations and formulate strategies for future biomonitoring studies.

4.3.1 Analytes of Interest

An analytical method was developed and validated for identification and quantitation of Group I analytes in human serum and urine. Group I was comprised of the pesticides ATR, DIM, IMI, LIN, and TM, as well as degradation products ETU, CAR, TCPy and OME. All analytes of interest are capable of forming *N*-nitroso compounds through interaction with nitrite. MCPA, a phenoxy herbicide, was also included in the study because even though it is not nitrosatable, it is often contaminated with NDMA [104]. In addition, Group I analytes are expected to be contaminants of concern in Atlantic Canadian environments in terms of toxicity and exposure, based on provincial pesticide sales reports and detections in air and groundwater samples [60,62,86,149].

Group II compounds included 15 PA*N*N compounds: *N*-ATR; *N*-CAR; *N*-DIM; *N*-ETU; *N*-IMI; *N*-LIN; *N*-OME; *N*-TCPy; and *N*-TM. In addition, PA*N*N compounds with more than one *N*-nitroso (N–N=O) functional group potentially formed from target analytes were also included in Group II: di-*N*-ATR; di-*N*-CAR; di-*N*-ETU; di-*N*-TM; tri-*N*-TM; and tetra-*N*-TM.

Group III was comprised of six biomarkers associated with target analytes. Atrazine mercapturate (AM), diaminochlorotriazine (DACT), and DEA are urinary metabolites of ATR. These ATR metabolites were included as priority biomarkers of exposure in the *Second Report on Human Biomonitoring of Environmental Chemicals in Canada;* however, more than 99% of all samples tested were below the detection limit of 0.03, 1, and 0.2 μg L^{-1}, for AM, DACT, and DEA, respectively [198]. Methyl 5-hydroxy-2-benzimidazole carbamate (5-HBC), a metabolite of both TM and carbendazim, [191] ethylene urea (EU), a metabolite of ETU, and 3,4-dichloroaniline (3,4-D), a metabolite of LIN [109,112], were included as Group III analytes. All 31 target and semi-target analytes are listed in Table 4-1.

Table 4-1. Molecular formula, molar mass, and theoretical *m/z* values for the molecular ion of each target and semi-target analyte. Parent compounds (Group I analytes) are highlighted in bold.

PA*N*N compound	Molecular formula	Molar mass (g mol^{-1})	$[M+H]^+$ theoretical mass (*m/z*)	$[M-H]^-$ theoretical mass (*m/z*)
ATR	$C_8H_{14}ClN_5$	215.68	216.10105	N/A
N-ATR	$C_8H_{13}ClN_6O$	244.08	245.09121	243.07666
di-*N*-ATR[a]	$C_8H_{12}ClN7O_2$	273.68	274.08138	272.06682
AM[b]	$C_{13}H_{22}N_6O_3S$	342.42	343.15469	341.14013
DACT[c]	$C_3H_4ClN_5$	145.55	146.02280	144.00825
DEA[d]	$C_6H_{10}ClN_5$	187.63	188.06975	186.05520
CAR	$C_9H_9N_3O_2$	191.19	192.07675	N/A
N-CAR	$C_9H_8N_4O_3$	220.06	221.06692	219.05236
di-*N*-CAR[a]	$C_9H_7N_5O_4$	249.18	250.05708	248.04253
DIM	$C_5H_{12}NO_3PS_2$	229.26	230.00690	N/A
N-DIM	$C_5H_{11}N_2O_4PS_2$	257.99	258.99706	256.98251
ETU	$C_3H_6N_2S$	102.16	103.03245	N/A
N-ETU	$C_3H_5N_3OS$	131.02	132.02261	130.00806
di-*N*-ETU[a]	$C_3H_4N_4O_2S$	160.15	161.01277	158.99822
EU[e]	$C_3H_6N_2O$	86.09	87.05529	85.04074
IMI	$C_9H_{10}ClN_5O_2$	255.66	N/A	254.04503
N-IMI	$C_9H_9ClN_6O_3$	284.04	285.04974	283.03519
LIN	$C_9H_{10}Cl_2N_2O_2$	249.09	N/A	247.00466
N-LIN	$C_9H_9Cl_2N_3O_3$	277.00	278.00937	275.99482
3,4-D[f]	$C_6H_5Cl_2N$	162.02	161.98718	159.97263
MCPA	$C_9H_9ClO_3$	200.62	N/A	199.01675
OME	$C_5H_{12}NO_4PS$	213.19	214.02974	N/A
N-OME	$C_5H_{11}N_2O_5PS$	242.01	243.01991	241.00535
TCPy	$C_5H_2Cl_3NO$	198.43	N/A	195.91292
N-TCPy	$C_5HCl_3N_2O_2$	225.91	226.91764	224.90308
TM	$C_{12}H_{14}N_4O_4S_2$	342.39	N/A	341.03837
N-TM	$C_{12}H_{13}N_5O_5S_2$	371.04	372.04309	370.02853
di-*N*-TM[a]	$C_{12}H_{12}N_6O_6S_2$	400.39	401.03325	399.01870
tri-*N*-TM[g]	$C_{12}H_{11}N_7O_7S_2$	429.39	430.02341	428.00886
tetra-*N*-TM[h]	$C_{12}H_{10}N_8O_8S_2$	458.39	459.01358	456.99902
5-HBC[i]	$C_9H_9N_3O_3$	207.19	208.07167	206.05711

[a]PA*N*N compounds formed by nitrosation at two sites on parent analyte
[b]AM=Atrazine mercapturate
[c]DACT = diaminochlorotriazine
[d]DEA= desethylatrazine
[e]EU = ethylene urea
[f]3,4-D = 3,4-dichloroaniline
[g] PA*N*N compounds formed by nitrosation at three sites on parent analyte
[h] PA*N*N compounds formed by nitrosation at four sites on parent analyte
[i]5-HBC = methyl 5-hydroxy-2-benzimidazole carbamate

4.3.2 Study Design

This biomonitoring study involved the profiling of nitrosatable pesticides, PA*N*N compounds, and other pesticide-derived biomarkers in human serum and urine for two populations living in areas of different pesticide use intensities: (1) 32 healthy adults residing at least five years in PEI, particularly in areas where groundwater nitrate contamination, an indicator of agricultural pesticide use, was more than 3 mg L^{-1}; and (2) 32 healthy adults residing in Halifax, NS, for at least five years, which represented as the urban area control group (age- and sex-matched). Data and biological samples for this project were provided by the Atlantic Partnership for Tomorrow's Health (Atlantic PATH) study. The Atlantic PATH study is part of the Canadian Partnership for Tomorrow Project, a pan-Canadian longitudinal cohort study examining the role of genetic, environmental, behavioural, and lifestyle factors in the development of cancer and chronic disease [199]. Atlantic PATH collected data from 31,173 individuals aged 35-69 across Atlantic Canada, including information on health and health-related measures, as well as biological samples including blood, urine, saliva, and toenails [200].

The number of participants in each sample population fits the criteria for a discovery study outlined by Dunn et al. (2011) [201]. A discovery study generally involves tens or low hundreds of samples from two independent populations. Rigorously designed discovery studies are small enough to be financially feasible as a pilot study but provide preliminary data essential for the design of large-scale epidemiological studies. Considering analytical costs, we selected a sample size of 32 participants per location. This study was approved by the Dalhousie Research Ethics Board (REB application #: 2017-4382).

4.3.3 Inclusion/Exclusion Criteria

Atlantic PATH analysts screened their dataset and identified 189 PEI participants who reported a minimum of a five-year residence history and well water as the primary source of drinking water. Postal code data for these 189 participants were cross-referenced with a groundwater nitrate concentration map to identify 38 participants residing in areas with groundwater nitrate concentration of 3 mg L^{-1} or more (Figure 4-1). Of these 38 participants, 32 were randomly chosen for inclusion in this study. For the Halifax, NS

group, 32 participants were randomly chosen from those with a minimum of a five-year residence history in Halifax and municipal water as the primary source of drinking water.

Certain types of illness may affect metabolism and, ultimately, the expression of pesticide-associated biomarkers in serum and urine. To account for potentially confounding or effect modifying factors associated with pesticide biomarker expression, participants with a diagnosis of cancer or conditions that could affect metabolism via kidney and/or liver damage (diabetes, liver cirrhosis, chronic hepatitis, lupus, or Crohn's disease) were excluded from the study.

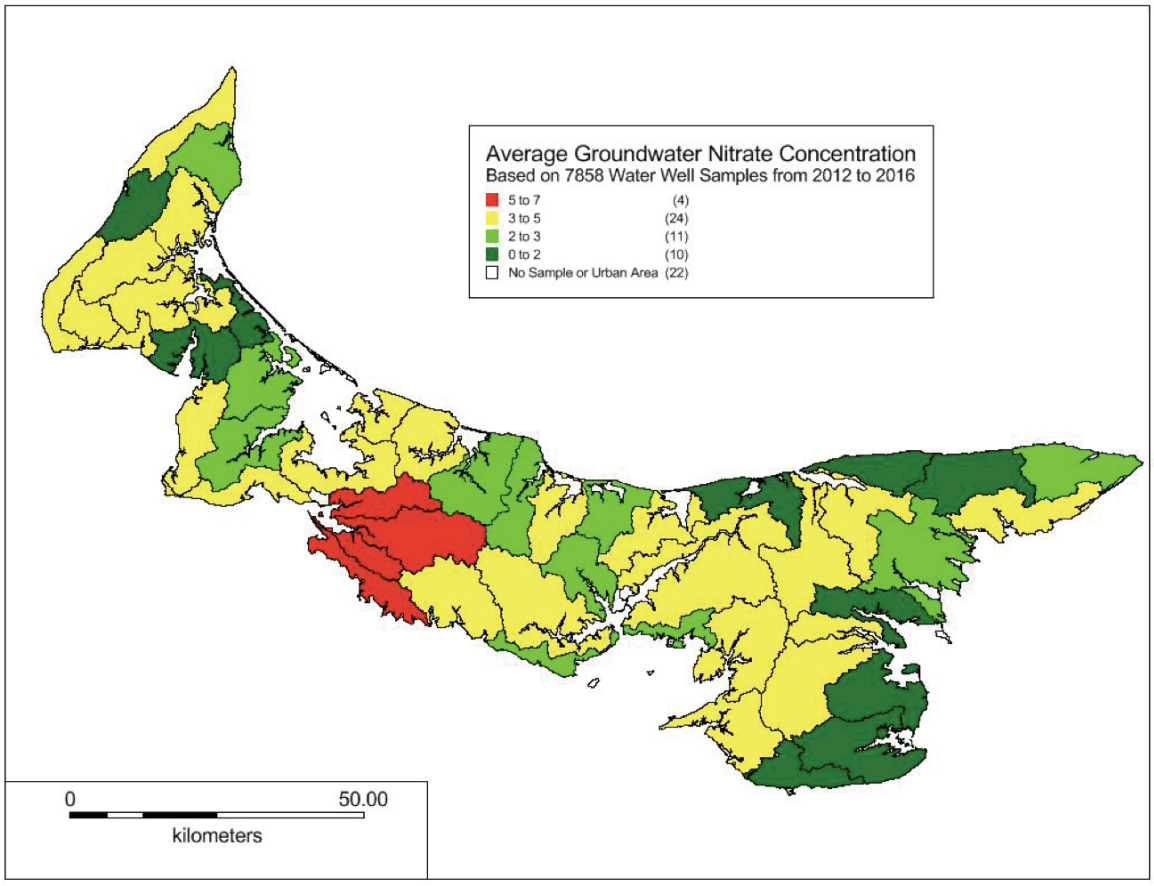

Figure 4-1. Average concentrations of groundwater nitrate in PEI (2012-2016) as an indicator of agricultural pesticide use (Government of Prince Edward Island. 2017. Groundwater Nitrate Concentration Map: 2012 to 2016 [202]).

4.3.4 Analytical Standards, Solvents, and Reagents

Analytical standards for the following target analytes were purchased individually from Chromatographic Specialties (Brockville, ON, CA): ATR, CAR, DIM, ETU, IMI, LIN, MCPA, OME, TCPy, and TM. Carbendazim-d3 was chosen as the IS and was obtained in neat form from Sigma Aldrich Canada Co. (Oakville, ON, CA). The tuning solutions for accurate mass calibration, Pierce LTQ Velos ESI Positive Ion Calibration Solution and Pierce ESI Negative Ion Calibration Solution, were provided by Thermo Fisher Scientific (Waltham, MA, US).

All solvents and reagents used in this study were of HPLC-grade. MeOH, ACN, and ACROS Organics formic acid (>98% pure) were obtained from Thermo Fisher Scientific (Fair Lawn, NJ, US). Human sera (SKU: S7023-50ML), Surine™ Negative Urine Control (SKU: S-020), and AcOH were purchased from Sigma-Aldrich Canada Co. (Oakville, ON, CA). Certified ACS NaOAc anhydrous fused crystals, certified $MgSO_4$ anhydrous powder, and certified ACS crystalline NaCl were obtained from Fisher Chemical (Fair Lawn, NJ, US). Ultrapure laboratory grade water was obtained from the Milli-Q plus system (Milli-Q water, Millipore, Bedford, MA, US). Ultra-high purity nitrogen for sample concentration was obtained from Praxair Canada (Dartmouth, NS, CA). SOLA™ HRP SPE cartridges (10 mg) were obtained from Thermo Scientific (Waltham, MA, US). Oasis HLB (30 mg) and Oasis PRiME HLB (10 mg) SPE cartridges were obtained from Waters (Milford, MA, US).

4.3.5 Sample Preparation

Following standard collection procedures, urine and serum samples were collected by Atlantic PATH between 2009 and 2015 and stored at −80 °C until analysis. Samples were analyzed in batches of seven or eight with three consecutive batches extracted each day for a total of 22 sample extractions per day. Samples were allowed to thaw at 4 ºC overnight. On the day of analysis, samples were prepared for the QuEChERS method by vortexing 1-mL aliquots for 15 seconds and transferring 500 µL of sample matrix to 1.5-mL microcentrifuge tubes. Samples were spiked to a final concentration of 100 µg L^{-1} with IS, vortexed for an additional 15 seconds and extracted in a fume hood using 500 µL of ACN with 4% AcOH for serum and 0.1% AcOH in ACN for urine. For serum, 200 mg

$MgSO_4$ and 50 mg NaOAc were added into the sample to facilitate phase separation and extraction of target analytes; for urine, 200 mg $MgSO_4$ and 50 mg NaCl were added. Samples were vortexed for 15 seconds to break up salt agglomerates, shaken vigorously by hand for one minute, then sonicated for 15 minutes. All samples were centrifuged at 4 ºC for 15 minutes at 15,800 g. A volume of 200 µL of the supernatant was transferred to a labelled autosampler vial, diluted 1:1 with Milli-Q water, vortexed for 15 seconds, and stored at 4 ºC in the autosampler tray. All extracted samples were analyzed within 24 hours.

4.3.6 Instrumentation

The Thermo Scientific Accela UHPLC system with the CTC Analytics PAL autosampler coupled to the Exactive Plus orbital ion trap mass spectrometer, equipped with a HESI source, was used for analysis of nitrosatable analytes and PA*N*N compounds (Thermo Fisher Scientific, MA, USA). Data analysis was performed using Thermo Scientific *Xcalibur* and *Tune* software. QuEChERS salts were weighed on a Denver Instrument P-114 analytical balance (Bohemia, NY, US). Samples were vortexed using the Thermo Scientific MaxiMix I vortex mixer and centrifuged using the Thermo Scientific Sorvall™ Legend™ X1R (75004261) centrifuge.

4.3.7 UHPLC/HRAM Orbital Ion Trap MS Analysis

The development of chromatographic and detection methods involving the targeted analysis of nitrosatable pesticides and the semi-targeted analysis of PA*N*N compounds of interest in this study is described in Chapter 2. Mean recoveries for all target analytes in serum ranged between 74 and 120% (%RSD <12). For urine, initial analyte recoveries ranged from 96% to 116% (%RSD ≤10). In summary, UHPLC separation was carried out using a Thermo Scientific Hypersil GOLD™ C18 analytical column (50 mm x 2.1 mm, 1.9 µm particle size) with a mobile phase flow rate of 400 µL min^{-1}. Mobile phase Solvent A consisted of 100% Milli-Q water and Solvent B was 100% MeOH. Solvent A began at 100% and was held for one minute. From minute one to seven, Solvent B was increased to 100% and held for one minute. Minutes eight to 15 show a decrease of Solvent B back down to 0% and 100% Solvent A is pumped for the remaining two minutes of the run for

a total run time of 17 minutes. The refrigerated autosampler tray held extracted serum and urine samples at 4 ºC.

HESI source parameters were optimized based on UHPLC flow rate and set to the following values: sheath gas flow rate, 50 au; auxiliary gas flow rate, 13 au; sweep gas flow rate, 0 au; spray voltage, 3.50 kV; capillary temperature, 263 ºC; S-lens RF level, 60.0 au; auxiliary gas heater temperature, 425 ºC. The HRAM MS was operated using the following scan parameter settings: scan type, full MS/AIF; *m/z* range, 55-800 m/z; resolution, 70,000; AGC target, 3e6; maximum IT, 200 ms; and collision energy, 20 eV. The orbital ion trap MS was also programmed to operate in polarity switching mode, a feature that allows the acquisition of data from both positive and negative mode scans in a single data file, to maximize the probability of detecting semi-targeted PA*N*N compounds and other pesticide-derived biomarkers.

4.3.8 Quality Assurance/Quality Control

The Exactive Plus orbital ion trap MS was evaluated for accurate mass calibration in both ionization modes prior to each sequence. Fresh mobile phase, calibration standards, blanks, and QC solutions were prepared each day of sample analysis. QC samples consisted of target analytes prepared in Milli-Q water at a concentration of 50 µg L^{-1}. A QC sample passed if the calculated amount of each standard was within 80 to 100% of the nominal concentration (i.e. 40 to 60 µg L^{-1}). Each batch consisted of no more than eight samples. With each batch, one method blank (MB) and one post-extraction spike control (PESC) was prepared. The MB was prepared in the exact manner as the samples, except Milli-Q water was used instead of biomatrix. This blank was used to evaluate batch contamination. To prepare the PESC, 200 µL of supernatant from a random duplicate sample in each batch was transferred to a labelled autosampler vial and spiked to a final concentration of 25 µg L^{-1} target analytes and 100 µg L^{-1} IS. The sample was topped up to 400 µL with Milli-Q water, vortexed for 15 seconds and stored at 4 ºC until analysis. The PESC was used to observe behaviour of the analyte and IS in the sample matrix. Since a known concentration was added to the PESC, analyte response was expected to increase by 25 µg L^{-1} and that of the IS by 100 µg L^{-1}. Deviations from expected responses would illustrate additional effects of the matrix for individual samples.

Each sample sequence began with two Milli-Q water blanks, a seven-point calibration curve, followed by two more Mill-Q water blanks and a QC check before the injection of samples. A method blank was first injected followed by a batch containing no more than eight samples. Between each sample batch, two blanks and a QC were injected. After all samples were injected, two blanks, a final QC, and three analytical standards (Levels 2, 4, and 6 at 5, 25, and 100 μg L^{-1}, respectively) were run; these three standards were used to evaluate the consistency of the initial calibration curve from the beginning of the sequence. The end of the sequence was marked by a final blank and column wash in preparation for the next sequence.

4.3.9 Data Processing and Biomarker Identification

Group I analytes were identified in serum and urine samples using the criteria recommended by the European Commission [203]. Target analyte identification was confirmed when the following three criteria were met: (i) the theoretical mass value of the molecular ion matched its experimental exact mass value with a mass error of less than 5 ppm; (ii) the theoretical mass value of at least one fragment ion matched its experimental exact mass value with a mass error of less than 5 ppm; and (iii) molecular and fragment ions had fully overlapping retention times. Quantitation of Group I analytes was carried out using calibration standards prepared at seven different concentrations in Milli-Q water to construct a seven-point calibration curve for each analyte. As the validity of creatinine correction for pesticide analysis in urine has been debated in pesticide exposure science [204], only free form analytes were measured.

Group II and III semi-target analytes were tentatively identified using an approach that was designed to be fit-for-purpose. First, theoretical mass values for molecular ions in both positive and negative ionization modes were individually extracted from sample chromatograms and visually inspected for screening based on the following criteria: (i) suspect analyte response was greater than 2E-05; (ii) a fully formed peak was distinct from the background; and (iii) the suspect molecular ion exact mass was within 5 ppm of theoretical mass. Two analytes from Group II (*N*-ATR and *N*-ETU) were previously synthesized in the lab and their experimental exact masses (within 5 ppm) and retention times were used to assist in tentative identification in samples. A workflow for compound

identification is illustrated in Figure 4-2. When possible, predicted and/or experimental fragmentation data was gathered from the literature and accurate mass spectra databases, such as mzCloud, MetFrag, Competitive Fragmentation Modeling for Metabolite Identification (CFM-ID), and MassBank of North America (MoNA).

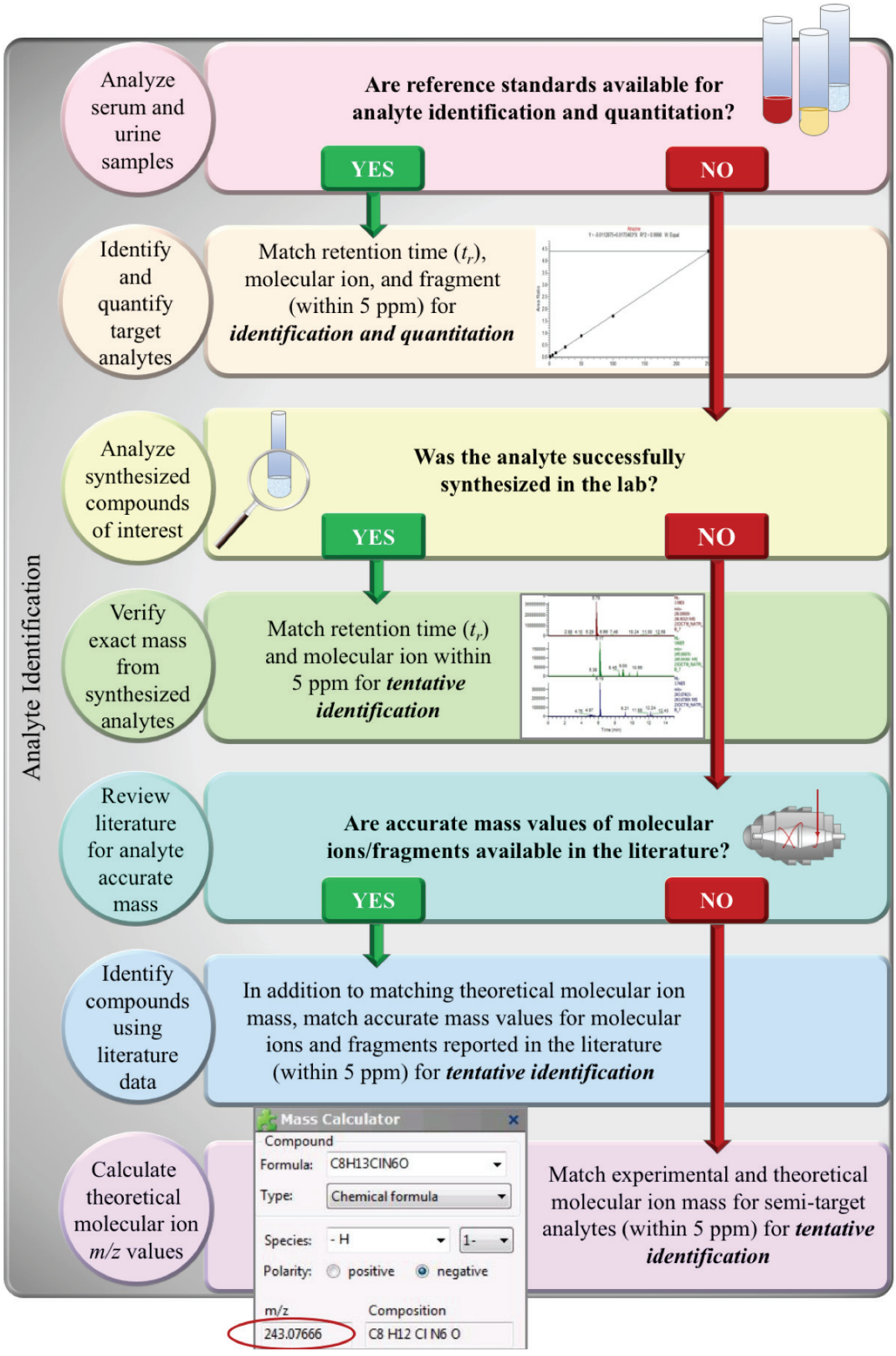

Figure 4-2. Compound identification workflow for target and semi-target analytes.

As accurate quantitation and unequivocal identification is not possible without certified analytical standards, a peak area ratio technique was formulated to measure relative responses of Group II and Group II analytes among individual samples. Once identified using the *Tune* and *Xcalibur* software, analyte peak area was divided by the IS peak area and reported as a percentage (e.g. 100**N*-ETU peak area/IS peak area). This ratio represented the relative response of each biomarker among individual samples.

4.3.10 Statistical Analysis and Population Characteristics

Testing difference between provinces

In addition to biomarker measurement, data for self-reported health score, number of daily servings of fruits and vegetables, smoking status, number of full-term births, and number of breastfeeding months were included as they may influence the expression of pesticide-associated biomarkers. For each continuous variable, normal distribution was tested using a Shapiro-Wilks test, and variance was tested using Levene's test for equal variance. If the variables violated assumptions of normality, a two-sample Wilcoxon Rank Sum Test was used to test for a significant difference between provinces. If the normality assumption was met, a two-sample t-test with equal or unequal variance was employed, depending on Levene's test result. These variables include self-reported general health, number of daily servings of fruits and vegetables, analyte concentration (both serum and urine), total number of analytes detected (serum and urine), and for female participants (if applicable), the number of live births the participant has given and number of months the participant has breastfed. Categorical variables (smoking status and detection frequency of each analyte in both urine and serum) were tested for differences between provinces using a chi-squared test.

4.4 Results and Discussion

4.4.1 Participant Characteristics

Although participants were age- and sex-matched between the two provinces, 78% of the sample population was female. The mean age among all participants was 64.3 years. Overall, NS participants self-rated health scores were higher than those of the PEI participants. There was a significant difference in smoking status with more PEI

participants reported having ever smoked. For female participants, the number of breastfeeding months was significantly greater in PEI. All other participant characteristics are shown in Table 4-2.

Table 4-2. Comparison of participant characteristics between PEI and NS.

Variable	Measure	N	PEI	NS	Total	P value
Sex	% Male % Female	64	22 78	22 78	22 78	1.000
Age	Mean (SD)	64	64.3 (6.4)	64.3 (6.4)	64.3 (6.4)	1.000
Health score[a]	Mean score (SD)	64	3.4 (0.8)	4.0 (0.7)	3.7 (0.8)	0.0077
Fruits and vegetables[b]	Mean number of servings per day (SD)	64	4.5 (2.0)	5.2 (2.9)	4.8 (2.5)	0.2813
Smoking status[c]	% Never smoked % Ever smoked	63	32 66	68 34	44 56	0.008
Live births	Mean # of births (SD)	33	3 (1.0)	3 (1.5)	3 (1.2)	0.6314
Breastfeeding time	Mean # of months (SD)	26	16.6 (10.7)	9.6 (15.2)	13.4 (13.2)	0.0462

[a]Participants self-rated health scores used the following scale: 1=Poor; 2=Fair; 3=Good; 4=Very good; 5=Excellent

[b]"Ever smoked" is defined as having ever smoked at least 100 cigarettes, being a current occasional smoker, or being a current daily smoker while "never smoked" is defined as never smoking at least 100 cigarettes

4.4.2 Group I Analytes in Serum and Urine

Two target analytes, ETU and TCPy, were identified in serum and ATR, ETU, and MCPA were identified in urine. Initially, ETU concentrations in serum appeared to be unusually high (mean ETU concentration in serum of 37 $\mu g\ L^{-1}$) using the IS method. This may be due to a mismatch between ETU and the IS. For example, CAR-d3 shares most physicochemical properties with its non-deuterated counterpart, CAR. Therefore, the extraction recoveries of CAR and CAR-d3 from biomatrices would match closely. However, as CAR-d3 and ETU share fewer common physicochemical properties, calculations involving relative recoveries of the two are not well matched and discrepancies in quantitation occur. In an attempt to compensate for the IS incompatibility for ETU in

urine and serum, a matrix-matched calibration curve was constructed for each biomatrix using laboratory control samples (LCSs) at the following concentrations: 10, 25, 50 and 100 µg L^{-1} (Figure 4-3). ETU concentrations were recalculated using the matrix-matched calibration curves. ETU was identified in 38 of 63 serum samples (19 from each sample population) at concentrations above the MDL of 2.7 µg L^{-1} but below the LOQ of 9.5 µg L^{-1} (Table 4-3).

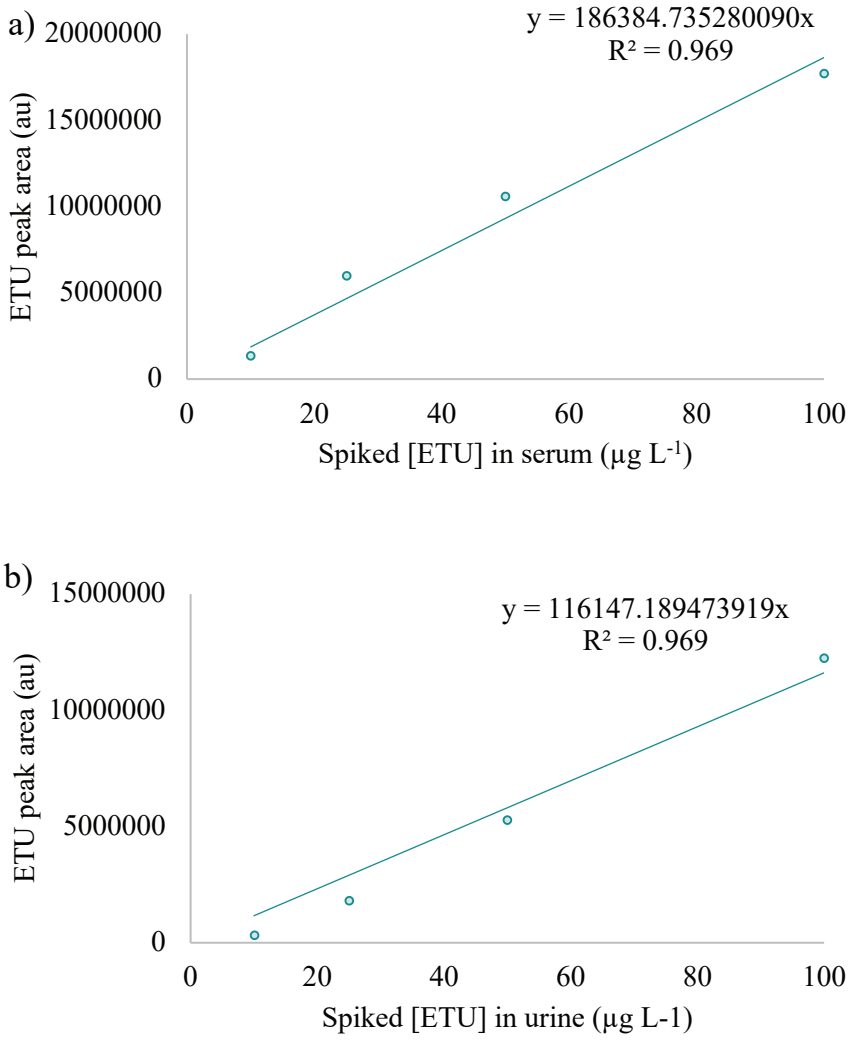

Figure 4-3. Matrix-matched calibration curves for ETU in a) serum and b) urine.

Table 4-3. Theoretical and exact *m/z* values for molecular ions, presence of an ion fragment with a matching retention time (t_r), and number of detections for each target analyte identified via in serum samples.

Analyte	Molecular ion theoretical mass	Mean exact mass of biomarker ion in samples (*m/z*)		t_r and frag match <5 ppm		Number of detections		P value
		PEI	NS	PEI	NS	PEI	NS	
ETU	103.03245	103.03242	103.03229	Yes	Yes	19	19	0.877
TCPy	195.91190	195.91254	ND[a]	Yes	---	2	0	0.157

[a]ND = not detected

The mean exact mass of the ETU molecular ion in the serum samples was 103.03236 with a retention time of 0.52 (± 0.03) minutes. The predicted fragment ion mass was identified as 86.0059 and the exact mass of the fragment was determined experimentally as 86.00654 using the reference standard (Figure 4-4). The average mass of the fragment ion in the serum samples was 86.00694 with a matching retention time of 0.51 (± 0.04) minutes. The mass error between the theoretical ETU molecular ion 103.03245 and observed values was less than 5 ppm for all detections. The mass error of the fragment ion was less than 5 ppm in 30 of the 38 detections and ranged from 5.7 to 7.7 ppm for the other 8 detections.

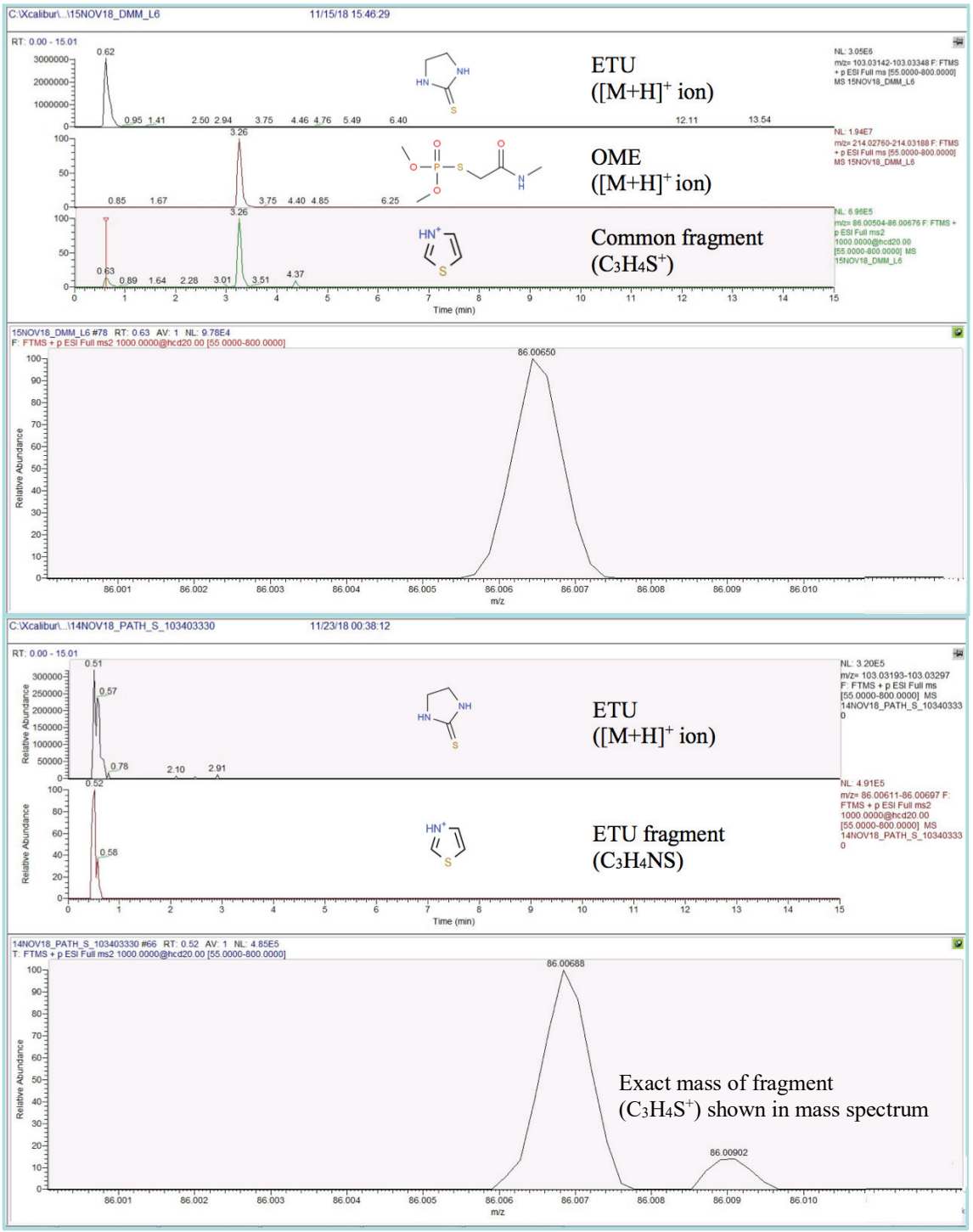

Figure 4-4. Chromatograms showing ETU confirmation using analytical standard (top) and in a serum sample (bottom).

TCPy was detected at concentrations above the MDL of 2.7 µg L^{-1} but below the LOQ of 8.1 µg L^{-1} in two serum samples, both from the PEI sample population. The mean

exact mass of the TCPy molecular ion was 195.91254 and eluted at a retention time of 5.51 (± 0.05) minutes. As fragment data for TCPy is lacking in the literature and databases that produce predicted fragmentation ions for compounds, no fragment was identified in either the analytical standards or samples. Compound identification was confirmed by matching retention time and theoretical and observed values for the TCPy molecular ion (Figure 4-5). The mass error between the theoretical TCPy molecular ion (195.91190) and observed values was less than 5 ppm for both detections.

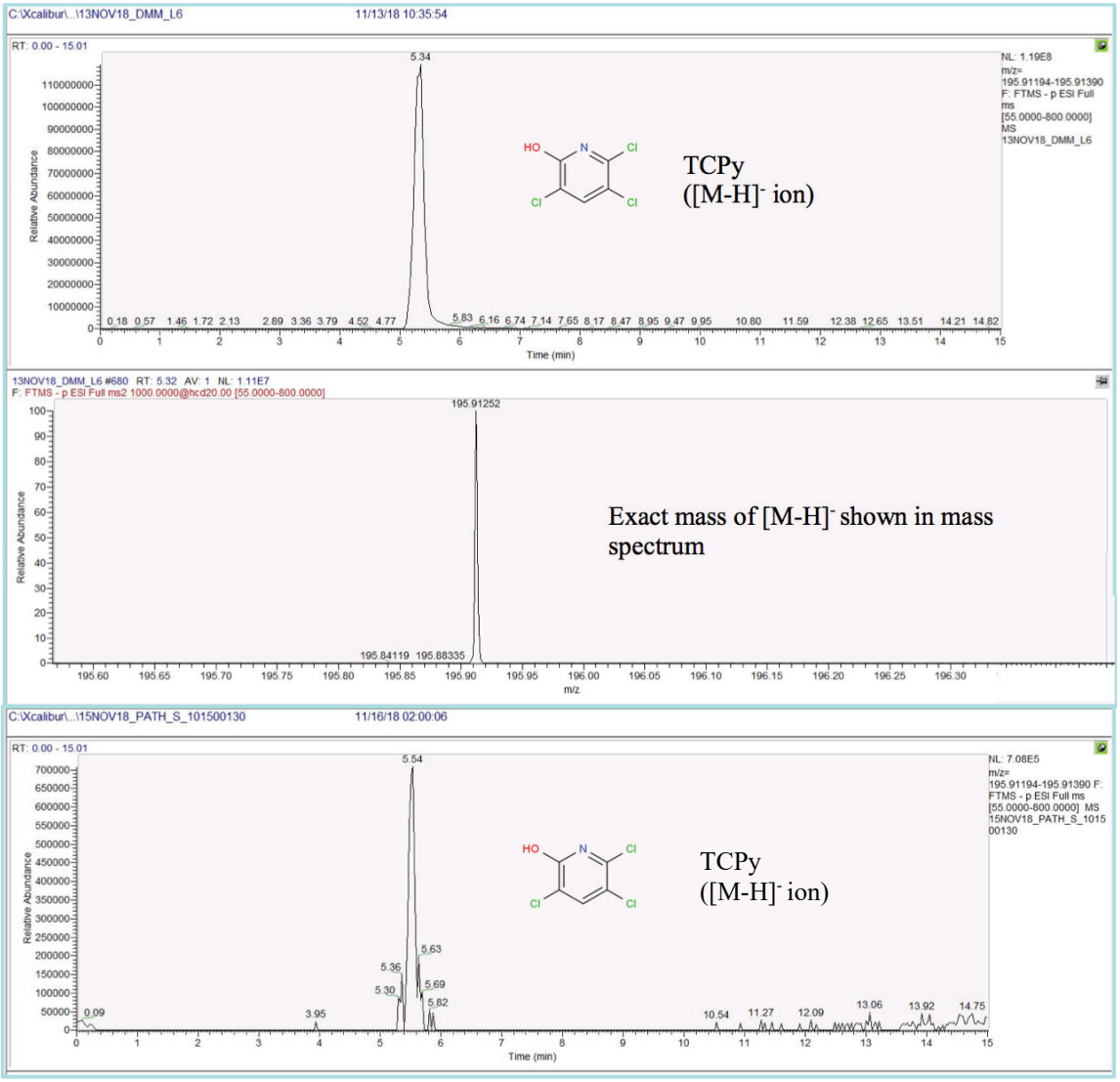

Figure 4-5. Chromatograms showing TCPy confirmation using analytical standard (top) and in sample (bottom).

ATR was identified in 3 of 64 urine samples at concentrations above the MDL of 1.9 µg L^{-1} but below the LOQ of 5.8 µg L^{-1} (Table 4-4). The theoretical value of ATR's molecular ion in positive mode was 216.10105 and its predicted fragment mass was 174.05410. Experimentally, the molecular and fragment ions in the analytical standard had exact mass values of 216.10060 and 174.05382, respectively. The mean exact mass of the ATR molecular ion in the urine samples was 216.10109 with a retention time of 5.73 (± 0.01) minutes. The average mass of the fragment ion in the samples was 174.05425 with a matching retention time of 5.74 (± 0.01) minutes. The mass error between theoretical and observed values for ATR molecular and fragment ions was less than 5 ppm for all three detections. Identification criteria for ATR are illustrated in chromatograms in Figure 4-6.

Table 4-4. Theoretical and exact *m/z* values for molecular ions, presence of an ion fragment with a matching retention time (t_r), and number of detections for each target analyte identified via in urine samples.

Analyte	Molecular ion theoretical mass	Mean exact mass of biomarker ion in samples (*m/z*)		t_r and frag match <5 ppm		Number of detections		P value
		PEI	NS	PEI	NS	PEI	NS	
ATR	216.10060	216.10125	216.10078[a]	Yes	Yes	2	1	0.554
ETU	103.03245	103.03227	103.03221	Yes	Yes	5	4	0.719
MCPA	199.01675	ND[a]	199.01588[a]	---	No	0	1	N/A

[a]ND = not detected
[b]Mean value not available for n=1

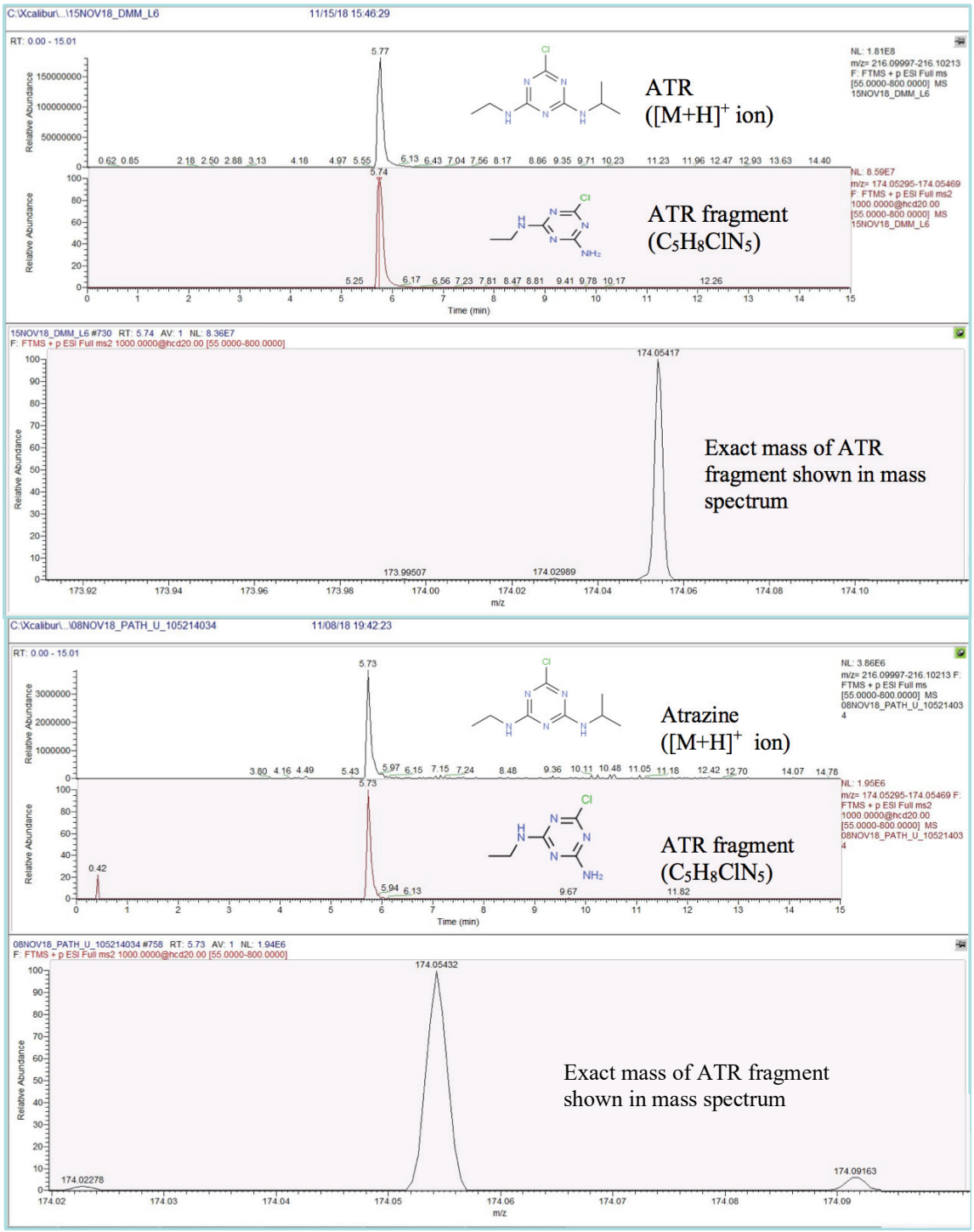

Figure 4-6. Chromatograms showing ATR confirmation of molecular and fragment ions shown with analytical standard (top) and in sample (bottom).

ETU was identified in urine samples using the same approach as with the serum samples. A total of nine urine samples contained ETU. Five PEI samples contained ETU in concentrations above the MDL of 2.6 µg L^{-1}. ETU was also detected in four NS urine samples at concentrations above the MDL but below the LOQ, with one sample having an ETU concentration above the LOQ of 8.7 µg L^{-1}. MCPA was detected in one NS sample at the MDL but the identity of the analyte could not be confirmed, as the retention time of its experimentally determined fragment, $C_7H_6ClO^-$, did not match that of its molecular ion (Figure 4-7).

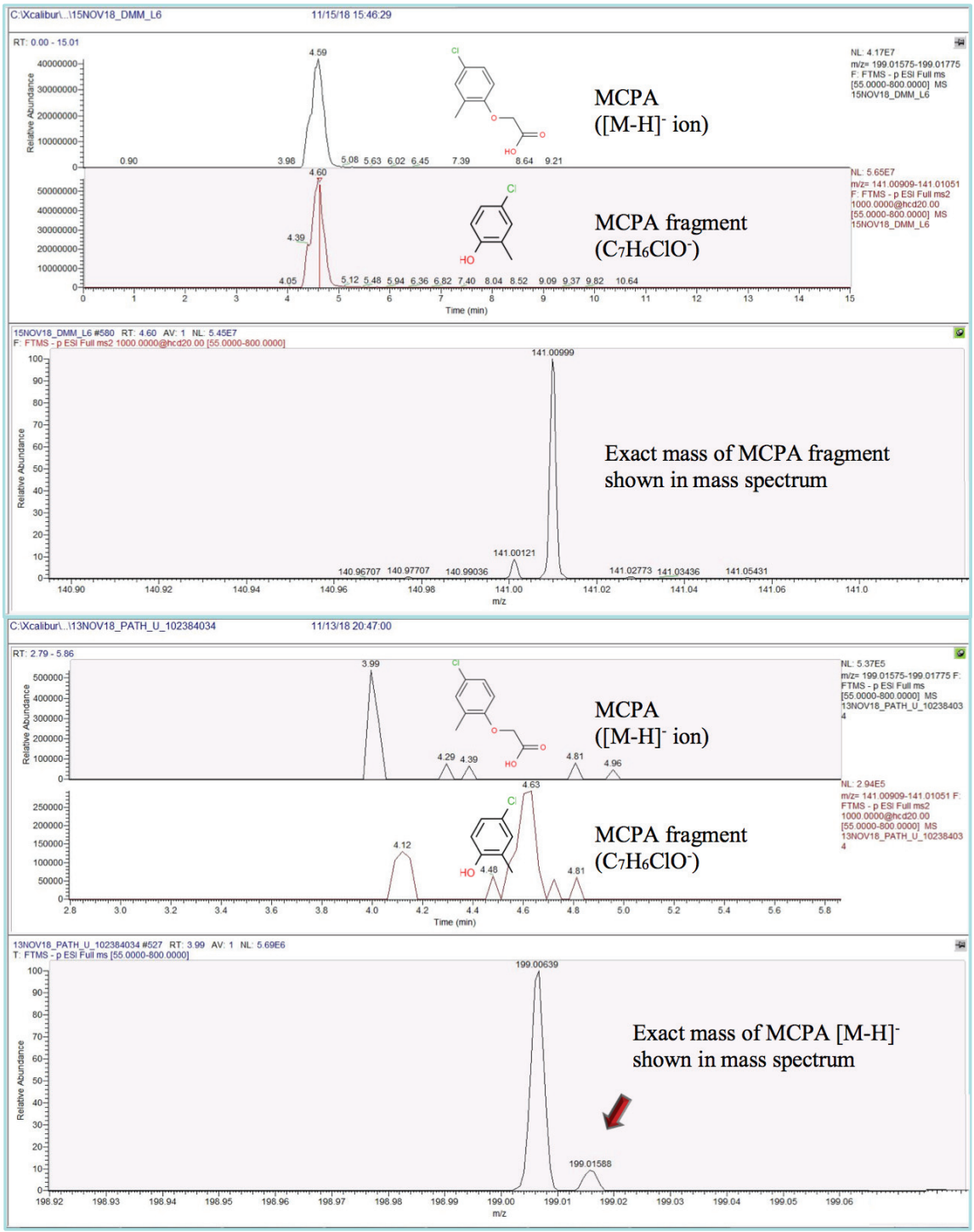

Figure 4-7. Chromatograms showing MCPA confirmation of molecular and fragment ions shown with analytical standard (top) and unmet identification criteria in urine sample (bottom).

It is apparent that the matrix-matched curve correction cannot entirely compensate for the incompatibility of the IS used in the recovery calculations of ETU, as some chromatograms from samples that were non-detects for ETU actually showed a peak for the analyte (Figure 4-8a). In contrast, some samples in which an ETU quantity was reported showed no peak where one was expected (Figure 4-8b). In addition, the reference serum used in method development recovery studies may not share the same matrix characteristics as sample serum, as inter-individual differences make each serum sample relatively unique. Furthermore, this extraction method was optimized for a suite of analytes rather than specifically for ETU. The responses generated in the serum LCSs used to construct these matrix-matched calibration curves reflected ETU recoveries as low as 54.8% in serum and 51.9% in urine using this method. Ideally, the IS method would be used with a deuterated version of ETU itself to correct these recovery issues and yield more accurate quantitation of the analyte.

a)

b)

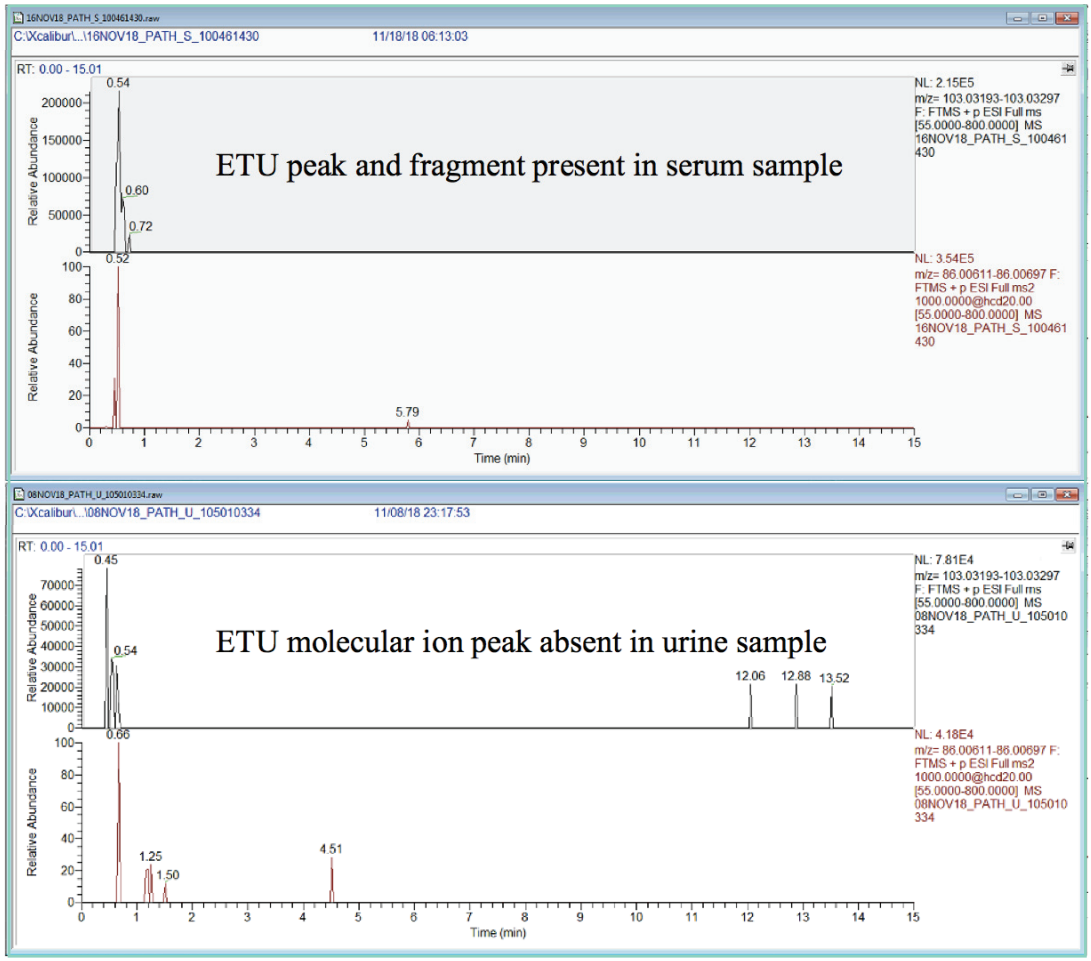

Figure 4-8. a) ETU peak and fragment detected in serum sample that was reported as NF ("not found") by processing method using unsuitable matrix-matched calibration curve and b) ETU molecular ion peak absent from urine sample that showed a concentration of 3.0 µg L^{-1}.

4.4.3 Tentative Identification of PA*N*N Compounds in Serum and Urine

Predicted mass spectra were identified for only two PA*N*N compounds: *N*-ATR and *N*-ETU. Fragments from these spectra were used as potential identifiers. Remaining PA*N*N compounds could be tentatively identified using only the theoretical mass of their molecular ions. Six PA*N*N compounds (*N*-ATR, di-*N*-CAR, *N*-DIM, *N*-IMI, *N*-LIN, and *N*-OME) were tentatively identified in serum by matching their theoretical molecular ion masses to those of experimental ions found in samples with a mass error below 5 ppm (Table 4-5). A biomarker with the same accurate mass as the *N*-ATR negative mode molecular ion (with a mass error within 5 ppm) was detected in six PEI serum samples

while 15 detections were observed for the biomarker in NS serum samples (t_r = 3.87 ± 0.06 minutes). An analyte with a molecular ion mass matching that of *N*-OME in positive ionization mode (243.01991) was detected in all PEI serum samples and in 29 of the NS serum samples with a mean retention time of 0.36 ± 0.02 minutes. The *N*-DIM positive mode ion was also frequently detected as a possible serum biomarker in 28 and 22 of the PEI and NS samples, respectively (t_r = 0.363 ± 0.004 minutes). The number of tentative detections for three other PA*N*N compounds in serum were significantly fewer. The remaining PA*N*N compounds, di-*N*-CAR, *N*-IMI, and *N*-LIN, were tentatively identified in three or fewer serum samples.

Table 4-5. Ionization mode, theoretical and exact mass values for molecular ions, and number of detections for each PA*N*N compound tentatively identified in serum samples.

Analyte	Ionization mode	Molecular ion theoretical mass	Mean exact mass of biomarker in samples (*m/z*)		Number of tentative detections		P value
			PEI	NS	PEI	NS	
N-ATR	–	243.07666	243.07725	243.07713	6	15	0.013
di-*N*-CAR	+	250.05708	ND[a]	250.05792[b]	0	1	0.306
N-DIM	+	258.99706	258.99777	258.99742	28	22	0.105
N-IMI	+	285.04974	285.04883[b]	ND[a]	1	0	0.321
N-LIN	+	278.00937	ND[a]	278.00832	0	3	0.071
	–	275.99482	275.99550[b]	ND[a]	1	0	0.321
N-OME	+	243.01991	243.02028	243.02001	32	29	0.144

[a]ND = not detected
[b]Mean value not available for n=1

A biomarker matching the exact mass of *N*-ATR was observed in all 64 urine samples and matches for *N*-ATR molecular ions in both ionization modes were present in all but one urine sample (Table 4-6). Mean retention times for positive and negative mode molecular ions were 4.17 ± 0.22 minutes (n=64) and 4.14 ± 0.17 minutes (n=63), respectively. Chromatograms showing peaks extracted for these ions in serum and urine of the same individual, as well as a notable shift in analyte retention time between the two

biomatrices, are shown in Figure 4-9. The expression of both positive and negative molecular ions indicates that the relative response for this biomarker may be higher in urine than in serum. The magnitude of biomarker response was high enough to see the less prominent ion in almost all urine samples whereas it was not seen in any of the serum samples. This may be attributable to a higher concentration of biomarker present or decreased matrix effects in urine.

Table 4-6. Ionization mode, theoretical and exact mass values for molecular ions, and number of detections for each PA*N*N compound tentatively identified in urine samples.

Analyte	Ionization mode	Molecular ion theoretical mass	Mean exact mass of biomarker in samples (*m/z*)		Number of tentative detections		P value
			PEI	NS	PEI	NS	
N-ATR	–	243.07666	243.07759	243.07691	32	32	1.000
di-*N*-ATR	+	274.08138	274.08132	ND[a]	2	0	0.151
	–	272.06682	272.06770	272.06744	4	5	0.719
N-CAR	+	221.06692	ND[a]	221.06653	0	2	0.151
	–	219.05236	219.05228[b]	219.05223	1	5	0.086
di-*N*-CAR	+	250.05708	250.05649	250.05689	8	3	0.098
	–	248.04253	248.04164	248.04150[b]	6	1	0.045
di-*N*-ETU	+	161.01277	161.01350	161.01252	3	2	0.641
N-IMI	+	285.04974	285.05057	285.05058	4	4	1.000
N-LIN	+	278.00937	278.00941	278.00950	4	6	0.491
N-OME	+	243.01991	243.01959[b]	ND[a]	1	0	0.313
	–	241.00535	241.00465	241.00552	17	11	0.131
N-TM	–	370.02853	ND[a]	370.03026	0	3	0.076
di-*N*-TM	–	399.01870	ND[a]	399.01880[b]	0	1	0.313

[a]ND = not detected
[b]Mean value not available for n=1

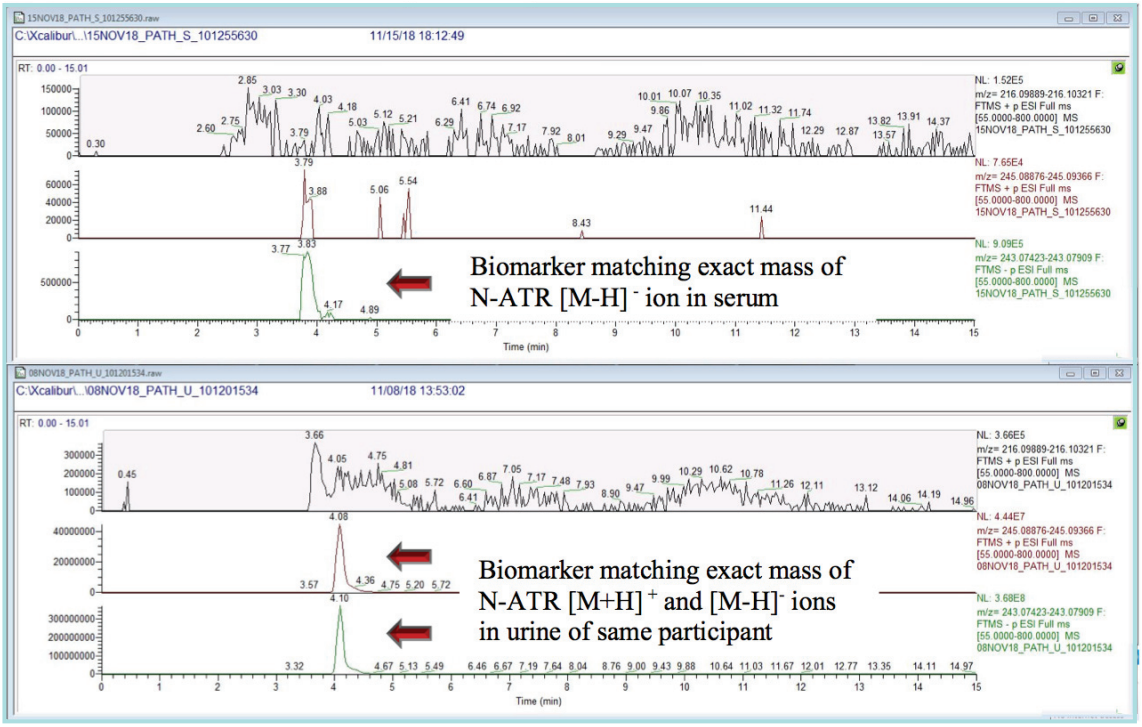

Figure 4-9. Chromatograms showing peaks extracted for *N*-ATR molecular ions in serum (top) and urine (bottom) of the same individual, as well as a notable shift in analyte retention time from 3.83 minutes in serum to 4.10 minutes in urine.

Di-*N*-ATR was tentatively identified by its negative mode molecular ion in four and five urine samples from PEI and NS sample populations, respectively (t_r = 4.40 ± 0.26 minutes) and by its positive ion in only two samples (t_r = 4.90 ± 0.04 minutes). Some samples had both molecular ions present whereas some had one or the other (Figure 4-10). Similarly, *N*-CAR, di-*N*-CAR, and *N*-OME were tentatively identified by both molecular ions. Seven of eight possible detections for *N*-CAR were observed in the NS urine samples whereas 14 of 18 possible detections for di-*N*-CAR were seen in the PEI urine samples. Interestingly, mean retention time for analytes matching the mass of the *N*-CAR $[M+H]^+$ ion was 3.62 ± 0.33 minutes and that for its negative mode molecular ion ranged from to 0.43 to 4.11 minutes. Analytes matching di-*N*-CAR theoretical masses showed consistency in retention time for the positive mode ion (3.13 ± 0.73 minutes) but a wider range for the negative mode ion (0.46 to 4.22 minutes). Only one of 28 tentative detections for *N*-OME were due to the presence of a matching positive mode molecular ion whereas all tentative detections in serum were exclusively positive mode matches. Of note, retention time for

N-OME tentative detections in the PEI sample population was 4.06 ± 0.83 minutes (with only one detection under 3.78 minutes) whereas retention time for the NS urine samples showed a much greater variation with a mean retention time of 1.60 ± 1.26 minutes.

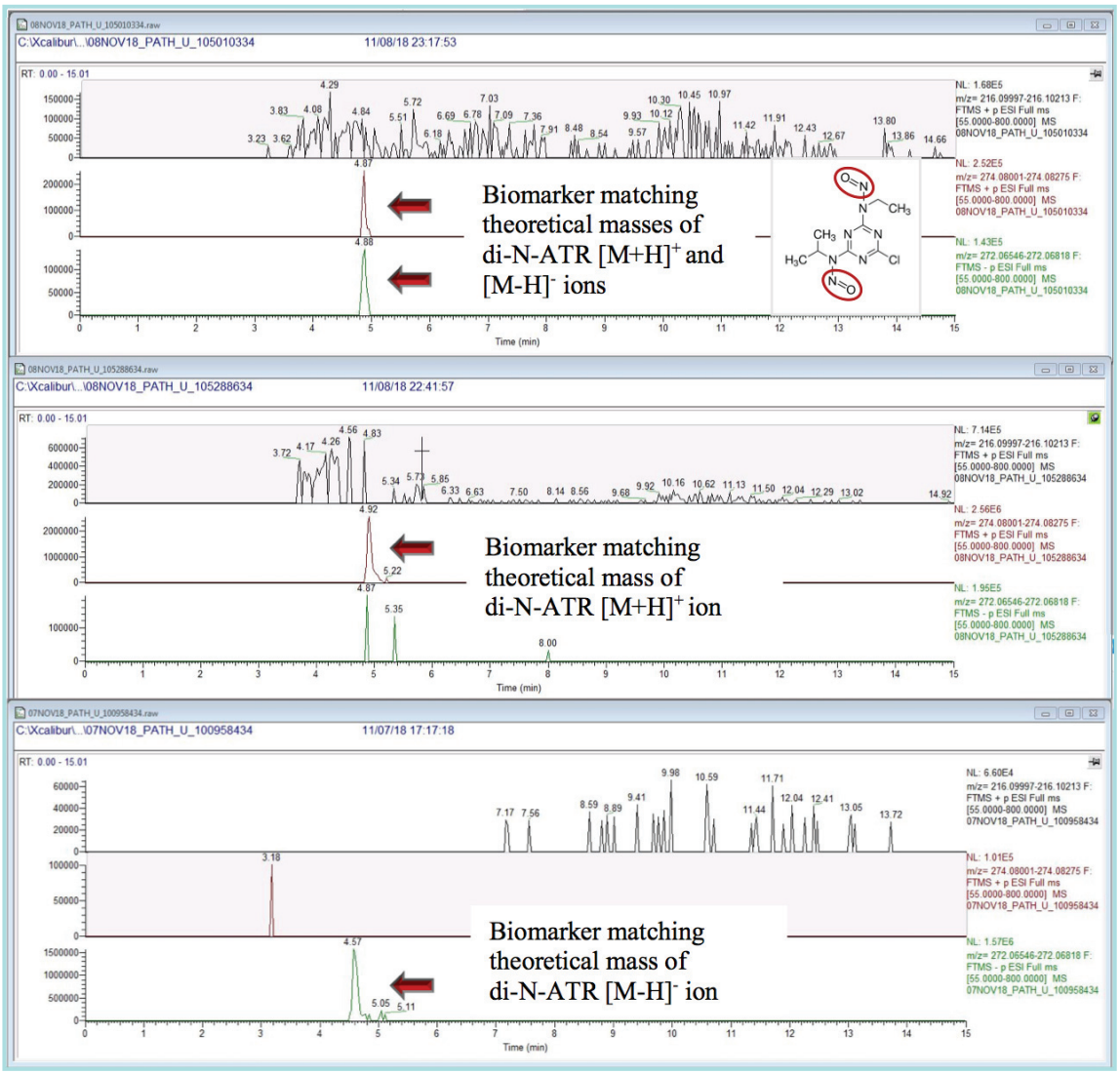

Figure 4-10. Chromatograms showing peaks extracted for both positive and negative di-*N*-ATR molecular ions (top), positive mode only (middle), and negative mode only (bottom) in three different urine samples.

The presence of either molecular ion, or both at non-overlapping retention times, suggests that more than one compound having a molecular ion within the 5-ppm mass error match the mass of those for theoretical ions of di-*N*-ATR, *N*-CAR, and *N*-OME. All tentative detections for di-*N*-ETU (t_r = 0.61 ± 0.11 minutes), *N*-IMI (t_r = 3.37 ± 0.05

minutes), and *N*-LIN (t_r = 4.05 ± 0.41 minutes) were based on matches for positive mode molecular ions with a total of five, eight and 10 detections, respectively. *N*-TM (t_r = 3.91 ± 0.37 minutes) and di-*N*-TM were tentatively identified in only NS urine samples (three and one detection, respectively) and only with a mass match for the negative mode molecular ion.

Since *N*-ATR is one of the two PA*N*N compounds successfully synthesized in the laboratory and for which a predicted mass spectrum was available, retention time and fragment ions were considered to aid in identification of this biomarker in both serum and urine. The retention time of the synthesized analyte in water was 6.18 ± 0.02 minutes (n=2) while the mean retention time of the biomarker in serum was 3.87 ± 0.06 minutes (n=24). An illustration of the earlier retention time of the tentatively-identified *N*-ATR in a serum sample is shown in Figure 4-11. While this difference in retention times does not support a match between the biomarker and *N*-ATR, it is not enough to rule out the possibility that the compound detected in the samples is *N*-ATR, as analyte retention time can shift with different injection solvents and sample pH (i.e. water at pH ~ 2.5 versus serum extract). Further spectral analyses revealed a more likely match between the biomarker presenting as *N*-ATR and indolyl-3-acryloylglycine (IAG) (Appendix B).

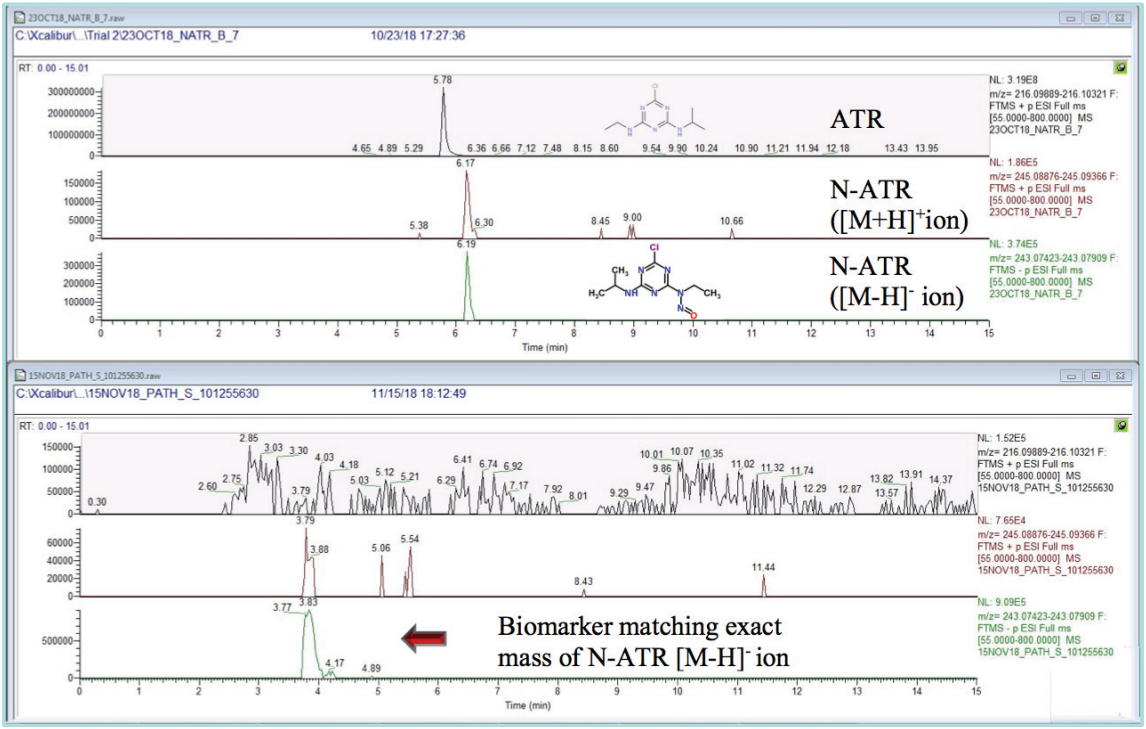

Figure 4-11. Chromatograms showing confirmation of synthesized *N*-ATR (top) and different retention time of biomarker matching exact mass of *N*-ATR in serum sample (bottom).

4.4.4 Tentative Identification of Other Biomarkers in Serum and Urine

Molecular ions for ATR metabolites AM and DEA were detected in both biomatrices with a mass error of less than 5 ppm (Tables 4-7 and 4-8). Previous work has shown that AM was identified by the molecular ion 343.15468 in positive ionization mode [205]. Another study reported the AM fragment $C_8H_{16}N_5S$ with an experimental exact mass of 214.1126, along with the protonated molecular ion of experimental mass 343.1543 [206]. The *Tune* software calculated the theoretical mass of the $[M+H]^+$ ion and fragment for AM as 343.15469 and 214.11209, respectively. These theoretical values are consistent with experimental masses determined in the literature and were therefore used for tentative identification of AM in biological samples. AM and its fragment were detected in both serum and urine of one PEI participant (Figure 4-12). It should be noted that the parent compound ATR was not detected in the individual's serum or urine. If this biomarker is, in fact, AM, then ATR appears to have been completely metabolized and eliminated from the individual's serum and urine.

Table 4-7. Ionization mode, theoretical and exact mass values for molecular ions, and number of possible detections for each Group III metabolite tentatively identified in serum samples.

Analyte	Ionization mode	Molecular ion theoretical mass	Mean exact mass of biomarker in samples (*m/z*)		Number of tentative detections		P value
			PEI	NS	PEI	NS	
AM	+	343.15469	343.15384[b]	ND[a]	1	0	0.321
DEA	+	188.06975	188.06980	188.07052	5	21	<0.001

[a]ND = not detected
[b]Mean value not available for n=1

Table 4-8. Ionization mode, theoretical and exact mass values for molecular ions, and number of possible detections for each Group III metabolite tentatively identified in urine samples.

Analyte	Ionization mode	Molecular ion theoretical mass	Mean exact mass of biomarker in samples (*m/z*)		Number of tentative detections		P value
			PEI	NS	PEI	NS	
AM	+	343.15469	343.15387[b]	ND[a]	1	0	0.313
DEA	+	188.06975	188.07055	188.07045	24	26	0.545
5-HBC	+	208.07167	208.07228	ND[a]	3	0	0.081

[a]ND = not detected
[b]Mean value not available for n=1

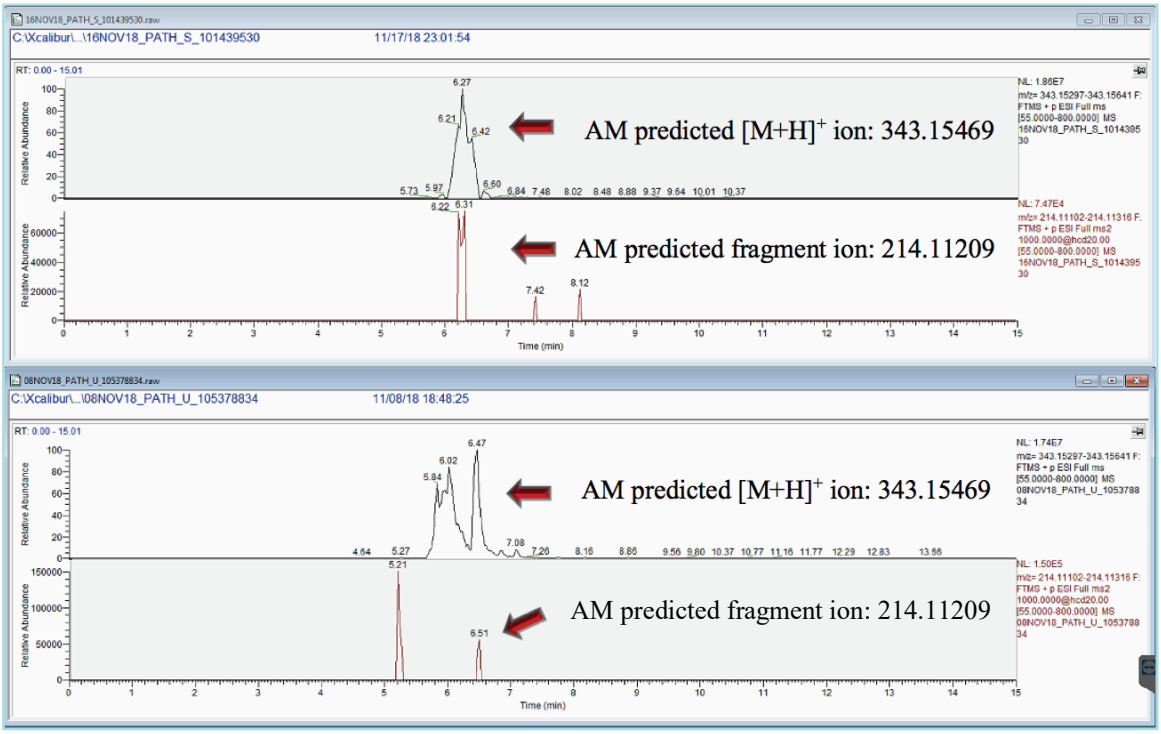

Figure 4-12. Chromatograms showing peaks extracted for theoretical *m/z* values of AM molecular and fragment ions in serum (top) and urine (bottom) of the same individual.

The fragment $C_3H_5ClN_5$ is a known fragment of DEA and its exact mass has been experimentally determined to be 146.0219 with a molecular ion mass of 188.0691 (MoNA Spectrum AU301601 for DEA). The *Tune* software calculated the theoretical mass of the $[M+H]^+$ ion and fragment for DEA as 188.06975 and 146.02280, respectively. The theoretical value for the $[M+H]^+$ ion is within a 5-ppm mass error of the experimental value whereas the theoretical fragment mass has a 6.2 ppm mass error from the experimental value. Since the experimental value found in the literature has one fewer significant digit, the theoretical value for the fragment $C_3H_5ClN_5$ (as well as the for the molecular ion) was used for tentative identification of DEA in biological samples. Extraction of these theoretical ions for DEA in a sample with the highest peak area for this biomarker showed a match for both ions at a retention time of 3.05 minutes (Figure 4-13). All other samples showing a response for the biomarker near this retention time were considered tentative matches for DEA.

Of the five PEI serum samples showing peaks matching the DEA biomarker retention time (t_r = 3.07 ± 0.03 minutes), two showed a peak for the fragment at an

overlapping retention time. In contrast, 21 NS serum samples showed the presence of the biomarker at the expected retention time (t_r = 3.04 ± 0.02 minutes) with 10 sample chromatograms having a peak for the DEA fragment ion within a 5-ppm mass error. There was not a significant difference in the biomarker's retention time between biomatrices. PEI and NS urine samples showed mean retention times of 3.02 ± 0.03 minutes (n=24) and 3.03 ± 0.04 minutes (n=26), respectively. Two and three of the PEI and NS urine sample chromatograms, respectively, showed a peak for the DEA fragment at the expected retention time. As mentioned previously, analytes may still be present at the expected retention time but fragments with lower ion intensities may not generate a response at low analyte concentrations.

As there is limited information on the spectral characteristics of 5-HBC, predicted *m/z* values for the analyte's fragments were used for tentative identification. Peaks for the positive mode molecular ion and fragment with a *m/z* value of 176.04545 were found at overlapping retention times in three urine samples from the PEI sample population. An example of the detection in a participant's urine sample is shown in Figure 4-14. The mean retention time of the biomarker was 3.91 ± 0.01 minutes (n=3).

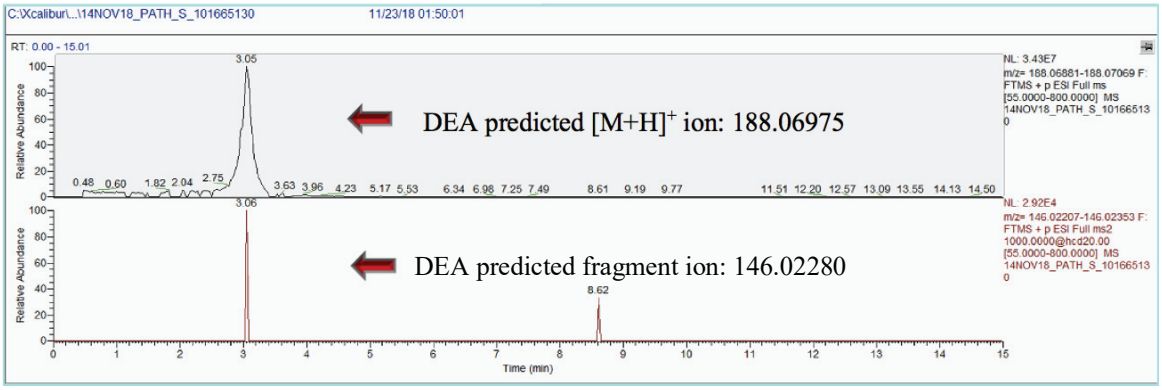

Figure 4-13. Chromatogram showing peaks extracted for theoretical *m/z* values for DEA molecular and fragment ions in a serum sample.

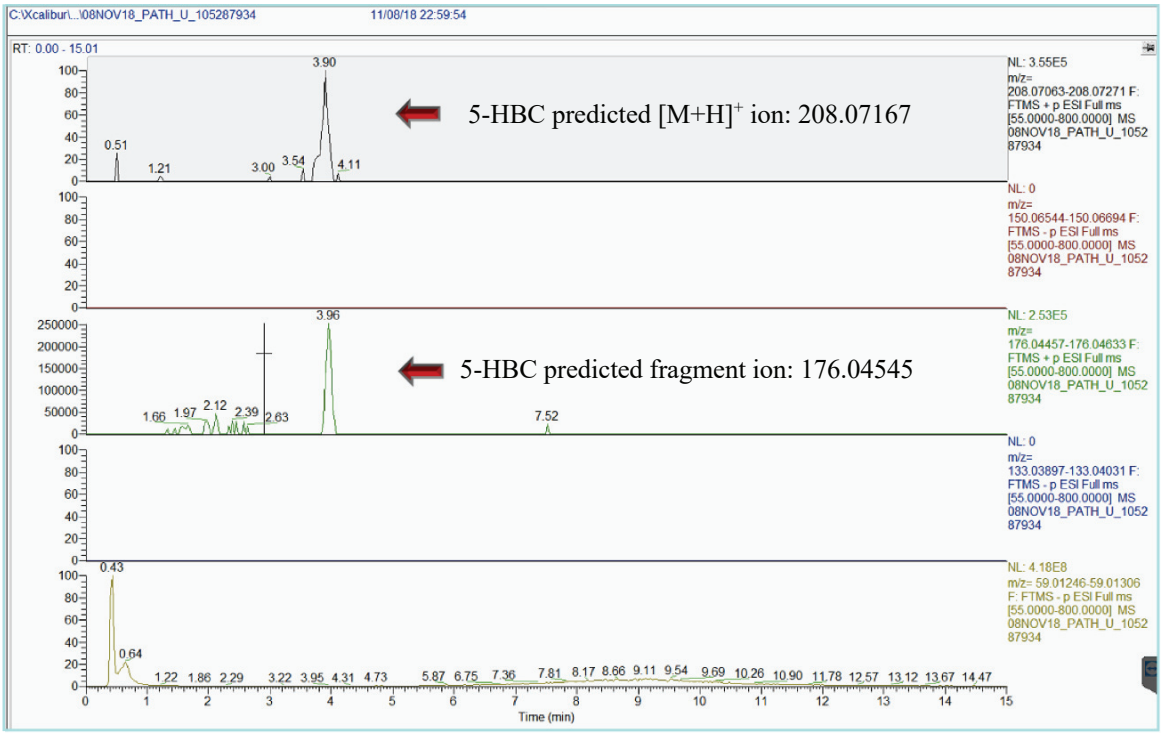

Figure 4-14. Chromatogram showing extraction of predicted 5-HBC *m/z* values for the molecular ion plus four fragments in a urine sample. One fragment (*m/z* = 176.04545) generated a peak with a retention time matching that of the molecular ion.

Of the 31 target and semi-target analytes, CAR, DIM, IMI, LIN, MCPA, OME, TM, DACT, *N*-ETU, EU, 3,4-D, *N*-TCPy, tri-*N*-TM, and quat-*N*-TM were not detected in any of the serum or urine samples. There were no significant differences between provinces in number of detections in serum or urine for Group I target analytes. Only two detections for target analytes were above the LOQ: one NS participant had a urinary ATR concentration of 16.5 µg L^{-1} and another NS participant had a urinary ETU concentration of 24.3 µg L^{-1}. In serum, there was a significantly higher number of *N*-ATR tentative detections in NS ($p = 0.013$); however, this compound more closely matches identification criteria for IAG rather than for *N*-ATR. In urine, significantly more tentative identifications were reported in the PEI samples for di-*N*-CAR ($p = 0.045$). CAR, the parent compound for di-*N*-CAR, was not detected in any of the serum or urine samples above the MDL. For Group III analytes, there was a significantly higher number of tentative identifications for the ATR metabolite DEA in NS serum samples ($p < 0.001$).

It was initially hypothesized that pesticide biomarkers would be more frequently detected and in higher concentrations in the PEI sample population biofluid samples, as it

was assumed that PEI residents have a greater level of pesticide exposure due to the province's intense potato farming industry. In an effort to include participants with a greater probability of being exposed to routinely applied pesticides, PEI participants with postal codes matching those in areas where groundwater nitrate contamination, an indicator of agricultural pesticide use, was more than 3 mg L^{-1} were selected for this study. However, postal code regions do not coincide with watershed boundaries (Figure 4-15). Even if a participant resides in a postal code region that contains part of a nitrate-contaminated watershed, the residence may still be outside of the watershed of interest and pesticide exposure may be minimal. Therefore, it remains unknown if there was a difference in the degree of pesticide exposure between the two sample populations.

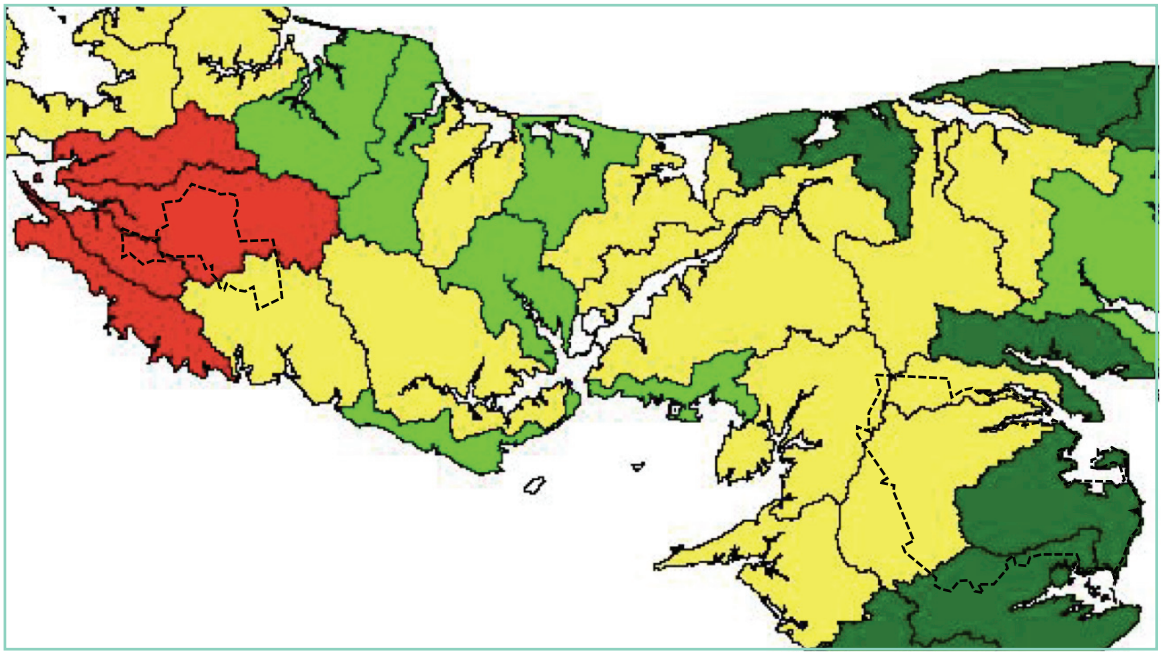

Figure 4-15. A cropped section of the Groundwater Nitrate Concentration Map: 2012 to 2016 showing that postal code boundaries (black dotted lines, obtained by Map Data ©2019 Google) do not coincide with watershed boundaries. Participants in the smaller postal code zone (left) may reside in an area with groundwater nitrate concentrations of 5 to 7 mg L^{-1} (red) or 3 to 5 mg L^{-1} (yellow). Similarly, participants residing in the larger postal code zone (right) may obtain well water from a watershed having nitrate concentrations of 2 mg L^{-1} or less, which may be indicative of minimal pesticide exposure.

Despite the uncertainty of pesticide exposure for participants between the two provinces, ETU was found in 60% of all serum samples and was the most frequently detected target analyte in urine. ETU is a common metabolite of EBDCs, a group of widely used fungicides [207]. It is possible that ETU exposure in these two populations occurred through consumption of food or water that contained either ETU or parent EBDC residues that were subsequently metabolized to ETU. In any case, biomonitoring of this analyte should be further examined in these populations because ETU is a common metabolite of two parent compounds (mancozeb and metiram) that are two of the most widely used fungicides in PEI, with a combined amount of 343,492 kg a.i. sold in 2014 [86].

The U.S. EPA classifies ETU as a Group B Probable Human Carcinogen [11]. In October 2018, Health Canada's PMRA reissued a Proposed Re-evaluation Decision document (PRVD2018-17) for mancozeb and its associated end-use products (e.g. ETU) due to a critical omission of the risk management proposal in the July 2013 Proposed Re-evaluation Decision (PRVD2013-01) [193]. Based on the dietary and environmental risk assessments, the 2013 proposal was to recommend the cancellation of all uses for mancozeb, except for greenhouse tobacco. However, due to the omission of the risk management proposal, the final decision (RVD2018-21) that was issued in June 2018 finding the use of mancozeb acceptable for foliar application to potatoes was revoked in October 2018. While PRVD2018-17 incorporates this proposed cancellation of mancozeb, Canada has seen an additional five years of continued use and exposure of mancozeb and its carcinogenic metabolite, ETU [182]. This is especially a concern for PEI groundwater contamination because ETU is the only metabolite of mancozeb expected to be found in groundwater where soils are permeable and water tables are shallow.

The Health Canada PMRA cancer risk assessment for ETU lists the following as primary sources of ETU exposure: drinking water (54.8% of total exposure), milk (9.0% of total exposure), cereal grains (7.7% of total exposure), tomatoes (6.2% of total exposure), and potatoes (5.3% of total exposure) [193]. As a result, the cancer risk estimation from exposure to ETU in drinking water alone was found to be unacceptable. This is remarkable, considering data from only 10 Canadian water monitoring studies from 1987 and 2007 were available to the PMRA at the time of the assessment. Of these studies, ETU was a target analyte in only three of these studies, all of which took place in Quebec.

Two of these studies reported ETU in water at concentrations of 1.1 and 2.3 µg L^{-1}. In this doctoral work, it was shown that ETU was detected in two of five groundwater samples from a vulnerable PEI watershed. It is evident that ETU groundwater monitoring data are lacking not only in PEI, but nationwide and that they are paramount in assessing cancer risk of EBDC pesticide exposure and application.

The two PA*N*N compounds most frequently tentatively identified in serum were *N*-DIM (78%) and *N*-OME (95%). This is interesting because DIM, which forms *N*-DIM, is the parent compound of OME, which forms *N*-OME. Neither *N*-DIM nor *N*-OME was found in urine using the same ionization mode as in serum (positive) but a biomarker having a molecular ion matching that of *N*-OME in negative mode was detected in 44% of the urine samples. Furthermore, DEA was tentatively detected in 42% of serum samples and 78% of urine samples, indicating that exposure to ATR is relatively common in these two sample populations. To confirm the identity of these, or other PA*N*N compounds and semi-target analytes investigated in this study, a certified reference material should be obtained or synthesized and analyzed for comparison of chromatographic and mass spectral characteristics.

Given the complexity of pesticide and nitrite/nitrate exposures, and the potential for endogenous formation of PA*N*N compounds, reliable biomarkers for characterizing exposure to these potential carcinogens are essential in evaluating associations between exposure and cancer development in epidemiology studies. However, as little is known about the toxicokinetics of specific PA*N*N compounds in humans, it is difficult to choose an ideal biomonitoring medium. The majority of PA*N*Ns do not have commercially-available reference standards, making identification and quantitation difficult using traditional targeted analytical methods. Targeted analysis requires the use of reference standards to make comparisons of analyte characteristics (i.e. retention time, accurate mass of primary ions, and ion intensity ratios) between standards and compounds detected in the sample in order to confirm the identity of an analyte [208]. In addition, a calibration curve can be generated from a series of known concentrations of the analytical standard for reliable quantitation.

HRAM orbital ion trap MS is an advanced analytical technique that operates in full spectrum acquisition mode to allow screening for a countless number of organic

contaminants present in the sample in a single injection [81,209]. One major advantage of this approach is that reliable tentative identifications of semi-targeted compounds (e.g. novel PA*N*N compounds with known molecular formulas) can be made by matching theoretical and observed *m/z* values of parent and fragment ions with high accuracy when reference standards are unavailable. Unlike the conventional targeted approach, semi-targeted analysis using HRAM MS facilitates reliable tentative identification of organic contaminants (e.g. PA*N*N compounds) for which analytical standards may not be available [125,209].

The prominent strength of this study is its novelty in the biomonitoring of PA*N*N compounds. This is the first study of its kind to apply the QuEChERS method for extraction of this suite of nitrosatable pesticides and associated PA*N*N compounds from human serum and urine samples. This work included analyses of biomarkers in both serum and urine, the gold standards for biomonitoring studies [125]. The method is easy to execute, safe, cost-effective, and allows for analysis of about 250 samples per week. Furthermore, with the use of the HRAM orbital ion trap MS, the spectral data files can be mined retrospectively and indefinitely. This allows for the semi-targeted analysis of an infinite number of known and yet unknown biomarkers in these samples. The presence of PA*N*N compounds or other pesticide-related biomarkers in human serum or urine signifies the discovery of novel biomarkers that may be vital in carcinogenic risk assessment in PEI and other regions of intense agriculture.

The limitations of this study match those of many pesticide biomonitoring studies. Due to gaps in pesticide toxicokinetic data (e.g. metabolic pathways, half-lives, etc.), it is difficult to predict what form and in what bodily compartment (i.e. blood, urine, etc.) the analyte of interest will be found. In addition, analytes of interest may be present in conjugated forms in urine to enhance excretion or bound to serum proteins as adducts. The method used here only measures the free form of analytes in both serum and urine. Creatinine correction for pesticide analysis in urine was omitted from the study because it has been controversial in the pesticide exposure literature [204]. Due to this approach, it is expected that a proportion of the body burden of each biomarker remains unaccounted for. Moreover, other unknown intra- and inter-person variation (e.g. metabolic enzyme gene

expression, lifestyle factors, etc.) may greatly influence the expression of pesticide-associated biomarkers.

Exposure data in biomonitoring studies are often lacking, as they are in this case. Due to the absence of residential street addresses, it is undetermined whether the PEI participants reside in areas of intense agricultural production. In addition, direct analysis of participants' drinking water was beyond the scope of this study and it was therefore not confirmed that drinking water was a source of nitrate and nitrosatable pesticide exposure to the PEI participants. As such, it remains unknown if there was a difference in pesticide exposure between the two sample populations. Other drawbacks of this study are that the semi-targeted data-mining process is extremely time-consuming without metabolomic analysis software, which is costly. Also, predicted spectra sometimes differed from one database to another and from experimental values.

Future studies may involve larger sample sizes to better understand baseline levels of the biomarkers in the general population, and include participants known to reside in regions of intense agriculture. Biomonitoring data from healthy participants may be compared to those from cancer patients. In terms of the analytical method, the use of enzymes to release protein- and conjugate-bound analytes may be incorporated. Additionally, optimizing the method(s) with a focus on a smaller suite of biomarkers of interest (i.e. ETU/*N*-ETU, *N*-ATR, *N*-DIM, and *N*-CAR) are critical in lowering the method detection limit and obtaining reliable quantitation data. It would also be helpful to analyze fresh drinking water samples along with biological samples. In addition, spectral data from this project may be mined in search of additional environmental contaminants or biomarkers of concern in these particular serum and urine samples.

4.5 Conclusions

Several target and semi-target pesticide-derived biomarkers were detected in both serum and urine samples of individuals residing in PEI and NS. Of the Group I analytes, two pesticide metabolites, ETU and TCPy were found in serum. ETU was present in 60% of all serum samples. TCPy was detected in two of the total 63 serum samples with detections reported only in PEI samples. In urine, ATR was detected in three of 64 samples. Two PEI urine samples contained ATR at concentrations above the MDL and the third

ATR detection was in one NS urine sample at a concentration of 16.5 µg L^{-1}, well above the LOQ. ETU was also detected in a total of nine urine samples. Five of the PEI urine samples contained ETU with one sample having a concentration above the LOQ at 9.1 µg L^{-1}. ETU was detected in four NS urine samples. There was no significant difference in the number of detections between PEI and NS for any of the target compounds.

For the Group II and III analytes, tentative identifications were reported for six PA*N*N compounds (*N*-ATR, di-*N*-CAR, *N*-DIM, *N*-IMI, *N*-LIN, and *N*-OME) in serum, 10 PA*N*N compounds (*N*-ATR, di-*N*-ATR, *N*-CAR, di-*N*-CAR, di-*N*-ETU, *N*-IMI, *N*-LIN, *N*-OME, *N*-TM, and di-*N*-TM) in urine, and DEA in both serum and urine by matching their theoretical molecular ion masses to those of experimental ions found in samples with a mass error within 5 ppm of theoretical *m/z* values. Identity confirmation of these potential biomarkers requires the use of certified reference standards, which are not commercially available for a majority of these compounds. Unequivocal confirmation requires matching of sample analyte LC characteristics (retention time, peak shape) and mass spectral characteristics (ion fragments and intensities, isotopic ions, accurate mass) to those of its analytical standard [210].

The ultimate goal of this study was to advance pesticide-related biomarker research for assessing associations between exposure to agricultural pollutants and adverse health outcomes in future large-scale studies. Based on the results of this cross-sectional biomonitoring study, a majority of the PEI and NS participants involved in this study have been exposed to detectable concentrations of nitrosatable pesticides and may be exposed to potentially carcinogenic PA*N*N compounds due to endogenous formation. This work shows that biomonitoring of PA*N*N compounds in human serum and urine is feasible and future research may focus on confirming the identity of *N*-ATR, *N*-DIM, and *N*-CAR, as well as tailoring the method for ETU and *N*-ETU, as these analytes appear to be potential biomarkers of concern for the PEI and NS sample populations. While the presence of these biomarkers does not necessarily imply that adverse health effects will ensue, it is important to continue integrating biomonitoring data into epidemiological studies, which serves to elucidate potential health risks associated with these novel biomarkers.

Chapter 5. Conclusions and Future Perspectives

5.1 Conclusions

This interdisciplinary PhD dissertation outlines the achievement of three principal objectives: (i) the development and validation of an analytical method for analysis of nitrosatable pesticides and by-products in human serum and urine using UHPLC/HRAM orbital ion trap MS; (ii) the investigation of PA*N*N compound formation in water containing environmentally-relevant concentrations of nitrosatable pesticides and nitrite; and (iii) the identification of specific pesticide-derived biomarkers, including parent pesticides and their associated PA*N*N compounds, in human serum and urine from a healthy sample population in an area of intense agriculture in PEI (with groundwater as the sole drinking water source) and from a healthy sample population in Halifax, a non-agricultural urban area (with municipal water as the primary drinking water source). Each standalone project has been merged into a trilogy of research studies from three disciplines: analytical toxicology; hydrogeology; and epidemiology.

In Chapter 2 of this dissertation, three sample preparation methods were evaluated for extraction of nitrosatable pesticides and byproducts from human serum and urine. Methanol deproteinization resulted in ion enhancement of some target compounds and suppression of others. While SPE showed less ion enhancement than did deproteinization, significant analyte loss was observed. The QuEChERS method resulted in a revolutionary method for sufficient extraction of the target analytes from both serum and urine. Following analysis via UHPLC/HRAM MS, mean recoveries for all target analytes in serum ranged between 74.4 and 120.3% (%RSD <12). For urine, initial analyte recoveries ranged from 95.9 to 115.5% (%RSD ≤10). Findings from this study provided compatible analytical methods required to analyze PA*N*N compounds and their parent compounds in subsequent experiments of this PhD project.

Chapter 3 involved the investigation of PA*N*N compound formation in water from nine nitrosatable pesticides and degradation products that were individually reacted at environmentally-relevant concentrations with nitrite in acidic conditions. Of the nine analytes tested, only ETU showed evidence of PA*N*N compound formation and only under acidic conditions (i.e. ~ pH 2). *N*-ETU formation was further investigated in a pooled

groundwater sample collected from an agricultural region of PEI, where nitrate contamination is an ongoing issue. Evidence of *N*-ETU formation in the groundwater sample was observed at concentrations ranging from 7.5 to 20 µg L^{-1}. UHPLC/HRAM MS analysis confirmed in-house synthesis of *N*-ETU, the spectral characteristics of which provided compound identification. These results indicate that ETU is capable of forming the potentially carcinogenic *N*-ETU at environmentally-relevant concentrations at pH values comparable to that of gastric pH. Thus, the results of this study show that endogenous *N*-ETU formation may be a concern for individuals exposed to low concentrations of ETU and nitrite/nitrate.

In the first biomonitoring study of its kind to investigate PA*N*N compounds in human serum and urine, Chapter 4 utilizes the analytical method developed and validated in Chapter 2 and the PA*N*N compound formation experimental data in Chapter 3 to identify specific pesticide-related biomarkers in human serum and urine from the healthy PEI and NS sample populations. Ten nitrosatable pesticides and byproducts were extracted from serum and urine from 64 individuals and analyzed via UHPLC/HRAM MS. Two target analytes, ETU and TCPy were found in serum, while ATR and ETU were detected in urine. Interestingly, there were no significant differences in the frequency of target analyte detection in either biomatrix between provinces. Six and 10 PA*N*N compounds were tentatively identified in serum and urine, respectively. The two PA*N*N compounds that were most frequently tentatively identified in serum were *N*-DIM and *N*- OME. In urine, significantly more tentative identifications were found in PEI samples for di-*N*-CAR. Identity confirmation of these PA*N*N compounds requires the use of certified reference standards, most of which are not yet commercially available.

This innovative and interdisciplinary study intentionally cast a wide net of objectives which, if met, would serve as the foundation for future PA*N*N compound biomonitoring studies. The collective results of this dissertation provide numerous deliverables. First, the successful development of the analytical method not only allows future analyses of PA*N*N compounds and their parent compounds in serum and urine of other sample populations of interest, but also retrospective analysis of yet unknown biomarkers extracted from the analyzed samples. Since HRAM orbital ion trap MS

operates in full scan mode, spectral data from known and unknown biomarkers present in all analyzed serum and urine samples may be analyzed indefinitely.

Second, the screening of 10 nitrosatable pesticides and byproducts deemed contaminants of concern in PEI for *N*-nitroso compound formation under various conditions clearly shows that the monitoring of ETU and *N*-ETU formation should be a major focus of future biomonitoring studies in the province. *N*-ETU was repeatedly produced in several experiments and at initial ETU concentrations as low as 7.5 $\mu g\ L^{-1}$. Former studies of *N*-ETU exposure in mice and rats indicate that endogenous formation of *N*-ETU resulted in carcinogenesis and that *N*-ETU is a more potent carcinogen than is ETU [55–58]. Thus, even trace concentrations of ETU or its parent compounds (e.g. mancozeb and metiram) in PEI groundwater and other sources of exposure warrant exploration of endogenous *N*-ETU formation in potentially exposed humans.

Third, the biomonitoring of serum and urine samples from the PEI and NS populations showed that ETU was detected in 60% of all serum samples and in nine of 64 urine samples, despite the method's limitations in extracting ETU from the biomatrices. Two other target compounds, ATR and TCPy, were found in urine and serum, respectively. There was no significant difference in the number of detections between PEI and NS for any of the target compounds. Six and 10 PA*N*N compounds were tentatively identified in serum and urine, respectively, with *N*-DIM and *N*-CAR the most frequently detected in serum. In urine, significantly more tentative identifications were found in PEI samples for di-*N*-CAR. A critical point to make here is that although *N*-ETU itself was not tentatively identified in any of the serum or urine samples, it is possible the PA*N*N compound may not have been detected due to poor extraction recovery from the samples since the method was not ideally suited for ETU analysis. These data set up the framework for the next steps in PA*N*N compound biomonitoring research in PEI, NS, and other locations where exposure to trace amounts of nitrosatable pesticides is occurring. The central conclusion from this PhD work is that PA*N*N compounds should be investigated as important biomarkers of pesticide exposure and cancer risk assessment and that ETU and its PA*N*N compound, *N*-ETU, should be highlighted as contaminants of concern to PEI and NS residents.

5.2 Future Perspectives

Analytical method optimization

The analytical method developed herein shows the feasibility of extracting nitrosatable pesticides from human serum and urine by way of a simple, rapid, effective, and inexpensive method. Opportunely, small modifications to this method can be made in future studies to optimize extraction recoveries of priority pesticides, such as ETU and its PA*N*N compound, *N*-ETU. First, certified reference standards for the deuterated isotope of ETU (to be used as a compatible IS) and *N*-ETU, for unequivocal identification of the biomarker, would be integral tools in the optimization of a follow-up biomonitoring study. Second, since ETU has been found to participate in protein-binding and conjugation [211], the addition of a hydrolysis step could significantly increase the concentration of free-form ETU in biofluid samples. Other method modifications include further optimization of the pH of extraction solvents and the proportion of separation salts for enhanced extraction of ETU and *N*-ETU. For identity confirmation of other PA*N*N compounds without commercially-available reference standards, compound synthesis may provide an alternate route of biomarker identification.

Environmental analysis of nitrosatable pesticides and nitrate/nitrite

When biomarkers of pesticide exposure such as PA*N*N compounds are detected in human samples, it is important to investigate possible sources of exposure. Doing so serves to reduce the risk of exposure and potentially mitigate pesticide-related health effects. Future studies may integrate the analysis of this suite of target compounds and biomarkers in environmental samples, including groundwater and food samples, by utilizing the analytical methods developed in this work. Foremost, it is recommended that regular monitoring of ETU in PEI groundwater be implemented, as it is a potential groundwater contaminant based on its high water solubility (20,000 mg L^{-1}) and low K_{OC} (13 L kg^{-1}) [109,110]. Moreover, ETU is a common metabolite of mancozeb and metiram, two of the most widely used pest control products in PEI, with combined sales reaching 343,492 kg a.i. in 2014 [86]. Finally, regular monitoring of groundwater nitrate, which is converted to nitrite in the body, would be beneficial as nitrite is a key component of endogenous *N*-

nitroso compound formation. The monitoring of these PA*N*N compound substrates in the environment would be paramount in determining risk of *N*-ETU formation in the body.

Expanding the scope of epidemiological PANN biomarker studies

Following recommendations by Dunn et al. (2011), this work should be followed by a cross-sectional study involving thousands of participants, which would serve to validate the true utility of the biomarkers identified in the target population [201]. This large-scale PA*N*N compound biomonitoring study would aid in determining baseline levels of these biomarkers in the general population. In addition, subsets of sample populations based on exposure (participants known to have been exposed to nitrosatable pesticides and nitrate/nitrite) and outcome (participants diagnosed with different types of cancer) may also be compared to identify potential associations between PA*N*N compounds and cancer development.

While "snapshots" of PA*N*N compound biomarker levels in the target population provide useful pesticide exposure data and proof-of-concept for the analytical method, these types of cross-sectional studies do not consider the length of time between exposures and outcomes nor do they provide information about causality. Longitudinal studies that follow participants over time and compare cancer incidence rates with biomarker expression should be considered. Serum and urine samples may also be analyzed regularly over a certain period to see how the concentration of biomarker expression changes over time. These types of studies are designed such that exposure precedes outcome. For PA*N*N biomarkers to be instrumental in cancer risk assessments, evidence of a clearly defined causal relationship should be established between exposure to nitrosatable pesticides and carcinogenesis. A longitudinal study involving quantitation of PA*N*N biomarkers in thousands of PEI participants over a period of decades would be helpful in determining whether there exists a link between endogenous PA*N*N compound formation and cancer risk.

Although longitudinal cohort studies are of considerable value, they often take decades to complete as the longer the latency period of the outcome of interest, the longer the duration of the study. In the interim and in the face of uncertainty of quantifiable risk, we have the option to collect existing evidence, incorporating the data presented in this work, and assemble it purposefully to exercise the precautionary principle. In this case, we

have available to us some valuable information about the hazard and exposure risk of ETU. First, it is known that ETU has been flagged by Health Canada's PMRA as posing an unacceptable risk from exposure in drinking water. In this work, ETU was detected in two of five PEI groundwater samples and in 60% of serum samples from both sample populations, the latter of which shows that ETU exposure is widespread in this population. Considering that mancozeb, one of ETU's primary parent compounds, is the most commonly used pesticide in PEI, this population may be at an increased risk of ETU exposure and endogenous *N*-ETU formation. ETU is a probable human carcinogen and its endogenously-formed PA*N*N, *N*-ETU, may be a more potent carcinogen (based on animal toxicity studies). As such, PEI residents exposed to ETU may have an increased risk of developing cancer associated with these potential human carcinogens. With the focus of primary prevention of pesticide-associated cancers in PEI at the forefront, a judicious evaluation of current groundwater monitoring policies and future PA*N*N biomonitoring research is necessary to understand and mitigate the risks of pesticide exposure and endogenous PA*N*N formation.

References

[1] W. Zhang, Global pesticide use: Profile, trend, cost/benefit and more, Proceedings of the International Academy of Ecology and Environmental Sciences. 8 (2018) 1–27.

[2] L. Schinasi, M. Leon, Non-Hodgkin Lymphoma and Occupational Exposure to Agricultural Pesticide Chemical Groups and Active Ingredients: A Systematic Review and Meta-Analysis, International Journal of Environmental Research and Public Health. 11 (2014) 4449–4527. doi:10.3390/ijerph110404449.

[3] H.D. Bailey, C. Infante-Rivard, C. Metayer, J. Clavel, T. Lightfoot, P. Kaatsch, E. Roman, C. Magnani, L.G. Spector, E. Th. Petridou, E. Milne, J.D. Dockerty, L. Miligi, B.K. Armstrong, J. Rudant, L. Fritschi, J. Simpson, L. Zhang, R. Rondelli, M. Baka, L. Orsi, M. Moschovi, A.Y. Kang, J. Schüz, Home pesticide exposures and risk of childhood leukemia: Findings from the childhood leukemia international consortium, Int. J. Cancer. 137 (2015) 2644–2663. doi:10.1002/ijc.29631.

[4] G. Van Maele-Fabry, L. Gamet-Payrastre, D. Lison, Residential exposure to pesticides as risk factor for childhood and young adult brain tumors: A systematic review and meta-analysis, Environment International. 106 (2017) 69–90. doi:10.1016/j.envint.2017.05.018.

[5] S. k. Swain, N. Kaur, B. d. Banerjee, K. Thamineni, T. Sharma, Organochlorine Pesticides Exposure as a Risk Factor for Breast Cancer in Young Women: A Case Control Study, JGO. 4 (2018) 7s–7s. doi:10.1200/jgo.18.76300.

[6] A.-M. Lewis-Mikhael, A. Bueno-Cavanillas, T. Ofir Guiron, R. Olmedo-Requena, M. Delgado-Rodríguez, J.J. Jiménez-Moleón, Occupational exposure to pesticides and prostate cancer: a systematic review and meta-analysis, Occup Environ Med. 73 (2016) 134–144. doi:10.1136/oemed-2014-102692.

[7] S.A. Uyemura, H. Stopper, F.L. Martin, V. Kannen, A Perspective Discussion on Rising Pesticide Levels and Colon Cancer Burden in Brazil, Front. Public Health. 5 (2017). doi:10.3389/fpubh.2017.00273.

[8] T. VoPham, K.A. Bertrand, J.E. Hart, F. Laden, M.M. Brooks, J.-M. Yuan, E.O. Talbott, D. Ruddell, C.-C.H. Chang, J.L. Weissfeld, Pesticide exposure and liver cancer: a review, Cancer Causes Control. 28 (2017) 177–190. doi:10.1007/s10552-017-0854-6.

[9] R. Zendehdel, R. Tayefeh-Rahimian, A. Kabir, Chronic exposure to chlorophenol related compounds in the pesticide production workplace and lung cancer: a meta-analysis, Asian Pac. J. Cancer Prev. 15 (2014) 5149–5153.

[10] S. Koutros, D.T. Silverman, M.C. Alavanja, G. Andreotti, C.C. Lerro, S. Heltshe, C.F. Lynch, D.P. Sandler, A. Blair, B. Freeman, L. E, Occupational exposure to pesticides and bladder cancer risk, Int J Epidemiol. 45 (2016) 792–805. doi:10.1093/ije/dyv195.

[11] U.S. Environmental Protection Agency, Chemicals Evaluated for Carcinogenic Potential, Office of Pesticide Programs, 2015. http://npic.orst.edu/chemicals_evaluated.pdf (accessed April 13, 2016).

[12] S.S. Mirvish, Formation of N-nitroso compounds: Chemistry, kinetics, and in vivo occurrence, Toxicology and Applied Pharmacology. 31 (1975) 325–351. doi:10.1016/0041-008X(75)90255-0.

[13] U.S. EPA, Guidelines for Carcinogen Risk Assessment, Risk Assessment Forum, US EPA, Washington, DC, 2005.

[14] A. Blair, B. Ritz, C. Wesseling, L. Beane Freeman, Pesticides and human health, Occupational and Environmental Medicine. 72 (2015) 81–82. doi:10.1136/oemed-2014-102454.

[15] D.L. Sparks, Advances in Agronomy, Academic Press, San Diego, CA, 2013.

[16] W. Lijinsky, Chemical Structure of Nitrosamines Related to Carcinogenesis, in: Nitrosamines and Related N-Nitroso Compounds, American Chemical Society, 1994: pp. 250–266. doi:10.1021/bk-1994-0553.ch020.

[17] R. Preussmann, Carcinogenic N-nitroso compounds and their environmental significance, Naturwissenschaften. 71 (1984) 25–30.

[18] R. Dubrow, A.S. Darefsky, Y. Park, S.T. Mayne, S.C. Moore, B. Kilfoy, A.J. Cross, R. Sinha, A.R. Hollenbeck, A. Schatzkin, M.H. Ward, Dietary Components Related to N-Nitroso Compound Formation: A Prospective Study of Adult Glioma, Cancer Epidemiol Biomarkers Prev. 19 (2010) 1709–1722. doi:10.1158/1055-9965.EPI-10-0225.

[19] National Toxicology Program, 14th Report on Carcinogens, U.S. Department of Health and Human Services, 2016. https://ntp.niehs.nih.gov/ntp/roc/content/profiles/nitrosamines.pdf (accessed February 2, 2018).

[20] W. Lijinsky, How nitrosamines cause cancer, in: New Scientist, Reed Business Information, 1977: pp. 216–217.

[21] C. Ioannides, Cytochromes P450: Role in the Metabolism and Toxicity of Drugs and other Xenobiotics, Royal Society of Chemistry, 2008.

[22] P. Varelis, L. Melton, F. Shahidi, Encyclopedia of Food Chemistry, Elsevier, 2018.

[23] C.W. Jameson, D.B. Walters, Chemistry for Toxicity Testing, Butterworth-Heinemann, 2016. https://books.google.ca/books?hl=en&lr=&id=CXD-BAAAQBAJ&oi=fnd&pg=PA15&dq=n-nitrosamine+OR+nitroso+AND+%22ultimate+carcinogen%22&ots=X38yeZr--X&sig=K85IhXm0zW19nn124fXuK52CcTU#v=onepage&q=nitroso&f=false (accessed February 3, 2018).

[24] M.C. Archer, Mechanisms of action of N-nitroso compounds, Cancer Surv. 8 (1989) 241–250.

[25] A.M. Camus, O. Geneste, P. Honkakoski, J.C. Béréziat, C.J. Henderson, C.R. Wolf, H. Bartsch, M.A. Lang, High variability of nitrosamine metabolism among individuals: role of cytochromes P450 2A6 and 2E1 in the dealkylation of N-nitrosodimethylamine and N-nitrosodiethylamine in mice and humans, Mol. Carcinog. 7 (1993) 268–275.

[26] R.J. Graves, P.F. Swann, Clearance of N-nitrosodimethylamine and N-nitrosodiethylamine by the perfused rat liver: Relationship to the Km, and Vmax for nitrosamine metabolism, Biochemical Pharmacology. 45 (1993) 983–989. doi:10.1016/0006-2952(93)90240-W.

[27] G. Eisenbrand, C. Janzowski, Potential mechanism of action of nitrosamines with hydroxy, oxo, or carboxy groups, ACS Symposium Series (USA). (1994). http://agris.fao.org/agris-search/search.do?recordID=US9604043 (accessed February 11, 2018).

[28] M.G. Rhoades, J.L. Meza, C.L. Beseler, P.J. Shea, A. Kahle, J.M. Vose, K.M. Eskridge, R.F. Spalding, Atrazine and Nitrate in Public Drinking Water Supplies and Non-Hodgkin Lymphoma in Nebraska, USA, Environ Health Insights. 7 (2013) 15–27. doi:10.4137/EHI.S10629.

[29] I.B. Rogozin, V.B. Berikov, E.A. Vasunina, O.I. Sinitsina, The effect of the primary structure of DNA on induction of mutations by alkylating agents, Russian Journal of Genetics. 37 (2001) 704–710.

[30] R. Montesano, Alkylation of DNA and tissue specificity in nitrosamine carcinogenesis, J. Supramol. Struct. Cell. Biochem. 17 (1981) 259–273. doi:10.1002/jsscb.380170307.

[31] M. Dietrich, G. Block, J.M. Pogoda, P. Buffler, S. Hecht, S. Preston -Martin, A review: dietary and endogenously formed N-nitroso compounds and risk of childhood brain tumors, Cancer Causes Control. 16 (2005) 619–635. doi:10.1007/s10552-005-0168-y.

[32] K. Ikeda, K.G. Migliorese, H. Curtis, Analysis of nitrosamines in cosmetics, Journal of the Society of Cosmetic Chemists. 41 (1990) 283–333.

[33] A.R. Tricker, B. Spiegelhalder, R. Preussmann, Environmental exposure to preformed nitroso compounds, Cancer Surv. 8 (1989) 251–272.

[34] R.A. Scanlan, Formation and occurrence of nitrosamines in food, Cancer Res. 43 (1983) 2435s–2440s.

[35] Agency for Toxic Substances and Disease Registry (ATSDR), Toxicological profile for n-Nitrosodimethylamine, U.S. Department of Health and Human Services, Public Health Service., Atlanta, GA, 1989.

[36] M. Cantwell, C. Elliott, Nitrates, Nitrites and Nitrosamines from Processed Meat Intake and Colorectal Cancer Risk, J Clin Nutr Diet. 3 (2017) 27.

[37] A.S. Shamsuddin, S.N.S. Ismail, S.M. Sham, E.Z. Abidin, Nitrate in Groundwater and Excretion of Nitrate and Nitrosamines in Urine: A Review, (2014).

[38] P. Sivasinthujah, R. Srikaran, A.C. Thavaranjit, K. Velauthamurty, C.J. Tharmila, P. Abiman, P. Iyngaran, Contents of nitrate, nitrite and the occurrence of bacteria in fermented cooked parboiled rice and their potential ingestion in the diet, Journal of Microbiology and Biotechnology Research. 4 (2017) 56–61.

[39] J. Kobayashi, Effect of diet and gut environment on the gastrointestinal formation of N-nitroso compounds: A review, Nitric Oxide. (2017). doi:10.1016/j.niox.2017.06.001.

[40] D. Cova, C. Nebuloni, A. Arnoldi, A. Bassoli, M. Trevisan, A.A.M. Del Re, N-Nitrosation of Triazines in Human Gastric Juice, J. Agric. Food Chem. 44 (1996) 2852–2855. doi:10.1021/jf9501296.

[41] A.J. Cross, J.R.A. Pollock, S.A. Bingham, Haem, not protein or inorganic iron, is responsible for endogenous intestinal N-nitrosation arising from red meat, Cancer Res. 63 (2003) 2358–2360.

[42] C.J. Schorah, G.M. Sobala, M. Sanderson, N. Collis, J.N. Primrose, Gastric juice ascorbic acid: effects of disease and implications for gastric carcinogenesis, Am. J. Clin. Nutr. 53 (1991) 287S-293S.

[43] R.U. Hernández-Ramírez, M.V. Galván-Portillo, M.H. Ward, A. Agudo, C.A. González, L.F. Oñate-Ocaña, R. Herrera-Goepfert, O. Palma-Coca, L. López-Carrillo, Dietary intake of polyphenols, nitrate and nitrite and gastric cancer risk in Mexico City, Int. J. Cancer. 125 (2009) 1424–1430.

[44] International Agency for Research on Cancer, IARC Monographs on the Evaluation of the Carcinogenic Risk of Chemicals to Humans: Miscellaneous Pesticides. Volume 30, World Health Organization, Lyon, France, 1983.

[45] N.L. Wolfe, R.G. Zepp, J.A. Gordon, R.C. Fincher, N-Nitrosamine formation from atrazine, Bull. Environ. Contam. Toxicol. 15 (1976) 342–347. doi:10.1007/BF01812647.

[46] R.J. Gilliom et al, J.E. Barbash, C.G. Crawford, P.A. Hamilton, J.D. Martin, N. Nakagaki, L.H. Nowell, J.C. Scott, P.E. Stackelberg, G.P. Thelin, D.M. Wolock, Pesticides in the nation's streams and ground water, 1992-2001: the quality of our nation's waters, U.S. Geological Survey, Reston, VA, 2007.

[47] Health Canada, Guidelines for Canadian Drinking Water Quality: Guideline Technical Document – Atrazine, 1993. https://www.canada.ca/en/health-canada/services/publications/healthy-living/guidelines-canadian-drinking-water-quality-guideline-technical-document-atrazine.html (accessed February 8, 2018).

[48] L.F. Meisner, B.D. Roloff, D.A. Belluck, In vitro effects of N-nitrosoatrazine on chromosome breakage, Arch. Environ. Contam. Toxicol. 24 (1993) 108–112.

[49] P.C. Kearney, J.E. Oliver, C.S. Helling, A.R. Isensee, A. Kontson, Distribution, movement, persistence, and metabolism of N-nitrosoatrazine in soils and a model aquatic ecosystem, Journal of Agricultural and Food Chemistry. 25 (1977) 1177–1181.

[50] H.-R. Wei, M.G. Rhoades, P.J. Shea, Formation, Adsorption, and Stability of N-Nitrosoatrazine in Water and Soil, in: It's All in the Water: Studies of Materials and Conditions in Fresh and Salt Water Bodies, American Chemical Society, 2011: pp. 3–19. doi:10.1021/bk-2011-1086.ch001.

[51] C. Janzowski, R. Klein, R. Preussmann, Formation of N-nitroso compounds of the pesticides atrazine, simazine and carbaryl with nitrogen oxides., IARC Sci Publ. (1980) 329–339.

[52] G. Meli, R. Bagnati, R. Fanelli, E. Benfenati, L. Airoldi, Metabolic profile of atrazine and N-nitrosoatrazine in rat urine, Bulletin of Environmental Contamination and Toxicology. 48 (1992) 701–708.

[53] M. Yamamoto, T. Yamada, A. Tanimura, The Reaction of Ethylenethiourea with Nitrite and Transnitrosation by N-Nitrosoethylenethiourea, Chem. Pharm. Bull. 31 (1983) 3678–3683. doi:10.1248/cpb.31.3678.

[54] C.H. Lindh, M. Littorin, G. Johannesson, B.A.G. Jönsson, Analysis of ethylenethiourea as a biomarker in human urine using liquid chromatography/triple quadrupole mass spectrometry, Rapid Commun. Mass Spectrom. 22 (2008) 2573–2579. doi:10.1002/rcm.3647.

[55] M. Moriya, K. Mitsumori, K. Kato, T. Miyazawa, Y. Shirasu, Carcinogenicity of N-nitroso-ethylenethiourea in female mice, Cancer Letters. 7 (1979) 339–342. doi:10.1016/S0304-3835(79)80063-4.

[56] A. Yoshida, T. Harada, K. Maita, Tumor Induction by Concurrent Oral Administration of Ethylenethiourea and Sodium Nitrite in Mice, Toxicol Pathol. 21 (1993) 303–310. doi:10.1177/019262339302100306.

[57] K. Nishiyama, J. Ando-Lu, S. Nishimura, M. Takahashi, M. Yoshida, K. Sasahara, K. Miyajima, A. Maekawa, Initiating and promoting effects of concurrent oral administration of ethylenethiourea and sodium nitrite on uterine endometrial adenocarcinoma development in Donryu rats., In Vivo. 12 (1998) 363–368.

[58] J.P. Seiler, In vivo mutagenic interaction of nitrite and ethylenethiourea, Experientia. 31 (1975) 214–215. doi:10.1007/BF01990712.

[59] Agriculture and Forestry: Prince Edward Island Potatoes, (n.d.). http://www.gov.pe.ca/agriculture/index.php3?number=71616&lang=E (accessed July 22, 2013).

[60] S. Brimble, P. Bacchus, P.-Y. Caux, Pesticide utilization in Canada : a compilation of current sales and use data, Environment Canada Pesticide Program Coordinating Committee, Ottawa, ON, 2005.

[61] M.W. Priddle, R.E. Jackson, J.P. Mutch, Contamination of the Sandstone Aquifer of Prince Edward Island, Canada by Aldicarb and Nitrogen Residues, Ground Water Monitoring & Remediation. 9 (1989) 134–140. doi:10.1111/j.1745-6592.1989.tb01022.x.

[62] PEI Department of Communities, Land and Environment, Environment: Pesticide Monitoring Program, (n.d.). https://data.princeedwardisland.ca/Environment-and-Food/OD0004-Pesticide-Analysis-For-Drinking-Water/iy5f-uq43 (accessed March 3, 2016).

[63] Z. He, Sustainable potato production: global case studies, Springer, New York, 2012.

[64] Y. Jiang, G. Somers, Modeling effects of nitrate from non-point sources on groundwater quality in an agricultural watershed in Prince Edward Island, Canada, Hydrogeol J. 17 (2009) 707–724. doi:10.1007/s10040-008-0390-2.

[65] Government of Prince Edward Island, Department of Communities, Land and Environment, Fish Kill Information and Statistics, (2018). https://www.princeedwardisland.ca/en/information/communities-land-and-environment/fish-kill-information-and-statistics (accessed December 22, 2018).

[66] Prince Edward Island Legislative Assembly, Briefing on Fish Kills, Order of the Legislature, Charlottetown, PEI, 2017. http://www.assembly.pe.ca/sittings/2017spring/transcripts/17_2017-15-09-transcript.pdf (accessed December 22, 2018).

[67] Martec Limited., Mill River Estuary Modelling Study: Martec Report No. TP-02-36., (2002). www.gov.pe.ca/photos/original/tpw_millstudy.pdf (accessed November 6, 2011).

[68] Statistics Canada, Number of new cases and age-standardized rates of primary cancer (based on the November 2017 CCR tabulation file), by cancer type and sex: Table: 13-10-0747-01 (formerly CANSIM 103-0554), (2018). https://www150.statcan.gc.ca/t1/tbl1/en/cv.action?pid=1310074701 (accessed December 16, 2018).

[69] IARC, N-nitroso compounds analysis and formation; proceedings of a working conference held at the Deutsches Krebsforschungszentrum, Heidelberg, Federal Republic of Germany, 13-15 October 1971, International Agency for Research on Cancer, 1972. https://search.library.utoronto.ca/details?2520942&uuid=6516d4ed-7462-4366-83c4-bf8d18ef5c9b (accessed February 22, 2018).

[70] IARC, N-nitroso compounds in the environment: proceedings of a working conference held at the International Agency for Research on Cancer, Lyon, France, 17-20 October 1973, International Agency for Research on Cancer, 1975.

[71] IARC, N-nitroso compounds : occurrence and biological effects : proceedings of the VIIth International Symposium on N-nitroso Compounds held in Tokyo, 28 September-1 October 1981 / editors, H. Bartsch ... [et al.] ; technical editor for IARC, W. Davis, International Agency for Research on Cancer ; WHO Publications Centre USA, distributor], Lyon : [Albany, N.Y, 1982.

[72] World Health Organization, Nitrates, nitrites, and N-nitroso compounds: Conference proceedings by WHO Task Group on Environmental Health Criteria for Nitrates, 1976: Lyon, France, World Health Organization, Lyon, France, 1978.

[73] E.A. Walker, IARC, N-nitroso Compounds, Analysis, Formation, and Occurrence: Proceedings of the 6th International Symposium on N-nitroso Compounds Held in Budapest, 16-20 October 1979, International Agency for Research on Cancer, 1980.

[74] IARC, N-nitroso Compounds: Occurrence, Biological Effects, and Relevance to Human Cancer : Proceedings of the VIIIth International Symposium on N-nitroso Compounds, Held in Banff, Canada, 5-9 September, 1983, International Agency for Research on Cancer, 1984.

[75] H. Bartsch, IARC, Relevance of N-nitroso Compounds to Human Cancer: Exposures and Mechanisms : Proceedings of the IXth International Symposium on N-Nitroso Compounds, Held in Baden, Austria, 1-5 September 1986, International Agency for Research on Cancer, 1987.

[76] P.E. Oettinger, F. Huffman, D.H. Fine, D. Lieb, Liquid Chromatograph Detector for Trace Analysis of Non-Volatile N-Nitroso Compounds, Analytical Letters. 8 (1975) 411–414. doi:10.1080/00032717508058224.

[77] D.H. Fine, R. Ross, D.P. Rounbehler, A. Silvergleid, L. Song, Analysis of nonionic nonvolatile N-nitroso compounds in foods, Journal of Agricultural and Food Chemistry. 24 (1976) 1069–1071.

[78] D.H. Fine, Firooz. Rufeh, David. Lieb, D.P. Rounbehler, Description of the thermal energy analyzer (TEA) for trace determination of volatile and nonvolatile N-nitroso compounds, Anal. Chem. 47 (1975) 1188–1191. doi:10.1021/ac60357a073.

[79] J.F. Hotchkiss, J.F. Barbour, L.M. Libbey, R.A. Scanlan, Nitramines as thermal energy analyzer positive nonnitroso compounds found in certain herbicides, Journal of Agricultural and Food Chemistry. 26 (1978) 884–887.

[80] D. Tsipi, H. Botitsi, A. Economou, Mass Spectrometry for the Analysis of Pesticide Residues and Their Metabolites, John Wiley & Sons, Hoboken, NJ, 2015.

[81] A. Zhang, J.S. Chang, C. Gu, M. Sanders, Non-targeted Screening and Accurate Mass Confirmation of 510 Pesticides on the High Resolution Exactive Benchtop LC/MS Orbitrap Mass Spectrometer. Application Note: 51878, Thermo Fisher Scientific, San Jose, CA, USA, 2010. https://www.thermofisher.com/content/dam/tfs/ATG/CMD/CMD%20Documents/Application%20&%20Technical%20Notes/Mass%20Spectrometry/LC%20MS/LC%20MS%20for%20Endocrine%20Analysis/AN51878_Exactive-NonTargetedPesticideScreening(1).pdf (accessed May 29, 2017).

[82] W.-H. Chen, T.M. Young, NDMA Formation during Chlorination and Chloramination of Aqueous Diuron Solutions, Environ. Sci. Technol. 42 (2008) 1072–1077. doi:10.1021/es072044e.

[83] S.U. Khan, J.C. Young, N-Nitrosamine formation in soil from the herbicide glyphosate, Journal of Agricultural and Food Chemistry. 25 (1977) 1428–1430.

[84] W. Zwickenpflug, E. Richter, Synthesis and occurrence of nitrosated cyanazine in soil, Journal of Agricultural and Food Chemistry. 42 (1994) 2333–2337.

[85] L.P. Padhye, J.-H. Kim, C.-H. Huang, Oxidation of dithiocarbamates to yield N-nitrosamines by water disinfection oxidants, Water Research. 47 (2013) 725–736. doi:10.1016/j.watres.2012.10.043.

[86] Department of Communities, Land and Environment, PEI Government, Retail Pesticide Sales Report: 21 September 2015., (2015). http://www.gov.pe.ca/photos/original/cle_pest_rpt.pdf (accessed March 2, 2016).

[87] S. Teramoto, A. Shingu, Y. Shirasu, Induction of dominant-lethal mutations after administration of ethylenethiourea in combination with nitrite or of N-nitroso-ethylenethiourea in mice, Mutation Research/Fundamental and Molecular Mechanisms of Mutagenesis. 56 (1978) 335–340. doi:10.1016/0027-5107(78)90202-6.

[88] H. Tezuka, N. Ando, R. Suzuki, M. Terahata, M. Moriya, Y. Shirasu, Sister-chromatid exchanges and chromosomal aberrations in cultured chinese hamster cells treated with pesticides positive in microbial reversion assays, Mutation Research/Genetic Toxicology. 78 (1980) 177–191. doi:10.1016/0165-1218(80)90097-X.

[89] S. Teramoto, R. Saito, Y. Shirasu, Teratogenic effects of combined administration of ethylenethiourea and nitrite in mice, Teratology. 21 (1980) 71–78. doi:10.1002/tera.1420210109.

[90] M. Hirano, K. Maita, Y. Shirasu, Effect of N-nitroso-ethylenethiourea on germinal cells in male mice., The Japanese Journal of Veterinary Science. 46 (1984) 697–704.

[91] J.P. Seiler, Nitrosation in vitro and in vivo by sodium nitrite, and mutagenicity of nitrogenous pesticides, Mutation Research/Fundamental and Molecular Mechanisms of Mutagenesis. 48 (1977) 225–236. doi:10.1016/0027-5107(77)90164-6.

[92] L. Fishbein, Overview of potential mutagenic problems posed by some pesticides and their trace impurities., Environ Health Perspect. 27 (1978) 125–131.

[93] S.S. (Eppley I. for R. in C. Mirvish, P. Gannett, D.M. Babcook, D. Williamson, S.C. Chen, D.D. Weisenburger, N-Nitrosoatrazine: synthesis, kinetics of formation, and nuclear magnetic resonance spectra and other properties, Journal of Agricultural and Food Chemistry (USA). (1991). http://agris.fao.org/agris-search/search.do?recordID=US9176643 (accessed January 31, 2018).

[94] J. L'Haridon, M. Fernandez, V. Ferrier, J. Bellan, Evaluation of the genotoxicity of n-nitrosoatrazine, n-nitrosodiethanolamine and their precursors in vivo using the newt micronucleus test, Water Research. 27 (1993) 855–862. doi:10.1016/0043-1354(93)90150-G.

[95] C. Cox, Atrazine: toxicology, Journal of Pesticide Reform. 21 (2001) 12–20.

[96] R.D. Cox, C.W. Frank, L.D. Nikolaisen, R.E. Caputo, Screening procedure for determination of total N-nitroso content in urine, Analytical Chemistry. 54 (1982) 253–256.

[97] Simultaneous determination of four tobacco-specific N-nitrosamines (TSNA) in human urine, Journal of Chromatography B. 877 (2009) 1185–1192. doi:10.1016/j.jchromb.2009.03.009.

[98] R.M. Hicks, C.L. Walters, I. Elsebai, A.B. Aasser, M.E. Merzabani, T.A. Gough, Demonstration of nitrosamines in human urine: preliminary observations on a possible etiology for bladder cancer in association with chronic urinary tract infections., Proc R Soc Med. 70 (1977) 413–417.

[99] M. Yamamoto, T. Yamada, A. Tanimura, Volatile nitrosamines in human blood before and after ingestion of a meal containing high concentrations of nitrate and secondary amines, Food and Cosmetics Toxicology. 18 (1980) 297–299. doi:10.1016/0015-6264(80)90111-X.

[100] L. Lakritz, M.L. Simenhoff, S.R. Dunn, W. Fiddler, N-nitrosodimethylamine in human blood, Food and Cosmetics Toxicology. 18 (1980) 77–79. doi:10.1016/0015-6264(80)90014-0.

[101] A.A. Melikian, E.J. LaVoie, D. Hoffmann, E.L. Wynder, Volatile nitrosamines: Analysis in breast fluid and blood of non-lactating women, Food and Cosmetics Toxicology. 19 (1981) 757–759. doi:10.1016/0015-6264(81)90533-2.

[102] Government of Prince Edward Island, Pesticide Analysis for Drinking Water - Open Data, 2016. https://www.princeedwardisland.ca/en/service/pesticide-analysis-drinking-water-open-data (accessed November 28, 2017).

[103] R. Raina-Fulton, A review of methods for the analysis of orphan and difficult pesticides: glyphosate, glufosinate, quaternary ammonium and phenoxy acid herbicides, and dithiocarbamate and phthalimide fungicides, J AOAC Int. 97 (2014) 965–977.

[104] World Health Organization, N-Nitrosodimethylamine in Drinking water: Background document for development of WHO Guidelines for Drinking-water Quality, World Health Organization, Geneva, Switzerland, 2008. http://www.who.int/water_sanitation_health/dwq/chemicals/ndma_2add_feb2008.pdf.

[105] Toxnet HSDB, Atrazine, U.S. National Library of Medicine, Bethesda, MD, 2012. https://toxnet.nlm.nih.gov/cgi-bin/sis/search2/f?./temp/~4T9lnj:1 (accessed January 22, 2018).

[106] Toxnet HSDB, Carbendazim, U.S. National Library of Medicine, Bethesda, MD, 2016. https://toxnet.nlm.nih.gov/cgi-bin/sis/search2/f?./temp/~Ym7we8:1 (accessed December 18, 2018).

[107] U.S. EPA, Reregistration eligibility decision: Thiophanate-methyl, Washington, DC, 2005.

[108] Toxnet HSDB, Dimethoate, U.S. National Library of Medicine, Bethesda, MD, 2007. https://toxnet.nlm.nih.gov/cgi-bin/sis/search2/f?./temp/~C6NgNg:1 (accessed December 18, 2018).

[109] Toxnet HSDB, Ethylenethiourea, U.S. National Library of Medicine, Bethesda, MD, 2010. https://toxnet.nlm.nih.gov/cgi-bin/sis/search2/f?./temp/~VdxROg:1 (accessed December 18, 2018).

[110] R.C. Rhodes, Studies with manganese [14C]ethylenebis(dithiocarbamate) ([14C]maneb) fungicide and [14C]ethylenethiourea ([14C]ETU) in plants, soil, and water, Journal of Agricultural and Food Chemistry. 25 (1977) 528–533. doi:10.1021/jf60211a016.

[111] Toxnet HSDB, Imidacloprid, U.S. National Library of Medicine, Bethesda, MD, 2016. https://toxnet.nlm.nih.gov/cgi-bin/sis/search2/f?./temp/~3RXMb1:1 (accessed December 18, 2018).

[112] Toxnet HSDB, Linuron, U.S. National Library of Medicine, Bethesda, MD, 2001. https://toxnet.nlm.nih.gov/cgi-bin/sis/search2/f?./temp/~6eXbUe:1 (accessed December 18, 2018).

[113] Toxnet HSDB, MCPA, U.S. National Library of Medicine, Bethesda, MD, 2001. https://toxnet.nlm.nih.gov/cgi-bin/sis/search2/f?./temp/~82Cu7g:1 (accessed December 18, 2018).

[114] Toxnet HSDB, Omethoate, U.S. National Library of Medicine, Bethesda, MD, 2007. https://toxnet.nlm.nih.gov/cgi-bin/sis/search2/f?./temp/~T0tdPw:1 (accessed December 18, 2018).

[115] K. Paranjape, V. Gowariker, V.N. Krishnamurthy, S. Gowariker, The Pesticide Encyclopedia, CABI, 2014.

[116] A.M. Grumezescu, A.M. Holban, Food Safety and Preservation: Modern Biological Approaches to Improving Consumer Health, Academic Press, 2018.

[117] S. Baskaran, R.S. Kookana, R. Naidu, Contrasting behaviour of chlorpyrifos and its primary metabolite, TCP (3,5,6-trichloro-2-pyridinol), with depth in soil profiles, Soil Res. 41 (2003) 749–760. doi:10.1071/sr02062.

[118] Toxnet HSDB, Thiophanate methyl, U.S. National Library of Medicine, Bethesda, MD, 2009. https://toxnet.nlm.nih.gov/cgi-bin/sis/search2/f?./temp/~xjvMEp:1 (accessed December 18, 2018).

[119] Y. Soeda, S. Kosaka, T. Noguchi, The Fate of Thiophanate-methyl Fungicide and Its Metabolites on Plant Leaves and Glass Plates, Agricultural and Biological Chemistry. 36 (1972) 931–936. doi:10.1080/00021369.1972.10860358.

[120] R.E. Ney, Fate and Transport of Organic Chemicals in the Environment: A Practical Guide, Government Institutes, 1998.

[121] B. Hanson, C. Bond, K. Buhl, D. Stone, Pesticide Half-life Fact Sheet, National Pesticide Information Center, Oregon State University Extension Services., 2015. http://npic.orst.edu/factsheets/half-life.html (accessed December 22, 2017).

[122] National Research Council, Human Biomonitoring for Environmental Chemicals, National Academies Press, 2006.

[123] M.J. Chung, S.H. Lee, N.J. Sung, Inhibitory effect of whole strawberries, garlic juice or kale juice on endogenous formation of N-nitrosodimethylamine in humans, Cancer Letters. 182 (2002) 1–10. doi:10.1016/S0304-3835(02)00076-9.

[124] S. Gupta, R.C. Gupta, A.B. Gupta, S. Eskiocak, E.V.S. Prakasa Rao, K. Puttanna, A. Singhvi, Pathophysiology of Nitrate Toxicity in Human and its Mitigation Measures, Society for Conservation of Nature, New Delhi, India, 2010.

[125] V. Yusa, M. Millet, C. Coscolla, M. Roca, Analytical methods for human biomonitoring of pesticides. A review, Analytica Chimica Acta. 891 (2015) 15–31. doi:10.1016/j.aca.2015.05.032.

[126] D.B. Barr, J. Angerer, Potential Uses of Biomonitoring Data: A Case Study Using the Organophosphorus Pesticides Chlorpyrifos and Malathion, Environ Health Perspect. 114 (2006) 1763–1769. doi:10.1289/ehp.9062.

[127] L. Kapka-Skrzypczak, M. Cyranka, M. Skrzypczak, M. Kruszewski, Biomonitoring and biomarkers of organophosphate pesticides exposure-state of the art, Annals of Agricultural and Environmental Medicine. 18 (2011). http://yadda.icm.edu.pl/yadda/element/bwmeta1.element.agro-fc4ea557-2096-4250-acba-7969c01110a0/c/fulltext859.pdf (accessed September 26, 2016).

[128] D.B. Barr, L.L. Needham, Analytical methods for biological monitoring of exposure to pesticides: a review, J. Chromatogr. B Analyt. Technol. Biomed. Life Sci. 778 (2002) 5–29.

[129] W.B. Dunn, D. Broadhurst, P. Begley, E. Zelena, S. Francis-McIntyre, N. Anderson, M. Brown, J.D. Knowles, A. Halsall, J.N. Haselden, A.W. Nicholls, I.D. Wilson, D.B. Kell, R. Goodacre, Human Serum Metabolome (HUSERMET) Consortium, Procedures for large-scale metabolic profiling of serum and plasma using gas chromatography and liquid chromatography coupled to mass spectrometry, Nat Protoc. 6 (2011) 1060–1083. doi:10.1038/nprot.2011.335.

[130] K. Čonka, B. Drobná, A. Kočan, J. Petrík, Simple solid-phase extraction method for determination of polychlorinated biphenyls and selected organochlorine pesticides in human serum, Journal of Chromatography A. 1084 (2005) 33–38. doi:10.1016/j.chroma.2004.11.029.

[131] C.D. Sandau, A. Sjödin, M.D. Davis, J.R. Barr, V.L. Maggio, A.L. Waterman, K.E. Preston, J.L. Preau, D.B. Barr, L.L. Needham, D.G. Patterson, Comprehensive Solid-Phase Extraction Method for Persistent Organic Pollutants. Validation and Application to the Analysis of Persistent Chlorinated Pesticides, Analytical Chemistry. 75 (2003) 71–77. doi:10.1021/ac026121u.

[132] R. Cazorla-Reyes, J.L. Fernández-Moreno, R. Romero-González, A.G. Frenich, J.L.M. Vidal, Single solid phase extraction method for the simultaneous analysis of polar and non-polar pesticides in urine samples by gas chromatography and ultra high pressure liquid chromatography coupled to tandem mass spectrometry, Talanta. 85 (2011) 183–196. doi:10.1016/j.talanta.2011.03.048.

[133] J. Chen, C. Duan, Y. Guan, Sorptive extraction techniques in sample preparation for organophosphorus pesticides in complex matrices, Journal of Chromatography B. 878 (2010) 1216–1225. doi:10.1016/j.jchromb.2010.02.031.

[134] M. Anastassiades, S.J. Lehotay, D. Štajnbaher, F.J. Schenck, Fast and easy multiresidue method employing acetonitrile extraction/partitioning and "dispersive solid-phase extraction" for the determination of pesticide residues in produce, Journal of AOAC International. 86 (2003) 412–431.

[135] S.J. Lehotay, K.A. Son, H. Kwon, U. Koesukwiwat, W. Fu, K. Mastovska, E. Hoh, N. Leepipatpiboon, Comparison of QuEChERS sample preparation methods for the analysis of pesticide residues in fruits and vegetables, J Chromatogr A. 1217 (2010) 2548–2560. doi:10.1016/j.chroma.2010.01.044.

[136] S.J. Lehotay, K. Mastovska, A.R. Lightfield, Use of buffering and other means to improve results of problematic pesticides in a fast and easy method for residue analysis of fruits and vegetables, Journal of AOAC International. (2005). http://agris.fao.org/agris-search/search.do?recordID=US201301063111 (accessed May 19, 2018).

[137] L. Cherta, T. Portolés, J. Beltran, E. Pitarch, J.G.J. Mol, F. Hernández, D. Roberts, R. Rao, A Validated Method for the Analysis of 142 Pesticide Residues Using Atmospheric Pressure GC Coupled with Tandem Quadrupole Mass Spectrometry, (2014).

[138] R. Raina, Chemical Analysis of Pesticides Using GC/MS, GC/MS/MS, and LC/MS/MS, PESTICIDES Ť STRATEGIES FOR PESTICIDES ANALYSIS. (2011) 105.

[139] N.A. Parris, Instrumental Liquid Chromatography: A Practical Manual on High Performance Liquid Chromatographic Methods, Elsevier, 2011.

[140] G.W. Tindall, J.W. Dolan, LC Troubleshooting: Mobile Phase Buffers, Part II — Buffer Selection and Capacity, LCGC Europe. (2003). http://images.alfresco.advanstar.com/alfresco_images/pharma/2014/08/22/e5171cb5-7a69-4389-ad35-d4dd1b7c21a5/article-41697.pdf (accessed September 22, 2016).

[141] Q.A. Xu, Ultra-High Performance Liquid Chromatography and Its Applications, John Wiley & Sons, 2013.

[142] S.C. Moldoveanu, V. David, Selection of the HPLC Method in Chemical Analysis, Elsevier, 2016.

[143] LCGC Editors, HPLC Column Selection, LCGC Europe. 26 (2013). http://www.chromatographyonline.com/hplc-column-selection (accessed September 21, 2016).

[144] D. Guillarme, J.-L. Veuthey, Guidelines for the use of UHPLC Instruments, Web Site: Http://Unige. Ch/Sciences/Pharm/Fanal/Lcap/Guidelines. 20 (n.d.). http://www.hplc.eu/Downloads/UHPLC_Guide.pdf (accessed September 21, 2016).

[145] H. Heinzen, L.M.L. Nollet, A.R. Fernandez-Alba, Multiresidue Methods for the Analysis of Pesticide Residues in Food, CRC Press, 2017.

[146] H. Nair, W. Clarke, Mass Spectrometry for the Clinical Laboratory, Academic Press, 2016.

[147] R.H. Perry, R.G. Cooks, R.J. Noll, Orbitrap mass spectrometry: Instrumentation, ion motion and applications, Mass Spectrometry Reviews. 27 (2008) 661–699. doi:10.1002/mas.20186.

[148] R. Romero-González, A.G. Frenich, Applications in High Resolution Mass Spectrometry: Food Safety and Pesticide Residue Analysis, Elsevier, 2017.

[149] Health Canada, Pest Control Products Sales Report 2007-2008, Government of Canada, 2012. http://www.hc-sc.gc.ca/cps-spc/pubs/pest/_corp-plan/sales-2007-2008-ventes/index-eng.php (accessed July 9, 2013).

[150] S. Souverain, S. Rudaz, J.-L. Veuthey, Matrix effect in LC-ESI-MS and LC-APCI-MS with off-line and on-line extraction procedures, Journal of Chromatography A. 1058 (2004) 61–66. doi:10.1016/j.chroma.2004.08.118.

[151] US EPA, Definition and Procedure for the Determination of the Method Detection Limit, Revision 2, 2016. https://www.epa.gov/cwa-methods/procedures-detection-and-quantitation-documents (accessed August 23, 2018).

[152] H. Govers, C. Ruepert, T. Stevens, C.J. van Leeuwen, Experimental determination and prediction of partition coefficients of thioureas and their toxicity to Photobacterium phosphoreum, Chemosphere. 15 (1986) 383–393. doi:10.1016/0045-6535(86)90532-1.

[153] H. Bräunlich, H. Bernhardt, I. Bernhardt, Renal handling of 2-methyl-4-chlorophenoxyacetic acid (MCPA) in rats, Journal of Applied Toxicology. 9 (1989) 255–258. doi:10.1002/jat.2550090409.

[154] S.B. Rosso, M. Gonzalez, L.A. Bagatolli, R.O. Duffard, G.D. Fidelio, Evidence of a strong interaction of 2,4-dichlorophenoxyacetic acid herbicide with human serum albumin, Life Sci. 63 (1998) 2343–2351.

[155] D.M. Roberts, A.H. Dawson, L. Senarathna, F. Mohamed, R. Cheng, G. Eaglesham, N.A. Buckley, Toxicokinetics, including saturable protein binding, of 4-chloro-2-methyl phenoxyacetic acid (MCPA) in patients with acute poisoning, Toxicology Letters. 201 (2011) 270–276. doi:10.1016/j.toxlet.2011.01.011.

[156] B.K. Matuszewski, M.L. Constanzer, C.M. Chavez-Eng, Strategies for the Assessment of Matrix Effect in Quantitative Bioanalytical Methods Based on HPLC−MS/MS, Anal. Chem. 75 (2003) 3019–3030. doi:10.1021/ac020361s.

[157] I. Marchi, V. Viette, F. Badoud, M. Fathi, M. Saugy, S. Rudaz, J.-L. Veuthey, Characterization and classification of matrix effects in biological samples analyses, Journal of Chromatography A. 1217 (2010) 4071–4078. doi:10.1016/j.chroma.2009.08.061.

[158] Government of Prince Edward Island, PEI Department of Agriculture and Fisheries, Agriculture on PEI, (2017). https://www.princeedwardisland.ca/en/information/agriculture-and-fisheries/agriculture-pei (accessed November 6, 2011).

[159] M. Arias-Estévez, E. López-Periago, E. Martínez-Carballo, J. Simal-Gándara, J.-C. Mejuto, L. García-Río, The mobility and degradation of pesticides in soils and the pollution of groundwater resources, Agriculture, Ecosystems & Environment. 123 (2008) 247–260. doi:10.1016/j.agee.2007.07.011.

[160] J. Nouri, A.H. Mahvi, G.R. Jahed, A.A. Babaei, Regional distribution pattern of groundwater heavy metals resulting from agricultural activities, Environ Geol. 55 (2008) 1337–1343. doi:10.1007/s00254-007-1081-3.

[161] H. Andry, T. Yamamoto, T. Irie, S. Moritani, M. Inoue, H. Fujiyama, Water retention, hydraulic conductivity of hydrophilic polymers in sandy soil as affected by temperature and water quality, Journal of Hydrology. 373 (2009) 177–183. doi:10.1016/j.jhydrol.2009.04.020.

[162] S. Reichenberger, M. Bach, A. Skitschak, H.-G. Frede, Mitigation strategies to reduce pesticide inputs into ground- and surface water and their effectiveness; A review, Science of The Total Environment. 384 (2007) 1–35. doi:10.1016/j.scitotenv.2007.04.046.

[163] C.W. Fetter, Applied Hydrogeology: Fourth Edition, Waveland Press, 2018.

[164] Government of Prince Edward Island, Provincial Soil, (2015). https://www.princeedwardisland.ca/en/information/conseil-executif/provincial-soil (accessed December 22, 2018).

[165] B.J. Zebarth, S. Danielescu, J. Nyiraneza, M.C. Ryan, Y. Jiang, M. Grimmett, D.L. Burton, Controls on Nitrate Loading and Implications for BMPs Under Intensive Potato Production Systems in Prince Edward Island, Canada, Groundwater Monit R. 35 (2015) 30–42. doi:10.1111/gwmr.12088.

[166] V. Hakoun, P. Orban, A. Dassargues, S. Brouyère, Factors controlling spatial and temporal patterns of multiple pesticide compounds in groundwater (Hesbaye chalk aquifer, Belgium), Environmental Pollution. 223 (2017) 185–199. doi:10.1016/j.envpol.2017.01.012.

[167] A. Rahman, A GIS based DRASTIC model for assessing groundwater vulnerability in shallow aquifer in Aligarh, India, Applied Geography. 28 (2008) 32–53. doi:10.1016/j.apgeog.2007.07.008.

[168] L. Wu, H. Chang, X. Ma, A modified method for pesticide transport and fate in subsurface environment of a winter wheat field of Yangling, China, Science of The Total Environment. 609 (2017) 385–395. doi:10.1016/j.scitotenv.2017.07.116.

[169] J. Kjær, V. Ernstsen, O.H. Jacobsen, N. Hansen, L.W. de Jonge, P. Olsen, Transport modes and pathways of the strongly sorbing pesticides glyphosate and pendimethalin through structured drained soils, Chemosphere. 84 (2011) 471–479. doi:10.1016/j.chemosphere.2011.03.029.

[170] M. Sophocleous, Interactions between groundwater and surface water: the state of the science, Hydrogeology Journal. 10 (2002) 52–67. doi:10.1007/s10040-001-0170-8.

[171] J.C. Rozemeijer, H.P. Broers, The groundwater contribution to surface water contamination in a region with intensive agricultural land use (Noord-Brabant, The Netherlands), Environmental Pollution. 148 (2007) 695–706. doi:10.1016/j.envpol.2007.01.028.

[172] E.H. Hofkes, J.T. Visscher, others, Artificial groundwater recharge for water supply of medium-size communities in developing countries, International Reference Centre for Community Water Supply and Sanitation The Hague, 1986. http://www.samsamwater.com/library/Artificial_groundwater_recharge_for_water_supply_of_medium-size_communities_in_developing_countries.pdf (accessed April 6, 2016).

[173] PEI Department of Fisheries, Aquaculture and Environment, State of the Environment, (2003). www.gov.pe.ca/photos/original/fae_soe_report.pdf (accessed November 6, 2011).

[174] J. Mutch, Pesticide monitoring and fish kill investigations on Prince Edward Island, 1994-1999, Canadian Technical Report of Fisheries and Aquatic Sciences. (2002) 94-94–115.

[175] Canadian Council of Ministers of the Environment., Canadian Water Quality Guidelines for the Protection of Aquatic Life: Aldicarb., (1999). ceqg-rcqe.ccme.ca/download/en/140/ (accessed November 15, 2011).

[176] R.E. Jackson, J.P. Mutch, M.W. Priddle, Persistence of aldicarb residues in the sandstone aquifer of Prince Edward Island, Canada, Journal of Contaminant Hydrology. 6 (1990) 21–35. doi:10.1016/0169-7722(90)90009-6.

[177] M.M.T. Khan, A.E. Martell, Activation Of Small Inorganic Molecules, Academic Press, Inc., New York, NY, 1974.

[178] Q. Wu, H. Shi, Y. Ma, C. Adams, T. Eichholz, T. Timmons, H. Jiang, Determination of secondary and tertiary amines as N-nitrosamine precursors in drinking water system using ultra-fast liquid chromatography–tandem mass spectrometry, Talanta. 131 (2015) 736–741. doi:10.1016/j.talanta.2014.08.003.

[179] Health Canada, Guidelines for Canadian Drinking Water Quality—Summary Table, Water and Air Quality Bureau, Healthy Environments and Consumer Safety Branch, Health Canada, Ottawa, ON, 2017. https://www.canada.ca/en/health-canada/services/environmental-workplace-health/reports-publications/water-quality/guidelines-canadian-drinking-water-quality-summary-table-health-canada-2012.html (accessed February 28, 2018).

[180] Prince Edward Island Government, Drinking Water Quality Summary Results Open Data Portal, Socrata. (2018). https://data.princeedwardisland.ca/Environment-and-Food/OD0039-Drinking-Water-Quality-Summary-Results/jq4v-y6dv/data (accessed December 23, 2018).

[181] Agency for Toxic Substances and Disease Registry, Nitrate/Nitrite Toxicity: What is the Biologic Fate of Nitrates and Nitrites in the Body?, Atlanta, GA, 2013. https://www.atsdr.cdc.gov/csem/csem.asp?csem=28&po=9 (accessed February 27, 2018).

[182] Health Canada Pest Management Regulatory Agency, Proposed Re-evaluation Decision: Mancozeb and its Associated End-use Products (PRVD2018-17), Health Canada, Ottawa, ON, 2018.

[183] M.R. Carter, J.A. Macleod, Biological Properties of Some Prince Edward Island Soils: Relationship Between Microbial Biomass Nitrogen and Mineralizable Nitrogen, Can. J. Soil. Sci. 67 (1987) 333–340. doi:10.4141/cjss87-029.

[184] US EPA, FIFRA Scientific Advisory Panel Briefing Document for a Consultation on: Monitoring Strategies for Pesticides in Surface Derived Drinking Water, Washington, DC, 2000.

[185] M. Csuros, Environmental Sampling and Analysis for Technicians, CRC Press, Boca Raton, FL, 1994.

[186] M.Z. Bruckner, Montana State University, Ion Chromatography, Bio-Geochemical Methods. (2018). https://serc.carleton.edu/microbelife/research_methods/biogeochemical/ic.html (accessed January 6, 2019).

[187] PerkinElmer, Inc, The 30-Minute Guide to ICP-MS, Waltham, MA, 2011.

[188] Government of Prince Edward Island, Interpreting Drinking Water Quality Results, (2016). https://www.princeedwardisland.ca/en/information/communities-land-and-environment/interpreting-drinking-water-quality-results (accessed January 2, 2019).

[189] L.M.L. Nollet, D.A. Lambropoulou, Chromatographic Analysis of the Environment: Mass Spectrometry Based Approaches, Fourth Edition, CRC Press, Boca Raton, FL, 2017.

[190] M. Rechcigl, Handbook of Naturally Occurring Food Toxicants, CRC Press, 2018.

[191] Health Canada Pest Management Regulatory Agency, Proposed Re-evaluation decision: Thiophanate methyl., Health Canada, Ottawa, ON, 2011.

[192] J. Briggs, T. Whitwell, R.T. Fernandez, M.B. Riley, Effect of Integrated Pest Management Strategies on Chlorothalonil, Metalaxyl, and Thiophanate-methyl Runoff at a Container Nursery, (n.d.) 7.

[193] Health Canada Pest Management Regulatory Agency, Re-evaluation Decision RVD2018-21, Mancozeb and Its Associated End-use Products, Pest Management Regulatory Agency, Ottawa, ON, 2018. https://www.canada.ca/en/health-canada/services/consumer-product-safety/reports-publications/pesticides-pest-management/decisions-updates/reevaluation-decision/2018/mancozeb.html (accessed January 7, 2019).

[194] K. Sexton, L.L. Needham, James.L. Pirkle, Human Biomonitoring of Environmental Chemicals, American Scientist. 92 (2004). https://www.cdc.gov/biomonitoring/pdf/as_article_biomonitoring.pdf (accessed January 30, 2017).

[195] Prince Edward Island Department of Fisheries, Aquaculture and Environment, State of the Environment, Charlottetown, PEI, 2001.

[196] E. and C.C.C. Government of Canada, Environment and Climate Change Canada - Water - Groundwater, (2007). http://www.ec.gc.ca/eau-water/default.asp?lang=En&n=300688DC-1%A0 (accessed February 2, 2019).

[197] Mittelstaedt, Martin, “Pesticides are what is killing our kids” - The Globe and Mail, (2006). http://www.theglobeandmail.com/news/national/pesticides-are-what-is-killing-our-kids/article18179217/?page=all (accessed September 3, 2015).

[198] Health Canada, Second Report on Human Biomonitoring of Environmental Chemicals in Canada: Results of the Canadian Health Measures Survey Cycle 2 (2009–2011), Ottawa, Ontario, 2013.

[199] T.J.B. Dummer, P. Awadalla, C. Boileau, C. Craig, I. Fortier, V. Goel, J.M.T. Hicks, S. Jacquemont, B.M. Knoppers, N. Le, T. McDonald, J. McLaughlin, A.-M. Mes-Masson, A.-M. Nuyt, L.J. Palmer, L. Parker, M. Purdue, P.J. Robson, J.J. Spinelli, D. Thompson, J. Vena, M. Zawati, with the C.R.C. Consortium, The Canadian Partnership for Tomorrow Project: a pan-Canadian platform for research on chronic disease prevention, CMAJ. 190 (2018) E710–E717. doi:10.1503/cmaj.170292.

[200] E. Sweeney, Y. Cui, V. DeClercq, P. Devichand, C. Forbes, S. Grandy, J.M.T. Hicks, M. Keats, L. Parker, D. Thompson, M. Volodarsky, Z.M. Yu, T.J.B. Dummer, Cohort Profile: The Atlantic Partnership for Tomorrow's Health (Atlantic PATH) Study, Int J Epidemiol. 46 (2017) 1762–1763i. doi:10.1093/ije/dyx124.

[201] W.B. Dunn, D.I. Broadhurst, H.J. Atherton, R. Goodacre, J.L. Griffin, Systems level studies of mammalian metabolomes: the roles of mass spectrometry and nuclear magnetic resonance spectroscopy, Chem Soc Rev. 40 (2011) 387–426. doi:10.1039/b906712b.

[202] Government of Prince Edward Island, Groundwater Nitrate Concentration Map: 2012 to 2016, 2017. https://www.princeedwardisland.ca/sites/default/files/publications/average_nitrate_in_groundwater_maps.pdf (accessed November 24, 2017).

[203] European Commission, Guidance document on analytical quality control and method validation procedures for pesticide residues and analysis in food and feed., (2017) 46.

[204] D.T. Mage, R.H. Allen, G. Gondy, W. Smith, D.B. Barr, L.L. Needham, Estimating pesticide dose from urinary pesticide concentration data by creatinine correction in the Third National Health and Nutrition Examination Survey (NHANES-III), Journal of Exposure Science & Environmental Epidemiology. 14 (2004) 457–465. doi:10.1038/sj.jea.7500343.

[205] M. Roca, N. Leon, A. Pastor, V. Yusà, Comprehensive analytical strategy for biomonitoring of pesticides in urine by liquid chromatography–orbitrap high resolution mass spectrometry, Journal of Chromatography A. 1374 (2014) 66–76. doi:10.1016/j.chroma.2014.11.010.

[206] G. Mendaš, M. Vuletić, N. Galić, V. Drevenkar, Urinary metabolites as biomarkers of human exposure to atrazine: Atrazine mercapturate in agricultural workers, Toxicology Letters. 210 (2012) 174–181. doi:10.1016/j.toxlet.2011.11.023.

[207] S. Mandic-Rajcevic, F.M. Rubino, E. Ariano, D. Cottica, S. Negri, C. Colosio, Exposure duration and absorbed dose assessment in pesticide-exposed agricultural workers: Implications for risk assessment and modeling, International Journal of Hygiene and Environmental Health. 222 (2019) 494–502. doi:10.1016/j.ijheh.2019.01.006.

[208] F. Hernández, J.V. Sancho, M. Ibáñez, E. Abad, T. Portolés, L. Mattioli, Current use of high-resolution mass spectrometry in the environmental sciences, Anal Bioanal Chem. 403 (2012) 1251–1264. doi:10.1007/s00216-012-5844-7.

[209] F. Hernández, T. Portolés, M. Ibáñez, M.C. Bustos-López, R. Díaz, A.M. Botero-Coy, C.L. Fuentes, G. Peñuela, Use of time-of-flight mass spectrometry for large screening of organic pollutants in surface waters and soils from a rice production area in Colombia, Science of The Total Environment. 439 (2012) 249–259. doi:10.1016/j.scitotenv.2012.09.036.

[210] F. Hernández, M. Ibáñez, T. Portolés, M.I. Cervera, J.V. Sancho, F.J. López, Advancing towards universal screening for organic pollutants in waters, Journal of Hazardous Materials. 282 (2015) 86–95. doi:10.1016/j.jhazmat.2014.08.006.

[211] E. Ekman, M. Maxe, M. Littorin, B.A.G. Jönsson, C.H. Lindh, High-throughput method for the analysis of ethylenethiourea with direct injection of hydrolysed urine using online on-column extraction liquid chromatography and triple quadrupole mass spectrometry, Journal of Chromatography B. 934 (2013) 53–59. doi:10.1016/j.jchromb.2013.06.035.

[212] S. Naz, H. Gallart-Ayala, S.N. Reinke, C. Mathon, R. Blankley, R. Chaleckis, C.E. Wheelock, Development of a Liquid Chromatography–High Resolution Mass Spectrometry Metabolomics Method with High Specificity for Metabolite Identification Using All Ion Fragmentation Acquisition, Analytical Chemistry. 89 (2017) 7933–7942. doi:10.1021/acs.analchem.7b00925.

[213] D. Cavanna, L. Righetti, C. Elliot, M. Suman, (in press). The scientific challenges in moving from targeted to non-targeted mass spectrometric methods for food fraud analysis: a proposed validation workflow to bring about a harmonized approach, Trends in Food Science & Technology. (2018). doi:10.1016/j.tifs.2018.08.007.

[214] S.T. Hassib, E.A. Taha, E.F. Elkady, G.H. Barakat, RP-LC Method for the Determination of Seven Antiviral Drugs and Bioanalytical Application for Simultaneous Determination of Lamivudine and Penciclovir in Human Plasma, Chromatographia. 81 (2018) 289–301. doi:10.1007/s10337-017-3441-9.

[215] Y.H. Hayun, M.O. Puspasari, Development of a high performance liquid chromatography method for simultaneous analysis of theophylline, guaifenesin and diphenhydramine in an elixir, Tropical Journal of Pharmaceutical Research. 16 (2017) 2501-2506–2506.

[216] M. Caban, N. Migowska, P. Stepnowski, M. Kwiatkowski, J. Kumirska, Matrix effects and recovery calculations in analyses of pharmaceuticals based on the determination of β-blockers and β-agonists in environmental samples, J Chromatogr A. 1258 (2012) 117–127. doi:10.1016/j.chroma.2012.08.029.

[217] W.M.A. Niessen, P. Manini, R. Andreoli, Matrix effects in quantitative pesticide analysis using liquid chromatography-mass spectrometry, Mass Spectrom Rev. 25 (2006) 881–899. doi:10.1002/mas.20097.

[218] United Chemical Technologies, Pesticide Residue Analysis in Whole Milk by QuEChERS and LC-MS/MS, UCT, Inc., Bristol, PA, 2013.

[219] J. Wilson, B. Wright, S. Jost, R. Smith, H. Pearce, S. Richardson, Can urinary indolylacroylglycine levels be used to determine whether children with autism will benefit from dietary intervention?, Pediatric Research. 81 (2017) 672–679. doi:10.1038/pr.2016.256.

Appendix A. Detailed Overview of Analytical Method Development

There are two distinct segments of analytical method development required for this project: instrument method development and sample preparation method development. It is critical to begin with instrument method development because before assessing the efficacy of a sample preparation method, it must first be verified that the instrument method can accurately detect and quantify target analytes. For this reason, the methods in this section are described in the order in which they were developed rather than the order they would be applied (i.e. sample preparation followed by sample analysis).

Instrument method development

Based on the physicochemical properties of the target compounds and the objective to incorporate semi-targeted analysis of PA*N*N compounds, an UHPLC/HRAM MS analytical platform was chosen. This platform can be operated using HESI, atmospheric pressure chemical ionization, or atmospheric pressure photoionization. The HESI source was selected based on previous work involving the analysis of 510 pesticide residues using this this ionization source [81]. A feature of the detector called "all ion fragmentation" (AIF) was also employed. AIF is a secondary ionization event that results in fragmentation patterns comparable to those generated by triple quadrupole MS. Although AIF mode allows for more in-depth analysis for analyte identification, this extra fragmentation may supress analyte signal [212].

Analytical Platform/Instrumentation

The Thermo Scientific Accela UHPLC system with the CTC Analytics PAL autosampler coupled to the Exactive Plus orbital ion trap mass spectrometer, equipped with the HESI source, was used for all sample analyses. Data analysis was performed using Thermo Scientific *Xcalibur* and *Tune* software. SPE was performed using the EluVac™ SPE vacuum manifold (LCTech GmbH, Dorfen, Germany). Samples were concentrated using the Thermo Scientific Reacti-Vap™ III 27-port evaporator (TS-18826) and Reacti-Therm™ III triple block (TS-18824) heating module ensemble. Centrifugation was done

using the Thermo Scientific Sorvall™ Legend™ X1R (75004261) centrifuge and salts were weighed on a Denver Instrument P-114 analytical balance (Bohemia, NY, US).

For optimization of ionization mode and injection solvent, starting chromatographic and detector conditions were established. A Hypersil GOLD™ aQ analytical column was installed and conditioned. The mobile phase consisted of 0.1% formic acid as Solvent A and 0.1% formic acid in MeOH as Solvent B. Solvent A was made by adding 1 mL of formic acid in 1,000 mL of Milli-Q water and Solvent B was made by adding 1 mL of formic acid in 1,000 mL of HPLC-grade MeOH. Solvent A began at 95% and was held for one minute. From minute one to seven, Solvent B was increased to 95% and held for one minute. Minutes eight to 15 show a decrease of Solvent B back down to 5% and 95% Solvent A is pumped for the remaining two minutes of the run for a total run time of 17 minutes.

Default HESI source parameters based on UHPLC flow rate were set to the following values: sheath gas flow rate, 50 au; auxiliary gas flow rate, 13 au; sweep gas flow rate, 0 au; spray voltage, 3.50 kV; capillary temperature, 263 ºC; S-lens RF level, 60.0 au; auxiliary gas heater temperature, 425 ºC. The orbital ion trap MS scan parameters were set to the following values: scan type, full MS/AIF; *m/z* range, 55-800 *m/z*; resolution, 70,000; automatic gain control target, 3e6; maximum IT, 200 ms; and collision energy, 20 eV.

Ionization Mode and Injection Solvent Selection

Standard solutions of each analyte were prepared in two different injection solvents (100% Milli-Q H_2O and 95%:5% H_2O:MeOH) and analyzed in both positive and negative HESI modes to determine which ionization mode, as well as injection solvent, resulted in a higher signal for each analyte. To make individual analyte solutions, 990 µL Milli-Q water was transferred to a labeled autosampler vial using a 100-µL glass syringe. A 10-µL glass syringe was used to add 10 µL of 100-µg mL^{-1} stock analyte solution to the vial for an intermediate concentration of 1,000 µg L^{-1}. The solution was vortexed for 15 seconds. A solution with a final concentration of 100 µg L^{-1} was made by combining 990 µL Milli-Q water and 10 µL of the 1,000 µg L^{-1} intermediate. This process was repeated using 95%:5% H_2O:MeOH as the injection solvent.

Initial injections showed that 100% Milli-Q H_2O was a better injection solvent than was 95%:5% H_2O:MeOH and half of the analytes ionized better in positive mode (ATR, CAR, DIM, ETU, and OME) while the other half ionized better in negative mode (IMI, LIN, MPCA, TCPy, and TM). Additionally, the Exactive Plus boasts a feature called "polarity switching", in which one full positive mode scan and one full negative mode scan are completed in under a second. Polarity switching allows the acquisition of data from both positive and negative mode scans in a single data file. To maximize the probability of detecting a greater number of semi-target analytes, both positive and negative ionization modes should be employed [213]. Therefore, the method was set to operate in polarity switching mode.

Master Mixes, Calibration Standards, and Intermediates

A master mix containing all target analytes was made to simplify the method development process. Master mixes facilitate the assessment of analyte responses for all target analytes in a single injection rather than multiple individual injections. Generally, a separate master mix is required for positive and negative ionization modes. In this case, where polarity switching was utilized, analytes designated to either ionization mode could be combined in the same solution. A double master mix (DMM) containing all 10 target analytes was made at a concentration of 1 μg mL^{-1} by adding 100 μL of each 100-μg mL^{-1} analytical standard to a 10-mL volumetric flask. The solution was topped up to the 10-mL mark with Milli-Q water.

Several intermediates were made for the IS (carbendazim-d3). The first intermediate was made by weighing 100 mg (0.1010 g) of solid analyte on a Denver Instrument P-114 analytical balance and adding it to 5 mL of HPLC-grade ACN in a clean 10-mL volumetric flask. The solution was topped up to 10 mL with ACN using a disposable glass pipet, vortexed for 15 seconds, and transferred to a labeled 10-mL amber glass vial with a final concentration of 10,000 μg mL^{-1}. The second intermediate was made by adding 1 mL of the first intermediate to a 10-mL volumetric flask, topped up with ACN to 10 mL, and vortexed for 15 seconds for a final concentration of 1,000 μg mL^{-1}. A third intermediate (required for making calibration standards) was made by adding 100 μL of the second intermediate to 9,000 μL ACN in a 10-mL volumetric flask for a final

concentration of 10 µg mL^{-1} IS. A fourth IS intermediate (for sample preparation method development) was made by adding 1 mL of the third intermediate to a 10-mL volumetric flask and topped up with ACN to 10 mL for a final concentration of 1 µg mL^{-1}.

The DMM and third IS intermediate was used to make calibration standards, which are prepared at several known concentrations to construct a calibration curve for the purpose of quantitation. Calibration standards were prepared at seven different concentrations in Milli-Q water to represent a seven-point calibration curve for each analyte (Table A-1).

Table A-1. Standard concentrations for a seven-point calibration curve for each analyte.

Calibration level	Volume of 1 µg mL^{-1} DMM added (µL)	Volume of 10 µg mL^{-1} IS added (µL)	Final IS concentration (µg L^{-1})	Final calibration standard concentration (µg L^{-1})
Level 1	10	100	100	1
Level 2	50	100	100	5
Level 3	100	100	100	10
Level 4	250	100	100	25
Level 5	500	100	100	50
Level 6	1000	100	100	100
Level 7	2500	100	100	250

Optimization of HESI Source Parameters

In addition to default settings for the UHPLC flow rate of 400 µL min^{-1}, the HESI source parameters were further optimized. Sheath gas, an inner coaxial nitrogen supply that is applied to help nebulize the liquid sample as it exits the ESI nozzle, was optimized within the following values: 40, 50, and 60 au. The auxiliary gas, an outer coaxial gas that may be used in conjunction with sheath gas to help disperse and/or evaporate sample, was optimized within the values 0, 10, 15, and 20 au. Sweep gas is a third nitrogen source that aids in solvent declustering and adduct reduction. Sweep gas flow rates were assessed at 0, 3, and 5 au. Spray voltage is the voltage applied to the spray needle in the HESI source to ionize sample particles. Spray voltage was tested at 3.5, 4, and 5 kV. The capillary temperature is the temperature of the ion transfer capillary and was evaluated at 250, 300,

and 350 ºC. Lastly, heating the auxiliary gas aids solvent evaporation. Auxiliary gas heater temperature was assessed at 100, 200, 300, and 400 ºC.

Column Optimization

Three analytical columns obtained from Thermo Fisher Scientific were tested for optimal retention and separation of target analytes: Hypersil GOLD™ aQ; Hypersil GOLD™; and Acclaim™ Trinity Q1 (Table A-2). All method development involving the Acclaim™ Trinity Q1 column was carried out in the absence of alcohols, as they degrade the column packing material.

Table A-2. Analytical column stationary phase, length, inner diameter, and particle size.

Column	Stationary phase	Length (mm)	Inner diameter (mm)	Particle size (µm)
Acclaim™ Trinity Q1 (Thermo Scientific)	Tri-mode (WCX, WAX, RP)	100	2.1	3
Hypersil GOLD™ (Thermo Scientific)	C18	50	2.1	1.9
Hypersil GOLD™ aQ (Thermo Scientific)	C18	20	2.1	12

Mobile Phase Optimization

MeOH and ACN were chosen as organic solvents for mobile phase optimization. ACN is favourable because it has a relatively lower viscosity, reduces back pressure, and may produce cleaner peak shapes [214]. However, MeOH is advantageous due to its lower cost and toxicity, as well as its higher polarity, which reduces the probability of buffer precipitation [215]. Three combinations of mobile phase solvents were tested for best analyte retention: (i) 100% Milli-Q water and 100% MeOH; (ii) 100% Milli-Q water and 100% ACN; and (iii) 0.1% formic acid in Milli-Q water and 0.1% formic acid in MeOH or ACN, depending on which organic solvent resulted in better peak shape and separation when used without the addition of acid.

UHPLC/HRAM Orbital Ion Trap MS Method Summary

Best analyte retention and separation was achieved with the Thermo Scientific Hypersil GOLD™ C18 analytical column (50 mm x 2.1 mm, 1.9 µm particle size) with a mobile phase flow rate of 400 µL min^{-1}. The optimal mobile phase combination of three tested was 100% water (Solvent A) and 100% MeOH (Solvent B). Solvent A began at 100% and was held for one minute. From minute one to seven, Solvent B was increased to 100% and held for one minute. Minutes eight to 15 showed a decrease of Solvent B back down to 0% and 100% Solvent A was pumped for the remaining two minutes of the run for a total run time of 17 minutes (Table A-3). The refrigerated autosampler tray held samples at 4 ºC.

Table A-3. Optimized UHPLC mobile phase gradient and flow rate.

Time	Solvent A: 100% H_2O (%)	Solvent B: 100% MeOH (%)	Flow rate (µL min^{-1})
0 minute	100	0	400
0-1 minute	100	0	400
1-7 minutes	0	100	400
7-8 minutes	0	100	400
8-15 minutes	100	0	400
15-17 minutes	100	0	400

For the HESI source parameters, analyte peak areas were highest using the default settings for a 400 µL min^{-1} flow rate, which were thereafter restored to the following values: sheath gas flow rate, 50 au; auxiliary gas flow rate, 13 au; sweep gas flow rate, 0 au; spray voltage, 3.50 kV; capillary temperature, 263 ºC; S-lens RF level, 60.0 au; auxiliary gas heater temperature, 425 ºC. The orbital ion trap MS scan parameters were set to the following values: scan type, full MS/AIF; *m/z* range, 55-800 *m/z*; ionization mode, polarity switching; resolution, 70,000; AGC target, 3e6; maximum IT, 200 ms; and collision energy, 20 eV.

Quality Assurance/Quality Control (QA/QC)

A number of QA/QC tools were employed in this study, including QC samples, solvent blanks, IS, LCSs, matrix post-extraction (MPE) spike samples, MBs, and reagent

water control (RWC) samples. QC samples are utilized to ensure analyte quantitation, retention times, and peak shape and height are reproducible with no systematic drift [129]. To assess consistency of the LC-MS, QC samples were injected throughout each sequence after every 10 injections or less. QC samples consisted of a mix of all target analytes in Milli-Q water at a concentration of 50 μg L^{-1}. Solvent blanks are samples of pure solvent that contain neither IS nor target analytes. These blanks are used to ensure target analytes do not carry over and remain in the chromatographic system from one injection to the next. For these experiments, solvent blanks were injected in duplicate at the beginning and end of each sequence, as well as throughout the sequence, usually before and after every QC injection.

An IS is defined as an isotopically-labeled compound, similar to the target analyte in structure and physicochemical properties, that can be added to samples before sample preparation is performed as a surrogate standard or after extraction [216]. The IS is helpful in assessing the extraction efficiency of a sample preparation method. A known concentration of the IS is often added to a test volume of sample matrix and is quantified after all sample preparation procedures have been performed on the sample. Environmental or biological samples often contain analytes of interest and the presence of any IS in the original sample would skew recovery experiments. Therefore, it is essential that the selected IS is not present in the sample. This exclusion is achieved by using isotopically-labeled ISs. In this study, carbendazim-d3 was used as the isotopically labeled IS and was added to all calibration levels and test samples for a final sample concentration of 100 μg L^{-1}. The sample preparation method was considered acceptable when recoveries (measured concentrations) of spiked concentration of IS and target analytes were between 80 and 120% (relative standard deviation, RSD < 20%). Test samples that did not yield an IS recovery within this range after optimization of the sample preparation and instrument methods were re-tested.

Four types of control samples were used in the development of sample preparation methods: MB, LCS, RWC, and MPE spiked controls. MBs were made by adding a known concentration of IS to test volumes of analyte-free matrix. These blanks are used to test for contamination during the sample preparation process. Test samples was considered uncontaminated if target analyte responses in MBs were undetected. An LCS is a

laboratory-made sample designed to represent a real-world sample. LCSs consisted of analyte-free sample matrix spiked with known concentrations of IS and analytes of interest *before* any sample preparation steps were performed. Mean LCS analyte concentrations are utilized to calculate both extraction process efficiency and matrix effects.

RWCs were made by spiking a test volume of Milli-Q water with IS and target analytes and were also subjected to the sample preparation process. Although analyte recoveries from RWCs were not used in any method performance calculations, they were helpful in demonstrating relative analyte loss due to the extraction process itself rather than by matrix effects. A perfect extraction technique would show identical analyte concentrations in the RWCs (subjected to the extraction process) and spiked controls (not subjected to the extraction process), as the reagent water used in RWCs matched both the injection solvent of the analytical standards and the initial mobile phase gradient. MPE spiked controls are used to assess matrix effects, which are defined as analyte signal suppression or enhancement caused by constituents present in the matrix [217]. MPE spiked controls were made by spiking analyte-free sample matrix with IS and target analytes *after* completion of all sample preparation and extraction procedures. Each test sample batch consisted of one MB, three to five LCSs (depending on the type of experiment), one MPE spike control, and one RWC.

Sample Preparation Method Development

Sterile frozen liquid human sera (50 mL) and Surine™ Negative Urine Control (50 mL) were chosen as test sample matrices. Stock matrix was allowed to thaw at 4 ºC overnight and was aliquoted in volumes of 1 mL and refrozen. Three different techniques were evaluated for the extraction of target analytes from biological matrices: deproteinization, SPE and QuEChERS. Of these three techniques, the one that resulted in the highest recoveries for the most analytes was selected for further optimization and validation. Method parameters were optimized by preparing a series of sample batches, each having a different method modification. Each batch was analyzed and subsequently modified until a recovery efficiency between 75 and 125% was obtained for each analyte, at which point the method was approved to undergo validation procedures. The optimized sample preparation method for the extraction of target analytes from the matrices was

deemed applicable to the semi-targeted PA*N*N compounds of interest, as the chemical structures of the nitrosatable pesticides are similar to their *N*-nitrosamine counterparts. For each experiment, 1-mL aliquots of stock matrix were allowed to thaw refrigerated at 4 ºC overnight. Urine sample preparation for targeted analysis used methods optimized for serum as a starting point.

Deproteinization procedure

The deproteinization approach involved methods adapted from procedures for non-targeted metabolomic analysis described in the Nature Protocols publication entitled, *Procedures for large-scale metabolic profiling of serum and plasma using gas chromatography and liquid chromatography coupled to mass spectrometry* [129]. LCS test samples (n=3) were made by adding 300 µL of stock serum, 50 µL each of a 1-µg mL^{-1} analyte master mix and IS intermediate, and 900 µL MeOH to a labeled 1.5-mL microcentrifuge tube. One MB was prepared by adding 300 µL serum, 50 µL IS intermediate, 100 µL Milli-Q water, and 900 µL MeOH to a labeled 1.5-mL microcentrifuge tube (Figure A-1). One MPE spiked control was prepared by adding 300 µL serum, 900 µL MeOH, and 150 µL Milli-Q water to a labeled 1.5-mL microcentrifuge tube; 50 µL each of a 1-µg mL^{-1} analyte master mix and IS intermediate were added after sample preparation steps were completed. A RWC was made by adding 300 µL Milli-Q water, 50 µL each of a 1-µg mL^{-1} analyte master mix and IS intermediate, and 900 µL MeOH; this test sample represents extraction of analytes in pure water rather than serum. Each sample in the batch was vortexed for 15 seconds and then centrifuged at room temperature for 15 minutes at 15,800 g. The addition of MeOH to serum samples and subsequent centrifugation serves as a "deproteinization step", which precipitates high-molecular-weight species from the sample. A volume of 1110 µL of the supernatant was transferred to a separate 1.5-mL centrifuge tube and evaporated under a gentle nitrogen stream at room temperature using the Reacti-Vap™/Reacti-Therm™ system.

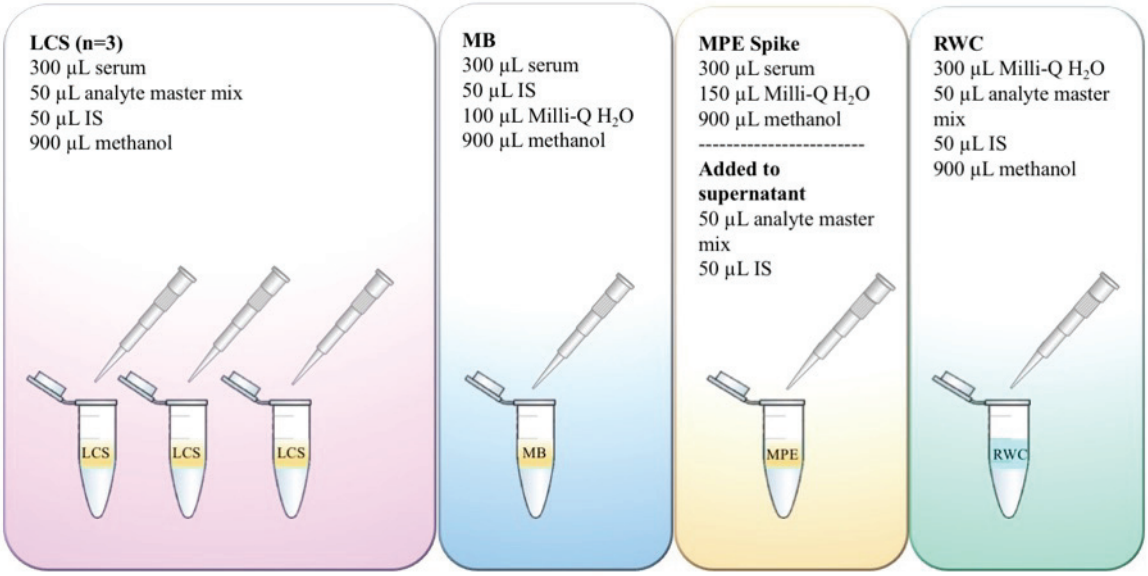

Figure A-1. Serum deproteinization experiment batch consisting of three LCSs, and one each of MB, MPE, and RWC.

To assess analyte loss during the nitrogen evaporation process, three different sample evaporation volumes were compared (Figure A-2). One batch of samples was evaporated to dryness and reconstituted in 250 µL of Milli-Q water. These samples were evaporated to dryness to obtain an injection solvent similar to the mobile phase starting conditions, as mismatched injection solvent and initial mobile phase may change analyte retention times. A second batch was evaporated to 125 µL and diluted 1:1 with Milli-Q water. This batch has a reduced risk of analyte loss, as the sample is evaporated down to only 50%, but the injection solvent is approximately 1:1 Milli-Q water:MeOH. A third batch was evaporated down to 250 µL and left unmodified. Following reconstitution, each test sample was vortexed for 15 seconds and centrifuged at 4 ºC for 15 minutes at 15,800 g. A volume of 225 µL of the supernatant was transferred to a 2-mL amber glass autosampler vial fitted with a 400 µL glass insert (to ensure that the sample level would be accessible to the autosampler syringe needle) and stored at 4 ºC until analysis.

Figure A-2. Nitrogen stream concentration of the three separate batches of serum samples (left) and markings showing different sample concentration volumes (right).

SPE procedure

Samples were prepared by spiking 200 µL serum with 20 µL each of a 1-µg mL^{-1} analyte master mix and IS intermediate in a 1.5-mL microcentrifuge tube and vortexed for 15 seconds (n=3). Three types of SPE cartridges were tested for optimal analyte retention: SOLA™ HRP (10 mg), Oasis HLB (30 mg), and Oasis PRiME HLB (10 mg). Generic methods for sample pre-treatment, as described by the manufacturers, varied with SPE cartridge type. For the SOLA™ HRP cartridges, 0.1% (v/v) aqueous formic acid was added up to 400 µL after the addition of standards. For the Oasis HLB and PRiME HLB cartridges, serum was diluted 1:1 with 4% (v/v) aqueous phosphoric acid and spiked with standards following acidification for a total test sample volume of 650 µL. This acidification step was performed to help release target analytes from serum proteins. All samples were shaken vigorously by hand for one minute, vortexed for 15 seconds, and then centrifuged at 4 ºC for 15 minutes at 15,800 g.

The SOLA™ HRP cartridges were conditioned with 500 µL MeOH and then equilibrated with 500 µL Milli-Q water. For each sample, the entire serum supernatant was loaded onto the cartridge followed by a wash volume of 500 µL 95 %:5 % Milli-Q water:MeOH solution. All cartridges were then eluted with 200 µL MeOH with 0.1% (v/v) aqueous formic acid followed by 200 µL Milli-Q water for a 1:1 dilution. The Oasis HLB cartridges were conditioned with 500 µL MeOH and then equilibrated with 500 µL Milli-Q water. The entire serum supernatant was loaded onto the cartridge followed by a wash volume of 500 µL Milli-Q water. The cartridge was then eluted with 500 µL MeOH followed by 200 µL Milli-Q water for a 1:1 dilution. The Oasis PRiME HLB cartridges need neither conditioning nor equilibration. The entire serum supernatant was loaded onto the cartridge followed by a wash volume of 500 µL Milli-Q water. The cartridge was then eluted with 500 µL MeOH followed by 200 µL Milli-Q water for a 1:1 dilution. All extracted samples were stored at 4 ºC until analysis. Serum SPE batch preparation is shown in Figure A-3.

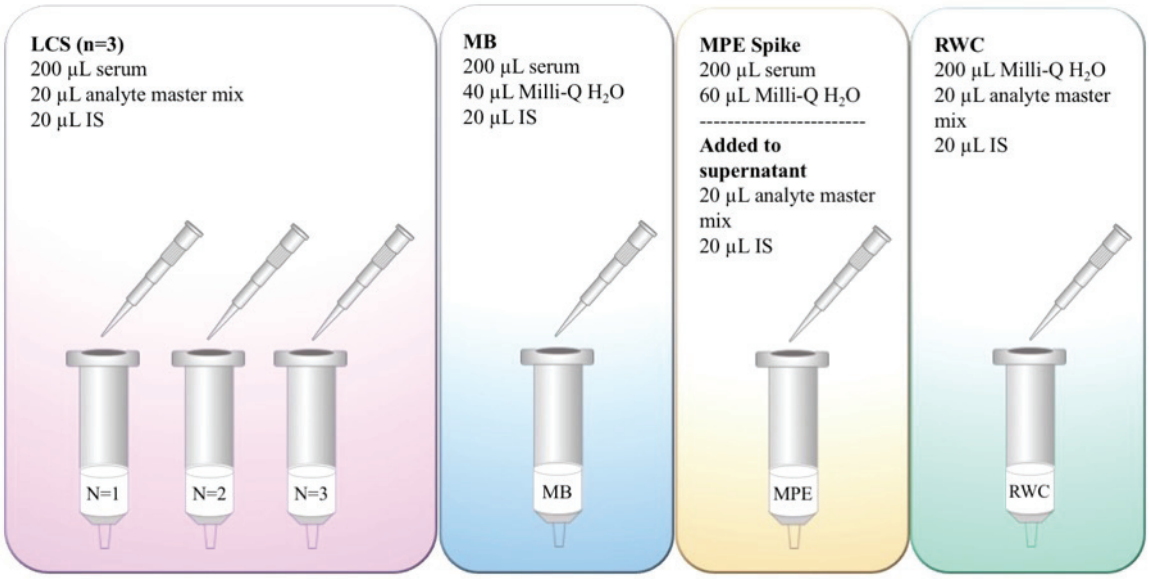

Figure A-3. Serum SPE experiment batch consisting of three LCSs, and one each of MB, MPE, and RWC.

QuEChERS

The methods used in this study were adaptions of the QuEChERS method described by UCT, Inc. in the protocol entitled, *Pesticide Residue Analysis in Whole Milk by QuEChERS and LC-MS/MS* [218]. Serum and Surine™ test samples were prepared by

vortexing 1-mL aliquots for 15 seconds and transferring 500 µL of sample matrix to 1.5-mL microcentrifuge tubes. Test samples (n=3) were spiked with 50 µL each of a 1-µg mL^{-1} analyte master mix and IS intermediate and vortexed for an additional 15 seconds. To each tube, 500 µL of extraction solvent (100% ACN, or 0.1%, 0.5%, 1%, or 4% AcOH in ACN) were added and samples were shaken vigorously by hand for one minute. One of three premade QuEChERS salt mixtures (250 mg $MgSO_4$ only, 200 mg $MgSO_4$ + 50 mg NaOAc, or 200 mg $MgSO_4$ + 50 mg NaCl) was added to the sample to facilitate phase separation and extraction of target analytes. The salts were weighed on a Denver Instrument P-114 analytical balance with masses within 0.3 mg considered acceptable. Samples were vortexed for 15 seconds to break up salt agglomerates and shaken vigorously by hand for one minute. In some trials, the samples were sonicated for either 15 or 30 minutes. All samples were centrifuged at 4 ºC for 15 minutes at 15,800 g. This created a three-layer system (Figure A-4). A volume of 200 µL of the supernatant was transferred to a labelled autosampler vial, diluted 1:1 with Milli-Q water, vortexed for 15 seconds, and stored at 4 ºC until analysis. Biomatrix QuEChERS batch preparation is shown in Figure A-5.

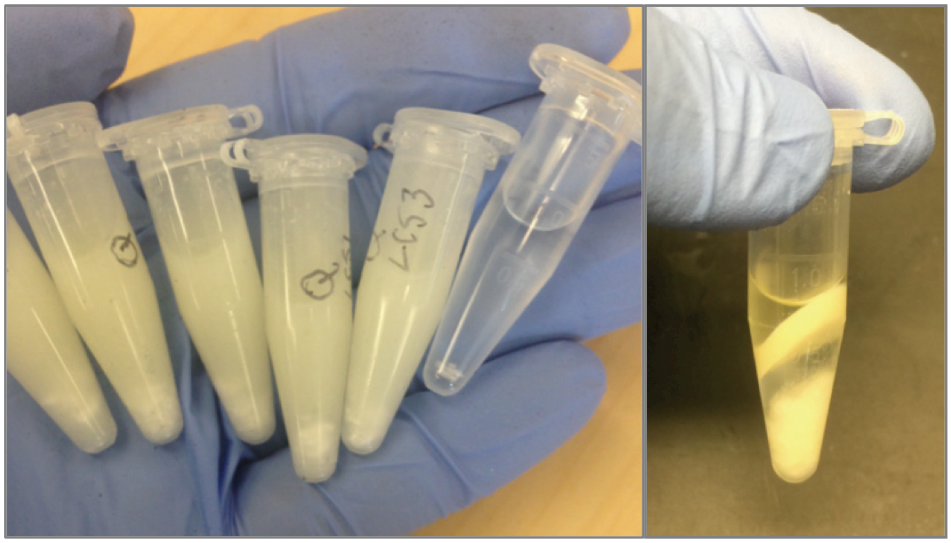

Figure A-4. Serum samples before centrifugation (left) and a three-layer system formed after centrifugation (right) during QuEChERS sample preparation.

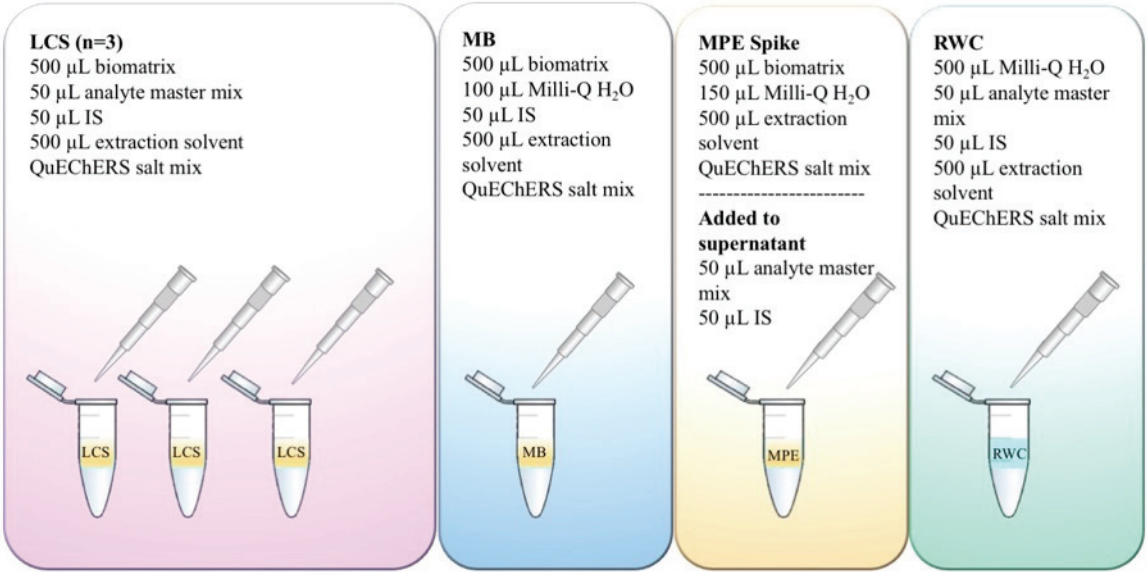

Figure A-5. Biomatrix QuEChERS experiment batch consisting of three LCSs, and one each of MB, MPE, and RWC.

Method Validation Procedures

Once optimized, analytical methods require validation to demonstrate that they are fit for purpose. The degree of validation depends on the scope and objectives of the project. The validation parameters applied to these methods include specificity, linearity, accuracy (recovery and process efficiencies), precision (intra-day precision, and inter-day precision), matrix effects, method detection limit, and limit of quantitation. Specificity is the ability of a method to accurately differentiate between a target analyte and other substances present in the sample matrix. Chromatographic peaks of each analytical standard for target compounds and IS were identified by their retention times and by confirming a match between the *Tune* software's calculated theoretical *m/z* and experimentally determined *m/z*. Determination of the recovery and process efficiencies, and matrix effects in quantitative bioanalytical methods using HPLC-MS has been detailed by Matuszewski *et al*. (2003) [156] and adapted for this study.

Recovery efficiency (RE (%)) of the extraction method was evaluated by assessing analyte recoveries of test sample replicates at two different concentrations (25 and 50 µg L^{-1}) and reported as %RSD of mean analyte peak area. Recovery was measured by entering mean observed concentrations for LCSs and a MPE spiked control into Eq. (1).

$$RE\ (\%) = \frac{mean\ test\ sample\ concentration}{matrix\ post{-}extraction\ spiked\ control\ concentration} \times 100 \qquad (1)$$

Process efficiency (PE (%)) of the optimized extraction method for each sample matrix was determined using five replicates at two different analyte concentrations, 25 and 50 µg L^{-1}, and calculated for each analyte using Eq. (2).

$$PE\ (\%) = \frac{mean\ test\ sample\ concentration}{concentration\ of\ spiked\ controls} \times 100 \qquad (2)$$

Intra-day precision was evaluated at 50 µg L^{-1} (n=3) by repeating the extraction procedure twice within a 24-hour period. Inter-day precision was evaluated at 50 µg L^{-1} and spiked samples (n=3) were analyzed daily for a period of three consecutive days.

The ME (%) value was calculated for each analyte at three different analyte concentrations (10, 25, and 50 µg L^{-1}) by entering the values obtained for the MPE spike concentration and spiked control concentration into Eq. (3).

$$ME\ (\%) = \frac{matrix\ post{-}extraction\ spiked\ control\ concentration}{spiked\ control\ concentration} \times 100 \qquad (3)$$

The MDL was determined using the U.S. EPA procedures outlined in *Definition and Procedure for the Determination of the Method Detection Limit, Revision 2* [151]. First, MDLs were estimated to be around 1 µg L^{-1} from previously determined quantitation limits for several target analytes [81]. A concentration ten times this estimate (10 µg L^{-1}) was used to experimentally determine MDLs for each analyte. Ten spiked samples and 10 method blank samples were processed through all steps of the method (three test samples per day over two days and four on the third day) and analyzed. MDLs for each analyte in spiked samples and method blanks were then calculated; the greater of the two determined for each analyte represented the MDL. The LOQ was calculated as ten times the standard deviation of the 10 replicate spiked sample measurements.

Statistical Analysis

Initial recovery experiments conducted to assess the most efficient sample preparation technique were carried out using replicates of three. Mean recovery values were recorded, and standard deviation was calculated to determine error bars. Method validation experiments were carried out in replicates of either three or five measurements. Process and recovery efficiencies were calculated along with %RSD values for five replicate measurements. Intra- and inter-day precision was represented by %RSD calculated from replicates of three.

Analytical method validation procedures

The molecular formula for each target analyte was entered into the *Tune* software's *Mass Calculator* to calculate theoretical *m/z* of ions generated in positive and negative ionization modes. Standards of target analytes were injected individually, and the theoretical *m/z* values were extracted from the resulting chromatograms. Compound identification was confirmed by matching theoretical and experimental *m/z* values from the mass spectrum at each chromatographic peak corresponding to the target analyte (within 5 ppm). Chromatographic peaks of each analytical standard for target compounds and IS (Figure A-6) were further identified by retention time (t_r) (Table A-4).

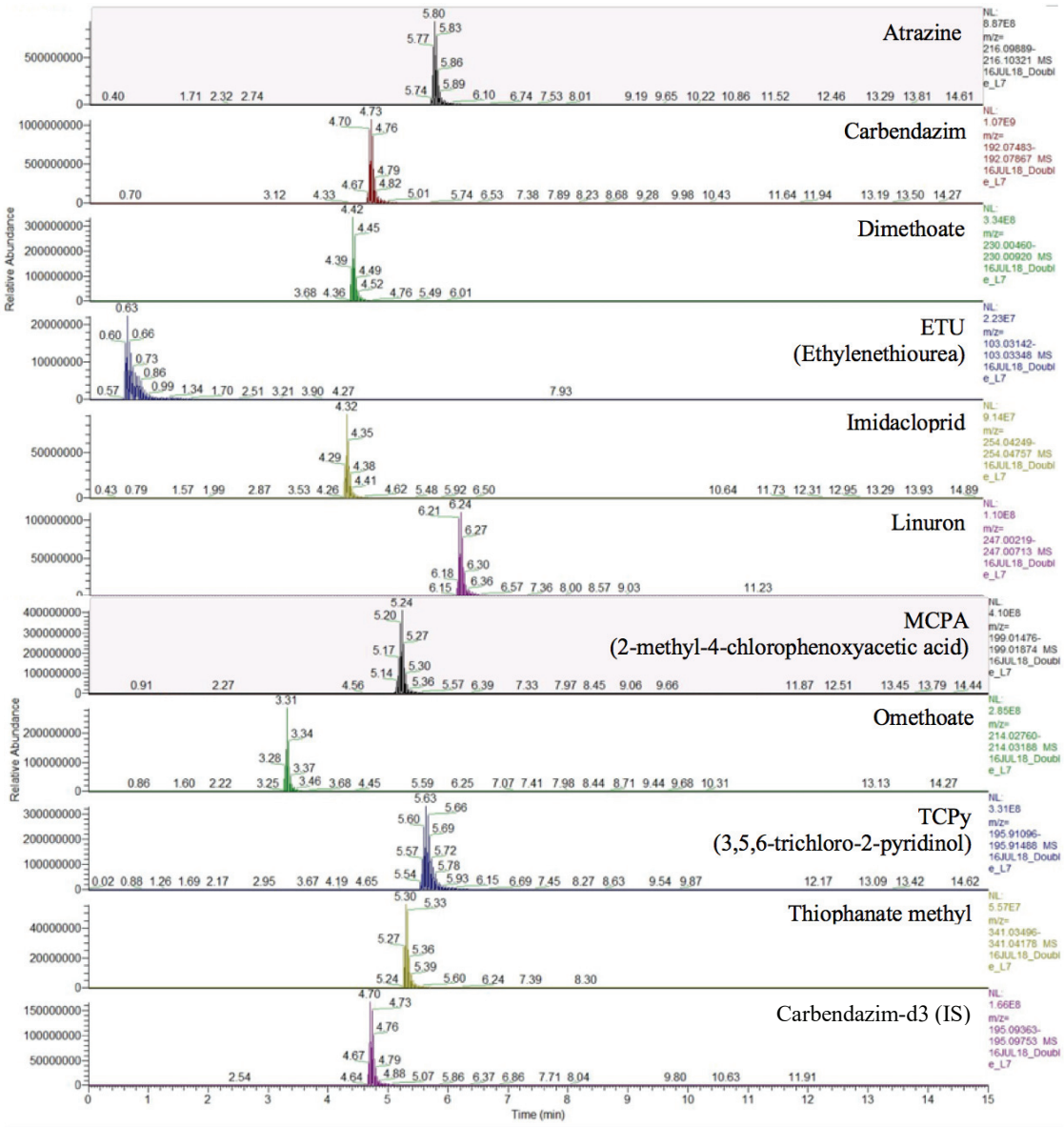

Figure A-6. Representative chromatogram of a standard mixture of 10 target analytes and IS. Peaks were displayed by extracting the *m/z* values generated by the Exactive Plus Tune software.

Table A-4. Theoretical *m/z* values extracted from chromatograms, ionization mode (positive, +, or negative, –) and retention times (t_r) for each analyte used for identification of target analytes; seven-point calibration curves generated linear regression equations and corresponding R^2 values.

Analyte[1]	Theoretical mass (*m/z*)	Ionization mode	t_r (min)	Linear regression equation	R^2
ATR	216.10105	+	5.80	Y = -0.0112875 + 0.0175463*X	0.9998
CAR	192.07675	+	4.73	Y = 0.0090075 + 0.0183376*X	0.9999
DIM	230.00690	+	4.42	Y = 0.00440021 + 0.00474638*X	0.9999
ETU	103.03245	+	0.63	Y = 0.00114833 + 0.000396687*X	0.9992
IMI	254.04503	–	4.32	Y = 0.00161635 + 0.00078102*X	0.9991
LIN	247.00466	–	6.24	Y = -0.00133009 + 0.00140702*X	0.9996
MCPA	199.01675	–	5.24	Y = 0.00976771 + 0.00707869*X	0.9994
OME	214.02974	+	3.31	Y = 0.000861952 + 0.00442353*X	0.9997
TCPy	195.91292	–	5.63	Y = 0.00822632 + 0.00726235*X	0.9999
TM	341.03837	–	5.30	Y = -0.0030802 + 0.00127105*X	0.9992
CAR-D3*	195.09558	+	4.70	---	---

**Internal standard carbendazim-d3*

[1]ATR = atrazine; CAR = carbendazim; DIM = dimethoate; ETU = ethylenethiourea; IMI = imidacloprid; LIN = linuron; MCPA = 2-methyl-4-chlorophenoxyacetic acid; OME = omethoate; TCPy = 3,5,6-trichloro-2-pyridinol; TM = thiophanate methyl.

To assess linearity, Milli-Q water was spiked with a master mix containing all target analytes at seven different concentrations: 1, 5, 10, 25, 50, 100, and 250 μg L^{-1}. Each calibration level was also spiked with 100 μg L^{-1} IS for internal calibration. A calibration curve was generated for each analyte and linearity was evaluated using the correlation coefficient (R^2) (Figure A-7).

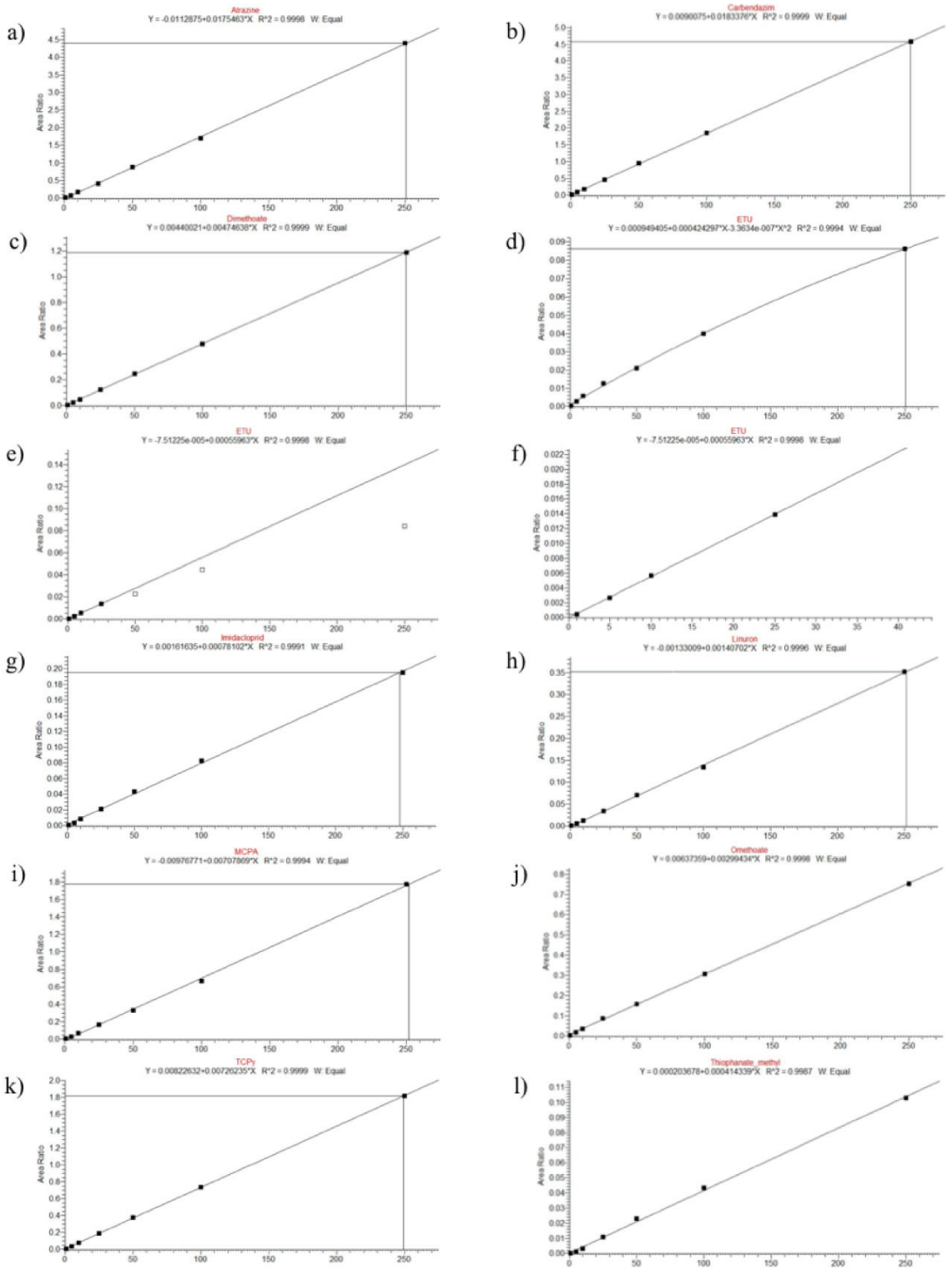

Figure A-7. Linearity depicted by calibration curves for a) ATR; b) CAR; c) DIM; d) ETU comprised of seven calibration points, showing nonlinearity; e) ETU comprised of four calibration points, showing linearity with exclusion of points with higher concentration; f) ETU comprised of four calibration points, zoomed in on lower calibration range; g) IMI; h) LIN; i) MCPA; j) OME; k) TCPy; and l) TM.

Appendix B. Tentative Identification of Biomarker Presenting as *N*-ATR

For the compound in question presenting as *N*-ATR in both serum and urine samples, the following information was gathered to characterize the expression of the biomarker: (i) throughout the injection sequences, there was no gradual increase or decrease in either *N*-ATR molecular ion response among the samples, indicating that neither contamination nor analyte carryover were likely explanations for the biomarker response; (ii) peak areas of each molecular ion varied widely among participants with large standard deviations (mean *N*-ATR/IS peak areas for PEI and NS urine samples were 10.8 ± 9.5 and 14.2 ± 13.2 a.u., respectively), which suggests that the biomarker is expressed with a high degree of variation in the two sample populations; (iii) retention times for the *N*-ATR molecular ions are consistent among injections for the same biomatrix, but there is a notable (0.27 minutes) difference in mean retention time of the negative *N*-ATR molecular ion between serum (3.87 ± 0.06 minutes, n=24) and urine (4.14 ± 0.17 minutes, n=63) and a more marked difference in retention time in biological samples and that of synthesized *N*-ATR in Milli-Q water; (iv) the biomarker was undetected in blanks injected before and between each sample batch; (v) reagent blanks (Milli-Q water and IS) prepared along with each batch showed no response for *N*-ATR molecular ions; and (vi) examination of the synthesized *N*-ATR chromatogram revealed that its molecular ion peak area ratio ($[M-H]^-$:$[M+H]^+$) ion showed a greater response with a mean peak area of 1.8, whereas the urinary biomarker's mean molecular ion peak area ratio was determined to be 5.2 from sample chromatograms.

While it is not possible to unequivocally identify these PA*N*N compounds without an analytical standard, further evidence of the biomarker's identity was collected by the use of fragmentation data. Since the Exactive Plus orbital ion trap MS used in this study employed AIF technology, which applies a collision energy of 20 eV throughout the analysis to continuously generate fragment ions, potential fragment masses can be extracted from sample chromatograms to help identify unknown biomarkers. To test the usefulness of the predicted mass spectra approach, predicted mass spectra were generated for *N*-ATR and *N*-ETU using the CFM-ID program (Figure B-1). Each predicted spectrum displays several potential fragments using electrospray ionization (ESI) with a collision

energy of 20 V. The top five predicted fragments were extracted from chromatograms for synthesized *N*-ATR in negative ionization mode (243.07666 $[M-H]^-$; 225.06610; 58.06622; 215.04536; and 83.0614) and *N*-ETU in positive ionization mode (132.02261 $[M+H]^+$; 73.03964; 101.01680; 55.02907; and 99.00115) (Figure B-2). Extraction of predicted ions for *N*-ATR fragmentation did not result in identity confirmation through a secondary fragment whereas *N*-ETU matched both its molecular ion and a secondary fragment.

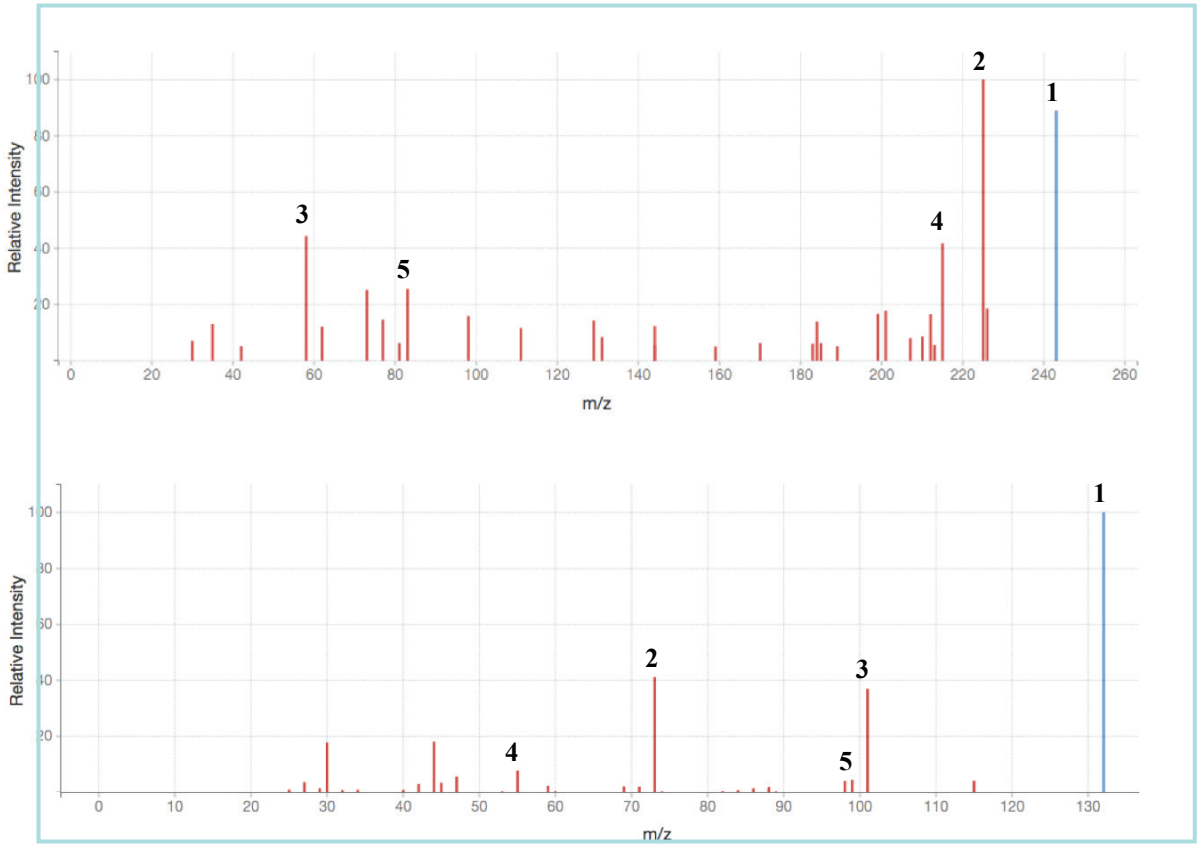

Figure B-1. Predicted mass spectra of *N*-ATR in negative ionization mode (top) and *N*-ETU in positive ionization mode (bottom) with a collision energy of 20 V. Five ions with highest intensities above *m/z* value of 50 were selected for analyte identification.

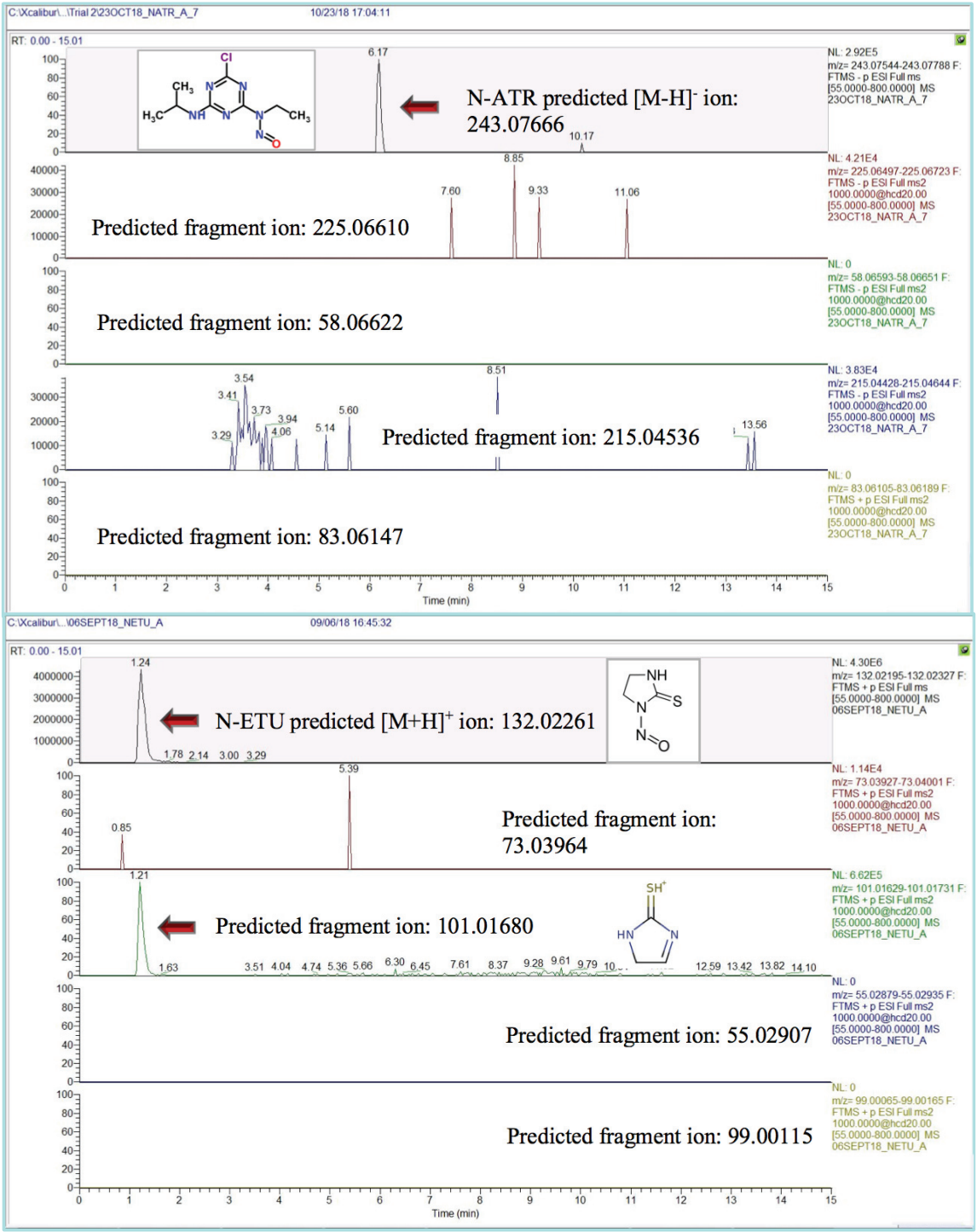

Figure B-2. Extractions of predicted fragment ions from *N*-ATR (top) and *N*-ETU (bottom) chromatograms of synthesized compounds. Only the molecular ion matched for *N*-ATR whereas *N*-ETU matched with both its molecular ion and a secondary fragment.

The sample that produced the highest response of unknown biomarker was analyzed using the Q-Exactive orbital ion trap MS. Unlike the Exactive Plus, the Q-

Exactive contains a quadrupole that allows the filtering of ions before a secondary fragmentation. This means that as opposed to fragmenting all ions (including interfering ions generated from the thousands of constituents that may be present in the sample), only ions matching the mass of the biomarker's molecular ion were further fragmented. This cleaned up the mass spectrum substantially and allowed determination of ion fragments contributing to the biomarker in question. Comparative mass spectra between the Exactive Plus and the Q-Exactive are shown in Figure B-3.

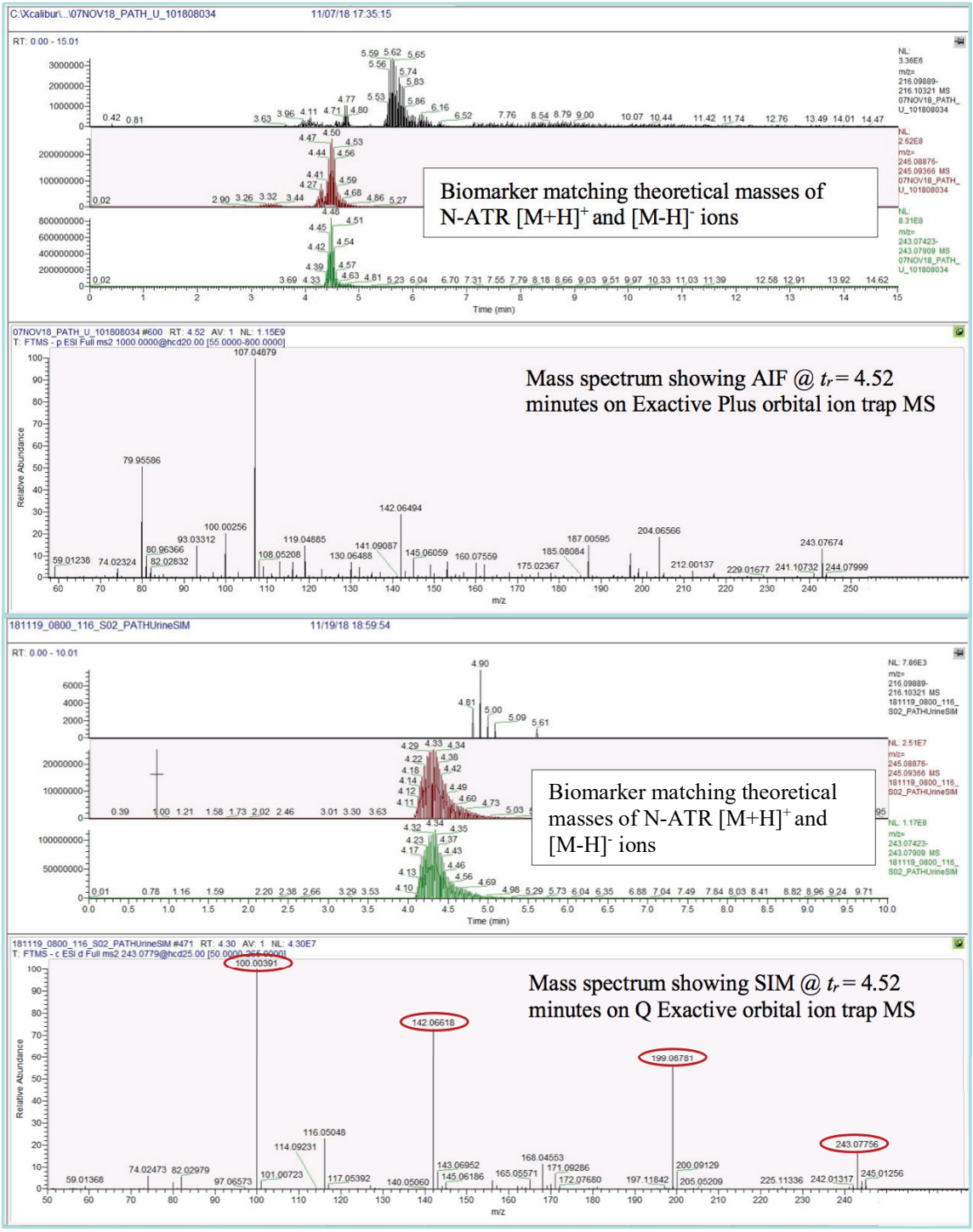

Figure B-3. Comparison of unknown biomarker fragmentation using the Exactive Plus orbital ion trap MS (top) and the Q-Exactive orbital ion trap MS (bottom). The Exactive Plus uses AIF, which does not filter ions from interfering sample constituents, whereas the Q-Exactive MS is able to selectively fragment only ions that match the molecular ion of the unknown biomarker via selected ion monitoring (SIM).

After a thorough and lengthy search of potential candidates for this biomarker using possible chemical formulas suggested by the *Xcalibur* software and the ion fragments generated by the Q-Exactive orbital ion trap MS, the compound indolyl-3-acryloylglycine (IAG) was investigated as a potential match. IAG has a molecular weight of 244.085 g mol^{-1} and its theoretical *m/z* value 243.07752 is only 3.5 ppm apart from that of *N*-ATR, 243.07683. In children, an association has been identified between increased concentrations of urinary IAG and autism spectrum disorders (ASD) with coexisting gastrointestinal issues [219]. A predicted mass spectrum of this potential biomarker revealed several potential fragment ions for comparison: 243.07752; 74.02475; 199.08769; 225.06695; and 168.04549 (Figure B-4). Extraction of predicted fragment ions for IAG in a serum and urine sample from the same participant showed a match for one and two predicted fragments, respectively, at an overlapping retention time (Figure B-5).

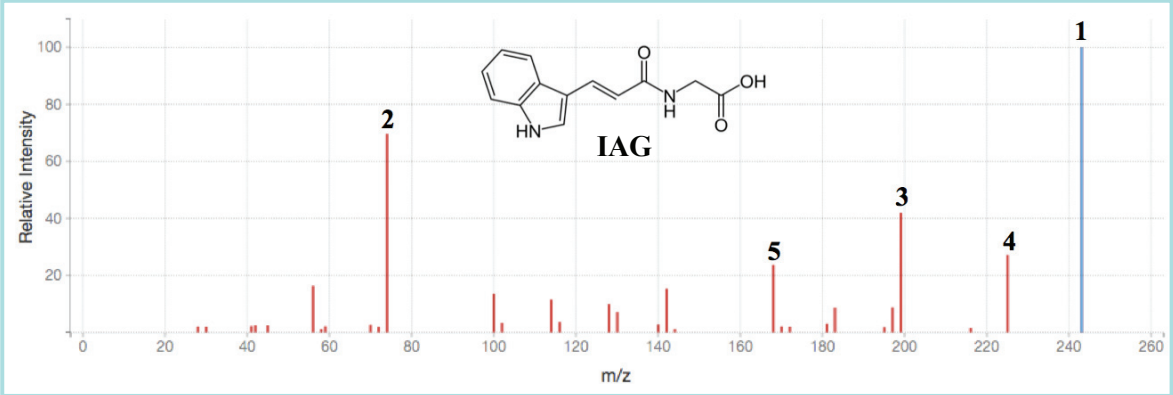

Figure B-4. Predicted mass spectrum of IAG in negative ionization mode with a collision energy of 20 V.

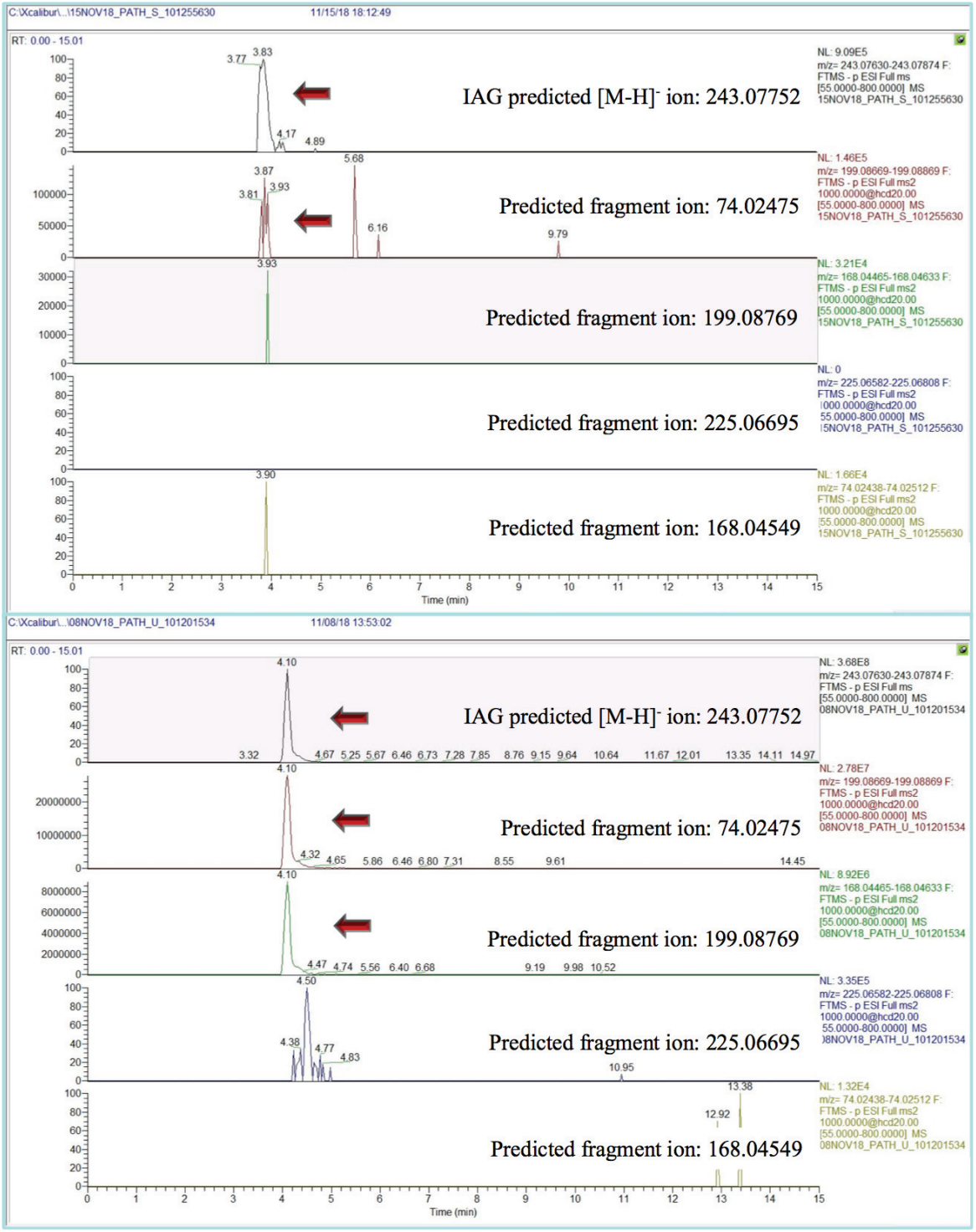

Figure B-5. Extraction of predicted fragment ions for IAG in serum (top) and urine (bottom) of the same individual. Although IAG and *N*-ATR have molecular ion masses within 5 ppm of each other, the presence of one predicted secondary IAG fragment in serum and two predicted IAG secondary fragments in urine suggest that this biomarker is IAG rather than *N*-ATR.

After observing a more likely match between the biomarker and IAG, all biological sample chromatograms were subsequently reanalyzed and extracted for five IAG predicted fragment ions. Of the six tentative detections in the PEI serum samples, four showed a small response for the secondary fragment. For the NS serum samples, the sample with the largest peak area for the biomarker showed responses for three additional predicted ions; a slight response was seen for one secondary fragment in eleven samples. Interestingly, all 31 PEI urine samples containing the biomarker clearly presented with two or more predicted fragments matching the retention time of the IAG molecular ion. In contrast, only 12 of the 32 NS urine samples showed two or more predicted IAG fragments at the expected retention time and 11 samples showed a peak for one matching secondary fragment. Three other samples generated a slight response for one secondary fragment and the remaining six samples showed no secondary fragments. Although the presence of a secondary fragment at an overlapping retention time is critical for compound identification, fragments with lower relative ion intensities may not generate a response at low analyte concentrations.